GEOLOGY OF THE THERON MOUNTAINS, ANTARCTICA

By

D. BROOK

A thesis submitted for the degree of Doctor of Philosophy under the Special Regulations of the University of Birmingham.

June 1972

Frontispiece. View of the northern part of the Theron Mountains showing Lenton Bluff and the escarpment to the north-east of it.

SUMMARY

The oldest rocks exposed in the Theron Mountains are an approximately 700 m. thick sequence of terrestrial, water-lain clastic sediments. They consist largely of arkosic, feldspathic and quartzitic fine-grained sandstones and siltstones with thin shales and mudstones and subordinate carbonaceous beds and coals. Minor breaks in the succession are of only local significance and there were variable local environments of deposition. There are glossopterid fossils indicative of a Lower Permian age.

These sediments were intruded during the Jurassic by great thicknesses of dolerite, mainly in the form of sills but with occasional thin dykes. Field, petrographical and chemical evidence indicates major differences between these dolerites and the Ferrar dolerites of Jurassic age elsewhere in eastern Antarctica. Comparison with other Mesozoic tholeiitic rocks of the Southern Hemisphere confirms the distinction of two separate magmatic provinces but modifies their geographical limits. A model is postulated to explain the origin of these magmatic provinces in relation to their association with the break-up and dispersal of Gondwanaland.

Minor local tilting and faulting occurred in association with and subsequent to the intrusive activity and there was pervasive thermal metamorphism of most of the sediments.

There is no record of tectonic events since the end of the Jurassic but there may have been some block-faulting, resulting in a graben now occupied by "Main Glacier".

Glacial and periglacial processes have been the dominant factors in determining the landforms of the Theron Mountains since the last glaciation of Antarctica.

CONTENTS

Page

Page

Page

LIST OF FIGURES

LIST OF TABLES

CHAPTER I

INTRODUCTION

A. LOCATION

The Theron Mountains, which are situated on the inland edge of the Filchner Ice Shelf (Fig. 1), trend north-east to south-west for a distance of about 120 km. The area described here (Figs. 2 and 3), lying between lat. 78°45'S., long. 26°50'W. and lat. 79°30'S., long. 30°20'W., includes the whole of the mountain range.

B. PREVIOUS INVESTIGATIONS

This study is based on the first detailed field mapping of the Theron Mountains, though they have been visited by earlier workers. First discovered from the air on 6 February 1956 during the Trans-Antarctic Expedition (Stephenson, 1966), the mountains were visited and specimens were collected by K.V. Blaiklock and R. Goldsmith on 18 December 1956. Further visits were made by aircraft and specimens were collected from Coalseam Cliffs by V.E. Fuchs on 22 January and by P.J. Stephenson on 18 November 1957. Much of the area south-west of Lenton Bluff was photographed

from the air during these and other early exploratory flights and a map of the area was compiled and published in 1963 by the Directorate of Overseas Surveys.

Stephenson (1960, 1966) published brief accounts of the geomorphology and geology of the mountains, including a brief discussion of the petrology and geochemistry of dolerite intrusions from the Theron Mountains and Whichaway Nunataks. Blundell (Blundell and Stephenson, 1959; Stephenson, 1966) investigated the palaeomagnetism of dolerite samples from the Theron Mountains and Whichaway Nunataks. Coal samples were examined by Brown and Taylor (1960) and Plumstead (1962) reported on the plant fossils. Rex (1971) has reported K-Ar age determinations on dolerite specimens collected by the author.

During the present study, glaciological and biological observations were also made and these aspects of the field work have been discussed by Wornham (1969), Lindsay and Brook (1971) and Brook and Beck (in press).

In December and January 1967-68, the U.S. Navy squadron VX6 completed trimetrogon air photography of the entire mountain range.

C. SCOPE OF THE PRESENT STUDY

The field work was carried out between November 1966 and December 1967 from the British Antarctic Survey station at Halley Bay (lat. 75°30'S., long. 26°42'W.).

In the southern summer of 1966-67, the author mapped the whole area of the mountains and was assisted by the geomorphological observations of A. Johnston, D.K. McKerrow and C.M. Wornham. Transport was by dog sledge and the field work was supported by depots laid by a tractor party. Parts of the area between Mount Faraway and Goldsmith Glacier were re-visited in the early part of the following summer season but time was limited by the necessity of reconnoitring an overland route to the Shackleton Range. During this period C.M. Wornham completed the glaciological studies begun in the previous season.

Because of the general steepness of slopes in the Theron Mountains, reconnaissance geological mapping has been done primarily by means of vertical sections of individual cliffs (Figs. 4 and 5). A map of the Theron Mountains at a scale of 1 : 40,000 has been compiled by A. Johnston, but even at this scale standard horizontal mapping is hardly feasible. Johnston also drew the original map on which Figs. 2, 3 and 4 are based.

Physiographical and geomorphological observations based on the work of Johnston, McKerrow, Wornham and the author are discussed in detail. A detailed stratigraphical succession in the sediments is difficult to establish for various reasons and many of the dolerite intrusions are only of local extent but, where possible, correlations are made. Studies of the palaeobotanical material and the palaeomagnetism of dolerite samples collected by the author will be made in due course.

Detailed petrographical studies of the dolerite intrusions are compared with those of other Southern Hemisphere dolerites. Chemical analyses of 95 specimens of dolerite have been completed by X-ray fluorescence techniques. Because of the radical differences in the chemistry of the dolerites of the Theron Mountains and other Jurassic dolerites of Antarctica, the geochemical study has been extended to include published analyses of Jurassic dolerites from Dronning Maud Land (20 analyses), Ferrar dolerites from Antarctica (148 analyses), Jurassic dolerites from Tasmania (110 analyses), and Karroo dolerites (154 analyses) and basalts (70 analyses) from South Africa.

CHAPTER II

PHYSIOGRAPHY AND GLACIAL GEOMORPHOLOGY

A. PHYSIOGRAPHY

Forming the southern margin of a lobe of the Filchner Ice Shelf, the main feature of the Theron Mountains is the steep north-east-facing scarp (Frontispiece) considered by Stephenson (1966) as a fault scarp on the basis of its linearity and constant trend. The presence of a similar, south-west-facing, crevassed ice scarp parallel to the range and about 50 km. to the north-west suggests the possibility that the mountains form the southern edge of a graben occupied by a major ice stream (here called "Main Glacier") flowing south-westwards into the Filchner Ice Shelf.

No direct evidenc of major faulting was found and little can be inferred of tectonic events since the end of the Jurassic. The Theron Mountains could have been uplifted prior to the last glaciation of Antarctica and the present landforms may have been created under quite different conditions and only modified subsequently by the action of ice.

The frontal scarp of the mountains is formed by four main cliffs separated by three narrow glaciers flowing approximately in a northerly direction. North-east of Goldsmith Glacier, the escarpment is continuous, although rock outcrops are sparse until the long cliff immediately north-east of the mouth of the glacier. Between Goldsmith and Jeffries Glaciers the scarp consists of an ice cliff at about 600 m., which is breached by occasional rock outcrops, and the prominent cliff of Lenton Bluff, which rises to over 950 m. at station Z.499; at this point it is about 580 m. above the surface of "Main Glacier". South-west of Jeffries Glacier the scarp front swings round smoothly from Marø Cliffs to form the eastern margin of the unnamed southern glacier. South-west of the unnamed southern glacier, the escarpment is continuous for a further 50 km. as Coalseam Cliffs and the ice cliffs (with occasional windows of dolerite), which decrease in height south-westwards before being swamped by the outflow of Slessor Glacier south-west of Parry Point.

The main physiographical features of the frontal scarp are caused by the differential resistance to erosion of the sediments and dolerite, the thicker dolerite sills forming near-vertical cliffs between which buttresses of sediments and thin sills with a cliff-and-ledge topography

are separated by extensive talus slopes (Fig. 6). Thin dykes also intrude the sediments and these may form wall-like projections up to 6 m. high (Fig. 7).

The frontal scarp of the mountains is backed by a broad undulating ice plateau, virtually devoid of rock outcrops, which descends to the south, gently at first and and then more steeply, culminating in the ice-cliff margin of Slessor Glacier. The only major rock outcrops south-east of the scarp front are alongside the three tributaries of "Main Glacier", Goldsmith, Jeffries and the unnamed southern glacier; these glaciers arise indefinitely from the ice plateau but they are well defined in their lower reaches and they are bounded by rock and ice cliffs (Figs. 8 and 9) separated by short, steep tributary glaciers.

B. WEATHERING AND EROSION

The main detailed features of the landscape are caused by frost action but other erosive agents are locally important.

The mean annual temperature in the Theron Mountains is about -22 to -26°C. and the mean of over 200 temperature measurements taken at various locations and at various times of day by A. Johnston and M.M. Samuel between

Fig. 6. Stewart Buttress and part of Coalseam Cliffs, viewed from the north-west, showing the three main cliff-forming sills (basal, middle and upper sills) separated by gentler slopes on the sediments.

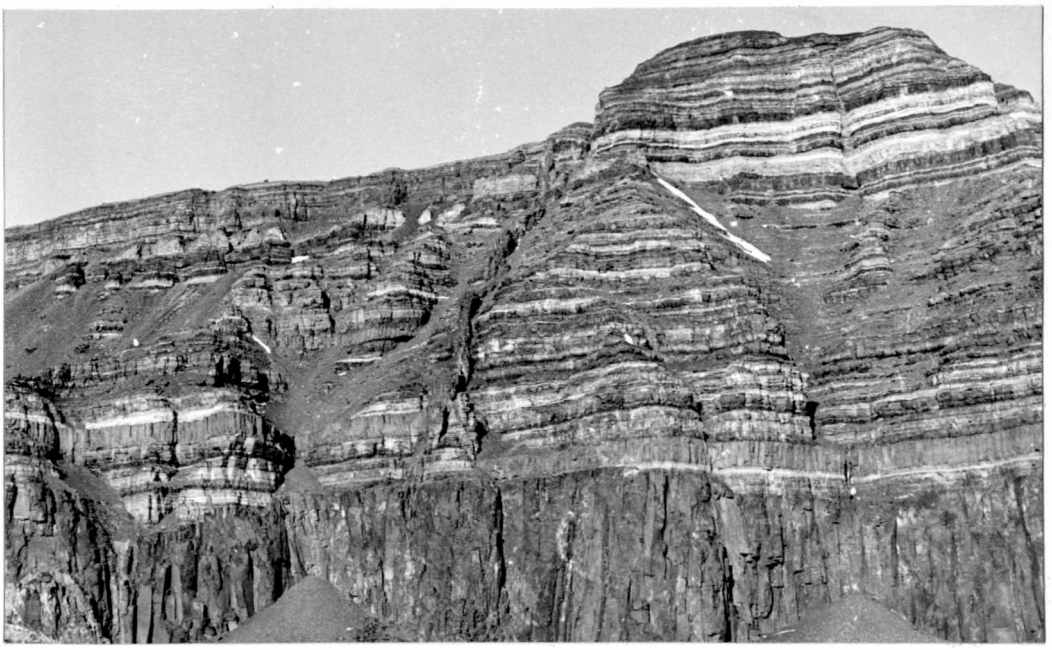

Fig. 7. Part of the south-western end of Lenton Bluff (Z.472 and 498), viewed from the north. The complex system of younger dykes form wall-like projections from the intruded sediments; the cliff-forming basal sill is succeeded by a cliff-and-ledge topography in the sediments and thin sills above it.

Fig. 8. View from about 8 km. north-west of the scarp front of Jeffries Glacier showing the distinct but interrupted scarp on its eastern margin.

Fig. 9. View from the same position as Fig. 8 of Marø Cliffs north-east of the central ice fall and the small cirque on the western margin of Jeffries Glacier.

November 1966 and February 1967 is -9.3°C. In the immediate environment of rock outcrops, however, air temperatures during the summer months rise sufficiently to cause melt during the day. Fracturing is common when water thus produced freezes in cracks due to falling temperatures at night and loud reports of the falling of blocks of rock and ice were often heard near rock outcrops. Fractured material falls from cliff faces, resulting in fresh joint-block faces with extensive screes and angular blocky weathering, particularly of dolerite sills. Frost-shattered material remains in situ on gentler slopes, resulting in large areas of felsenmeere and spheroidal weathering of dolerite.

Although the erosive power of wind carrying ice particles is significant at low temperatures and sand-blasting can be very effective near the surface in an arid area, the rocks of the Theron Mountains show little evidence of wind erosion. Wind erosion on snow, however, is extremely effective and sastrugi, windscoops, snow dunes and blue ice areas are common, especially on and alongside "Main Glacier", where air flow is channelled parallel to the scarp.

During the summer months there is considerable melt and small streams, which are effective to some extent in transporting and eroding material, are common. Although the streams were not generally highly charged with debris,

mud slurries were occasionally seen on Coalseam Cliffs. Small gullies on moraines and felsenmeere are probably attributable to melt streams, possibly accentuated by nivation.

In an arid, frigid climate, such as that of Antarctica, chemical weathering is restricted but it is not ineffective. Exfoliated, spheroidal boulders of dolerite, for example, may have weathered crusts up to several millimetres thick. Cavernous weathering (cf. Van Autenboer, 1964; Juckes, 1969b) was not observed.

No evidence of chemical precipitation, such as that of gypsum (Van Autenboer, 1964; Stephenson, 1966) or calcite (Juckes, in press) was seen in the Theron Mountains. The only encrustations observed are of organic origin, associated with bird colonies, but they are not as well developed as those in Heimefrontfjella (Ardus, 1964).

C. GLACIERS

The main flow of ice is from the polar plateau in the north-east towards the Filchner Ice Shelf and it is channelled in two large ice streams on either side of the Theron Mountains. Within the mountain range itself ice flow is dominantly towards these two ice streams, either over the scarp or channelled in tributary glaciers.

1. Major ice streams

Slessor Glacier, to the south of the Theron Mountains, was not examined in detail but it appears to be a rapidly moving ice stream of large dimensions, over 60 km. wide and 160 km. or more in length. It is bounded on both sides by ice cliffs and extensive areas of crevassing.

"Main Glacier" is about 50 km. wide and over 100 km. long and it flows south-westwards parallel to the escarpment of the Theron Mountains. It descends from over 600 m. near Tailend Nunatak to under 200 m., merging imperceptibly with the Filchner Ice Shelf somewhere south-west of Mount Faraway. Major crevasse belts, ice-movement vectors and blue-ice areas have been shown by Wornham (1969, fig. 1).

2. Tributaries of "Main Glacier"

Flowing north-westwards for 25-30 km., Goldsmith Glacier descends from the plateau at about 1,050 m. to "Main Glacier" at about 530 m. It is 5-7 km. wide and there are well defined crevassed zones at the margins. It is fed by small tributary glaciers from the north-east and south-west. Ice-movement vectors have been given by Wornham (1969).

Jeffries Glacier is 4-5 km. wide and flows north-north-westwards for over 20 km., descending from over 1,050 m. to about 370 m. Small tributary glaciers descend from the plateau and, on its south-western side, small cirques near the mouth of the glacier (Fig. 9) are partly fed by ice from the plateau above. Ice-movement vectors have been given by Wornham (1969). A prominent ice tongue with pressure ridges extends for over 1.5 km. into "Main Glacier". The crests and northern sides of pressure ridges are formed of blue ice; this could have been formed either by ablation (Wornham, 1969) or by horizontal compression under flow (Crary and Wilson, 1961).

Flowing north-north-westwards, the unnamed southern glacier is about 4 km. wide and 13 km. long. It descends from over 840 m. to under 300 m. An ice tongue, marked by blue ice, extends from the foot of the ice fall halfway down. The main source area is to the south and east, for the catchment area on Mount Faraway is of limited extent. On its eastern side, three prominent tributary glaciers, all less than 5 km. long and 1.5-2.0 km. wide, meet the glacier in ice falls; these are followed downstream by progressive waves of blue ice probably formed in the manner described by Crary and Wilson (1961). Ice-movement vectors have been given by Wornham (1969).

3. Minor glacial features

Although ice flows over the scarp in many places and the smooth profiles of other parts strongly suggest bevelling by ice, no indications of striations were seen. The ice has probably retreated since the last glaciation but the absence of trim lines noted by Wornham (1969) and the presence of extensive felsenmeere, which would have destroyed any original striations, does not indicate very recent retreat. There is no evidence of multiple glaciation such as that described from Victoria Land (Pewe, 1960; Bull and others, 1962).

The snow slope which breaches the middle sill of Coalseam Cliffs beneath Mount Faraway, and other snow-filled depressions on cliff faces, are similar to the type III niche glaciers described by Groom (1959).

D. MORAINES AND MELT POOLS

Moraines and melt pools are common along the margins of "Main Glacier" and in the lower reaches of the three tributary glaciers but they are absent from the plateau area of the Theron Mountains.

1. Moraines

Lateral moraines, consisting either of debris ridges or of isolated boulders on the crest of a small snow ridge, extend parallel to the scarp for several hundred metres from the foot of talus slopes (Fig. 10). Moraine ridges vary in height from <1 m. to about 10 m. and inter-moraine depressions may be snow-covered or infilled by melt pools.

The grain-size of morainic material varies from sand and silt to boulders a few metres across. Though its composition is variable, there is no material which could not have been locally derived.

Englacial moraine was seen in isolated areas in crevasses in "Main Glacier" and Jeffries Glacier.

2. Melt pools

Melt pools of varying size occur among the moraines (Fig. 10). Even in high summer, their surface is usually ice-covered but where rock debris forms the shore of the pool, there may be an ice-free zone at the margin. They are up to 4 m. deep and they are connected by streams of varying size which flow on a surface of ice, often fluted, or moraine.

Fig. 10. Moraine ridge which disappears beneath the snow surface at the south-western end of Lenton Bluff (Z.471). At the foot of the scree, in the foreground, is a melt pool with ice mounds; the melt pool merges almost imperceptibly with the ablation blue ice between it and the moraine.

Circular to elliptical ice mounds similar to those in the Sør-Rondane (Van Autenboer, 1962) and the Shackleton Range (Stephenson, 1966) occur on many pools (Fig. 10). They vary in size but are generally 2-10 m. in diameter and 0.2-1.5 m. in height. Crevasses radiating from the centre of the mounds pinch out at the margins. The ice in the mounds is white with numerous air bubbles, quite distinct from the bluer ice of the pools, but no cellular structure (Cailleux, 1962) was observed. They are considered to be expansion mounds caused by freezing water at depth.

In the blue-ice area north-west of Marø Cliffs, cryoconite holes (cf. Crohn, 1959; Van Autenboer, 1962) are common. They are typically circular patches of darker blue ice in the surrounding blue ice which is richer in air bubbles. They may have a small amount of water resting on and around the debris to which they are due.

E. PATTERNED GROUND

Patterned ground is common throughout the Theron Mountains on the tops of cliffs but none was observed in front of the cliffs, on scree or moraine. This is probably due to instability because of their rapid rate of transport but the difference in altitude and consequently in micro-climate may be significant.

Occurrences of patterned ground in the Theron Mountains are sorted polygons, nets and stripes (Washburn, 1956) and they are similar to the sorted circles described by Juckes (in press) except that they usually occur as a network and not singly. Patterned ground is more abundant and more noticeable on mantle formed of fissile sandstone and siltstone but it is also present on mantle formed of dolerite.

Stephenson (1961; 1966) has recorded instances of "fossil" patterned ground in the Shackleton Range, 130 km. to the south. These are on a relatively large scale compared to most occurrences in the Theron Mountains, where areas of suitable gradient for patterned ground formation are less extensive. The occurrences in the Shackleton Range are of non-sorted polygons and stripes and only the stripes of station Z.510, which seem to disappear beneath the snow cover and to be perfectly formed at the snow margin, are likely to be of similar form.

Melt-water gullies similar to those described from Heimefrontfjella by Worsfold (1967) are present in some of the screes and moraines and in a small dry valley on top of Lenton Bluff. Their somewhat erratic pattern and consequent lack of symmetry excludes them from Washburn's (1956) definition of patterned ground.

F. SUMMARY

The main physiographical feature of the Theron Mountains is the undulating snow-covered plateau area with isolated nunataks, which terminates abruptly to the north-west in the scarp of the Theron Mountains and to the south in the ice-cliff margin of Slessor Glacier. Local physiographical features are controlled largely by differential resistance to erosion of the sediments and dolerite and by slope and aspect. Frost action is the dominant erosive agent but wind, water and chemical weathering are locally significant.

The main glacial activity is restricted to "Main Glacier" and its three tributaries. Cirque and niche glaciers are also present. Moraines are locally derived and they are restricted to "Main Glacier" and the lower reaches of its tributaries. Melt pools, often with expansion mounds on them, are similarly restricted. There is little evidence of recent glacial retreat and none of multiple glaciation.

Patterned ground is restricted to cliff tops but it is present throughout the mountain range. One possible example of "fossil" patterned ground was seen.

CHAPTER III

STRATIGRAPHY

The stratigraphy of the Theron Mountains is summarized in Table I, and Figs 4, 5 and 3 illustrate the geology of the area and the stations visited. This area is unusual in eastern Antarctica in that no Basement Complex is exposed within more than 150 km., and the stratigraphy is therefore relatively simple.

1. Lower Permian sediments

The age of the sedimentary rocks of the Theron Mountains has been established by Plumstead (1962) as probably not younger than Lower Permian on the basis of the glossopterid flora collected by the Trans-Antarctic Expedition.

Correlation of the sediments between individual rock outcrops is rendered difficult by lateral variation in the sediments, the lack of unmistakable marker horizons and the variation in horizon, thickness and altitude of the dolerite sills and by minor local faulting.

Stephenson (1966) suggested that the sequence can be divided by a sedimentary "break" near the middle of the succession at Mount Faraway; this was not seen north-

TABLE I

SUMMARY OF THE STRATIGRAPHY, METAMORPHISM AND TECTONIC HISTORY OF THE THERON MOUNTAINS, ANTARCTICA

Age	Rock types	Metamorphism	Tectonics
Recent			Erosion
?			? Faulting
Jurassic	Dolerite sills and dykes	Thermal metamorphism of sediments	Minor tilting and faulting associated with intrusion
Lower Permian	Victoria Group sediments, including coals (continental)		Sedimentation with some penecontemporaneous erosion

east of Coalseam Cliffs, where the same stratigraphical horizon would appear to be present. Possibly the hiatus is only of local significance in the Coalseam Cliffs area. Stephenson (1966) suggested it is not of great significance and Plumstead's (1962) identification of Phyllotheca in the sediments above the depositional break tends to support this suggestion.

The term Theron Formation was proposed by Stephenson (1966) to include all the sedimentary rocks of the Theron Mountains. The term is not used here because it is not considered to be in accordance with accepted codes of stratigraphical nomenclature. A formation is defined by the American Commission on Stratigraphic Nomenclature (1961) as a body of rock characterized by lithological homogeneity, prevailingly but not necessarily tabloid, and mappable at the Earth's surface and traceable in the sub-surface. It is not sufficient, therefore, to apply a geographical name to a sequence of sedimentary rocks in which no type section has been established, of which no boundaries have been defined and whose dimensions and shape are unknown. Since neither the base nor the top of the sedimentary sequence is exposed in the Theron Mountains, it cannot be defined as a formation and it is only a mappable unit in that it is distinct from the Jurassic dolerite intrusions; these form part of a

different group and they are not a different formation within the same group. The lithological characteristics of the Lower Permian sediments are variable but they are not sufficiently distinct from other Lower Permian sediments of eastern Antarctica to warrant classification as a separate formation, except possibly by nature of their geographical isolation. Although no units of formational significance within the sedimentary sequence were recognized by the author, more detailed study may show their existence. If this is so, the whole sequence cannot be referred to as a single formation.

Continental sediments of Devonian to Jurassic age are widespread in eastern Antarctica and they have been referred to the Beacon Group (Grindley and Warren, 1964). Barrett and others (1971) re-defined the Beacon Supergroup as a largely flat-lying non-marine sequence from Devonian or older to Jurassic in age, which rests unconformably on a Precambrian and Lower Palaeozoic basement and is intruded and overlain by Jurassic basaltic rocks. They divided the Beacon Supergroup into the Taylor Group, a quartzose sandstone succession of Devonian or older age, and the Victoria Group, a heterogeneous sequence of glacial beds, carbonaceous and non-carbonaceous alluvial-plain sediments and volcaniclastic strata of Permo-Carboniferous to Jurassic age. The sediments of the

Theron Mountains are equivalent to parts of the Victoria Group.

Correlation with beds of Lower Gondwana age in other southern continents is confirmed by Plumstead's (1962) palaeobotanical work.

2. Jurassic dolerite intrusions

The Lower Permian sediments are intruded by numerous sills and dykes of Jurassic age (Rex, 1971) but no extrusive equivalents are present within the mountain range, though basaltic flows occur in nearby Dronning Maud Land (Juckes, in press; Aucamp and others, 1971). Although different phases of intrusion are present, these are not separable on the basis of whole-rock K-Ar age determinations, all of which lie in the range 154-169 m. yr. (Rex, 1971).

The term Faraway dolerites was proposed by Stephenson (1966) to include all the Jurassic dolerite intrusions of the Theron Mountains. This term is not used here for the same reason that the term Theron Formation has been abandoned in that it does not conform to accepted stratigraphical nomenclature. Some of the dolerite intrusions of the Theron Mountains are radically different, petrographically and chemically, from other Jurassic dolerite intrusions of eastern Antarctica; others, however,

cannot be distinguished by mineralogical, textural or chemical characteristics. The almost complete gradation between these end-members eliminates the possibility of subdividing the dolerite intrusions into different formations and the variation in characteristics renders impracticable the use of a single formational name. They are, therefore, referred to simply as the Jurassic dolerite intrusions of the Theron Mountains.

Jurassic dolerites co-extensive with sediments of the Beacon Supergroup are widespread in eastern Antarctica and they have been referred to the Ferrar dolerites by Harrington (1958). Grindley (1963) re-defined the Ferrar Group to include the Ferrar dolerites and their extrusive equivalents, the Kirkpatrick basalts.

Correlation with other southern continents is shown in Fig. 11.

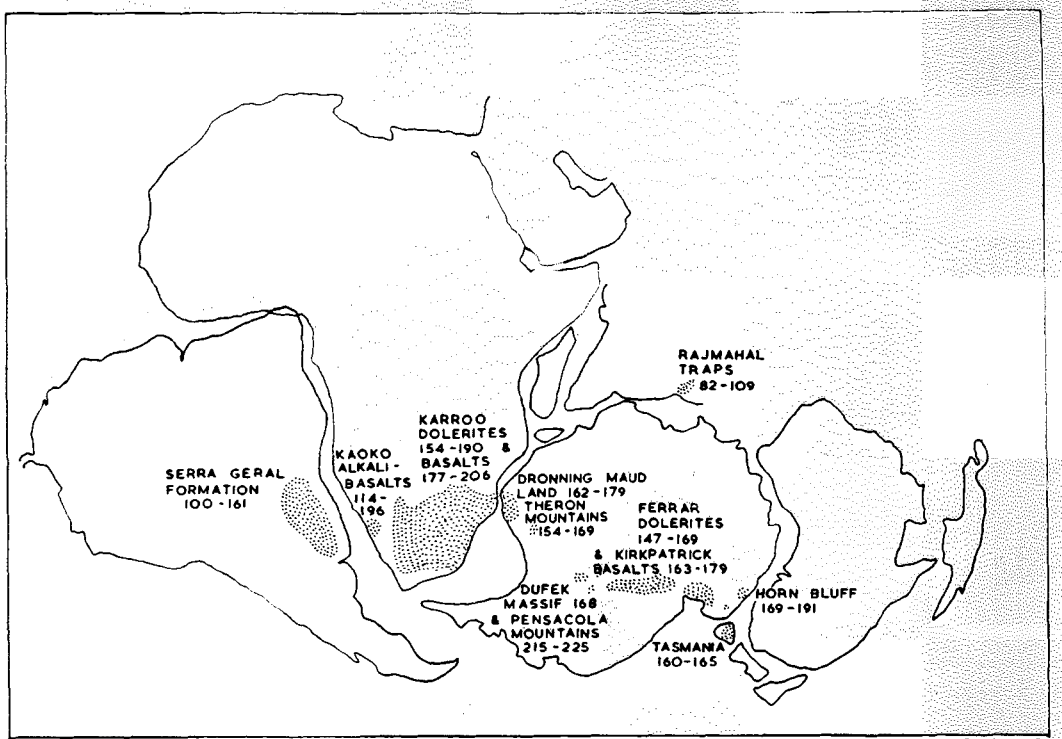

FIG. 11. RECONSTRUCTION OF GONDWANALAND (After SMITH & HALLAM, 1970) SHOWING LOCATION AND RADIOMETRIC AGES (M.YR.) OF SOME MESOZOIC BASALTIC ROCKS

SOURCES:

THERON MOUNTAINS	–	REX, 1971
DRONNING MAUD LAND	–	REX, 1967; 1971
FERRAR DOLERITES	–	McDOUGALL, 1963; COMPSTON & OTHERS, 1968
KIRKPATRICK BASALTS	–	ELLIOT, 1971a
DUFEK MASSIF	–	FORD, 1971
PENSACOLA MOUNTAINS	–	FORD, 1971
HORN BLUFF	–	PICCIOTTO & COPPEZ, 1962
TASMANIA	–	McDOUGALL, 1961
RAJMAHAL TRAPS	–	McDOUGALL & McELHINNY, 1970
KARROO DOLERITES	–	McDOUGALL, 1963
KARROO BASALTS	–	MANTON, 1968
KAOKO ALKALI-BASALTS	–	SIEDNER & MILLER, 1968
SERRA GERAL FORMATION	–	CREER & OTHERS, 1965; AMARAL & OTHERS, 1966; McDOUGALL & RÜEGG, 1966; VANDOROS & OTHERS, 1966; MELFI, 1967

CHAPTER IV

LOWER PERMIAN SEDIMENTS

A. DISTRIBUTION AND FIELD RELATIONS

Most of the outcrops of the Theron Mountains consist of sub-horizontal sediments intruded by dolerite sills and dykes but the relative thicknesses of the sedimentary sequence and dolerite intrusions are variable. The majority of sedimentary exposures are in the cliffs of the scarp front (Figs. 4 and 5) and alongside the tributaries of "Main Glacier". On the tops of the cliffs and on the few outcrops south-east of the scarp front, exposures are poor, being largely mantled by scree in the small ice-free areas that there are.

North-east of Goldsmith Glacier, sediments are sparsely distributed and only appear in the outcrops immediately north-east of the glacier. They occur above the 200 m. thick dolerite sill which is present throughout most of the mountain range from Tailend Nunatak to Coalseam Cliffs.

The scarp front between Goldsmith Glacier and the unnamed southern glacier is capped for much of its length by a 200 m. thick sill (here called the scarp-capping

sill), below which are exposed varying thicknesses of sediments intruded by other dolerite sills. The small outcrops north-east of Lenton Bluff have only 100-120 m. of sediments but Lenton Bluff has over 200 m. of sediments intruded by a 30 m. sill near the base of the sequence and by a number of minor sills and dykes between this and the scarp-capping sill. Marø Cliffs have a similar thickness of rocks below the scarp-capping sill but dolerite sills are thicker and more numerous, forming about half the sequence.

Above the scarp-capping sill on the scarp front between Goldsmith Glacier and the unnamed southern glacier, sediments are present only at the summit of Lenton Bluff (station Z.499) and at two or three places on top of Marø Cliffs (Z.451 and 452).

South-east of the scarp front between Goldsmith Glacier and the unnamed southern glacier, sediments are exposed below the scarp-capping sill only in the cliffs on the south-west side of Jeffries Glacier (Z.497 and 504) and at the base of the cliffs beneath point 3300 (Z.480). Most outcrops south-east of the scarp front have a thin sequence of sediments above the scarp-capping sill, the maximum thickness exposed being about 120-150 m. in the outcrops on the eastern flank of the unnamed southern glacier (Z.453, 454 and 493).

South-west of the unnamed southern glacier, the thickest sedimentary sequence in the Theron Mountains is in Coalseam Cliffs; over 900 m. of sediments and dolerites are exposed, of which about 200-250 m. consists of dolerite sills varying in individual thickness from <1 to about 60 m. About halfway up the sequence is the sedimentary "break" described by Stephenson (1966). This "break" cannot be traced for any distance along the cliffs north-east of Stewart Buttress or south-west of Mount Faraway and it is not seen in beds at approximately the same altitude on point 2600. It is considered to represent a hiatus of only local significance in the immediate area of Coalseam Cliffs; its absence elsewhere may alternatively be due to this horizon not being represented north-east of Stewart Buttress because of the disruption caused by dolerite intrusion.

No sediments are exposed south-west of Coalseam Cliffs.

B. LITHOLOGY

Most of the outcrops show only a part of the succession, the thickness and horizon exposed being variable. The most complete sequence is at Mount Faraway and Stewart

Buttress, where the total thickness of dolerite and sediments is in excess of 900 m. Nowhere in the Theron Mountains is either the top or the base of the succession exposed. No units of formational significance have been recognized within the sediments. Any hiates present are of only local significance.

The succession in individual exposures appears relatively simple to determine because of the different weathering colours when viewed from a distance. Closer approach, however, shows this simplicity to be only apparent, the colour of weathered faces often varying independently of lithology. Lithological variations in the sediments, both lateral and vertical, take place only gradually in most instances, increasing the difficulty of correlation between individual outcrops. No distinctive lithological units on which correlation can definitely be based have been observed; some units can be traced for a certain distance but the effects of variation in horizon, frequency and thickness of dolerite sills render them impracticable as marker bands. Minor local faulting and intrusion-faulting, observed or not, also hinder correlation.

1. Area north-east of Goldsmith Glacier

Sedimentary exposures north-east of Goldsmith Glacier are poor and only a thin sequence is seen in the long cliff north-east of the mouth of the glacier (Z.467

and 487) and in the outcrops on its north-eastern margin (Z.463, 465, 466 and 509). A composite section from these geological stations, with very approximate thicknesses, is given below.

Station No.	Lithology	Approx. thickness (m.)
Z.463	Dark greenish grey, fine-grained calcareous sandstone, yellow-brown-weathering medium-grained sandstones	10
	Snow-covered gap between outcrops	150
Z.465	Yellow and reddish brown-weathering, flaky fine-grained sandstones and sandy mud-stones, some dark grey to black shales with fragmental plant remains	20
	Dolerite sill	6
	Snow-covered gap between outcrops	20
Z.487	Alternations of dark shales and silt-stones and light grey siltstone and sandstones	15
	Slight local disconformity	
	Light grey laminated siltstones and fine-grained sandstones, darker grey mudstones with plant fragments and thin coals	20
	Dolerite sill	30
	Alternations of light grey to buff silt-stones and fine-grained sandstones with thin dark shales; some thin beds appear to wedge out laterally	20
	Dolerite sill	200

The sediments above the 30 m. thick sill at station Z.487 (Fig. 12) commonly show cross lamination, and slump bedding and slump balls are a feature of some horizons. Lensoid beds of soft, friable, white-weathering, fine-grained

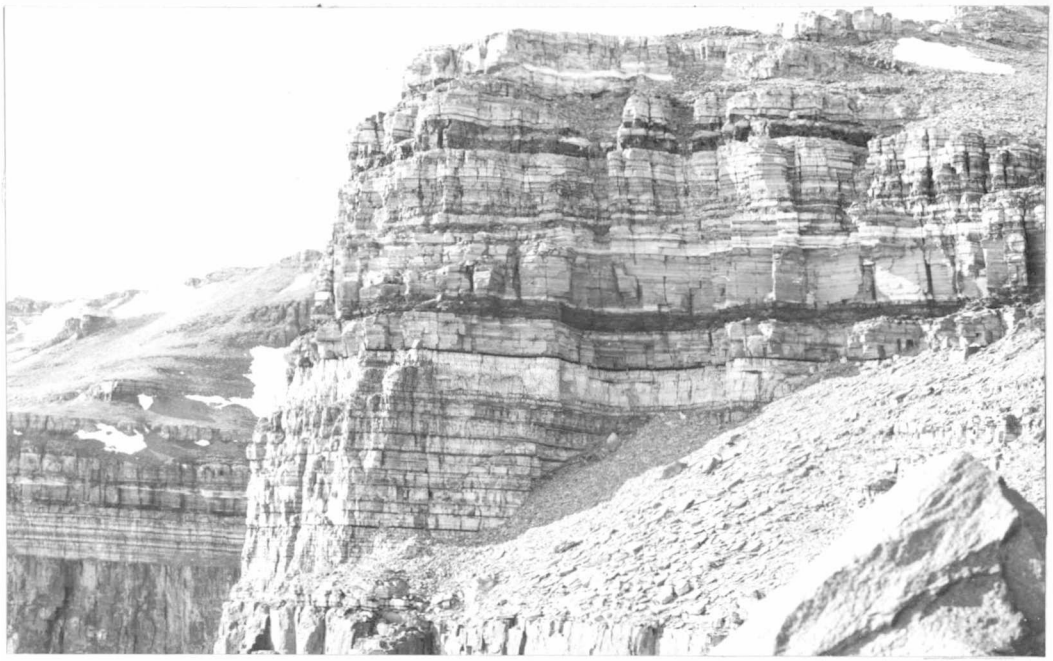

Fig. 12. Photograph of part of the sequence of sediments exposed above the upper (30 m.) sill at station Z.487. The black shaly mudstone in the middle of the sequence is about 1 m. thick.

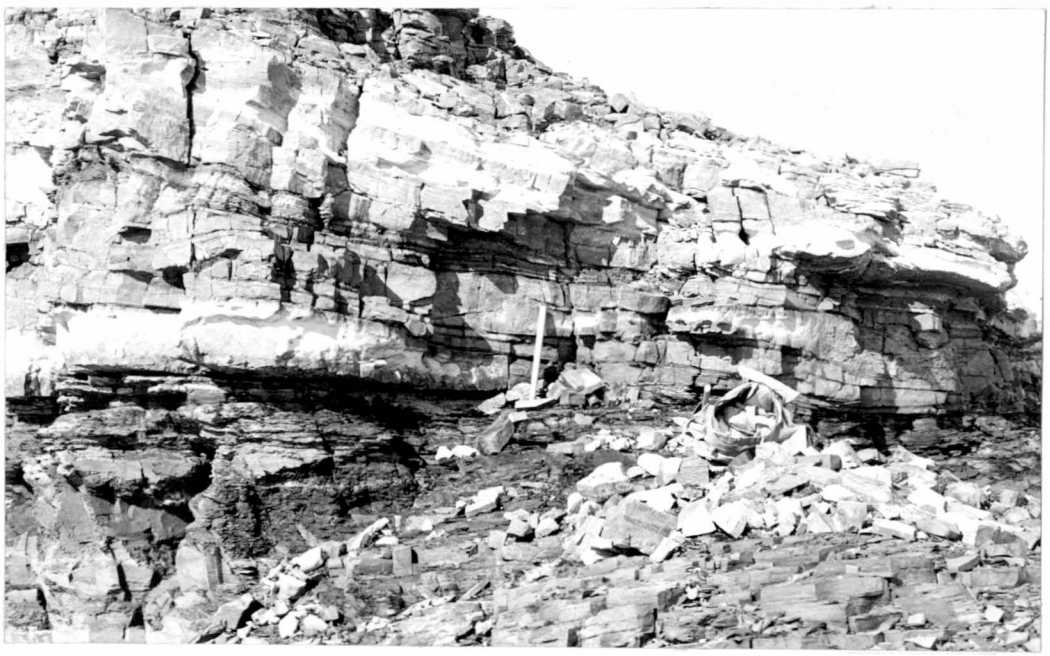

Fig. 13. Slight local disconformity, overlain by mud-flake breccia and coarse arkosic sandstone, about 15-20 m. below the summit of station Z.487. The sandstones above the disconformity are very irregularly bedded and impersistent; the hammer shaft is about 55 cm. long.

calcareous sandstones are also present. The interbedded mudstones are black and shaly with abundant plant fragments and thin coal streaks, often only millimetres in thickness.

The slight disconformity at station Z.487 (Fig.13) is only of local significance. It overlies dark grey to black shale and mudstone containing plants and the base of the beds above is very slightly transgressive. Above the disconformity, dark grey medium-grained sandstones with black mudstone fragments form, in places, a mud-flake breccia; lenses of light yellow-grey, slightly calcareous arkosic sandstone and friable, light grey, faintly laminated arkosic sandstones are intercalated. These are overlain by medium to dark grey, laminated medium-grained sandstones with occasional light grey mudstone pellets. The disconformity may have been caused by a slight local increase in erosion due to migration of a stream channel.

Muddy siltstones at station Z.465 show small-scale faulting which is probably contemporaneous with sedimentation; normal faults dipping north-eastwards at 30-60^{o} have an easterly downthrow of 5-15 cm. They are of localized effect and are probably caused by slight movements during deposition of the siltstones, though they could be the result of stresses set up during intrusion

of the dolerites. The sandy mudstones here contain bands and nodules of calcareous mudstone which may be concretionary in origin.

2. Area between Goldsmith and Jeffries Glaciers

The scarp front between Goldsmith and Jeffries Glaciers is capped by the scarp-capping sill; only at station Z.499 do sediments occur above it. South-east of the scarp front, however, a total thickness of about 50 m. of sediments, intruded by thin dolerite sills, is exposed above the scarp-capping sill. Up to 100 m. of sediments are exposed beneath the scarp-capping sill between Goldsmith Glacier and Lenton Bluff and almost 200 m. of sediments are present in Lenton Bluff. A composite section with very approximate thicknesses is given below.

Station No.	Lithology	Approx. thickness (m.)
Z.459	Light grey to white, yellow and some reddish, medium-grained sandstones and thinly bedded, light grey to black mudstones and shales	10
Z.460	Dolerite sill	<10
	Light grey to yellow, medium-grained sandstones	10
	Dark grey, iron-stained shaly mudstones with thin flaky sandstones	5
Z.461	Dolerite sill	<5
	Interbedded yellow to red sandy mudstones and dark shales	10
	Dolerite sill	5
Z.488	Buff-weathering fine-grained sandstones and sandy mudstones, some dark shales with poorly preserved plant material	10
	Dolerite sill (scarp-capping sill)	200
Z.507, 498	Interbedded light grey laminated siltstones and dark grey shales and mudstones with thin coals	20-30
Z.507, 499	Massive, thickly bedded, light grey to buff, fine- to medium-grained sandstones with interbedded coal and black mudstones	50
Z.499, 498	Alternating thinly bedded laminated siltstones and shales, thin dolerite sills (up to 5 m. thick)	80
Z.471, 492, 198	Light grey to buff fine-grained sandstones and siltstones	20
	Laminated siltstones with thin dark shales	15
	Dolerite sill (Basal sill of Lenton Bluff)	30
Z.471, 472	Alternations of light and dark grey laminated siltstones, dark grey to black shales and mudstones and occasional buff, fine-grained feldspathic and quartzitic sandstones	20

Beneath the basal sill of Lenton Bluff (Z.471), carbonaceous paper shales and plant-rich mudstones are present. Many of the sandstones have irregular laminae and lenticular interbeds of darker finer-grained material and some of the non-laminated siltstones and mudstones contain slump balls of laminated siltstone and fine-grained sandstone.

Between the basal sill of Lenton Bluff and the scarp-capping sill, siltstones are almost invariably laminated due to the presence of carbonaceous and micaceous material and cross lamination on a small scale is a common feature. Ripple-marking is fairly frequent at the tops of fine-grained sandstones interbedded with siltstones and shales (Fig. 14). The ripple marks are usually oscillation ripples with orientation varying between individual beds; though possible interference ripples were seen in some of the scree material, none were seen in situ. Occasional soft and friable calcareous sandstone beds often rest on an irregular surface of irregularly laminated siltstone or fine-grained sandstone. Scour-and-fill structures and load casts (Fig. 15) are a feature of some horizons. Calcareous and ferruginous mudstone bands and nodules occur within the shales and commonly show deformation of the bedding.

Fig. 14. Ripple marks trending approximately north—south on the surface of a siltstone bed on the top of Lenton Bluff (Z.498); the hammer shaft is about 55 cm. long).

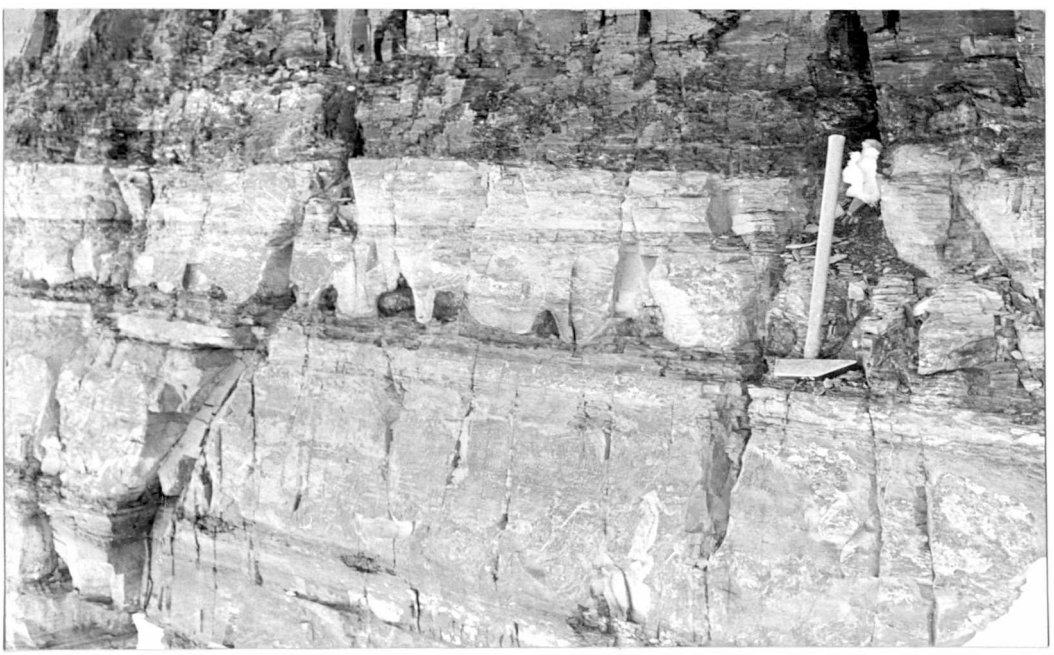

Fig. 15. Load-cast structures at the base of a thin sandstone bed in the middle of the sequence at station Z.507; the hammer shaft is about 55 cm. long.

Some shales and mudstones have interbedded coal streaks, often less than 2 mm. but up to 10 cm. thick; carbonized plant remains are common at some horizons. At least ten coal horizons, up to 1-2 m. thick, are present in the 50 m. sequence of massive sandstones at station Z.499. Individual coal bands, often less than 3 cm. but up to 20 cm. thick, are separated by medium to dark grey mudstone bands (Fig. 16) and they are usually more abundant near the top of mudstone horizons. In these massive sandstones, lenses of yellowish-weathering medium-grained sandstone 2-10 m. in length are common near the top of the sequence, as is slumping of laminated medium-grained sandstones (Fig. 17).

3. Area between Jeffries Glacier and the unnamed southern glacier

Between Jeffries Glacier and the unnamed southern glacier, the top of Marø Cliffs is mainly formed by the scarp-capping sill but thin sedimentary cappings are preserved in places (Z.451 and 452). On the eastern margin of the unnamed southern glacier, 120-150 m. of sediments, intruded by thin sills, occur above the scarp-capping sill in the ridge leading eastwards from point 3300 (Z.453 and 493) and in the outcrop south of point 3300 (Z.454).

Fig. 16. Part of the 1.2 m. thick coal about 3 m. below the scarp-capping sill in the middle of Lenton Bluff (Z.499); 2-3 cm. coal bands are separated by black carbonaceous mudstones; the hammer shaft is about 55 cm. long.

Fig. 17. Slump ball of laminated medium-grained sandstone in more homogeneous fine-grained sandstones and siltstones in the middle of Lenton Bluff (Z.499); about 10 cm. of the hammer head is visible.

Fig. 18. Penecontemporaneous deformation at the base of a calcareous sandstone lens in the middle of the succession in Marø Cliffs (Z.502); the hammer head is about 20 cm. long.

The sequence of sediments and dolerites exposed below the scarp-capping sill in Marø Cliffs and on the south-western margin of Jeffries Glacier has about the same thickness as that at Lenton Bluff but the proportion of dolerite is far greater, amounting in places to over half the total thickness. Sills are more abundant, thicker and more persistent than at Lenton Bluff but they are also much more variable in horizon and this makes correlation, even within the outcrop, and hence detailing of a composite section difficult.

Lithologically, the sediments are similar to those already described from Lenton Bluff (p. 28) and consist largely of alternating light and dark grey siltstones and shales and more massive, light grey to buff, fine- to medium-grained sandstones. Carbonaceous shales and coals are commonly interbedded with laminated siltstones and fine-grained sandstones; most of the coals have been thoroughly thermally metamorphosed by the intrusion of the dolerites. Ripple marks, cross lamination and wedging out of thin beds are common; scour-and-fill structures and load casts are also present. Grey-green calcareous sandstone lenses showing penecontemporaneous deformation (Fig. 18) are present at some horizons. Dendritic mineralization patterns radiating from calcite veins commonly occur on bedding planes.

The upper part of the sequence, above the scarp-capping sill, is apparently less variable and consists almost entirely of light grey and yellow, fine- to medium-grained sandstones with some siltstones near the top. They are generally thinly bedded and hard with a flaky fracture but some are softer and with sand-blast pits to windward (north-east).

4. Area south-west of the unnamed southern glacier

The thickest sequence of sediments in the Theron Mountains is at Coalseam Cliffs, where, beneath Stewart Buttress and Mount Faraway, about 700 m. of sediments are exposed between dolerite sills varying in individual thickness from <1 to about 60 m. This is also the only sequence previously described in part. During the Trans-Antarctic Expedition, the ridge between stations Z.477 and 457 was briefly traversed by Stephenson (1966), who has also described from photographs the sedimentary "break" beneath Stewart Buttress; specimens were collected from the lower part of Coalseam Cliffs near station Z.477 by V.E. Fuchs and these were included in Stephenson's descriptions. Dolerite sills vary in horizon and persistence and are omitted from the composite section, with very approximate thicknesses, given below.

Station No.	Lithology	Approx. thickness (m.)
Z.456, 495	Thinly bedded light grey siltstones and fine-grained sandstones, mainly mantled by scree; occasional dark shale horizons	>40
	Light grey to buff, medium-grained cross-bedded sandstones with thin bands of friable, white arkosic and calcareous sandstone	30
Z.479, 458	Alternating light to dark grey siltstones and fine-grained sandstones, light grey to buff more massive sandstones and dark grey to black shales and mudstones with interbedded coals and fragmental plant remains	120
Z.479	Fine- to medium-grained sandstones showing cross bedding on a megascopic scale	50
	Sedimentary "break"	
Z.479, 494	Alternating light and dark grey siltstones and shales, light grey to buff and dark grey siltstones and fine-grained sandstones, thin coals and coal shales	60
Z.475	Black carbonaceous mudstone and coal	4-5
	Massive, buff arkosic sandstones with thin interbedded siltstones and shales	30
Z.475, 478	Thin alternations of light and dark grey siltstones, buff, feldspathic sandstones, dark grey mudstones and shales, occasional thin coals and coal shales; sandstones thicker but less common in lower part but increase rapidly in frequency near top	60-70
Z.475, 474, 501	Three units of massive buff-weathering sandstones and siltstones with interbedded coals and shales separated by alternations of light grey siltstones and fine-grained sandstones and dark grey shales and mudstones with thin coals	60-70
	Alternating light grey siltstones and sandstones and dark grey shales and mudstones with thin coals; thickness and frequency of sandstones increase upwards	70

Station No.	Lithology	Approx. thickness (m.)
Z.474	Dark shales and mudstones and medium to dark grey mudstones and muddy siltstones, subordinate massive quartzitic sandstones and light grey siltstones	5-10
Z.477, 478, 500, 501	Alternating light to medium grey siltstones and fine-grained sandstones and dark grey shales and mudstones	10

At station Z.477, some of the shales are coaly with fragmental plant matter and one 0.8 m. coal seam occurs immediately beneath the basal sill; it consists of carbonaceous material distributed in black shiny layers a few millimetres thick between medium grey mudstone layers up to 1 cm. thick.

Throughout most of the sequence, well-indurated, quartzitic, arkosic and slightly calcareous sandstones and siltstones are present and they are often laminated; cross lamination is common and irregular and contorted laminations are also present. Slump bedding is a feature of some siltstones interbedded with shales. Calcareous or ferruginous nodules and bands are present at some horizons. Wedging out of thin beds of sandstone and shale is common but such changes are usually gradual and difficult to appreciate.

The massive buff-weathering sandstones of stations Z.475 (Fig. 19) and 501 are alternately thickly and thinly bedded and they often show a faint lamination in the form

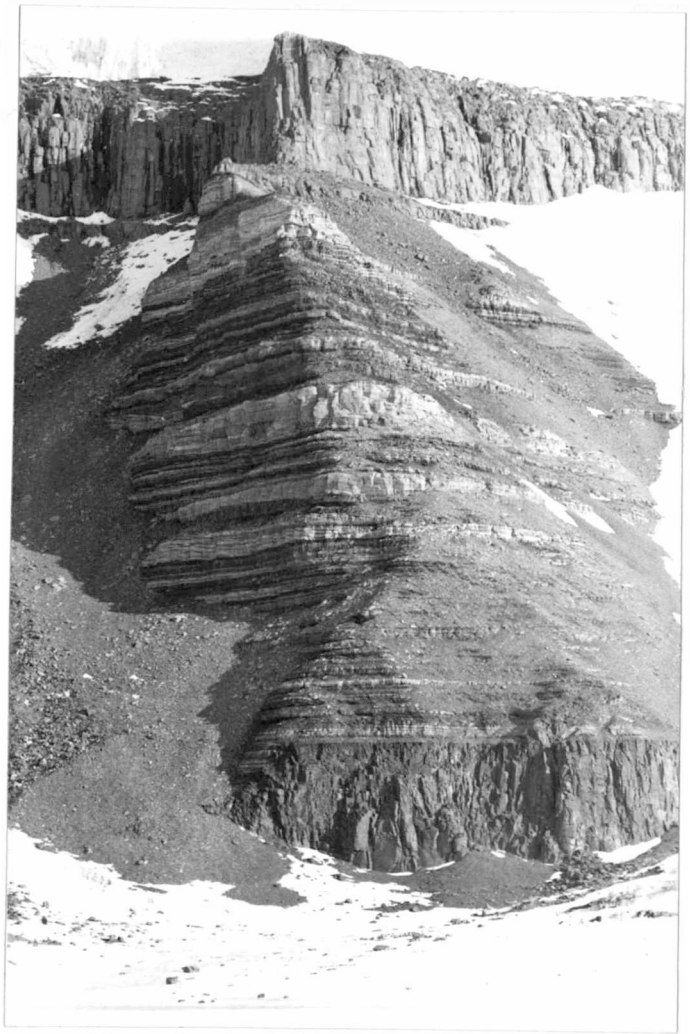

Fig. 19. The sedimentary sequence between the basal and middle sills of Coalseam Cliffs at station Z.475; about 250 m. of sediments occur between the two sills.

of very thin carbonaceous partings. Coals are more abundant in this part of the sequence than elsewhere; at least ten coals or coal shales up to 1 m. thick were observed in the 60 m. sequence of sandstone at station Z.501. The coals are usually underlain and often overlain by dark grey laminated mudstone or black shale, frequently containing plant remains; no evidence of plants growing in situ was seen.

The 4-5 m. thick carbonaceous mudstone and coal at station Z.475 has hexagonal jointing imposed by the dolerite sill immediately above it. About 3 m. of black carbonaceous mudstones with recognizable plant stems and thin interbeds of coaly paper shales are overlain by about 1 m. of coal; the coal is muddy with the proportion of mud decreasing upwards.

The sedimentary "break" beneath Stewart Buttress and Mount Faraway has been described, principally from photographs, by Stephenson (1966). It was visited only at station Z.479 and it is not as pronounced as it appears to be in photographs. The beds above appear to exhibit cross bedding on a megascopic scale before passing upwards into more "normal" sediments at stations Z.479 and 458. The "break" cannot be traced for any great distance north-east of Stewart Buttress or south-west of Mount Faraway and it does not appear in beds at approximately the same altitude on point 2600. It is considered to represent a deltaic

influx or migrating meander channel of only local significance in the immediate area of Coalseam Cliffs. The sediments above the "break" are generally similar to those below it except that carbonaceous beds are apparently less frequent.

5. Summary

The attitude of the sediments in all exposures examined, except over short distances, is very nearly horizontal and there is no evidence of major faulting between individual exposures. It seems likely, therefore, that the sediments exposed throughout the Theron Mountains are equivalent, in whole or in part, to the succession at Coalseam Cliffs. Exact correlation is not possible but the sequences along the scarp front between Goldsmith Glacier and the unnamed southern glacier are probably equivalent to the lower parts of the succession at Coalseam Cliffs. The sequences north-east of Goldsmith Glacier and south-east of the scarp front between Goldsmith Glacier and the unnamed southern glacier are probably equivalent to the middle and/or upper parts of the succession at Coalseam Cliffs. It is not clear whether the horizon of the sedimentary "break" is exposed north-east of Stewart Buttress or whether intrusion of the scarp-capping sill has caused beds equivalent to those below the "break" to be present at a greater altitude than at Coalseam Cliffs.

The sediments examined are almost universally of fine grade and show varying proportions of three basic lithological types: light grey to buff fine-grained sandstones, light and dark grey laminated siltstones, and dark grey shales and mudstones. These often grade into one another or are thinly interbedded. Occasional medium-grained sandstones and calcareous sandstone lenses are present but no conglomerates were observed. Coals and carbonaceous shales are ubiquitous throughout the succession but they are more abundant interbedded with thick sandstone sequences. Calcareous and ferruginous bands and nodules occur at some horizons. Flame, scour-and-fill and slump structures, ripple marks and cross lamination are common and cross bedding also occurs. Lateral variations in lithology are considerable but are difficult to detect; wedging out of thin beds is a common occurrence.

The Lower Permian sediments of the Theron Mountains are lithologically similar to the Victoria Group coal measures of eastern Antarctica.

In Heimefrontfjella, Juckes (in press) described a 160 m. sequence of Permo-Carboniferous sediments overlying peneplaned basement rocks and his middle and upper units are similar to some of the sediments of the Theron Mountains, though probably slightly older. Stephenson (1966)

considered the sediments of the Whichaway Nunataks to be slightly older than those of the Theron Mountains; coals are absent and shales uncommon but the sandstones are similar to those of the Theron Mountains. Cross-bedded quartz-sandstones with carbonaceous beds and thin coals have been described from the Patuxent Mountains (Schmidt and others, 1964) and cross-bedded arkosic sandstones with beds of silty sandstone, dark shale with plant remains and seams of high-ash coal occur in the Horlick Mountains (Long, 1964), in the mountain areas on the eastern margin of the Ross Ice Shelf and in Victoria Land. Carbonaceous shales in the Mount Glossopteris Formation of the Horlick Mountains (Long, 1964) are closely associated with the coal beds; the latter grade into carbonaceous shales both upwards and downwards. In the Pecora Formation of the Pensacola Mountains (Williams, 1969), impure coals with streaks and lenses of brittle vitrain in a dull, massive, brownish black matrix are similar to those of the Theron Mountains.

Many of the Victoria Group coal measures overlie Permo-Carboniferous glacial beds (Barrett and others, 1971) but the base of the sequence in the Theron Mountains is not exposed. Varvites, such as those of the Buckley Coal Measures in the Queen Alexandra Range (Grindley, 1963) were not observed.

Homotaxial Lower Gondwana coal measures have been described from other continents in the Southern Hemisphere. The Middle Ecca Coal Measures of the Karroo System of South Africa (Du Toit, 1954) are lithologically similar; they differ in containing more frequent beds of coarser grade and in that the majority of coals possess sandstone floors and pass upwards into shaly coal and dark shales with thin sandstones; the coals of the Theron Mountains grade upwards and downwards into dark mudstone and shale with plant remains. The Barakar stage of the Lower Gondwana of the Indian sub-continent (Jacob, 1952) and the Lafonian Sandstone of the Falkland Islands (Adie, 1952) are close lithological and stratigraphical correlatives, though the latter do not contain coals.

C. PETROGRAPHY

The sediments of the Theron Mountains are mainly siltstones and fine-grained sandstones of variable composition within fairly narrow limits. Many show recrystallization of any matrix or cement. This may be due to diagenesis, to load metamorphism to lower zeolite facies or to thermal metamorphism by the dolerite intrusions on a regional scale, as suggested in Victoria Land (Skinner, 1965).

Grain-size and sorting have been estimated visually in thin section, sphericity by comparison with fig. 2 of Wadell (1932) and roundness by comparison with plate I of Krumbein (1941). Mineral percentages have been estimated visually.

1. Sandstones

In thin section most of the sandstones are well sorted and of fine grade (average grain diameter 0.2 mm.); others, which are less well sorted, contain coarser material up to 0.4 mm. in diameter. One specimen (Z.487.13b) from above the slight local disconformity north-east of Goldsmith Glacier contains isolated, flattened mud pellets up to 5 mm. in length. Many of the finer-grained sandstones are finely laminated; this is often a sorting characteristic, though it may be due to, or accentuated by, concentrations of carbonaceous material. Sphericity of grains varies between about 0.60 and 0.85, with a mean of about 0.75; there does not appear to be any marked correlation between grain-size and sphericity. Roundness similarly varies indiscriminately with grain-size; it ranges from 0.3 to 0.5 and only rarely attains 0.7.

Quartz, feldspar and lithic fragments are major constituents of the sandstones and abundant carbonaceous

matter is commonly present. Cement, not very abundant in most cases, is usually siliceous but one or two specimens have a calcareous cement. Most of the sandstones have a fine-grained matrix, at least partly recrystallized, of quartz, sericite and chlorite. The heavy mineral fraction (estimated from thin sections) is variable but it includes large amounts of garnet, zircon and mica and smaller amounts of tourmaline and haematite.

The most abundant constituent of the sandstones is quartz, which is generally in excess of 40 per cent of the rock. Grains with undulose and uniform extinction in the sandstones as a whole occur in about equal proportions; they may occur together or separately. Some grains are composite. Overgrowths of secondary silica are common and often increase in abundance as dolerite sills are approached.

Feldspar varies in abundance from less than 10 to over 35 per cent of the rock and usually consists of about equal proportions of acid plagioclase and alkali-feldspar. The latter, particularly, is often sericitized or clouded with opaque dust. Alkali-feldspar is dominantly orthoclase but small amounts of microcline and microperthite were observed in some thin sections. Plagioclase is invariably well twinned on the albite law and rarely on the combined Carlsbad-albite law. Some grains show deformation

in the form of curved twin lamellae (cf. Barrett, 1969a, fig. 4); others have been fractured *in situ*.

Lithic fragments are not very abundant. They are usually fine-grained, altered and unidentifiable; where they are in contact with matrix material, both matrix and lithic fragments are often recrystallised, commonly obliterating grain margins. Quartz mosaics and quartz-feldspar intergrowths are present and rare grains have a vaguely igneous appearance; volcanic arenites such as those figured by Barrett (1969a) are not present. Specimen Z.487.13b has sporadically distributed pellets of muddy siltstone resulting from penecontemporaneous erosion of siltstones while the sandstones were being deposited.

Carbonaceous material is ubiquitous in the sandstones, usually as minute grains and flakes, often forming a coating between other mineral grains. It is commonly systematically distributed in such a way as to impart a lamination to the sandstones; this may be parallel to the bedding, cross lamination or irregular, and in many cases it has been deformed by slumping.

Detrital mica flakes are abundant in some of the sandstones and they are frequently bent and twisted between other grains. Up to 0.8-1.0 mm. long, they are usually muscovite but some are a mixture of muscovite and chlorite;

biotite is virtually absent. Garnet is abundant in some specimens, usually as sub-rounded grains about 0.1 mm. in diameter. Small clusters of minute angular grains of garnet appear to be remnants of sub-rounded grains fractured *in situ*. Zircon is not as common as garnet and it is usually well rounded and of small grain-size. Tourmaline and haematite were occasionally observed.

Some sandstones have a concentration of heavy minerals in association with thin, finer-grained, often carbonaceous laminae (e.g. Z.498.13); this is like graded bedding on the basis of density instead of grain-size. The muddy siltstone pellets of specimen Z.487.13 are armoured with heavy minerals, particularly garnet, and there is a far greater concentration of heavy minerals around the pellets than elsewhere in the rock (Figs. 20 and 21).

The fine-grained matrix of the sandstones is often unidentifiable but in some cases it is seen to consist of minute quartz, chlorite (most commonly penninite) and sericite. Interstitial authigenic sphene is present in many sandstones and in specimen Z.505.2 it is abundant and of larger grain-size. Specimen Z.471.4 is a highly altered fine-grained arkose and the matrix and much of the feldspar have been largely replaced by clinozoisite and prehnite; the amount of matrix is, because of this, difficult to

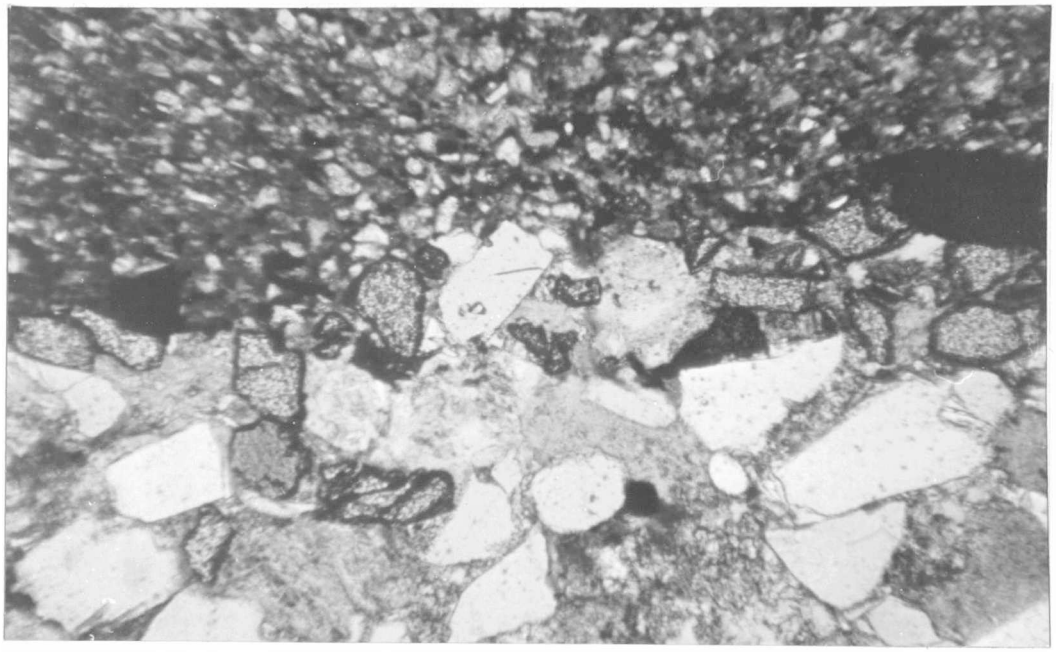

Fig. 20. Photomicrograph of a muddy siltstone pellet in medium-grained sandstone which grades into mud-flake breccia, showing its armouring by heavy minerals, especially garnet (Z.487.13b, ordinary light, x 65).

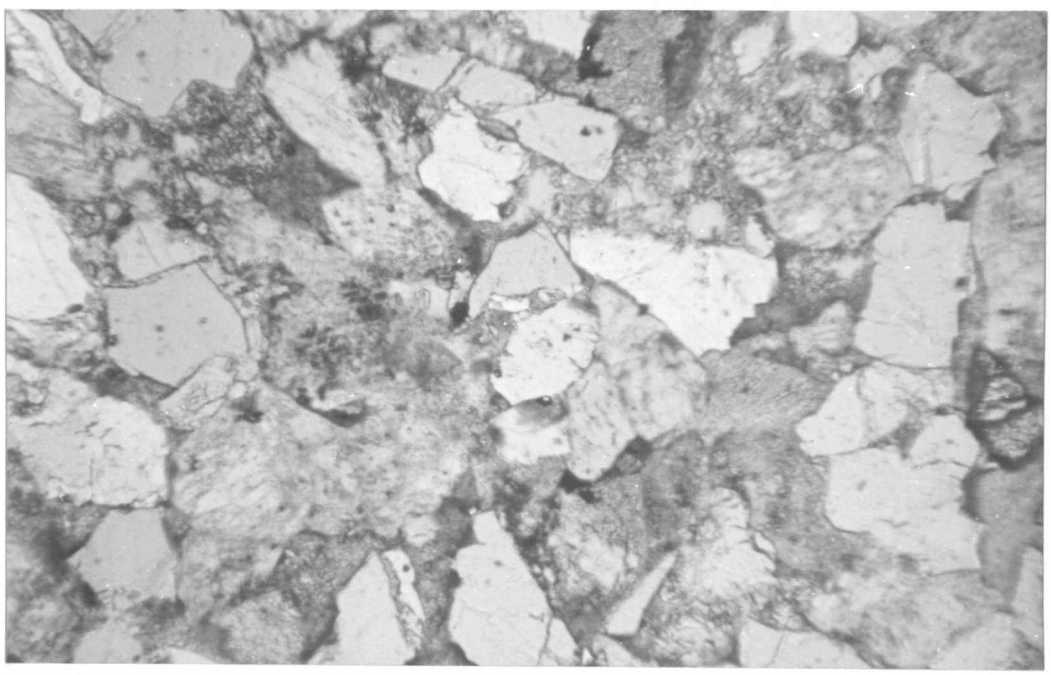

Fig. 21. Photomicrograph of medium-grained sandstone about 1 cm. from the muddy siltstone pellet of Fig. 2 , showing the general sparsity of heavy minerals (Z.487.13b, ordinary light, x 65).

estimate. The amount of matrix varies in individual thin sections, and often in different parts of one thin section, but it is usually smaller in the coarser-grained sandstones.

2. Siltstones

In thin section the siltstones differ from the sandstones largely in grain-size alone, with only minor differences in composition.

Sorting, sphericity and roundness are variable, but, like the sandstones, there is no apparent correlation of these parameters with grain-size. Most of the siltstones examined are finely laminated, largely due to the presence of carbonaceous material; some show slump features.

The siltstones are usually feldspathic or arkosic. Lithic fragments are even less readily discernible than in the sandstones but they appear to be similar. Carbonaceous material is probably more abundant than in the sandstones. Heavy minerals are not as common as in the sandstones and the abundance of zircon is apparently equal to or greater than that of the garnet. The matrix is generally more recrystallized than that of the sandstones and sericitic mica and authigenic sphene are more abundant. Specimen Z.507.1 is cut by calcite veins which also contain epidote.

3. Mudstones, shales and coals

Most of the finer-grained rocks sectioned are from xenoliths or contacts with dolerite intrusions and they have been thoroughly thermally metamorphosed. Even some distance from dolerite contacts, the mudstones are largely recrystallized, showing an abundance of sericitic mica (e.g. Z.502.5). These changes may be simply diagenetic or they may be the result of very low-grade (zeolite facies) regional or thermal (on a regional scale) metamorphic reactions.

Calcareous and possibly sideritic concretions are also present.

4. Discussion

The Lower Permian sediments of the Theron Mountains range in composition from feldspathic to arkosic sandstones and siltstones with subordinate carbonaceous, quartzitic and calcareous sandstones, siltstones and mudstones. They are usually of fine grade and they are mostly fine-grained sandstones and siltstones. Mudstones, shales and coals are slightly metamorphosed like the fine-grained matrix of sandstones and siltstones. This metamorphism may be due to load effects of the weight of sediments above or it may be a contact effect of the dolerite intrusions.

Hamilton (1965) considered that all the sediments of the Beacon Supergroup near its type section had been slightly metamorphosed by dolerite sills, with a total thickness near to that of the sediments, which were intruded at temperatures near 1,000° C. Metamorphism is obvious in the field in hornfelsed or metasomatized rocks within 1-2 m. of contacts. Away from contacts, the appearance of rocks in hand specimen is that of unaltered sedimentary rocks but pervasive metamorphism is apparent in thin sections. The argillaceous fractions have been reconstituted to fine-grained mica and most of the quartz has been recrystallized marginally to form mosaics and, locally, interlocking grains. Much of the feldspar has been sericitized and the bituminous to anthracitic character of coals is probably due to thermal metamorphism. Skinner (1965) also concluded that the regional alteration of the sediments of the Beacon Super-group between Byrd and Starshot Glaciers in Victoria Land was due to the widespread effects of dolerite sill injection; at the immediate contact with dolerite, the sediments have been more strongly metamorphosed to albite-epidote hornfels facies. In South Africa, Du Toit (1954) noted that coals within a distance from a dolerite intrusion about equal to its thickness are affected by the intrusion and that sediments in contact with dolerite intrusions invariably exhibit a

certain amount of alteration. Obvious hornfelsic baking of the sediments of the Theron Mountains does not extend very far from intrusive contacts but most of the sediments are slightly altered.

Brown and Taylor (1960) concluded that coal samples collected during the Trans-Antarctic Expedition had been thermally metamorphosed to different degrees under strong confining pressures, with a significant absence of vesicles in their samples. They suggested the coals were of bituminous rank prior to metamorphism. Many of the coals seen by the author, in Marø Cliffs, particularly, have been burnt by dolerites and specimen Z.475.3, from Coalseam Cliffs, has had hexagonal jointing imposed by the thick sill immediately above it. Specimens from the contacts of sills at Coalseam Cliffs (Z.478.6) and Marø Cliffs (Z.501.5) are intimate mixtures of dolerite and coal with hydrothermal quartz and calcite and there are abundant vesicles in the coal.

Schopf and Long (1960) suggested that the semi-anthracitic rank of the coals of Mount Glossopteris in the Horlick Mountains, which do not appear to have been affected by igneous activity, is proportional to the maximum previous overburden; this indicates a greater thickness of cover at Mount Glossopteris than elsewhere in Antarctica or in South Africa and eastern Australia.

Mudge (1968) suggested that nearly all concordant igneous masses in flat-lying sedimentary rocks were intruded into a zone ranging from 915-2,290 m. in depth; the depth of overburden of dolerite sills in the Taylor Glacier region of Victoria Land is given as 915-2,440 m.; this would imply a lithostatic pressure of 200-500 bar, which may be sufficient to impart some load metamorphism. The load effects of the overlying sediments in the Theron Mountains, as shown by load casts (Fig. 15), are considerable and the bituminous rank of coals prior to thermal metamorphism suggests there may have been some load metamorphism.

The alteration of the sediments is considered to be caused by the accentuation and increase in intensity of load metamorphism due to the contact effects of dolerite intrusion.

D. PALAEOBOTANY, AGE AND CORRELATION

The only fossil material present in the sediments of the Theron Mountains are leaf and stem impressions and coals, which are present throughout the succession and throughout the mountain range. Trace fossils and other Problematica noted by Vialov (1962) in Victoria Land were not seen. The only specific identifications of fossil material are those by Plumstead (1962) of fossils collected

during the Trans-Antarctic Expedition (Table II); these included possible insect wings but no evidence of any invertebrate fauna has been seen by the author.

1. Distribution of plant fossils

North-east of Goldsmith Glacier, the most prolific locality for plant fossils is at station Z.487. About 7 m. below the summit of the ridge, thin, light to medium grey, thinly bedded and irregularly laminated coarse-grained siltstones contain carbonaceous impressions of leaves and stems, some tentatively identified as Glossopteris and Vertebraria. Details of venation of leaves can be seen despite the coarseness of the matrix. Slightly lower down in the succession, a dark grey to black shaly mudstone about 2 m. thick has abundant plant impressions, both whole leaves and fragmental material. They are preserved as orange-brown carbonized coatings on bedding planes and the cell structure of woody stems is discernible.

Thin dark grey to black shales and mudstone partings with abundant leaf and stem impressions occur near the base of the sequence at station Z.508. They occur as dark carbonaceous impressions on bedding planes and much of the fine detail is preserved. At a slightly higher horizon at station Z.507, four thin coaly shales with abundant plant matter are interbedded with thinly bedded

TABLE II

FLORA IDENTIFIED BY PLUMSTEAD (1962) FROM FOSSIL SITES COLLECTED DURING THE TRANS-ANTARCTIC EXPEDITION

Upper horizon (above the sedimentary "break" above the middle sill of Coalseam Cliffs, near station Z.458)	*Phyllotheca australis* Brong.
Middle horizon (below the thick wedging sill of point 2600, near station Z.478)	*Glossopteris* cf. *longicaulis* Feist. *Glossopteris browniana* Brong. *Glossopteris stricta* Bunb. *Glossopteris fuchsii* Plumstead *Glossopteris parallela* Feist. *Glossopteris* cf. *cordata* Dana *Glossopteris antarctica* Plumstead *Cordaicarpus* Geinitz sp. *Arberiella* Pant sp. *Arberia* cf. *minasica* White ? *Hirsutum* Plumstead sp. Scale leaves of *Glossopteris* Unidentifiable stems Insect wing cases
Lower horizon (below the basal sill of Coalseam Cliffs, near station Z.477)	*Annularia* Sternberg sp. *Glossopteris formosa* Feist. *Vertebraria indica* Royle Unidentifiable stems Algal markings or worm tracks ?

sandstones. Only the lowest shale was collected and this shows preservation of very fine detail; the plants are similar to those at station Z.487 in having an orange-brown carbonized coating.

Interbedded with the siltstones and sandstones of Lenton Bluff are coal and plant-bearing mudstone and shale horizons, usually about 1 m. thick but attaining 3 m. in cases; the aggregate thickness is in excess of 20 m. Most of the fossil material consists of poorly preserved fragmental stems but occasional horizons contain whole leaves with finely preserved detail.

Little plant material is preserved at Marø Cliffs because the coals and coal shales there have been largely burnt by dolerite intrusions. The material present occurs in black mudstone and shales and is largely fragmental.

Fossil material from three horizons in Coalseam Cliffs has been described by Plumstead (1962). Plant fossils are more frequent and better preserved in the lower part of the succession (Z.477), at least four coal or fossiliferous horizons being present below the basal sill. Whole leaves and stems are well preserved and show fine detail as orange-brown carbonized coatings on black mudstone interbedded with dark grey siltstones in two of these horizons but others possess only fragmental stems.

Higher in the succession, plants tend to be less well preserved and more fragmental, except in the thin black shale about 5 m. below the thick wedging sill of point 2600 (Z.478). Above the sedimentary "break" at Stewart Buttress, coals and plants are present but not abundant; they were sampled only at station Z.458, where very fragmental plant remains occur in thinly bedded black shales with occasional coal partings.

2. Age and correlation

The specific identifications of Plumstead (1962), shown in Table II, indicate an Upper Carboniferous to Lower Permian age. There is no evidence to indicate anything other than a Lower Permian age for all the sediments of the Theron Mountains.

The Lower Permian sediments of the Theron Mountains are representatives of the Victoria Group of the Beacon Supergroup (Barrett and others, 1971); homotaxial formations are the Lower Gondwana sediments of other Southern Hemisphere continents.

Juckes (in press) has described a 160 m. sequence of Victoria Group sediments resting on the peneplaned basement rocks of Heimefrontfjella and overlain and intruded by Jurassic basaltic rocks. The flora collected by Juckes has been examined by Plumstead (in press), who considered that

they are probably of Upper Carboniferous age and possibly represent the oldest Glossopteris flora yet discovered in Antarctica. Plumstead (1962) considered that the sediments of the Whichaway Nunataks showed floral affinities with those of the Theron Mountains but that they were probably slightly older.

In the Horlick Mountains (Long, 1964), the Shackleton Glacier area (La Prade, 1970), the Queen Alexandra Range (Grindley, 1963), the Beardmore Glacier area (Barrett, 1969b) and southern Victoria Land (Allen, 1962; Webb, 1963; Hamilton and Hayes, 1963; and others) a more complete sequence of the Beacon Supergroup is exposed. This includes Devonian sandstones and siltstones with marine intercalations, Upper Carboniferous glacial beds, Permian sandstones and coal measures, Triassic arkosic arenites and coal measures and Upper Triassic to Jurassic volcaniclastic strata. The Permian coal measures are of about the same age as those of the Theron Mountains (Lower—Middle Permian) except for the Mount Glossopteris Formation of the Horlick Mountains, which is considered by Doumani and Tasch (Long, 1964) to be of Upper Permian age, and the Pecora Formation of the Pensacola Mountains (Williams, 1969).

Lower Gondwana sediments of other Southern Hemisphere continents are of Upper Carboniferous to Jurassic age and Plumstead (1964) considered the following formations

to be homotaxial with the Permo-Carboniferous plant-bearing formations of eastern Antarctica:

The Damuda System, ranging from the Karharbari stage to the Raniganj Series, of India

The Middle Ecca Series of the Karroo System of South Africa

The Lower Bowen Series of Queensland

The Greta Coal Measures and the lower part of the Newcastle Coal Measures of New South Wales

The north-eastern Canning Basin of Western Australia

The Bonito Group of the Tubarao Series of Brazil

The base of Piso II in the Paganzo System of Argentina

The Lafonian System of the Falkland Islands

The Sakoa Formation of Madagascar

The Mersey System of Tasmania

E. PROVENANCE AND DEPOSITIONAL ENVIRONMENT

1. Provenance

The orientation of such features as cross bedding, cross laminations and ripple marks varies between individual beds but it generally indicates a south-westerly provenance, as inferred by Stephenson (1966). This roughly parallels

current directions figured by Barrett and others (1971) in the post-glacial Permian of the Victoria Group of the Transantarctic Mountains.

The mineral composition of the sediments, especially the abundance of garnet in the heavy mineral fraction, is consistent with derivation from a metamorphic terrain, probably composed of gneisses and gneissic granites. Colourless and pale pink garnet are present in some of the rocks of the Shackleton Range (Stephenson, 1966) and the gneisses, amphibolites and schists of the Shackleton metamorphics seem a likely source for many of the constituents of the sediments. A certain admixture from an acid volcanic source is possibly indicated by the presence of twinning on the combined Carlsbad-albite law in some feldspars and by some of the finer-grained lithic fragments. This is not nearly so strongly developed as in the Beardmore Glacier area (Barrett, 1969a,b; Barrett and Elliot, 1971).

The sphericity and roundness of the mineral grains do not indicate transport of either prolonged or very short duration but the generally fine grain-size of the sediments suggests that the source was not in the immediate vicinity. The source area had probably not been subjected to very deep weathering and there had been only a moderate amount of re-working.

2. Depositional environment

Stephenson (1966) noted that the complete absence of marine fossils and the presence of coal and plant remains indicates that the sediments were deposited in a terrestrial environment. No features strongly indicative of aeolian deposition were observed in the field and the sediments are probably wholly water-lain clastic deposits.

The continental land surface on which the sediments were deposited is not exposed and it is not known whether glacial conditions preceded sedimentation, as they did elsewhere in Antarctica. There is no definite evidence of the climatic conditions prevailing during sedimentation, though the absence of tillites or evaporites suggests a temperate climate.

Lateral and vertical variations in lithology on a small and large scale indicate variable local environments. Although different lithologies are repeated throughout the succession, there is little evidence of a regular repetition and cyclic sedimentation, such as that in the Falla Formation of Victoria Land (McGregor, 1965) cannot be inferred.

No plant remains were found in a position of growth and the macerated nature of much of the plant fossil material, especially in association with coals, suggests that it was deposited in water; Plumstead (1962) suggested a paludal environment for the upper fossiliferous horizon

collected by Stephenson. The thin interlamination of coal and mudstone (Fig. 16) and the separation of mudstone beds by carbonaceous partings support the suggestion that the coal is allochthonous.

Oscillation ripple marks (Fig. 14) and the fine lamination of many of the siltstones indicates small areas of relatively shallow stagnant water. The lamination of many of the sandstones and siltstones, however, is irregular and there are other signs, in the form of scour-and-fill structures, of penecontemporaneous erosion. This is supported by the slight local disconformity and thin mud-flake breccia at the base of a sandstone bed at station Z.487 (Fig. 13). Armoured mud balls on the scale figured by Juckes (in press) were not seen but the mud pellets armoured by garnet (Z.487.13; Fig. 20) are probably of similar origin; they may indicate lateral shift of a stream channel. Load casts on the base of some beds (Fig. 15) probably followed original irregularities caused by scour and fill.

Local deltaic features or migrating meander channels are suggested by the cross bedding on a megascopic scale above the sedimentary "break" beneath Stewart Buttress. Other examples of large-scale cross bedding were noted and small-scale cross lamination and cross bedding are common; they are variable in orientation.

Slump balls (Fig. 17) and slump-bedded units throughout the succession indicate the presence in some areas of moderately steep slopes covered by meta-stable unconsolidated sediments. The small-scale faulting at station Z.465 may have resulted from slumping of underlying beds while the sediments were only partly consolidated. Penecontemporaneous deformation (Fig. 18) is also seen in other units.

The variable local environments suggest that erosion of the source area was probably fairly rapid with occasional intervals of quiet deposition. The sediments were apparently deposited on a low-lying alluvial plain under fluvial, fluvial-deltaic and lacustrine conditions (cf. Webb, 1963; Williams, 1969; Matz and others, 1971).

CHAPTER V

JURASSIC DOLERITE INTRUSIONS

A. DISTRIBUTION AND FIELD RELATIONS

Jurassic dolerite intrusions are ubiquitous in the Theron Mountains and form at least a part of every rock outcrop. North-east of station Z.487 and south-west of Mount Faraway (Fig. 4), only dolerite is exposed but elsewhere both dolerite and sediments are present and the intrusive relations can clearly be seen. Extrusive equivalents are absent, either never deposited or since removed by erosion.

Both dykes and sills occur but the majority of intrusions are in the form of sills, ranging from <1 to >200 m. in thickness. Dykes are far less common and they were observed at few localities; they are thinner, usually 1-2 m. but up to 7 m. wide, and less persistent. The relationships between dykes and sills are not always clear but they appear to have been intruded at about the same time; a sub-division into dykes and sills for descriptive purposes is purely arbitrary and is not used here.

There were apparently at least three phases of intrusion (p. 63); sills, transgressive sills and dykes are associated with all phases. The difference between the time of intrusion of the phases is probably not significant. Layering of two different types is seen in two sills alongside Jeffries Glacier and in Marø Cliffs (p. 66).

Few intrusions can definitely be traced beyond the confines of individual outcrops; exceptions are the scarp-capping sill and the middle sill of Coalseam Cliffs, which can be traced for 60 and 50 km., respectively. Other sills are less persistent and many do not persist the whole length of individual outcrops.

Where sills crop out along the scarp front they form, because of their prominent columnar jointing, near-vertical cliffs and, because of their resistance to erosion, gullies cut through them only occasionally. On top of the cliffs and on many of the rock outcrops south-east of the scarp front slopes are not as steep and spheroidal weathering of the dolerite is a common feature, especially in the medium- to coarse-grained parts of the thicker sills and dykes; thinner sills and dykes and the fine-grained margins of the thicker sills tend to show more angular, blocky weathering, even on gentler slopes. The dolerites are usually more resistant than the enclosing sediments,

resulting in a cliff-and-ledge topography with sills, and wall-like projections of dykes (Figs. 6 and 7).

1. Scarp-capping sill

The base, or, north-east of station Z.487, all of most of the outcrops north-east of Goldsmith Glacier is formed by a thick reddish brown-weathering sill which is at least 200 m. thick. The base of the sill is not exposed and the top is seen only alongside Goldsmith Glacier (Z.466 and 487). Where exposed, the upper contact appears to be largely concordant and essentially horizontal.

This sill can be traced across Goldsmith and Jeffries Glaciers, forming a capping to much of the escarpment and the base of many outcrops south-east of the scarp front. It appears to continue across the unnamed southern glacier as the thick wedging sill noted by Stephenson (1966) in Coalseam Cliffs beneath point 2600.

Both upper and lower contacts of the sill appear to be generally concordant, though irregular in detail. No xenoliths, apophyses of dolerite or pendant blocks of sediments were observed.

Near the south-western end of Lenton Bluff (Z.498), the lower contact appears to dip southwards at about 15° and it has tilted the sediments for a short distance. Alongside

Jeffries Glacier and the unnamed southern glacier, the top of the sill appears to dip gently (< 5°) southwards; the sill probably thickens in this direction.

Near the south-western end of Marø Cliffs (Z.481, 482), the scarp-capping sill apparently bifurcates and a lower 20-30 m. thick branch sill is separated from the upper 200 m. thick parent sill by a thin sequence of sediments (Fig. 22). Both the horizon and the altitude of the apparent branch sill decrease north-eastwards in a series of steps and it appears to continue across Jeffries Glacier as the basal sill of Lenton Bluff, where 200 m. of sediments and dolerite separate the parent and branch sills. It apparently cuts the first-phase sill of Marø Cliffs and is cut by the third-phase sill and by the younger transgressive sill of Lenton Bluff; it is considered to be the second of at least three phases of intrusion present in Marø Cliffs and Lenton Bluff (p. 63).

At the extreme north-eastern end of Coalseam Cliffs (Z.494), the thick wedging sill is about 200 m. thick and it wedges out south-westwards to less than 10 m. within 2.5 km.; 4 km. south-west of the north-eastern end of the cliffs it appears to wedge out completely. In the cliffs beneath point 2600, slightly curved jointing in the sill suggests there was some flowage to the south-west in the

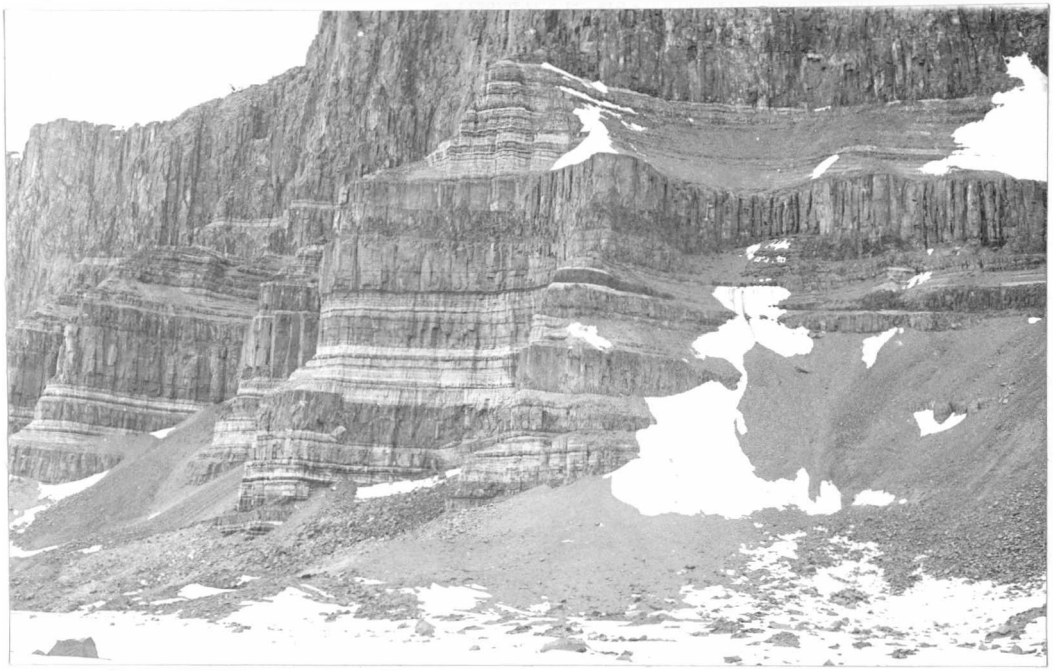

Fig. 22. Different intrusive phases of Marø Cliffs: the light-coloured first-phase sill is intruded by the darker-coloured third-phase sill; the second phase of intrusion is represented, left of centre, by the apparent branch sill, separated by a thin screen of sediments, from the scarp-capping sill. The relationships of other sills are unknown.

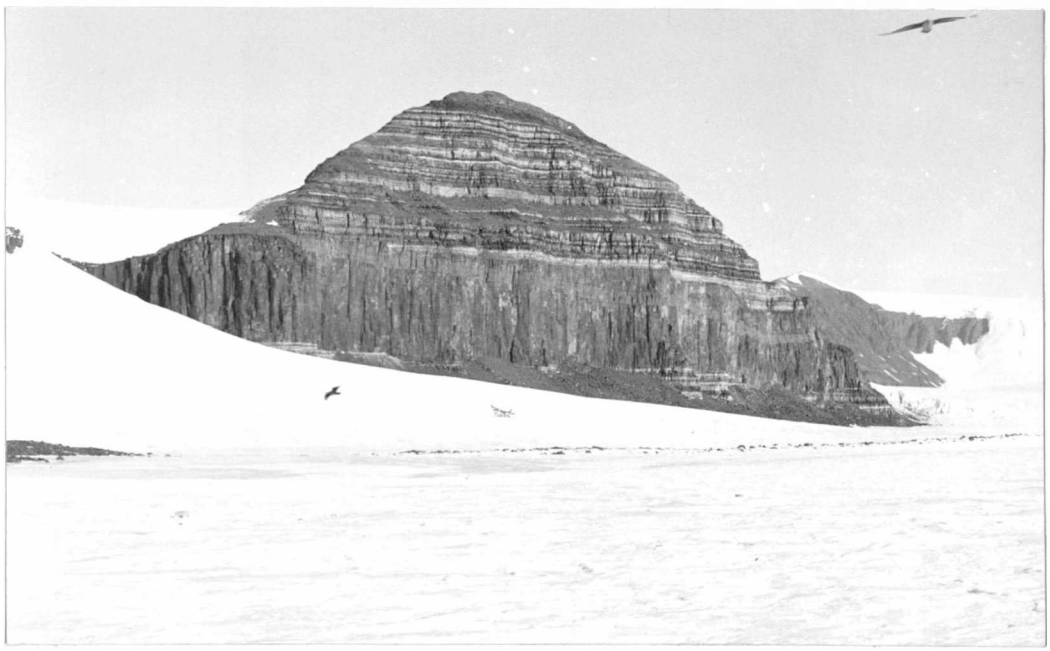

Fig. 23. Different intrusive phases of Lenton Bluff: the basal sill is cut by the younger transgressive sill which is about 4-5 m. thick.

lower part of the sill after it was partly consolidated. At station Z.478, there is some indication of possible auto-intrusion along the lower contact. The sill is chilled against the sediments below but a thin discontinuous wedge of fine-grained dolerite is interspersed between it and the sediments. The sill is also chilled against the fine-grained dolerite and it is transgressive across the chilled contact of the fine-grained dolerite with the sediments.

The scarp-capping sill covered an approximate area of at least 600 km.^{2} before dissection by erosion and the volume of dolerite in this sill alone was at least 120 km.^{3}

2. Different intrusive phases

In Marø Cliffs, the cliffs beneath point 3300 and Lenton Bluff, at least three phases of intrusion are present; the relationships between any pair of phases are clear but complete correlation is not possible. The different phases are characterized not only by the cutting of one sill by another but also by their different weathering colours (Figs. 22 and 23), indicative of different compositions.

The oldest recognizable phase is a light orange-brown-weathering sill about 30 m. thick which is present throughout Marø Cliffs and in the cliffs beneath point 3300

(Z.480). The second phase of intrusion is represented by the apparent branch sill of the scarp-capping sill, which continues across Jeffries Glacier as the basal sill of Lenton Bluff. The third phase is represented by a deep reddish brown-weathering sill which is less continuous than the first and second phases, but which cuts them both. A possible fourth phase is represented by the younger, light orange-brown-weathering sills and dykes which cut the basal sill of Lenton Bluff. Exact relationships between the different phases of intrusion in different areas are not clear and, though one sill can be traced across Jeffries Glacier, others cannot. They are, therefore, treated geographically.

a. Marø Cliffs

At the south-western end of Marø Cliffs (Z.481) and beneath point 3300 (Z.480), the first-phase sill is intruded by the third-phase sill, which is 5-10 m. thick (Fig. 22). The contacts of these two sills are clearly intrusive and the third-phase sill is markedly chilled. For much of the length of the cliffs the third-phase sill is intrusive into the first-phase sill or is separated from it by a thin screen of sediments, often coal. Just southwest of the central ice fall in Marø Cliffs (Z.482), the apparent branch sill of the scarp-capping sill appears to

be cut by the third-phase sill and, north-east of the ice fall (Z.483 and 502), it appears to cut the first-phase sill.

At the north-eastern end of Marø Cliffs (Z.483), a thin light orange-brown-weathering sill intrudes the sediments beneath the apparent branch sill, cuts through it at a steep angle and continues north-eastwards intruding the sediments above it. It is very similar to and may be continuous with the younger transgressive sills and dykes of Lenton Bluff.

b. Lenton Bluff

The basal sill of Lenton Bluff, a continuation of the apparent branch sill of the scarp-capping sill, forms the base of the cliffs for most of their length. It varies in thickness, averaging about 30 m., and it weathers a dark reddish brown. Both upper and lower contacts are transgressive on a small scale. Xenoliths (Fig. 24), pendant blocks of sediments and apophyses of dolerite into the overlying sediments are common; there is some associated hydrothermal mineralization.

At the south-western end of Lenton Bluff (Z.471), this basal sill is cut by a younger transgressive, light orange-brown-weathering sill about 5 m. thick (Fig. 23). It clearly intrudes the basal sill and is chilled against it at station Z.471 but farther north-east it intrudes the

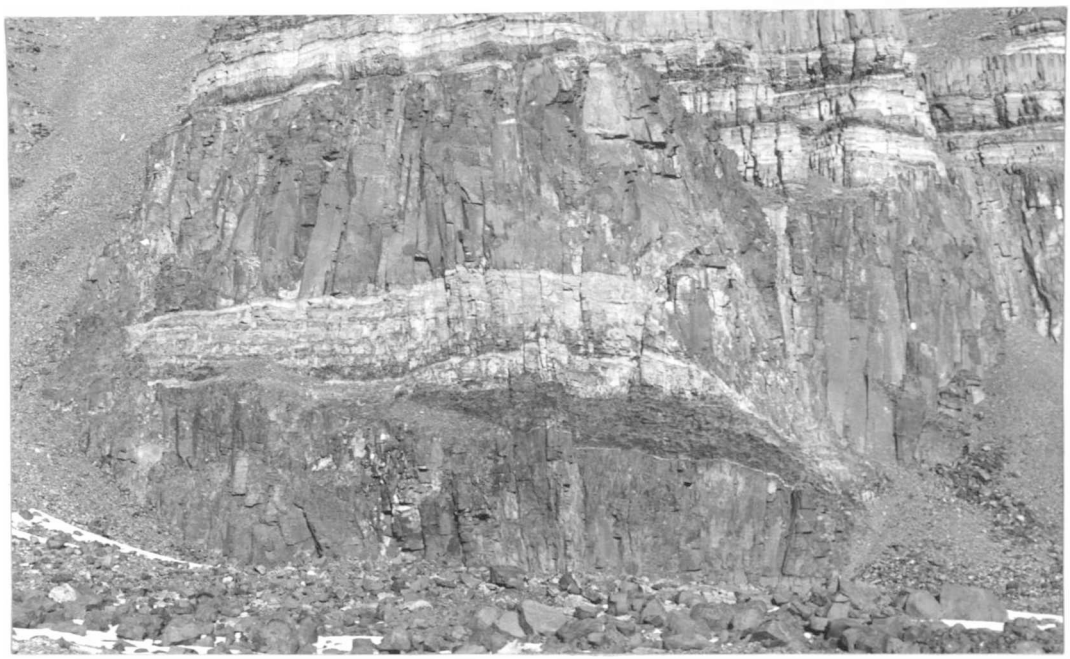

Fig. 24. Part of the basal sill at Lenton Bluff showing the largest xenolith at station Z.472; the xenolith attains a maximum thickness of about 10 m.

sediments above it. About 1.5 km. north-east of Jeffries Glacier (Z.498; Fig. 7), the younger sill becomes part of a complex system of dykes and thin sills which extend through all the sediments in this part of Lenton Bluff.

3. Layered sills

Two isolated examples of layering were seen in the dolerite intrusions of the Theron Mountains. They are both in sills which cannot be traced for any great distance, in the cliffs alongside Jeffries Glacier and in Marø Cliffs.

a. Jeffries Glacier

Near the base of the cliffs along the western margin of Jeffries Glacier (Z.497), a light reddish brown-weathering sill about 50 m. thick intrudes the sediments. The upper contact is slightly discordant but the lower one is essentially horizontal and it is not markedly transgressive. Xenoliths of sediments occur near the top of the sill and, at the northern end of the outcrop, a thin sill branches from the upper contact.

Approximately in the middle of the sill is a thin band of darker-weathering coarser-grained dolerite rich in mafic minerals (Fig. 25). It is variable in thickness, averaging about 1 m., and it is absent over short distances (< 1 m.); otherwise it is continuous throughout the exposed

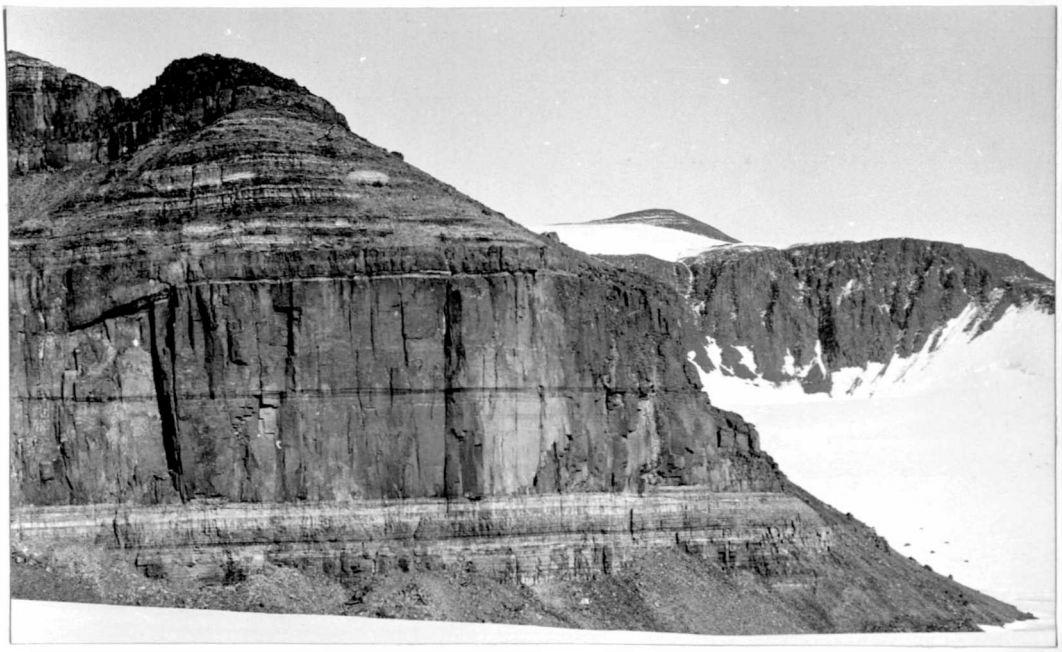

Fig. 25. Layered sill of Jeffries Glacier: View from Jeffries Glacier showing the mafic layer in the middle of the sill; occasional splitting of this layer is well shown.

section of the sill. Splitting of the mafic layer, with lenses of apparently normal dolerite between thin mafic bands, is common. Although the change in weathering colour into the mafic band is sharp, actual contacts are gradational and the mafic layer does not appear to be intrusive into the normal dolerite.

The mafic layer is similar to the olivine-diabase layer of the Palisades sill of New Jersey (Walker, 1940). The latter, however, averages 4.6 m. in thickness, ranging from 0.9-6.1 m., and occurs 9.1-18.2 m. above the lower contact of the 300 m. thick sill. The mafic layer of Station Z.497 is thinner, nearer the middle of the sill and it is developed in a sill only one-sixth the thickness of the Palisades sill.

Gunn (1962) noted a prominent coarse-grained hypersthene zone (band of norite) between about 60 and 120 m. above the base of the Upper Escalade sill of Victoria Land. This is similar to the mafic layer of station Z.497 except that the latter is apparently more mafic, considerably thinner and more restricted to the central part of the sill, which is only 50 m. thick.

b. Marø Cliffs

At the south-western end of Marø Cliffs (Z.481), the 30 m. thick sill which forms the base of the cliffs

shows pronounced rhythmic layering (Wager and Deer, 1939) for about 8 m. above the lower contact (Fig. 26). The layering is essentially horizontal and parallel to the lower contact of the sill. Individual layers vary in thickness, ranging from a few centimetres to about 1 m. and averaging about 70 cm. The layering is more pronounced on weathered surfaces and, though distinct, contacts between melanocratic and leucocratic layers are gradational (Fig. 27). The dolerite is chilled at the lower contact for a few centimetres and fine-grained for about 50 cm.; the layered material is medium-grained. Above the layered material, the sill consists of normal, medium-grained light brown-weathering dolerite.

Near the top of the sill is a very coarse-grained dolerite-pegmatite and about 1.8 m. below the upper contact a thin 15 cm. band of darker-weathering material parallels the upper contact (Fig. 28). Although coarse-grained, it is considerably finer in grain-size than the mass of dolerite-pegmatite which surrounds it. It grades upwards and downwards into the dolerite-pegmatite.

The upper contact of the sill is horizontal but a number of thin veins of re-mobilized sediments extend vertically down into the dolerite. The actual contact zone is a complex intermixture of chilled dolerite and metamorphosed

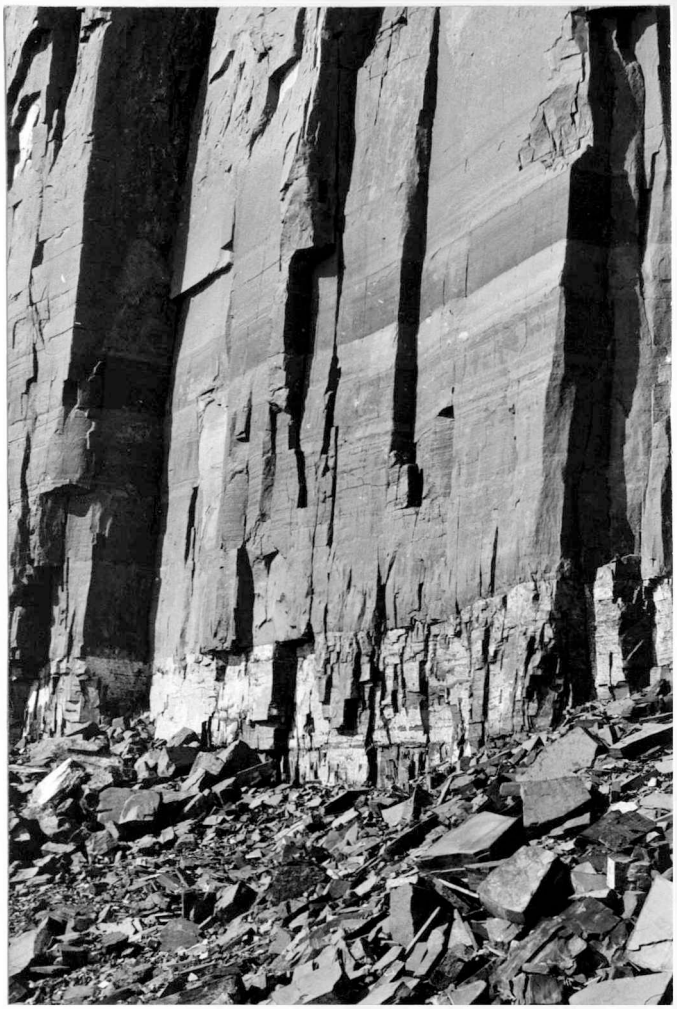

Fig. 26. Layered sill of Marø Cliffs: view of the lower part of the sill showing the rhythmic layering in the lower 8 m.

Fig. 27. Layered sill of Marø Cliffs: close-up of the rhythmic layering; the layers are quite distinct but contacts are gradational; the hammer shaft is about 55 cm. long.

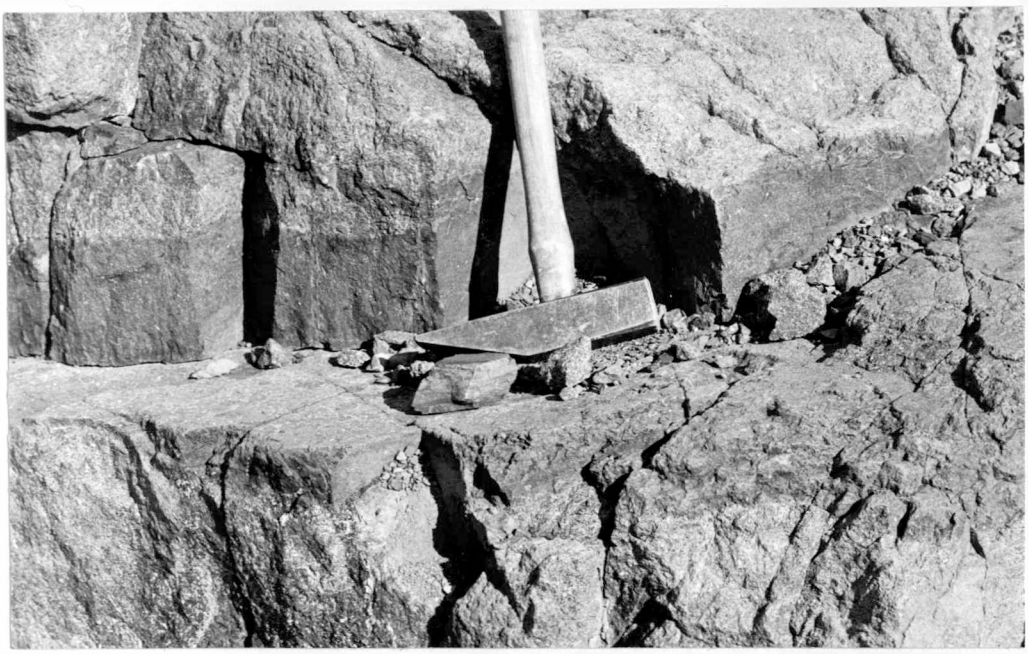

Fig. 28. Layered sill of Marø Cliffs; finer-grained darker-weathering band in dolerite-pegmatite about 1.8 m. below the upper contact; the hammer head is about 20 cm. long.

sediments. Contact effects are more pronounced around the upper reaches of this layered sill than in the lower parts and they include some partial melting, or at least re-mobilization, of the roof rocks, as was suggested to be the case in sills where crystal settling has had some effect (Irvine, 1970).

Rhythmic layering occurs in many intrusive igneous bodies (Wager and Brown, 1968). In Antarctica, it also occurs in the Thumb Point sheet (Skinner and Ricker, 1965) and the Mount Egerton sill (Gunn, 1963) of Victoria Land. These occurrences are similar in many ways to the sill described above but there are important differences.

The Thumb Point sheet is over 400 m. thick; 120-130 m. above the apparent base of the sill is a band of light and dark evenly layered fine-grained dolerite with layers ranging in thickness from 5-60 m. but averaging 10-20 cm. In the dolerite above the layered zone, grain-size increases steadily from normal fine-grained dolerite up to coarse pegmatoid.

The Mount Egerton sill is about 250 m. thick; concentrations of hypersthene with lenses of anorthositic rock start about 50 m. above the base, rise to a maximum and fall off gradually upward to about 90 m. above the base; the rhythmic layering is on a coarse scale. The overlying

dolerite is granophyric with pegmatoid and rare granophyre layers.

These two examples thus contrast with the layered sill of Marø Cliffs, which is only about 30 m. thick with layering in the lowest 8 m. and medium-grained dolerite above that, which grades into dolerite-pegmatite near the top of the sill.

4. Other intrusions

Other sills in the Theron Mountains are generally impersistent except for the basal and middle sills of Coal-seam Cliffs; they cannot be directly correlated between outcrops on the basis of field evidence alone. Dykes are rare and their relationships to sills are not always certain. These intrusions are considered geographically below.

a. Area north-east of the unnamed southern glacier

At station Z.487, a sill about 30 m. thick intrudes the sediments above the scarp-capping sill. Both upper and lower contacts are exposed and they appear to be concordant and horizontal. It may be equivalent to the sill capping the outcrop of station Z.466, though the top of the latter is not seen and its thickness is unknown. A vertical 20 cm. wide dyke extends from the upper contact of the 30 m. thick sill. It is fine-grained, dark reddish brown-weathering

and resistant to erosion, forming a wall-like feature projecting from the intruded sediments.

At station Z.509, the crest of the ridge is formed by a dark reddish brown-weathering dyke up to 7 m. wide. It is fine-grained closely jointed dolerite and shows pronounced spheroidal weathering. It is near-vertical at the top of the outcrop but it becomes progressively less steep in attitude lower down and, beneath a scree- and snow-covered area, it appears to merge with a 7 m. thick sill lower down in the sequence.

The sediments above the scarp-capping sill between Goldsmith Glacier and the unnamed southern glacier are intruded by a number of minor sills (< 10 m. thick) and rare dykes. Sills are concordant and essentially horizontal; they commonly weather a dark reddish brown and exhibit marked spheroidal weathering. At station Z.488, the uppermost sill appears to bifurcate south-westwards in two localities. In the ridge leading eastwards from point 3300 (Z.453), a 1-2 m. wide dyke is intruded along a fault plane which offsets a 15 m. thick sill lower down; it appears to lead into the sill forming the first shoulder on the ridge leading to point 3300 but exact relationships are not certain.

Numerous sills of variable thickness and characteristics and occasional thin dykes intrude the sediments below the scarp-capping sill. Many of these have been discussed above. The rock peak rising from the ice cliffs of the escarpment just south-west of the mouth of Goldsmith Glacier (Z.470, 489 and 508) is capped by the scarp-capping sill; intruded just below the base of this sill and separated from it by a thin screen of sediments 1-6 m. thick is a light orange-brown-weathering sill about 12 m. thick. At the base of the outcrop is a dark reddish brown-weathering sill about 30 m. thick. These may be related to the different intrusive phases of Lenton Bluff but, as they do not come into contact, the exact relationships are unknown.

At Marø Cliffs, rare vertical dykes 1-2 m. wide intrude the sediments beneath the scarp-capping sill and extend for a few metres into it (Fig. 29) at both the north-eastern (Z.483) and south-western (Z.481) ends of the cliffs. Their relationships with other sills were not seen.

b. Area south-west of the unnamed southern glacier

The relationships and nomenclature of the major sills in Coalseam Cliffs are shown in Fig. 5a. No dykes were observed.

The basal sill, which is about 30 m. thick, is continuous for the whole length of the cliffs. Although

Fig. 29. The 1 m. wide dyke at station Z.481: it terminates abruptly against the sediments, though 1-2 cm. dykelets penetrate a little farther down than shown; in its upper part it penetrates for a few metres into the scarp-capping sill; the hammer shaft is about 55 cm. long.

slightly transgressive on a small scale, partly due to intrusion-faulting, it is generally concordant. It is typically dark reddish brown-weathering and dark grey on fresh surfaces. Though chilled at both upper and lower contacts, it is generally fine- to medium-grained. It is usually free of xenoliths but, at the south-western end of the cliffs (Z.474), a number of sedimentary xenoliths up to 2-3 m. thick and 7-8 m. in length occur near the top of the sill.

The upper sill at point 2600 is of constant thickness (about 30 m.) but it does not continue south-west of the ice cliff between point 2600 and Stewart Buttress. It weathers a dark reddish brown compared to the light orange-brown of the middle sill so, although it occurs at about the same altitude, it is probably not the same sill. Thin veins of remobilized sediments intrude the sill up to about 7 m. above its base (Fig. 30).

The middle sill of Coalseam Cliffs is 50-60 m. thick and continuous for 50 km. from just north-east of Stewart Buttress to Parry Point. Assuming a south-easterly extension of only 10 km. before erosion, the volume of dolerite in this sill is 25 km.^{3}; this is probably an absolute minimum.

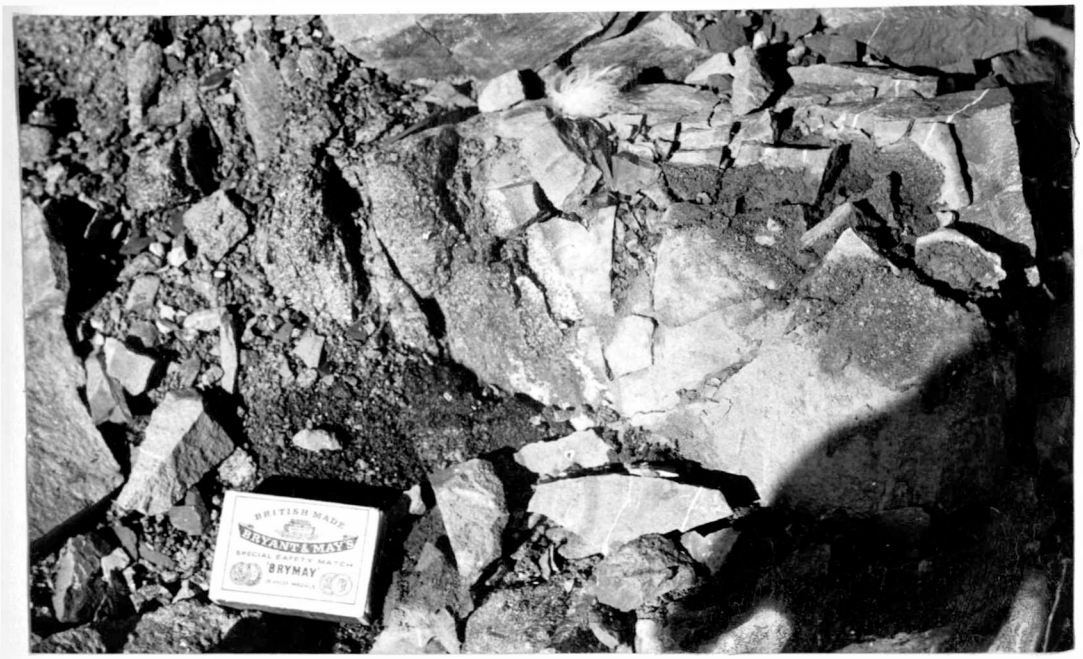

Fig. 30. Rheomorphic vein in coarse-grained rotten dolerite about 7 m. above the base of the upper sill of point 2600 (Z.494); it is poorly defined and there has been some reaction between the dolerite and the remobilized sediments.

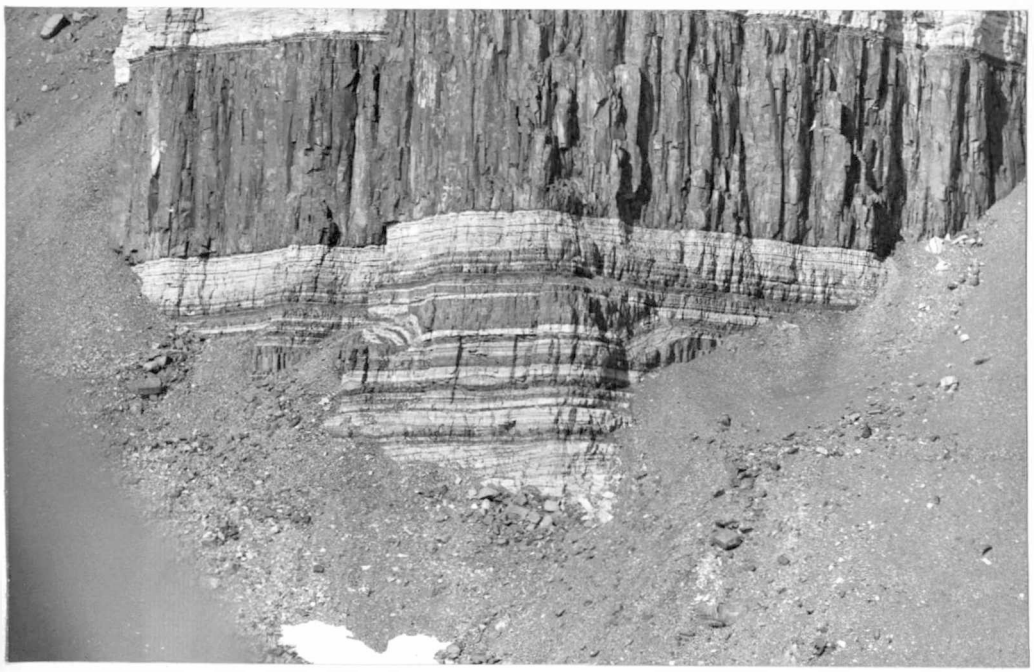

Fig. 31. Minor sill in the sediments beneath the basal sill of Coalseam Cliffs; small variations in attitude of the sill have tilted, over short distances, the intruded sediments.

The upper sill at Stewart Buttress and Mount Faraway is about 60 m. thick. It is apparently concordant and essentially horizontal in attitude.

Between these major sills, numerous minor sills intrude the sediments. They are up to 5 m. thick and often show great variations in horizon compared to their thickness. Over short distances they have tilted the sediments which they intrude (Fig. 31). They are variable in composition but no evidence of different phases of intrusion was observed. They are usually fine-grained and chilled at the contacts. Some have sharp regular contacts but others show a complex intermixture of partly mobilized sediments (especially coal) and chilled dolerite at the contact.

5. Summary and correlation

Detailed relationships between dolerite and sediments vary but all are clearly intrusive and there are no extrusive equivalents. Most intrusions are sills, dykes being rare, and they are often transgressive on a small scale, though generally concordant. Many are intruded along or very near coal seams.

The thickest and most extensive sill in the Theron Mountains is the scarp-capping sill, with a volume of at least 120 km.^{3} Other sills intrude the sediments both above

and below the scarp-capping sill; these are thinner, usually less than 60 m. and often 1-10 m., and less continuous. Exact relationships between sills of different thicknesses and compositions are not always clear but at least three and possibly four phases of intrusion have been recognized in Marø Cliffs (p. 64) and Lenton Bluff (p. 65).

Most of the thicker sills are alike in being medium- to coarse-grained with chilled margins, though compositions and hence weathering colours are variable. Thinner sills and dykes are uniformly fine-grained. Layering is seen only in the basal sills of stations Z.497 and 481. Granophyric dolerite is common in some sills, especially the scarp-capping sill and the middle sill of Coalseam Cliffs, and dolerite-pegmatite occurs near the top of the layered sill of Marø Cliffs.

Contacts are usually sharp with little sign of reaction between sediments and dolerite, though syntectic phenomena were noted in association with some sills, such as the basal sill of Lenton Bluff, the layered sill of Marø Cliffs and the upper sill of point 2600. Xenoliths and pendant blocks of sediments and apophyses of dolerite into the sediments are rare, though they are common in the basal sill of Lenton Bluff. Hydrothermal mineralization is seen in some sills and dykes, such as the basal sill and the younger dykes of Lenton Bluff.

Jurassic dolerite intrusions (Ferrar dolerites) co-extensive with sediments of the Beacon Supergroup have been described from many places in eastern Antarctica.

In Victoria Land, the Ferrar dolerites are mainly very thick sills (90-460 m.) and individual sills are of great extent. The volume of the Basement sill is over 800 km.^{3} (Hamilton, 1964) and that of the Peneplain sill is over 4,000 km.^{3} (Gunn and Warren, 1962). In the Nimrod—Beardmore—Axel Heiberg Glaciers region, Grindley and others (1964) noted sills ranging in thickness from as little as 10 m. to over 500 m., averaging 60-200 m. Dolerite sills 10-200 m. thick, and in places their extrusive equivalents, have also been noted in the Horlick Mountains (Long, 1964), the Pensacola Mountains (Schmidt and others, 1964), the Whichaway Nunataks (Stephenson, 1966) and western Dronning Maud Land (Juckes, in press; Hjelle and Winsnes, 1971; Aucamp and others, 1971).

Many of the features noted in the sills of the Theron Mountains are present in the Ferrar dolerites. Most of the sills are generally concordant, though inclined sheets are present (e.g. McGregor, 1965) and all have cross-cutting segments by which they shift from one stratigraphical level to another; changes in stratigraphical level are also accomplished by intrusion-faulting. Extreme local

irregularity of contacts is common but, though interfingering of dolerite and sediments and baking of the sediments has been noted, syntectic phenomena are uncommon. Hamilton (1964) suggested on the basis of geochemical evidence that there was some marginal reaction between the dolerite and the intruded sandstone and shale at the lower, moderately inclined contact of the sheet at the east base of Pyramid Mountain in Victoria Land. Xenoliths and rafts of sediments are a common feature of many of the sheets. Layering is uncommon and examples have been noted above (p. 67 and 69); it also occurs in the lopolithic Dufek intrusion of the Pensacola Mountains (Aughenbaugh, 1967).

Other Mesozoic tholeiitic rocks of the Southern Hemisphere are shown in Fig. 11.

The field characters of the Karroo dolerites of southern Africa are in many ways similar to those of the Theron Mountains. They occur as horizontal and inclined sheets and thin dykes and they can be traced over great distances; the lowest sheet north of Hopetown, Cape Province, covered at least 12,800 km.^{2} (Du Toit, 1954). Horizontal sheets follow more or less concordantly the bedding planes of invaded strata, especially along or next to coal seams in the Middle Ecca Series, but the majority of sheets are inclined and transgressive; there has been relatively

little tilting of the invaded strata. The sheets range in thickness from 15-150 m. but bodies 300-600 m. thick are found in the Eastern Province, Transkei and southern Natal. Different phases of intrusion have been proved in places by actual intrusive contacts. Walker and Poldervaart (1949) considered that the magma was extremely active towards the intruded sediments at all horizons and Mountain (1935) described veins of sedimentary material, derived from the floor of the sill, intruding the dolerite sill at Coedmore Quarries, Durban, Pale material occurring as inclusions and veins in the dolerite sheets of eastern Cape Province (Mountain, 1960) includes mobilized sediments and xenoliths of sedimentary origin. Du Toit (1954), however, considered syntectic phenomena at contacts to be rare compared with the normal sharp contacts showing no reaction whatsoever. Layering is uncommon but picrite segregations occur in the gabbro-norite of the lopolithic Insizwa sheet of Karroo age (Scholtz, 1936).

The Jurassic dolerites of Tasmania intrude horizontally bedded or gently tilted Permo-Carboniferous and Triassic sediments. They occur as sills, up to over 300 m. thick, occasional laccoliths and large ramifying dyke-like bodies (Edwards, 1942) and they are of great extent, the volume for present outcrops being about 3,100 $km.^3$

The Serra Geral Formation in South America covers a surface area of about 10^6 km.^{2} (Creer, 1962) and consists of flows of individual thickness up to 80 m., dykes a few to tens of metres thick and sills up to about 200 m. thick and covering hundreds of km.^{2} The total volume is estimated at 3.5×10^5 km.^{3} It is dominantly of Cretaceous age.

The Rajmahal Traps of India are a 600 m. thick sequence of sub-horizontal basaltic flows, individually 20-75 m. thick cropping out over an area of 3,900 km.^{2} (McDougall and McElhinny, 1970). They are of Cretaceous age. The Sylhet Traps are a series of basaltic lava flows and associated dolerite dykes overlying Archaean crystalline metamorphic rocks and overlain by Cretaceous sandstones (Athavale and others, 1962). The extent of exposure is small and that in thick forest regions.

B. PETROGRAPHY

The dolerite intrusions of the Theron Mountains are variable in petrography, ranging in composition from the extreme olivine-hypersthene-orthocumulates of the layered sills to the granophyric quartz-dolerites of the scarp-capping sill and the middle sill of Coalseam Cliffs. Some of the sills were sampled more extensively than others and these are considered separately below; the major

petrographical features of these and other intrusions are compared with those of other Jurassic dolerites of Antarctica and of other Southern Hemisphere continents.

Plagioclase compositions have been determined by the extinction angles on combined Carlsbad-albite twins and they are probably accurate to within about 5 per cent An content. Pigeonitic and augitic clinopyroxenes have been separated on the basis of optic axial angles estimated from interference figures but orthopyroxene and olivine compositions have not been determined. Fayalitic olivine has been distinguished from more magnesian olivine on the basis of the minerals associated with it and its optic axial angle, estimated from interference figures; in some cases this appears to be almost as low as that of augite.

Modal percentages have been calculated from thin sections using a Swift Automatic Point Counter and they are based on a minimum of 1,500 points. In porphyritic chilled marginal rocks the proportion of phenocrysts has probably been slightly over-estimated because of the gradation in grain-size between phenocrysts and groundmass crystals in many rocks. Olivine and pseudomorphs apparently after olivine have generally been counted together. Alteration products have not been differentiated and they include hornblende, biotite, chlorite and unidentified green and

brown material, some of which may be bowlingite or iddingsite.

1. Scarp-capping sill

This sill is formed of medium-grained granophyric quartz-dolerite of which the major constituents are plagioclase, clinopyroxene and a micrographic intergrowth of quartz and alkali-feldspar; skeletal and well formed iron ore crystals are present throughout and fayalitic olivine, apatite and zircon are common accessories; hornblende, biotite and chlorite occur as alteration products, though some may be of primary origin. Textural and compositional variations from the vitrophyric margins are rapid but there is relatively little variation higher than about 4-5 m. above the lower contact of the sill. Modal analyses of porphyritic rocks are given in Table III and of medium-grained rocks in Table IV.

The lower contact rock is a spherulitic porphyritic dolerite (Z.478.4a and 497.2) with microphenocrysts of plagioclase (An_{60-65}) and pigeonite within 0.1 mm. of the plane of contact. Within a few centimetres of the contact (Z.478.2 and 4b), the phenocrysts are in a hemicrystalline groundmass of plagioclase and pyroxene microlites and they occur as clusters of larger but slightly less idiomorphic

TABLE III

MODAL ANALYSES OF ROCKS FROM THE CHILLED MARGINS OF JURASSIC DOLERITE INTRUSIONS IN THE THERON MOUNTAINS, ANTARCTICA

Specimen number	Plagioclase	Pyroxene*	Olivine†	Counts	Plagioclase Composition	Name of sill
TAE 351/3	-	(1)	1		---	Scarp-capping sill
TAE 351/4	3	1	-		An_{60}	
Z.478.4	1.9	0.9	-	6,600	An_{60-65}	
Z.478.2	1.8	0.5	-	3,100	An_{60-65}	
Z.497.2	2.0	0.6	-	3,100	An_{58}	
Z.490.1	1.3	0.4	-	4,500	An_{55-60}	
Z.490.2	1.5	1.1	-	1,600	An_{66}	
Z.483.1a	6.3	-	-	2,100	Saussuritized	Apparent branch sill of the scarp-capping sill in Marø Cliffs
Z.472.7	10.4	3.8	0.7	4,500	An_{64}	Basal Sill of Lenton Bluff
Z.472.8	12.9		3.5	1,500	Albitized	
Z.472.9	9.4	3.7	0.6	7,900	An_{60-70}	
Z.472.12a	10.9	4.4	1.1	2,600	An_{66}	
Z.471.10	11.1	6.7	-	2,200	An_{60}	
Z.471.14	3.0	-	1.2	3,700	An_{60}	Younger transgressive sill of Lenton Bluff
Z.480.1a	10.9	0.3	8.5	2,900	An_{67}	Third-phase sill of Marø Cliffs
Z.480.2	8.8	0.5	5.6	3,300	An_{62}	
Z.475.2	-	-	2.7	5,900	---	Middle sill of Coalseam Cliffs
Z.478.10	11.8	-	5.7	3,600	An_{65-70}	Basal sill of Coalseam Cliffs
Z.477.3	9.4	p	5.4	7,300	An_{62-70}	
Z.478.12	10.7	-	3.6	1,500	An_{60-72}	
TAE 350/6	-	-	1		---	Miscellaneous other intrusions
TAE 351/7	1	-	1		An_{80-85}	
Z.464.1	6.4	-	2.7	1,900	An_{66}	
Z.487.3	7.1	1.0	2.8	3,600	Albitized	

* Figures in parentheses refer to orthopyroxene, others are clinopyroxene.

† Pseudomorphs of bowlingite and magnetite apparently after olivine have been counted with olivine.

p = present.

a. Scarp-capping sill

a. Scarp-capping sill

TAE 351/3 Porphyritic chilled dolerite. Upper contact of the thick wedging sill of point 2600 (Stephenson, 1966, table 3, analysis 8).

TAE 351/4 Fine-grained porphyritic dolerite. About 9 m. below the upper contact of the thick wedging sill of point 2600 (Stephenson, 1966, table 3, analysis 9).

Z.478.4 Porphyritic chilled dolerite. Lower contact of the thick wedging sill of point 2600; in contact with a thin wedge of fine-grained dolerite.

Z.478.2 Porphyritic chilled dolerite. Lower contact of the thick wedging sill of point 2600; in contact with sediments.

Z.497.2 Porphyritic chilled dolerite. Lower contact of the scarp-capping sill in the cliffs along the south-western margin of Jeffries Glacier.

Z.490.1 Porphyritic chilled dolerite. Lower contact of the scarp-capping sill in the escarpment between Goldsmith Glacier and Lenton Bluff.

Z.490.2 Porphyritic chilled dolerite. Lower contact of the scarp-capping sill in the escarpment between Goldsmith Glacier and Lenton Bluff.

b. Apparent branch sill of the scarp-capping sill

Z.483.1a Hydrothermally altered chilled dolerite. Lower contact of the apparent branch sill of the scarp-capping sill in Marø Cliffs.

c. Basal sill of Lenton Bluff

Z.472.7 Porphyritic chilled dolerite. Contact with sedimentary xenolith in lower part of sill.

Z.472.8 Altered chilled dolerite. Contact with sedimentary xenolith in lower part of sill.

Z.472.9 Porphyritic chilled dolerite. Contact with sedimentary xenolith in lower part of sill.

Z.472.12a Porphyritic chilled dolerite. Contact with sedimentary xenolith in lower part of sill.

Z.471.10 Porphyritic chilled dolerite. Lower contact of the sill.

d. Younger transgressive sill of Lenton Bluff

Z.471.14 Porphyritic chilled dolerite. Upper contact of the sill, in contact with the basal sill of Lenton Bluff.

e. Third-phase sill of Marø Cliffs

Z.480.1a Porphyritic chilled dolerite. Upper contact of the sill in the cliffs beneath point 3300; in contact with the first-phase sill.

Z.480.2 Porphyritic chilled dolerite. Lower contact of the sill in the cliffs beneath point 3300; in contact with the first-phase sill.

f. Middle sill of Coalseam Cliffs

Z.475.2 Porphyritic chilled dolerite. Lower contact of the sill at the south-western end of Coalseam Cliffs.

g. Basal sill of Coalseam Cliffs

Z.478.10 Porphyritic chilled dolerite. Upper contact of the sill, beneath point 2600.

Z.477.3 Porphyritic chilled dolerite. Lower contact of the sill, beneath point 2600.

Z.478.12 Porphyritic chilled dolerite. Lower contact of the sill, beneath point 2600.

h. Miscellaneous other intrusions

TAE 350/6 Porphyritic chilled dolerite. Contact of the thin sill immediately below the basal sill of Coalseam Cliffs (Stephenson, 1966, table 3, analysis 7).

TAE 351/7 Chilled dolerite. Top contact of the thin sill which is the lowest sill beneath the basal sill of Coalseam Cliffs.

Z.464.1 Porphyritic chilled dolerite. Upper contact of the sill immediately above the scarp-capping sill on the south-western margin of Goldsmith Glacier.

Z.487.3 Porphyritic chilled dolerite. Upper contact of the 30 m. sill above the scarp-capping sill in the long cliff immediately north-east of the mouth of Goldsmith Glacier.

TABLE IV

MODAL ANALYSES OF SPECIMENS FROM JURASSIC DOLERITE INTRUSIONS IN THE THERON MOUNTAINS, ANTARCTICA

Specimen number	Micro-pegmatite	Plagio-clase	Clino-pyroxene	Ortho-pyroxene	Olivine*	Iron ore	Alter-ation	Matrix	Counts	Plagioclase Composition
TAE 351/6	25	33	29	-	(p)	7	p	-		An_{56}
Z.455.1	33.2	29.4	24.0	-	(2.9)	6.2	4.4	-	3,000	An_{60}
Z.468.1	43.9	31.7	13.5	-	(2.7)	3.2	5.0	-	1,900	An_{60}
Z.484.1	41.0	27.1	20.4	-	(2.4)	4.2	4.8	-	1,500	An_{60}
Z.485.1	31.1	31.6	23.0	-	(1.0)	3.9	9.4	-	2,300	An_{56}
Z.486.1	30.5	31.3	22.4	-	(2.3)	7.3	6.2	-	3,000	An_{57}
Z.487.1	27.2	31.7	27.5	-	-	8.8	4.9	-	3,200	An_{40-50}
Z.508.1	29.8	34.6	21.7	-	(2.4)	4.4	7.2	-	3,600	An_{55}
Z.478.1	31.1	24.5	21.2	-	(1.1)	4.3	17.9	-	2,100	An_{55}
Z.483.5	34.3	25.2	20.2	-	-	5.3	15.0	-	2,000	An_{45-55}
Z.483.9	27.8	34.6	23.7	-	0.4	5.6	8.0	-	2,000	An_{45-50}
Z.480.1b	-	45.6	23.6	-	-	1.5	15.9	13.4	2,400	An_{65}
Z.481.11	-	41.3	18.5	-	7.0	5.5	16.7	11.0	1,600	An_{70}
Z.483.6	-	36.1	17.7	-	2.4	5.7	27.6	10.8	2,000	An_{75}
Z.471.15	-	44.0	30.6	-	6.6	1.8	17.0		1,500	
Z.498.3	-	41.7	23.3	-	-	n.d.	11.2	23.8	1,600	
Z.471.13c	-	44.9	32.9	-	3.8	1.8	16.6		1,800	An_{64}
Z.481.2	-	29.5	17.7	17.0	24.8	3.9	7.1		2,500	An_{50-76}
Z.481.1	-	37.2	21.5	12.1	16.2	2.7	10.3		2,800	An_{45-70}
Z.497.10	-	29.0	9.2	18.0	30.4	2.8	10.6		4,600	An_{60}
Z.497.9	-	48.2	21.5	12.8	1.3	2.6	13.6		2,000	An_{70}
Z.479.2	22.5	42.9	25.1	6.6	-	1.3	1.6	-	2,700	An_{72}
Z.473.1	53.1	21.1	10.2	-	(4.1)	2.7	8.8	-	3,600	An_{35-47}
Z.476.1	27.5	30.4	29.3	-	(0.5)	5.1	7.2	-	3,600	An_{40-50}
Z.479.3	24.7	45.2	16.1	8.3	-	1.0	4.6	-	2,700	An_{66}
Z.475.1	18.3	42.4	21.1	11.0	p	1.2	6.0	-	1,800	An_{65-70}
Z.474.1	-	47.9	n.d.	-	14.0	n.d.	38.1		3,400	An_{65-70}
Z.478.11	-	47.6	17.0	-	3.3	4.6	27.5		2,300	An_{70}
Z.500.1	-	43.9	18.0	-	14.7	4.7	18.7		2,800	An_{68}
Z.477.4	-	52.4	20.9	-	11.8	6.4	8.5		1,900	An_{64}
Z.464.2	9.0	44.3	33.1	-	9.6	2.1	1.8	-	2,300	An_{70}
Z.464.3	14.6	48.5	31.1		-	4.0	1.6	-	2,500	
Z.461.1	14.8	41.5	26.7	-	-	2.6	14.4	-	2,900	
Z.461.2	-	48.3	36.9	-	5.4	2.0	4.7	2.7	1,600	
Z.509.1	-	38.0	27.8	-	-	3.5	12.5	18.1	1,700	
Z.453.3	-	38.0	30.2	-	0.4	n.d.	1.2	30.3	2,000	An_{68}
Z.453.1	-	52.9	35.3	-	9.6	1.8	0.4	-	3,500	An_{60-65}
Z.477.11	-	39.2	26.2	-	-	n.d.	3.6	31.0	3,200	

* Figures in parentheses refer to fayalitic olivine, others are magnesian olivine.

p = present.

n.d. = not determined (usually counted with matrix).

Alteration products include hornblende, biotite, chlorite, etc.

a. Scarp-capping sill

a. Scarp-capping sill

TAE 351/6 Granophyric quartz-dolerite. Near the centre of the thick wedging sill of point 2600 (Stephenson, 1966, table 3, analysis 10).

Z.455.1 Granophyric quartz-dolerite. About 40-50 m. below the upper contact on the eastern margin of the unnamed southern glacier.

Z.468.1 Granophyric quartz-dolerite. Near the centre of the sill on the south-western margin of Goldsmith Glacier.

Z.484.1 Granophyric quartz-dolerite. Upper third of the sill at Tailend Nunatak.

Z.485.1 Granophyric quartz-dolerite. About 150 m. below the upper contact in the escarpment between Tailend Nunatak and Goldsmith Glacier.

Z.486.1 Granophyric quartz-dolerite. About 150 m. below the upper contact in the escarpment between Tailend Nunatak and Goldsmith Glacier.

Z.487.1 Granophyric quartz-dolerite. About 150 m. below the upper contact in the long cliff immediately north-east of the mouth of Goldsmith Glacier.

Z.508.1 Granophyric quartz-dolerite. About 50 m. above the lower contact in the escarpment between Goldsmith Glacier and Lenton Bluff.

Z.478.1 Altered quartz-dolerite. About 6-7 m. above the lower contact of the thick wedging sill of point 2600.

Z.483.5 Altered quartz-dolerite. About 6-7 m. above the lower contact in Marø Cliffs.

b. Apparent branch sill of the scarp-capping sill

Z.483.9 Altered quartz-dolerite. Near the centre of the sill in Marø Cliffs.

c. First-phase sill of Marø Cliffs

Z.480.1b Altered dolerite. Near the centre of the sill at its contact with the third-phase sill in the cliffs beneath point 3300.

d. Third-phase sill of Marø Cliffs

Z.481.11 Ophitic olivine-dolerite. Near the centre of the sill at the south-western end of Marø Cliffs.

Z.483.6 Altered ophitic olivine-dolerite. Near the centre of the sill at the north-eastern end of Marø Cliffs.

e. Younger sills and dykes of Lenton Bluff

Z.471.15 Subophitic olivine-dolerite. About 1 m. below the upper contact of the sill which cuts the basal sill of Lenton Bluff.

Z.498.3 Intergranular dolerite. About 0.8 m. from the contact of a dyke in the sediments between the scarp-capping sill and the basal sill of Lenton Bluff.

Z.471.13c Intergranular to subophitic dolerite. Centre of the dyke which cuts the sediments beneath the basal sill of Lenton Bluff.

f. Layered sills

Z.481.2 Pyroxene-olivine-orthocumulate from a melanocratic layer in the lower part of the layered sill of Marø Cliffs.

Z.481.1 Plagioclase-pyroxene-olivine-orthocumulate from a leucocratic layer in the lower part of the layered sill of Marø Cliffs.

Z.497.10 Olivine-hypersthene-orthocumulate from the mafic layer approximately in the middle of the 50 m. layered sill on the south-western margin of Jeffries Glacier.

Z.497.9 Normal dolerite from beneath the mafic layer in the 50 m. layered sill on the south-western margin of Jeffries Glacier.

g. Middle sill of Coalsack Cliffs

Z.497.9 Normal dolerite from beneath the mafic layer in the 50 m. layered sill on the south-western margin of Jeffries Glacier.

g. Middle sill of Coalseam Cliffs

Z.479.2 Subophitic two-pyroxene dolerite. About 3 m. below the upper contact beneath Stewart Buttress.

Z.473.1 Granophyric dolerite. Upper part of the sill in a dolerite window in the ice cliffs between Coalseam Cliffs and Parry Point.

Z.476.1 Granophyric dolerite. Upper part of the sill in a dolerite window in the ice cliff at Parry Point.

Z.479.3 Subophitic two-pyroxene dolerite. About 10 m. above the lower contact beneath Stewart Buttress.

Z.475.1 Subophitic two-pyroxene dolerite. About 2 m. above the lower contact at the south-western end of Coalseam Cliffs.

h. Basal sill of Coalseam Cliffs

Z.474.1 Porphyritic olivine-dolerite, approaching a troctolitic composition. Just above the contact of a sedimentary xenolith about 6 m. below the upper contact at the south-western end of Coalseam Cliffs.

Z.478.11 Altered ophitic olivine-dolerite. Near the centre of the sill beneath point 2600.

Z.500.1 Ophitic olivine-dolerite. Lower part of the sill beneath Stewart Buttress.

Z.477.4 Ophitic olivine-dolerite. About 3 m. above the lower contact beneath point 2600.

i. Other intrusions

Z.464.2 Subophitic olivine-dolerite. Near the top of the sill immediately above the scarp-capping sill on the south-western margin of Goldsmith Glacier.

Z.464.3 Subophitic two-pyroxene quartz-dolerite. Near the centre of the sill immediately above the scarp-capping sill on the south-western margin of Goldsmith Glacier.

Z.461.1 Subophitic quartz-dolerite. Lower part of the first sill above the scarp-capping sill on the north-eastern margin of Jeffries Glacier.

Z.461.2 Olivine-dolerite. Near the upper contact of the first sill above the scarp-capping sill on the north-eastern margin of Jeffries Glacier.

Z.509.1 Intergranular dolerite. Near the centre of the 6 m. dyke on the north-eastern margin of Goldsmith Glacier.

Z.453.3 Intersertal dolerite. Centre of a 1-2 m. dyke along a fault plane in the ridge leading eastwards from point 3300.

Z.453.1 Olivine-dolerite. Near the centre of the 15 m. sill which is offset by a fault in the ridge leading eastwards from point 3300.

Z.477.11 Intersertal dolerite. Centre of the thin sill which is the lowest sill beneath the Basal Sill of Coalseam Cliffs.

crystals than in the spherulitic zone. About 1 m. from the contact (Z.497.1 and 498.1), the dolerite is subvariolitic to subophitic with skeletal laths of plagioclase (An_{60}) and pigeonite, 0.8-1.0 mm. in length and 0.1-0.2 mm. in breadth, and granular to skeletal iron ore; poorly crystallized plagioclase and pyroxene mesostasis areas up to 2-3 mm. across occur between the major constituents. Both specimens are highly altered, brown and green chloritic alteration products being especially abundant in the mesostasis and in association with skeletal iron ore.

The central parts of the sill are subophitic to granophyric quartz-dolerites with varying proportions of the major constituents (Table IV).

Plagioclase (An_{55}) usually occurs as idiomorphic stumpy prisms twinned on the albite law and often on the combined Carlsbad-albite laws. Normal zoning is common and there is some weak oscillatory zoning. It is frequently subophitically enclosed by pyroxene and hornblende and often forms the cores to areas of micropegmatite. It also occurs interstitially as larger, poorly twinned and strongly zoned, less idiomorphic crystals rimmed by cloudy alkali-feldspar which grades into micropegmatite; these are probably of later generation than the well twinned idiomorphic prisms.

Clinopyroxene occurs as plates up to 2 mm. across but more commonly it is subprismatic in outline, although

still partly enclosing plagioclase laths. Simple twinning is a common feature in both prismatic and plate-like crystals of clinopyroxene. In the lower 50-60 m. of the sill, pigeonitic cores to crystals are rimmed by augitic margins; the latter has a faint pinkish tinge which often deepens in colour towards the rims of crystals. Higher in the sill, pink titaniferous augite is apparently the sole pyroxene, though pigeonite re-appears as the upper margin is approached; Stephenson (1966) recorded pigeonite phenocrysts from the fine-grained porphyritic dolerite about 9 m. below the upper contact of the thick wedging sill of Coalseam Cliffs and orthopyroxene phenocrysts from the upper contact material. Both pigeonite and augite show marginal alteration to brown hornblende and biotite which are in turn replaced by green and greenish brown chloritic material; fayalitic olivine may also be formed at the expense of pyroxene (Fig. 32).

Large areas of micropegmatite are present in most specimens examined. Clear quartz forms a micrographic intergrowth with cloudy alkali-feldspar in approximately equal proportions; this sometimes forms at the expense of plagioclase, either marginally or along twin planes. Clusters of apatite needles are a constant accessory in areas of micropegmatite.

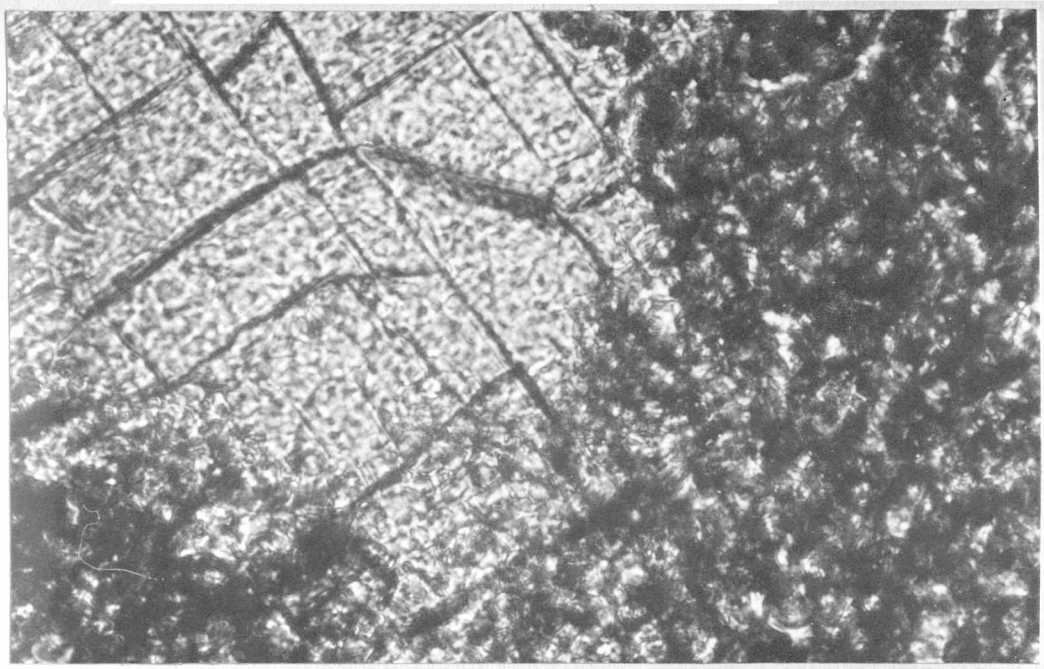

Fig. 32. Photomicrograph of clinopyroxene which is being marginally replaced by minute granular fayalite (Z.468.1, ordinary light, x 450).

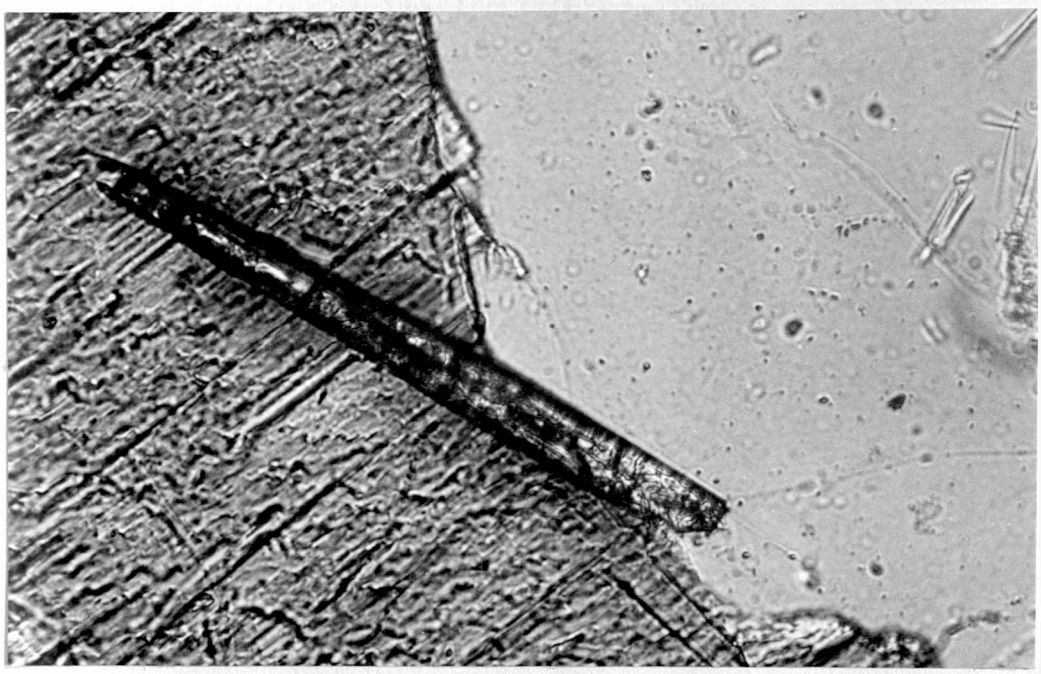

Fig. 33. Photomicrograph of a zircon needle penetrating hornblende with a slight halo effect (Z.487.1, ordinary light, x 450).

Fayalitic olivine, often replaced by a yellowish brown almost isotropic mineral (iddingsite or chlorophaeite) is a common accessory. Iron ore (ilmenite and titanomagnetite) occurs as well formed and skeletal crystals, the latter often being associated with bowlingitic alteration. Zircon is present in some specimens as needles (Fig. 33) or as minute crystals forming the cores to haloes in biotite and chlorite.

The thin wedge of fine-grained dolerite interspersed between the scarp-capping sill and the sediments at station Z.478 is petrographically distinct. It is a highly altered fine-grained porphyritic dolerite with idiomorphic phenocrysts, up to 1 mm. across, of chlorite and iron ore (Fig. 34), probably after olivine, in a fine-grained matrix of skeletal plagioclase (An_{65}) laths and allotriomorphic pyroxene, which often occurs in radiating fibrous clusters. Interstitial areas of brown devitrified glass with minute granular opaque minerals are more abundant nearer the contact of the scarp-capping sill (Z.478.4a) than in the middle of the thin wedge (Z.478.3). Idiomorphic haematite occurs in the groundmass and in veinlets of chlorite and a fibrous highly birefringent mineral.

The apparent branch sill of the scarp-capping sill in Marø Cliffs is considered with the different intrusive

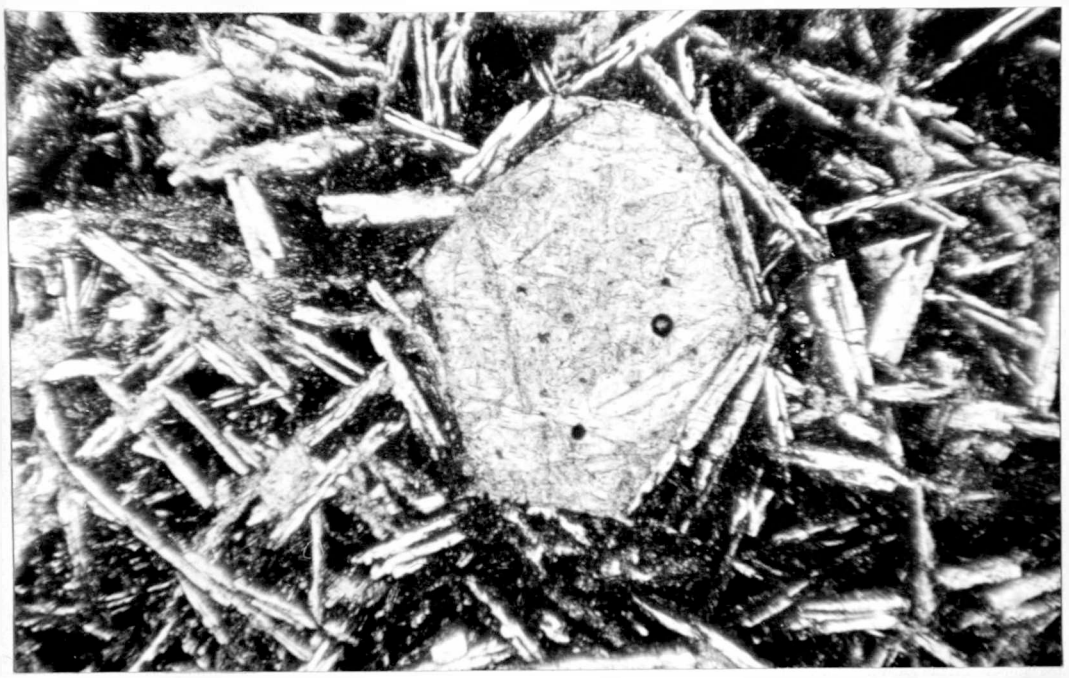

Fig. 34. Photomicrograph of fine-grained porphyritic dolerite intruded by the scarp-capping sill in Coalseam Cliffs. Idiomorphic phenocrysts of chlorite and (?) talc, probably after olivine, are set in a fine-grained groundmass of skeletal plagioclase and fibrous radiating pyroxene (Z.478.3, ordinary light, x 65).

phases of Marø Cliffs and Lenton Bluff, of which it forms a part.

2. Different intrusive phases

At least three phases of intrusion have been recognized in Marø Cliffs and Lenton Bluff on field evidence (p. 63). They are petrographically distinct (Tables III and IV). Correlation with other minor intrusions on the basis of petrography is uncertain.

a. Marø Cliffs

In Marø Cliffs and the cliffs beneath point 3300, the first phase of intrusion is characterized by the absence of olivine and by the presence in holocrystalline specimens of a poorly crystallized cloudy, quartzo-feldspathic mesostasis. In specimen Z.483.7, from about 0.8 m. above the lower contact, idiomorphic pseudomorphs of calcite, bowlingite, magnetite and quartz may be after olivine but other near-contact rocks (Z.481.9 and 502.1) are not markedly porphyritic and olivine is absent; they consist of radiating clusters of skeletal laths of plagioclase and pyroxene with intersertal areas of partly devitrified glass. The central parts of the sill (Z.480.1b and 3) consist of altered, medium- to coarse-grained subophitic dolerite with a cloudy felsic mesostasis; alteration may be due to hydrothermal activity or to thermal metamorphism by the third-phase sill.

The second phase of intrusion in Marø Cliffs is the apparent branch sill of the scarp-capping sill; it is an inequigranular, medium-grained, subophitic to intergranular dolerite with a poorly crystallized groundmass which occasionally develops as micropegmatite. The lower contact (Z.483.1a) is a highly altered, porphyritic hemicrystalline dolerite with saussuritized phenocrysts of plagioclase (Fig. 35) up to 2 mm. long in a groundmass of plagioclase microlites and alteration products. Veinlets of quartz, albite, chlorite and epidote cut the rock and there are amygdales, about 0.4 mm. across, surrounded by a 0.1 mm. wide margin of radial green chlorite. The central parts of the sill (Z.483.8 and 9) consist of medium-grained intergranular to subophitic dolerite with rare glomeroporphyritic clusters of idiomorphic plagioclase (An_{58}) crystals up to 4.0 mm. by 0.4 mm. Generally plagioclase occurs as well twinned crystals less than 1 mm. long enclosed by granular aggregates of neutral to pale pink, zoned and twinned pigeonite or as strongly zoned interstitial crystals which pass into alkali-feldspar and micropegmatite. Marginal alteration of pyroxene to brown hornblende is common and fayalitic olivine, largely altered to yellowish brown, strongly pleochroic iddingsite, is present in small amounts. Skeletal ilmenite and titano-magnetite are often associated

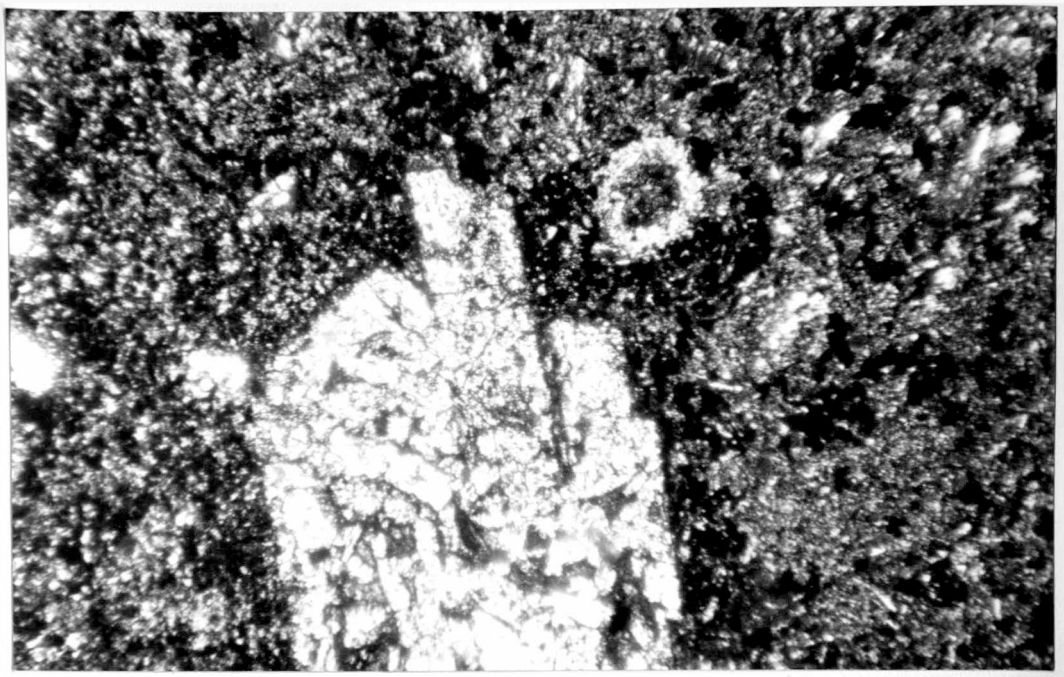

Fig. 35. Photomicrograph of highly altered porphyritic hemicrystalline dolerite at the lower contact of the apparent branch sill of the scarp-capping sill, which forms the second phase of intrusion in Marø Cliffs. Saussuritization of plagioclase phenocrysts and chloritization of the groundmass is probably of hydrothermal origin (Z.483.1a, ordinary light, x 65).

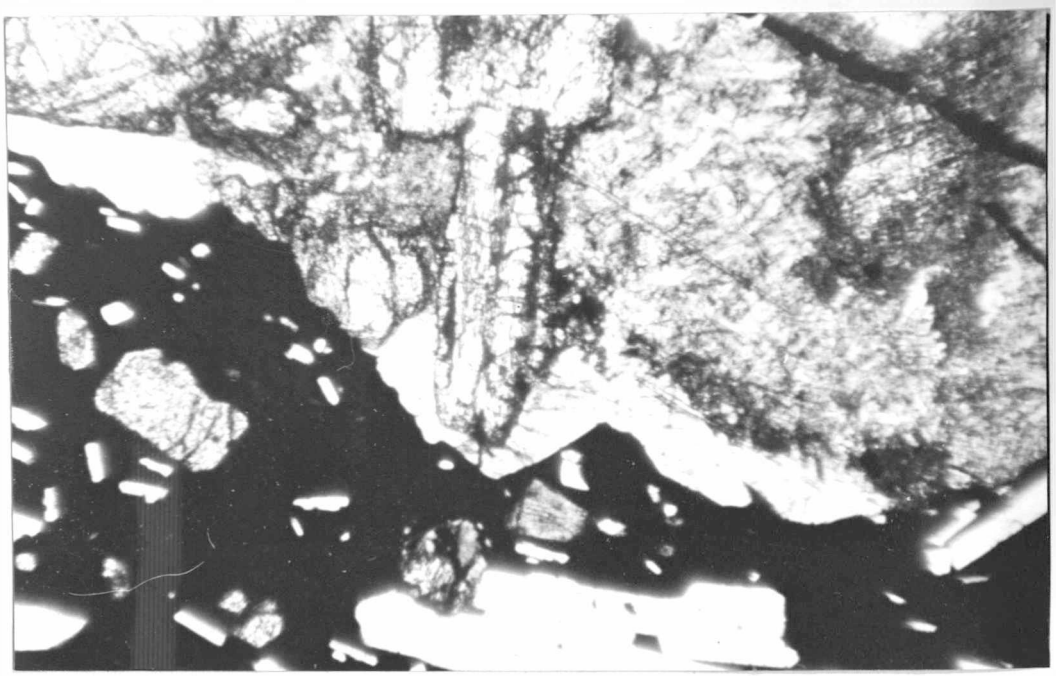

Fig. 36. Photomicrograph of the contact of the first- and third-phase sills in the cliffs beneath point 3300. The latter is vitrophyric, with idiomorphic phenocrysts of plagioclase and olivine, while the former is highly altered; the contact is sharp and there has apparently been little reaction (Z.480.1, ordinary light, x 65).

with iddingsite or viridite. The groundmass is a poorly crystallized intergrowth of clear quartz and cloudy, sericitized alkali-feldspar with abundant small apatite needles, minute brown biotite flakes and viridite, often penetrated by rods of iron ore.

The third phase of intrusion at Marø Cliffs is olivine-bearing throughout and textures vary from vitrophyric in contact rocks (Z.480.1a and 2) to ophitic in the central parts of the sill (Z.481.11 and 483.6). Idiomorphic phenocrysts of plagioclase (An_{67}) and olivine with rare pigeonite occur in a groundmass which is holohyaline at the contact with the first-phase sill (Fig. 36) and hemicrystalline with an acicular texture a few centimetres from that contact. In the central parts of the sill, plagioclase (An_{70-75}) laths are ophitically enclosed by pink titaniferous augite, which is commonly zoned and often altered to green chloritic material; small granular olivine crystals, often altered to bowlingite and magnetite, are also enclosed by pyroxene. Skeletal iron ore is common and the poorly crystallized, largely altered feldspathic mesostasis may contain secondary quartz.

b. Lenton Bluff

At Lenton Bluff, the basal sill, which is probably equivalent to the apparent branch sill of the scarp-capping

sill in Marø Cliffs, is the oldest phase of intrusion recognized. It is pigeonite- and olivine-bearing throughout and there is some variation in composition but the main variation is in texture. Chilled rocks occur not only at the upper and lower margins but also at the contacts of sedimentary xenoliths. The contact is sharp (Z.471.10) with a holohyaline margin about 0.1 mm. thick between the intruded sediments and the porphyritic hemicrystalline dolerite; there is some interdigitation of the two and small blebs of dolerite up to 0.5 mm. across are isolated within the sediments as much as 2-3 mm. from the contact. Idiomorphic phenocrysts, about 0.5 mm. by 0.2 mm. but up to 1.5 mm. by 0.8 mm., of plagioclase (An_{60}) are often rimmed by granular pigeonite crystals about 0.1 mm. across. Rare aggregates of magnetite, bowlingite and biotite surrounded by a "reaction rim" of biotite are probably pseudomorphs after olivine. The groundmass is generally cryptocrystalline with minute granular iron ore and secondary biotite but phenocrysts are often rimmed by about 0.05 mm. of holohyaline material. A vague cooling-contraction pattern with a pseudohexagonal pattern of lighter-coloured groundmass surrounding plagioclase microphenocrysts or incipient crystals is present.

At the contact with xenoliths (Z.472.9a and 12a), idiomorphic phenocrysts of plagioclase (An_{65}), pigeonite

and olivine attain 5, 2 and 1 mm. in length, respectively; pseudomorphs after olivine often form the cores to large pigeonite crystals which commonly partly enclose plagioclase in glomeroporphyritic clusters. Flow layering occurs in the groundmass (Fig. 37).

Within less than 1 m. of the contact (Z.471.11b and 472.9e), the rock is a porphyritic, fine-grained intergranular dolerite with sericitized and albitized phenocrysts of plagioclase in a groundmass of plagioclase (An_{59}) laths and granular pigeonite, chlorite, biotite and abundant iron ore. The lower part of the sill (Z.472.4 and 11) is a glomeroporphyritic, fine- to medium-grained, intergranular to subophitic dolerite. Plagioclase (An_{63}) laths, 0.8-1.0 mm. long, are subophitically enclosed by granular aggregates of pigeonite in a poorly crystallized groundmass of plagioclase, chlorite, pyroxene and rod-like iron ore with minute apatite needles and possibly alkali-feldspar and quartz. Large, hypidiomorphic, fayalitic olivine phenocrysts are associated with plagioclase phenocrysts up to 6 mm. long in glomeroporphyritic clusters. Small, granular groundmass olivines show marginal alteration and pseudomorphs of bowlingite and magnetite after olivine form the cores of some pyroxene crystals.

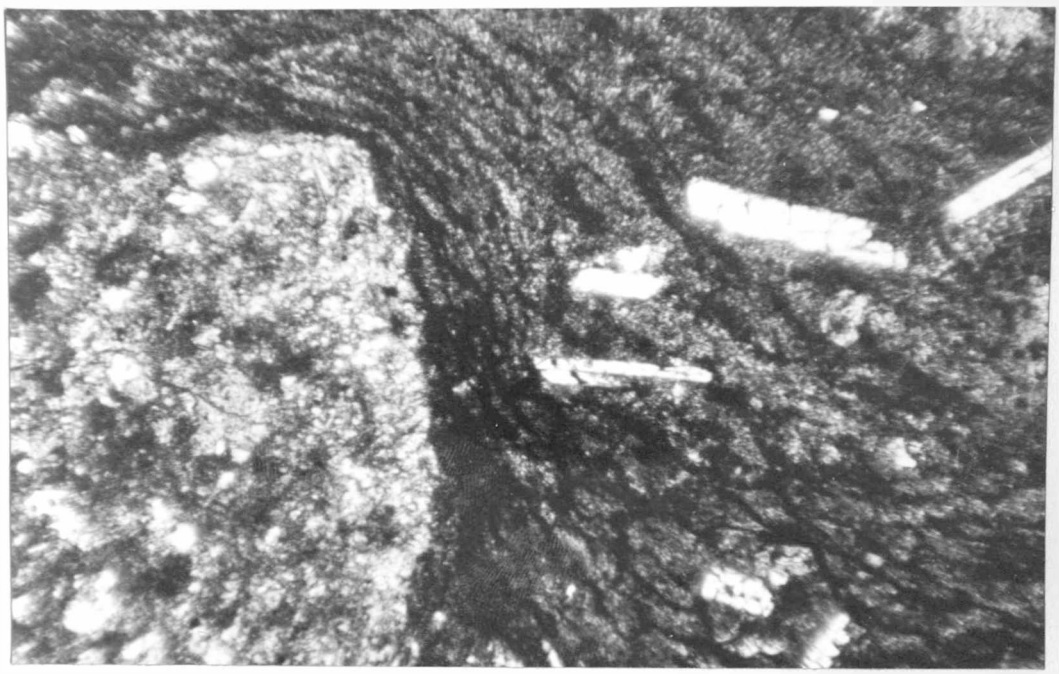

Fig. 37. Photomicrograph of the upper contact of a xenolith in the basal sill of Lenton Bluff. The vitrophyric dolerite shows flow layering (Z.472.12a, ordinary light, x 65).

The upper part of the sill (Z.471.16) is coarser-grained, olivine is absent, ilmenite occurs as well formed and skeletal crystals about 0.2 mm. across and there is a micropegmatitic mesostasis. It is highly altered, possibly due to thermal metamorphism by the younger transgressive sill, and granular aggregates of pyroxene appear to result from the breakdown of large plates rather than from separate nucleation during crystallization, as in the lower part of the sill.

The basal sill of Lenton Bluff is cut at station Z.471 by a younger transgressive sill about 5 m. thick. This continues as a system of thin dykes and sills at station Z.498 and it may be connected with the thin dyke beneath the basal sill at station Z.471. At the contact (Z.471.14) it is porphyritic with idiomorphic phenocrysts of plagioclase and bowlingite, after olivine, in a hemi-crystalline variolitic groundmass of plagioclase and pyroxene which is commonly altered to a lime-green chloritic material dotted with granular opaque minerals. The intersertal dolerite 1 m. below the contact (Z.471.15) contains some fresh olivine as well as pseudomorphs of bowlingite and magnetite. Sills from station Z.498 (Z.498.8 and 9) have an intergranular to intersertal texture with plagioclase laths separated by granular pigeonite in an altered hemi-

crystalline groundmass. Dykes from the same station (Z.498.3 and 5) consist of altered, fine-grained subvariolitic dolerite with short, stumpy laths of plagioclase in a chloritic groundmass with scattered, interstitial opaque minerals.

At the contact of the dyke below the basal sill (Z.471.13a), it is a fine-grained, slightly porphyritic, altered olivine-dolerite with pseudomorphs of viridite and iron ore, probably after olivine, in a variolitic groundmass of plagioclase, altered pyroxene and iron ore. The centre of the dyke (Z.471.13c) is a fine- to medium-grained, intergranular to subophitic olivine-dolerite with plagioclase (An_{64}) laths up to 2 mm. in length separated and partly enclosed by granular to plate-like augite which is often zoned from colourless cores to pink titaniferous rims; complex micrographic intergrowths are common. Idiomorphic to allotriomorphic pseudomorphs of magnetite and iddingsite are probably after olivine, though no remnants are preserved.

3. Layered sills

Two sills, one alongside Jeffries Glacier and the other in Marø Cliffs, show layering of different types. They are similar, however, in having mafic layers which are orthocumulates (Wager and others, 1960) in which olivine is a dominant cumulus mineral. Modal analyses are given in Tables IV and V.

a. Jeffries Glacier

The basal sill in the cliffs on the south-western margin of Jeffries Glacier (Z.497) has a mafic layer approximately through the middle of the sill (p. 66). Two specimens have been examined, one from the normal dolerite below the mafic layer (Z.497.9; Fig. 38) and one from the mafic layer itself (Z.497.10; Fig. 39).

The normal dolerite is a coarse-grained, olivine-bearing, two-pyroxene dolerite with an altered felsic mesostasis. Plagioclase (An_{70}) laths, 1-2 mm. long, with well defined twinning and weak normal zoning are partly enclosed by orthopyroxene and clinopyroxene and by a later generation of plagioclase; the latter is more equant than the twinned laths, is strongly zoned and shows poorly defined twinning. Orthopyroxene occurs as large sub-prismatic crystals up to 4 mm. long, which are commonly rimmed by clinopyroxene and altered along curving cracks and outwards from them along cleavages to yellowish green bowlingite; pseudomorphs of bowlingite after orthopyroxene occur rarely. Well developed crystal faces are rare and the orthopyroxene often partly encloses plagioclase laths. Clinopyroxene is most commonly built onto orthopyroxene crystals and subophitically encloses plagioclase laths but it also occurs as separate plates; the texture is nesophitic

Fig. 38. Layered sill of Jeffries Glacier: photomicrograph of part of the mafic layer, consisting of olivine, orthopyroxene and clinopyroxene with interstitial plagioclase (Z.497.10, ordinary light, x 65).

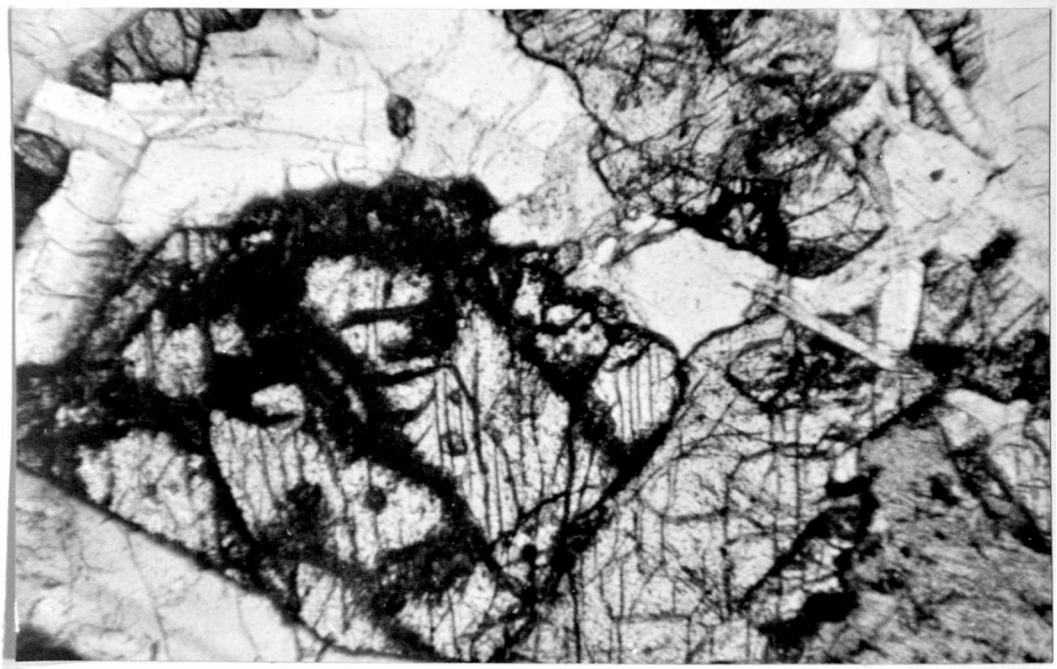

Fig. 39. Layered sill of Jeffries Glacier: photomicrograph of the normal dolerite below the mafic layer; plagioclase is more common and it is not dominantly interstitial (cf. Fig. 38) (Z.497.9, ordinary light, x 65).

(Walker, 1957). Clinopyroxene is neutral to pale pink in colour with faint colour zoning; the zoning probably ranges from pigeonitic cores to augitic margins. Fresh olivine is rare but large allotriomorphic pseudomorphs of bowlingite, (?) talc and magnetite moulded on plagioclase and rimmed by clinopyroxene are probably after olivine. The mesostasis consists of poorly crystallized feldspathic material, including alkali-feldspar and micropegmatites; apatite needles, minute biotite and chlorite flakes and rod-like magnetite are common.

The mafic layer is of slightly coarser grain-size and the ratio of femic to mafic minerals and the order of abundance of the main ferromagnesian minerals are reversed. Plagioclase (An_{70}) occurs as hypidiomorphic laths 1.5 mm. long and, dominantly, as interstitial strongly zoned crystals. Fresh olivine up to 2-3 mm. across is common; it occurs either as somewhat skeletal idiomorphic or as allotriomorphic crystals showing an ophitic relationship towards plagioclase; mantling by orthopyroxene and, more rarely, clinopyroxene, and alteration to magnetite and (?) talc are common. Orthopyroxene occurs as large sub-prismatic crystals up to 4 mm. long; bowlingitic alteration, which is typical of specimen Z.497.9 is absent. Clinopyroxene commonly mantles orthopyroxene and also occurs as subophitic plates 1-2 mm. across;

it is colourless to neutral and only rarely pale pink, and zoning and twinning are uncommon. The mesostasis consists largely of feldspathic material with fibrous chlorite and sericite, apatite needles, rare biotite flakes and rod-like iron ore; olivine is invariably altered and plagioclase develops a marginal rim of alkali-feldspar when in contact with the mesostasis.

Both of the above specimens are orthocumulates. Cumulus minerals are olivine, plagioclase and orthopyroxene in the mafic layer and plagioclase, orthopyroxene and clinopyroxene in the lower part of the sill; intercumulus minerals include plagioclase, clinopyroxene, iron ore and the poorly crystallized mesostasis. The mafic layer is relatively high in the sill and some of the textures suggest rapid crystallization of successive fractions rather than accumulation of crystals due to settling. Zoning of olivine, pyroxene and plagioclase suggest some intercumulus additions to cumulus minerals.

The mafic layer of this sill is similar to the olivine-diabase layer of the Palisades sill of New Jersey (Walker, 1940). The hypersthene-rich cumulates of the Ferrar dolerites and Kirkpatrick basalts of the Queen Alexandra Range (Grindley, 1963) and the "hypersthene-orthocumulates" of the Basement, Upper Escalade and Mount

Egerton sills of Victoria Land (Gunn, 1962; 1963) are in marked contrast petrographically (Table V).

b. Marø Cliffs

The basal sill at the south-western end of Marø Cliffs (Z.481) shows rhythmic layering in its lower 8 m. and dolerite-pegmatite near its upper margin. Specimens examined include both leucocratic (Z.481.1) and melanocratic (Z.481.2) layers, a complete section through the thin, finer-grained, darker-weathering band in the dolerite-pegmatite (Z.481.4 and 5) and the upper contact material near a thin rheomorphic vein (Z.481.6).

Both leucocratic (Fig. 40) and melanocratic (Fig. 41) layers are orthocumulates with varying proportions (Tables IV and V) of olivine, orthopyroxene and clinopyroxene as cumulus minerals, though plagioclase (An_{70}) is also a cumulus mineral in the leucocratic layer. The cumulus minerals, 0.5-2.0 mm. across, are idiomorphic and zoning is confined to the margins. Olivine is often skeletal, though showing good crystal form, and it is more altered in the leucocratic layer. Orthopyroxene and clinopyroxene mantle olivine in both specimens and the leucocratic layer has complex intergrowths of orthopyroxene and skeletal olivine with interstitial plagioclase. The intercumulus material is largely an intergrowth of strongly zoned

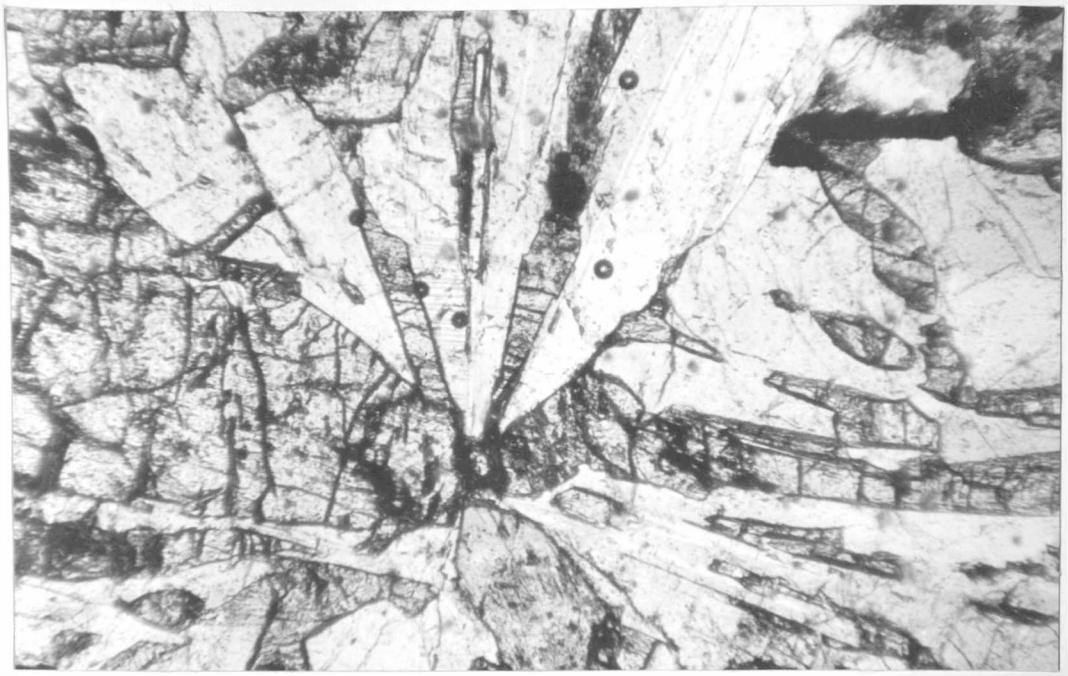

Fig. 40. Layered sill of Marø Cliffs: photomicrograph of a leucocratic layer showing a single nucleation centre and radiation from it of plagioclase, orthopyroxene and clinopyroxene (Z.481.1, ordinary light, x 65).

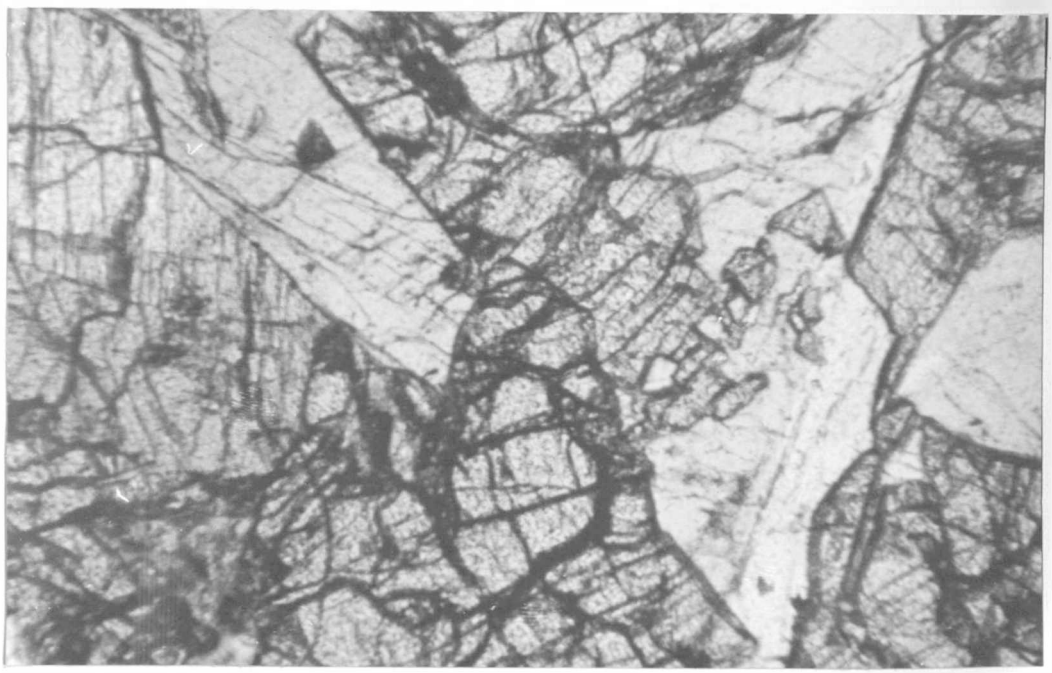

Fig. 41. Layered sill of Marø Cliffs: photomicrograph of a melanocratic layer consisting of olivine, orthopyroxene and clinopyroxene with interstitial plagioclase (cf. Fig. 40) (Z.481.2, ordinary light, x 65).

plagioclase (possibly as low as An_{45-50}) and pyroxene, the latter often growing along plagioclase twin planes. Pyroxene is zoned from colourless pigeonitic cores to pink augitic margins or from orthopyroxene to clinopyroxene. Slow crystallization of the intercumulus material has led in the leucocratic layer to radiation from one nucleation centre (Fig. 40) of orthopyroxene, clinopyroxene and plagioclase. A residual felsic mesostasis is present in small amounts and this includes alkali-feldspar, apatite, quartz and rod-like iron ore.

The dolerite-pegmatite near the top of the sill (Z.481.4) consists of long laths of plagioclase (An_{64}), 0.5-15.0 mm. long, clinopyroxene and rare orthopyroxene. Slivers of pyroxene along plagioclase twin planes are abundant and a complex intergrowth of the two minerals is common. Clinopyroxene is zoned from colourless pigeonitic cores to pink titaniferous augitic margins. Orthopyroxene, commonly altered to bowlingite, is rimmed by pigeonite. Plagioclase and alkali-feldspar are dominant in the poorly crystallized mesostasis and there is some micropegmatite; apatite needles, biotite flakes, viridite and long narrow rods of iron ore up to 3 mm. long are common.

The finer-grained, darker-weathering band (Z.481.5) is intergranular to subophitic; intergrowths of plagioclase

and pyroxene are rare. Pyroxene laths average 0.5 mm. but they are commonly strongly curved and attain 4 mm. in length; rod-like iron ore attains 2-3 mm. in length. Orthopyroxene is absent but altered cores to clinopyroxene may be pseudomorphs after orthopyroxene. The mesostasis is more abundant than in the dolerite-pegmatite and micropegmatite is common. Hornblende, biotite and chlorite alteration products are abundant.

Nearer the upper contact of the sill, at the contact of a rheomorphic vein (Z.481.6), plagioclase (An_{70}) and clinopyroxene occur as skeletal laths in variolitic clusters. Grain-size is variable and coarser-grained areas have interstitial micropegmatite and rare plagioclase—pyroxene intergrowths.

In the rhythmically layered part of the sill, zoning of plagioclase, pyroxene and to a certain extent olivine appears to result from intercumulus growth in rocks which are essentially orthocumulates. The large number of cumulus minerals (olivine, orthopyroxene, clinopyroxene, plagioclase) tends to obscure conclusive textural relationships. The coarse-grained segregations in the variolitic near-contact rock (Z.481.6) are similar to dolerite-pegmatite schlieren in the Palisades sill of New Jersey (Walker, 1940).

4. Middle sill of Coalseam Cliffs

This sill varies from porphyritic olivine-bearing contact rocks through a subophitic two-pyroxene quartz-dolerite to granophyric quartz-dolerite in the upper central parts of the sill. Modal analyses are given in Tables III and IV.

At the contact (Z.475.2), skeletal idiomorphic phenocrysts of olivine, often pseudomorphed by quartz and (?) talc, are set in a subvariolitic groundmass of plagioclase (An_{64}), orthopyroxene and clinopyroxene; the groundmass has intersertal areas of radiating clusters of fibrous pyroxene.

The lower parts of the sill (Z.475.1 and 479.3) consist of medium-grained, subophitic two-pyroxene dolerite with subordinate to no olivine and a dominantly micropegmatitic mesostasis. Plagioclase (An_{65-70}) occurs as idiomorphic stumpy prisms which are partly enclosed by pyroxene. Orthopyroxene occurs in prismatic crystals, up to 1.5 mm. long, and it is often overgrown in optical continuity by clinopyroxene. Small hypidiomorphic olivine crystals, or pseudomorphs of bowlingite, magnetite and chlorite after olivine, form the cores to orthopyroxene crystals within 2 m. of the lower contact (Z.475.1) but they are absent at about 10 m. from the contact (Z.479.3).

Clinopyroxene also occurs as separate plates of neutral to pale pink pigeonite; simple twinning is common and there is some polysynthetic twinning. The mesostasis consists of plagioclase, alkali-feldspar and quartz with clusters of apatite needles, minute biotite flakes and rod-like iron ore. Chloritic alteration of clinopyroxene and alkali-feldspar mantling plagioclase are common in contact with the mesostasis.

In the central parts of the sill (Z.473.1 and 476.1), granophyric dolerite contains an abundance of micropegmatite. Plagioclase (An_{40-50}) laths are partly enclosed by clinopyroxene and apparently primary green and brown hornblende and biotite but orthopyroxene is absent. Small, granular, fayalitic olivine crystals often form at the expense of pyroxene. Cores of plagioclase crystals are often sericitized or altered to micropegmatite and marginal rims of alkali-feldspar are common. Quartz occurs as discrete crystals in specimen Z.473.1 but it is mainly in micrographic intergrowth, in about equal proportions, with cloudy sericitized alkali-feldspar. Ilmenite occurs interstitially and as discrete idiomorphic crystals. Apatite needles, often long and curved, are abundant and zircon forms the cores to haloes in biotite. Small amounts of secondary calcite occur in specimen Z.473.1.

Nearer the upper contact (Z.479.2), medium-grained subophitic two-pyroxene dolerite is similar to that of the lower part of the sill. Plagioclase (An_{72}) is slightly more calcic, olivine is absent and clinopyroxene is more strongly zoned, from colourless pigeonitic cores to pink titaniferous augitic margins.

Differentiation is more marked petrographically in this sill than in any other in the Theron Mountains, except for the layered sills of Jeffries Glacier and Marø Cliffs. The upper central parts of the sill are much richer in micropegmatite (especially Z.473.1) and iron ore (especially Z.476.1) than either the upper or lower margins. Cryptic variation is marked in the plagioclase (An_{65-70} — An_{40-50} — An_{72}) and in the ferromagnesian minerals (Mg ol — cpx + opx + ol — cpx + opx — cpx + hbd + bt + Fa ol — cpx + opx).

5. Basal sill of Coalseam Cliffs

This sill is olivine-bearing throughout and the main variations are in texture as the contact is approached. It varies from vitrophyric olivine-basalt to medium-grained ophitic olivine-dolerite. Compositional variations are relatively limited (Tables III and IV). A cumulate approaching troctolitic composition occurs above the small

sedimentary xenolith at station Z.474. Specimen TAE 5 (Stephenson, 1966) is probably from this sill.

At the lower contact (Z.477.3 and 478.12), idiomorphic phenocrysts of plagioclase (An_{70}) and skeletal olivine are set in a devitrified glassy to intergranular groundmass of plagioclase (An_{55-60}) laths, granular pink augite, olivine and rod-like iron ore; the texture is seriate. Idiomorphic microphenocrysts of augite are rare but they appear within 5 mm. of the contact.

The central parts of the sill (Z.477.4, 500.1 and 478.11) consist of fine- to medium-grained ophitic olivine-dolerite. Idiomorphic laths, 0.5-2.0 mm. long, of plagioclase (An_{64-70}) are ophitically enclosed by plates, 2-4 mm. across, of pink titaniferous augite. Granular olivine, fresh except in specimen Z.478.11, commonly occurs in clusters and in augite plates. Interstitial and, rarely, skeletal ilmenite and magnetite are common. Plagioclase shows normal and oscillatory zoning and a cloudy felsic mesostasis is present but not abundant.

The upper contact rock (Z.478.10) is similar to that at the lower contact. Idiomorphic phenocrysts of plagioclase (An_{70}) and olivine are set in a cryptocrystalline to intergranular groundmass of plagioclase (An_{65}) laths, allotriomorphic pink augite, granular olivine, rod-like

iron ore and intersertal devitrified glass.

Just above the small sedimentary xenolith near the top of the sill at the south-western end of Coalseam Cliffs, a porphyritic cumulate (Z.474.1) approaches a troctolitic composition. One part of the rock (Fig. 42) has large idiomorphic phenocrysts of plagioclase (An_{65}), up to 4.0 mm. by 1.0 mm., and olivine, up to 1.5-2.0 mm. across, both of which contain inclusions of chilled material. The groundmass consists of 0.2 mm. long skeletal plagioclase laths and 0.1 mm. granular olivine crystals with intersertal cryptocrystalline material liberally dotted with granular and rod-like iron ore; the texture is hiatal. The rest of the rock (Fig. 43) has a seriate texture with hypidiomorphic to idiomorphic phenocrysts of plagioclase and olivine in a matrix of plagioclase (An_{65}) laths and granular olivine with intersertal cryptocrystalline material dotted with iron ore. The peculiar texture, compared to the rest of the sill, is probably due to localized settling and chilling in that part of the sill immediately above the xenolith.

6. Other intrusions

Specimens were collected from other sills and dykes in the Theron Mountains and those examined represent different parts of several intrusions.

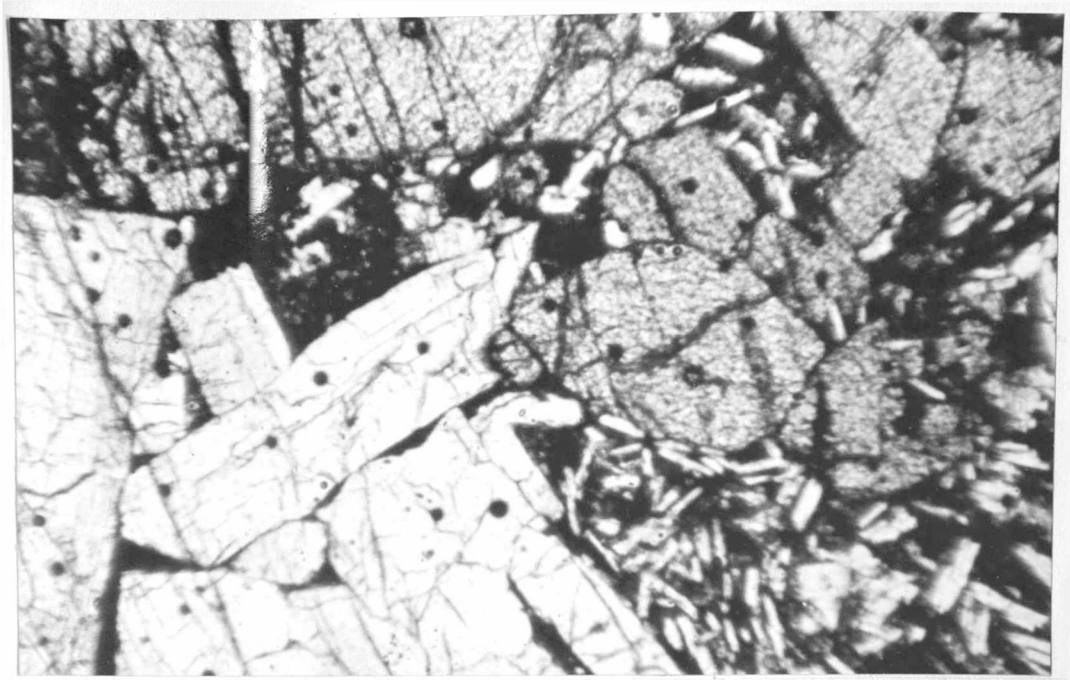

Fig. 42. Photomicrograph of part of the large glomeroporphyritic aggregate of specimen Z.474.1 showing the apparent chilling of the groundmass near olivine and plagioclase phenocrysts and the possible flow alignment of plagioclase laths in the groundmass (ordinary light, x 65).

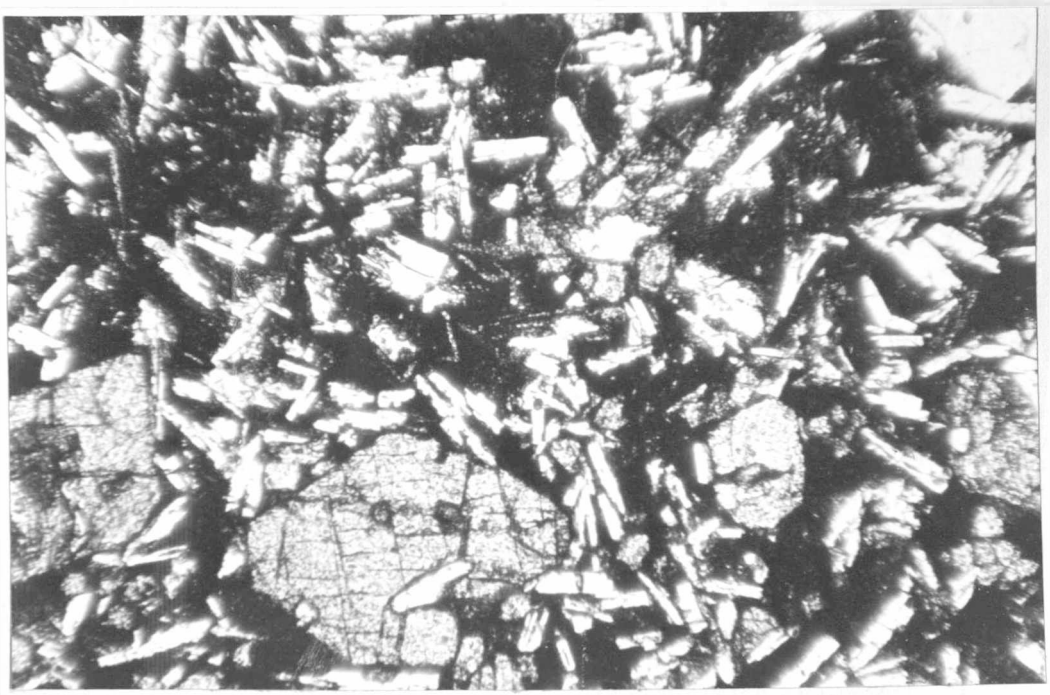

Fig. 43. Photomicrograph of part of specimen Z.474.1 some distance from the glomeroporphyritic aggregate of Fig. 42. Idiomorphic phenocrysts of plagioclase and olivine occur in a fine-grained groundmass with a seriate texture (ordinary light, x 65).

Textures are variable. They include porphyritic dolerites with a hemicrystalline groundmass (Z.453.2 and 487.3) and intersertal (Z.477.11 and 453.3), variolitic (Z.477.7) and intergranular (Z.509.1) textures in thinner intrusions. The central parts of thicker sills show sub-ophitic to ophitic textures (Z.461.1 and 487.2).

Composition is variable (Tables III and IV), ranging from olivine-dolerites (Z.453.1 and 466.3) to olivine-free dolerites with a granophyric mesostasis (Z.489.4); this variation also occurs within different parts of the same sill (Z.461.1 and 2; Z.464.1, 2 and 3). Plagioclase, often zoned, is of variable composition, usually between An_{55} and An_{75}. Pigeonite and augite are the common ferromagnesian minerals. Orthopyroxene is rare but in specimen Z.464.3 (Fig. 44), intergrowths of orthopyroxene and clinopyroxene surround cores of the former and are in turn surrounded by the latter. Micropegmatite is rare but it occurs in the central parts of some sills (Z.461.1, 464.3 and 487.2) and the contact rock of a rheomorphic vein in the upper sill of point 2600 (Z.494.1 and 2) consists mainly of micropegmatite surrounding plagioclase laths, with chlorite and subordinate biotite as the only ferromagnesian minerals. Iron ore occurs as skeletal and rod-like crystals and in the finer-grained rocks it is widely distributed as granular opaque crystals in the groundmass.

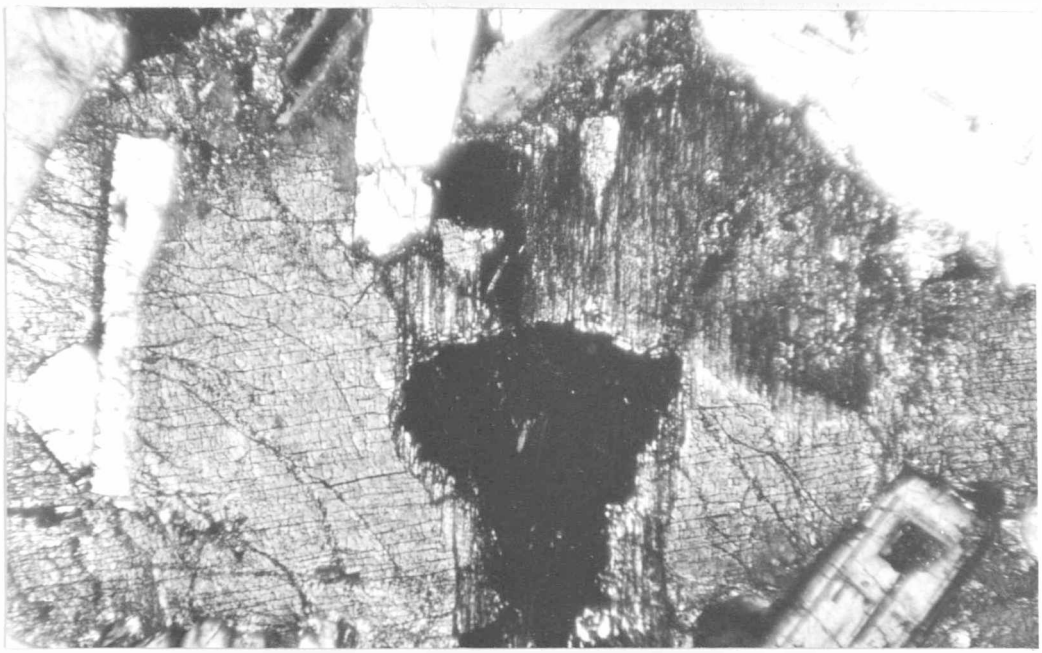

Fig. 44. Photomicrograph of subophitic two-pyroxene dolerite from a minor sill above the scarp-capping sill. Intergrowths of orthopyroxene and clinopyroxene surround cores of the former and, in turn, have a marginal rim of the latter (Z.464.3, crossed nicols, x 65).

7. Summary and comparative petrography

Petrographical variations in the Jurassic dolerite intrusions of the Theron Mountains are considerable. Modal analyses (Tables III and IV) show the main variations, which can be summarized as follows:

a. Chilled marginal rocks

i. Aphyric rocks are rare and hiatal and seriate textures are present; cooling-contraction and flow structures sometimes occur.

ii. Plagioclase is almost ubiquitous and it is often, with olivine, the first mineral to crystallize.

iii. Olivine, or pseudomorphs after olivine, is present in most sills except the scarp-capping sill. It is generally in excess of clinopyroxene.

iv. Orthopyroxene does not occur as phenocrysts, except as reported by Stephenson (1966).

v. Clinopyroxene is the dominant ferromagnesian phenocryst in the scarp-capping sill and the basal sill of Lenton Bluff but it is rare elsewhere. It crystallizes later than plagioclase and olivine when it occurs with them.

b. Holocrystalline rocks

i. Holocrystalline rocks are fine- to medium-grained with intergranular to subophitic and ophitic textures. Granophyric textures are common in the scarp-capping sill.

ii. Plagioclase is variable in composition and shows some cryptic variation, especially in the middle sill of Coalseam Cliffs. It is often of at least two generations, an earlier, well twinned and weakly zoned, and a later less idiomorphic, strongly zoned and poorly twinned generation. It is usually in excess of total ferromagnesian minerals.

iii. A micropegmatitic or cloudy felsic mesostasis is almost ubiquitous, even in olivine-dolerites. In some cases it is the most abundant single constituent.

iv. Magnesian olivine occurs in many sills, varying from 0-30 per cent of the rock; it is often pseudomorphed by bowlingite and magnetite and mantled by orthopyroxene and/or clinopyroxene. Fayalitic olivine is present in many granophyric quartz-dolerites, especially in the scarp-capping sill and the middle sill of Coalseam Cliffs; it often forms at the expense of clinopyroxene and is commonly pseudomorphed by a yellowish brown mineral which is probably iddingsite and/or chlorophaeite.

v. Orthopyroxene is rare, being of importance only in the layered sills of Jeffries Glacier and Marø Cliffs and the middle sill of Coalseam Cliffs.

vi. Clinopyroxene is ubiquitous; pigeonite and/or augite are present; zoning is common and its pinkish colour suggests it is often titaniferous.

vii. Hornblende and biotite may be primary in some of the granophyric quartz-dolerites.

viii. Accessory minerals include ilmenite, magnetite, titano-magnetite, possibly some pyrite and haematite, apatite and zircon.

ix. Alteration products include hornblende, biotite, chlorite, bowlingite, iddingsite, (?) chlorophaeite, (?) talc, sericite, quartz, calcite, albite, epidote and sphene.

c. Comparative petrography

Olivine-bearing basalts and dolerites similar to those of the Theron Mountains have been described from Heimefrontfjella (Juckes, in press) and Vestfjella (Brown, 1967; Juckes, 1968; Hjelle and Winsnes, 1971) in western Dronning Maud Land.

The variations in the Jurassic dolerites of the Theron Mountains and Dronning Maud Land are apparently

greater than those in the Ferrar dolerites of eastern Antarctica and there are significant petrographical differences.

The primary crystallizing phase in the Ferrar dolerites is usually orthopyroxene (Gunn, 1962). In the Theron Mountains olivine and/or plagioclase are the first minerals to appear and these are followed by clinopyroxene in most instances.

Gunn (1966) classified the Ferrar dolerites of Victoria Land, on the basis of petrography and chemistry, into olivine-, hypersthene- and pigeonite-tholeiites. Olivine-tholeiites are slightly undersaturated in silica and contain altered olivine microphenocrysts in a fine groundmass. Hypersthene-tholeiites contain 8-9 per cent of normative quartz and contain orthopyroxene, augite and plagioclase microphenocrysts. Pigeonite-tholeiites have 10-12 per cent of normative quartz and contain pigeonite, subcalcic augite, augite and plagioclase microphenocrysts. In volume pigeonite-tholeiites exceed hypersthene-tholeiites by a factor of 1.5-2.0 while olivine-tholeiite is present in comparatively minor quantities. Olivine has been reported in the Ferrar dolerites only from the Thumb Point sill (Skinner and Ricker, 1965), the Painted Cliffs sill (Grindley, 1963) and the Dufek Massif (Aughenbaugh, 1961), though

psuedomorphs, probably after olivine, have been reported from the dolerite of Horn Bluff (Browne, 1923) and the Mount Harmsworth dyke (Gunn, 1963). In Victoria Land (Gunn, 1966), hypersthene-tholeiites are apparently younger than pigeonite-tholeiites but no age relations for olivine-tholeiites can be deduced. Compston and others (1968) suggested that differentiation of olivine-tholeiites could give rise to hypersthene- and pigeonite-tholeiites.

Exact classification of the dolerites of the Theron Mountains into Gunn's types is not possible on petrographical grounds, though many of the sills appear to be olivine-tholeiites. The middle sill of Coalseam Cliffs appears to show differentiation from "olivine-tholeiite" margins, through "hypersthene-tholeiite" to end-members rich in iron ore and micropegmatite. In Marø Cliffs, "olivine-tholeiites" appear to bracket "pigeonite-tholeiites" in time of intrusion. In volume, "pigeonite-tholeiite" probably exceeds "olivine-tholeiite" by a factor of at least 2 but "hypersthene-tholeiite" is comparatively rare. In number of sills, "olivine-tholeiite" is by far the most abundant.

The Jurassic dolerites of Tasmania are very similar to the Ferrar dolerites. They have been extensively studied petrographically and chemically (Edwards, 1942; McDougall, 1962; 1964) and on the basis of density (Jaeger,

1964) and magnetic measurements (Jaeger and Joplin, 1954). The primary crystallizing phase is usually clinopyroxene and differentiation is through quartz-dolerites and fayalite-granophyres to granophyres. Jones and others (1966) suggest the presence of a central feeder beneath the Great Lake sheet, a typical form for Tasmanian dolerites, facilitates the formation of granophyres over the dykes.

Petrographical variations due to differentiation in individual sills and between different intrusions in the Theron Mountains are more similar to those of the Karroo dolerites of South Africa than to the Ferrar dolerites of Antarctica or the Jurassic dolerites of Tasmania. The primary crystallizing phase in the Karroo is commonly olivine, though in some cases it is orthopyroxene. Most of the dolerite types recognized by Walker and Poldervaart (1949) are represented in the Theron Mountains, though some are in very small quantities.

Closely related but of different age are the other Mesozoic tholeiites of the Gondwana continents (Fig. 11); these include the Serra Geral Formation of South America and the Rajmahal and Sylhet traps of India.

D. DOLERITE/SEDIMENT CONTACT PHENOMENA

Most of the sediments of the Theron Mountains have been affected by dolerite intrusion (p. 46) but obvious hornfelsic baking is visible in the field for <1 m. from the contacts of intrusions. The contacts of some sills show strong evidence of reaction between dolerite and sediments and many of the contacts are a complex intermixture of sediments and dolerite; rheomorphic veins of sedimentary material intruding the dolerite are present in places. Hydrothermal activity is generally located along or near contacts of intrusions.

1. Xenoliths

Xenoliths, which are entirely of sedimentary material, are generally rare in the Theron Mountains but they are common in the basal sill of Lenton Bluff. Both arenaceous and argillaceous material show strong indications of thermal metamorphism and hydrothermal activity is strongly associated. The main xenoliths examined are those in the basal sill near the south-western end of Lenton Bluff (Z.472).

The largest xenolith consists of about 3 m. of dark shaly mudstones overlain by 5-6 m. of light grey

quartzitic siltstones (Fig. 24). The upper contact is very irregular, with apophyses of dolerite within the xenolith, small isolated patches of sediments above the xenolith and deformation of the lamination of the siltstones. In the dolerite above the xenolith, fibrous radiating veins of chlorite and tremolite (identified by X-ray diffraction) occur on joint planes. In thin section (Z.472.3), they are also seen to contain minor quartz, epidote and feldspar. The dolerite itself is almost completely altered; idiomorphic phenocrysts of plagioclase are albitized and the groundmass consists of lime-green chloritic material with minute granular sphene (?).

The dolerite at the contact has been brecciated and intruded by rheomorphic veinlets derived from the siltstones. In thin section (Z.472.2), these consist of extremely fine-grained quartzo-feldspathic material with a tendency towards micrographic intergrowth. Secondary quartz is present and sphene and epidote are sporadically distributed; the latter are much more abundant in the intruded dolerite.

The lower contact, which is more regular than the upper one, is marked by a 15 cm. band of altered, yellowish green medium-grained sandstone, which passes upwards into hard, thinly bedded mudstones. In thin section (Z.472.9a), the contact is sharp but irregular, and small isolated pods

of sediment up to 2 mm. across are included within the dolerite. Reaction between the dolerite and sandstone is shown by the alteration of microphenocrysts near the contact, by green and brown alteration of the glassy groundmass of the dolerite and by a concentration of minute granular opaque minerals along the actual contact.

The matrix of the sandstone is completely altered to epidote, chlorite, orange-brown biotite and a colourless, moderately birefringent mineral with an extinction angle of about 45°; the latter sometimes occurs in radiating clusters. Quartz grains, up to 1 mm. across, have been strained and corroded and they are commonly separated by micropegmatitic intergrowths of quartz and feldspar. The relative abundance of quartz grains and matrix varies. A few centimetres above the contact (Fig. 45), sutured quartz grains with strongly undulose extinction are separated by interstitial areas of calcite, epidote, chlorite and possibly prehnite, or by micropegmatite. Finer-grained areas have isolated, corroded quartz grains in a matrix of fine-grained quartz, epidote and chlorite (Fig. 46). 15 cm. from the contact (Z.472.5), quartz grains are less corroded and some relic feldspar grains can be recognized; the matrix consists of minute quartz and feldspar, commonly intergrown, with abundant fibrous sheaves of sericitic

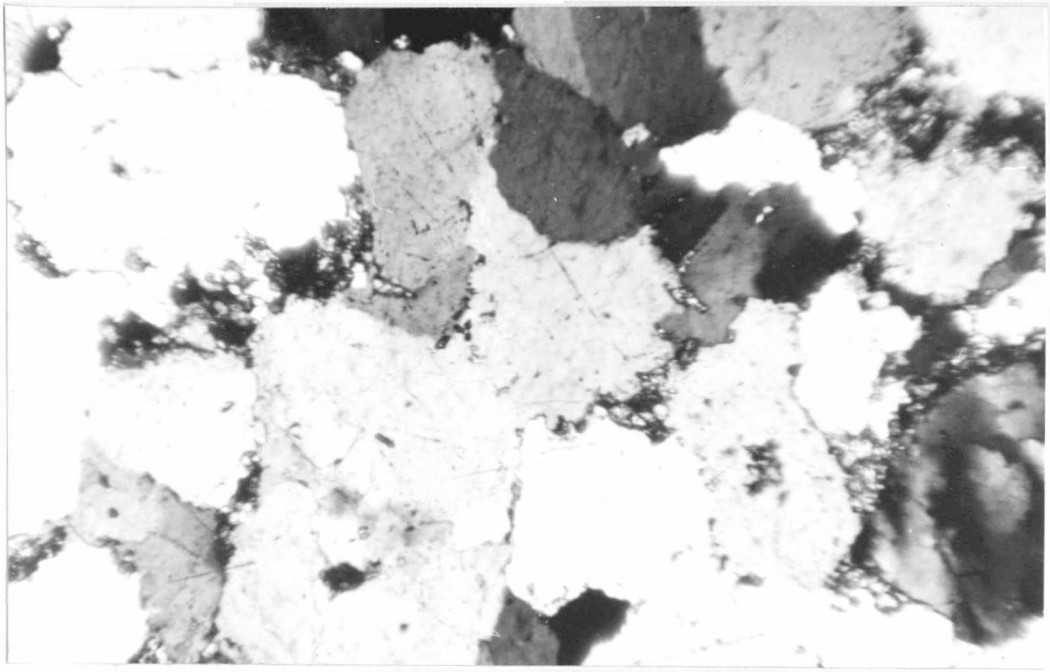

Fig. 45. Photomicrograph of sutured quartz grains separated by a recrystallized matrix of calcite, epidote and chlorite in the largest xenolith in the basal sill of Lenton Bluff (Z.472.6, crossed nicols, x 65).

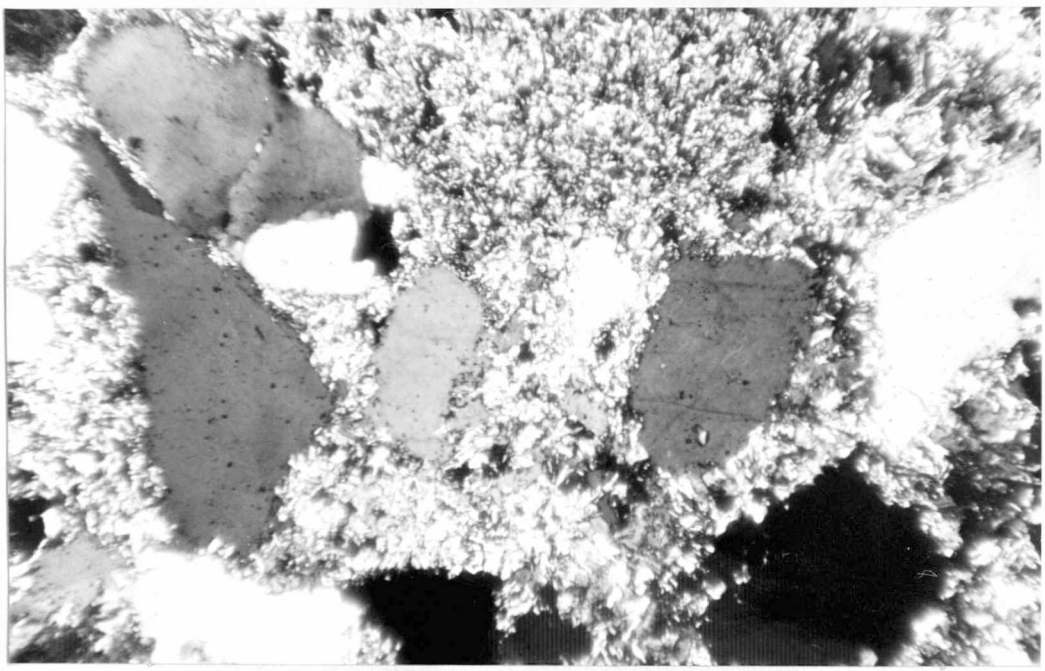

Fig. 46. Photomicrograph of finer-grained material from the largest xenolith in the basal sill of Lenton Bluff. Isolated corroded quartz grains are separated by a recrystallized matrix of quartz, feldspar, epidote, chlorite and calcite (Z.472.5, crossed nicols, x 65).

mica. The original texture and composition of the mudstone within 20 cm. of the contact (Z.472.10) has been completely masked by recrystallization of sericitic mica.

Just south-west of the largest xenolith is a small one consisting of fine-grained siltstones. Near the contact (Z.472.12a), chlorite and biotite are abundant but within a few millimetres they give way to sericitic mica; this suggests a slight basification similar to that suggested as the first phase of reaction between Karroo dolerites and intruded sediments in South Africa (Walker and Poldervaart, 1949). 5 cm. from the contact (Z.472.12c), chlorite and biotite are absent but sericitic mica is abundant. Feldspars in both specimens are cloudy but there has been little recrystallization of quartz and feldspar, possibly because the dolerite was cooler and more consolidated, as suggested by the flow layering in the vitrophyric dolerite contact rock (Fig. 37).

A short distance from the contact, the dolerite is highly altered and green in colour. It is cut by narrow veins consisting of andradite garnet on the walls, covered and partly surrounded (Fig. 47) by box-work calcite (both minerals have been identified by X-ray diffraction). In thin section (Z.472.13), the fine-grained porphyritic dolerite has idiomorphic phenocrysts of plagioclase (almost

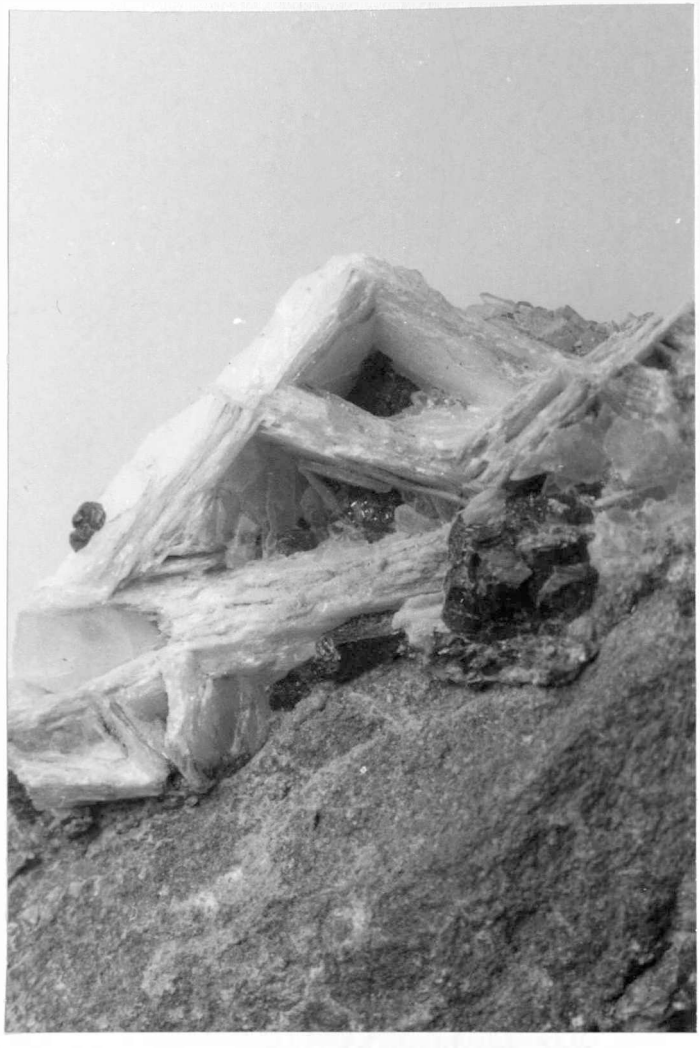

Fig. 47. Andradite garnets separated and enclosed by box-work calcite in a hydrothermal vein near a xenolith in the basal sill of Lenton Bluff (Z.472.13, x 2.5).

completely saussuritized) in a matrix of albitized plagioclase, lime-green epidote and chloritic material, iron ore and sphene.

Just north-east of the largest xenolith, the contact of a small xenolith is marked by extensive brecciation and mineralization. The main minerals noted were quartz, apophyllite (identified by X-ray diffraction), chalcopyrite, calcite and epidote.

Other small xenoliths occur in the basal sill of Lenton Bluff and in other sills, notably near the top of the layered sill of Jeffries Glacier and in the basal sill at the south-western end of Coalseam Cliffs (Z.474) but these were not closely examined.

2. Other contact rocks

a. Thermal metamorphism

Thermal metamorphism of intruded sediments is visible for <1 m. from the contacts of sills and dykes but petrographic examination of the sediments shows that it extends somewhat further (p. 46).

Mudstones and shales at intrusive contacts have been baked to hard flinty rocks with a conchoidal fracture (Z.497.2c) which in thin section show almost complete recrystallization. Coals have in all cases been thoroughly

coked and some have had hexagonal columnar jointing imposed (Z.475.3). Vesicles are abundant in some coals intruded by and included in a thin sill at Coalseam Cliffs (Z.478.6); the vesicles are filled by quartz and calcite.

In the siltstones and fine-grained sandstones many of the original minerals and textures have been preserved, except in the matrix, which is completely recrystallized. Feldspars are cloudy but they are often present right up to the contact. Corrosion of quartz grains at contacts with the matrix is common but suturing of quartz grains is rare; secondary overgrowths on quartz grains seem to increase as intrusive contacts are approached. Fusion of the siltstones to a glass, as described by Ackermann and Walker (1960) in the Karroo dolerites, is rare but some micropegmatite occurs in immediate contact with dolerite. The most pronounced effect of thermal metamorphism on the sandstones and siltstones is recrystallization of the matrix, usually to an indeterminate fine-grained, cloudy quartzofeldspathic aggregate. Prehnite and calcite are often present (Z.471.12) with minor clinozoisite; they are not restricted to contact rocks but they also occur in some sandstones at a distance from dolerite contacts (Z.471.4).

Most of the sediments of the Theron Mountains, even some distance from intrusive contacts, are considered to have been affected by thermal metamorphism (p. 46).

b. Rheomorphism

Rheomorphic veins, brecciating and intruding dolerite intrusions are rare but examples were noted from the floors of the basal sill of Lenton Bluff and the upper sill of point 2600 (Fig. 31) and from the roof of the layered sill of Marø Cliffs.

Complete fusion to glass has not occurred in any vein but there has been sufficient partial fusion for the mobile sediment to intrude the dolerite. The gradational contacts of specimens Z.471.11 and 494.1 and 2 suggest the dolerite was not fully consolidated at the time of intrusion and that there has been some reaction between the dolerite and sediments. Syntectic granophyre, such as described by Mountain (1935, 1960) from the Karroo dolerites of South Africa, appears to be absent, except immediately adjacent to the dolerite in specimens Z.471.11, 494.1 and 2 and possibly brecciating the coal in Z.481.6b.

Irvine (1970) suggested contact effects should be more pronounced around the upper reaches of a layered intrusion due to crystal settling than if the settled crystals had frozen to the roof. The layered sill of Marø Cliffs is considered to result from crystal settling (p.130). This is also the only one of the few cases of rheomorphism seen in which the rheomorphic and syntectic effects occur in the roof zone and not in the floor of the intrusion.

c. Hydrothermal activity

Hydrothermal mineralization is of limited occurrence but it is generally concentrated along or near intrusive contacts. The main minerals are quartz and calcite (Z.498.4) but epidote and prehnite in some contact sediments (Z.483.1) are probably of hydrothermal origin. The alteration of the phenocrysts in many of the contact dolerites, especially saussuritization of plagioclase (Z.483.1 and 487.4), is probably of hydrothermal origin; it is strongly associated with chloritization of the groundmass ferromagnesian minerals. In the intimate mixture of coal and dolerite at the contact of a thin sill in Marø Cliffs, a colloform texture (Fig. 48; Z.501.5) has developed in quartz-calcite veins.

E. AGE AND CORRELATION

The dolerite intrusions of the Theron Mountains are of Jurassic age; whole-rock K-Ar age determinations by Rex (1971) lie in the range 154-169 m.yr. This compares closely with basalts and dolerites from Heimefrontfjella (162-179 m.yr.; Rex, 1971) and dolerite from Vestfjella (168-172 m.yr.; Rex, 1967) in western Dronning Maud Land.

The Ferrar dolerites of eastern Antarctica have been dated as Middle Jurassic (147-169 m.yr.; McDougall,

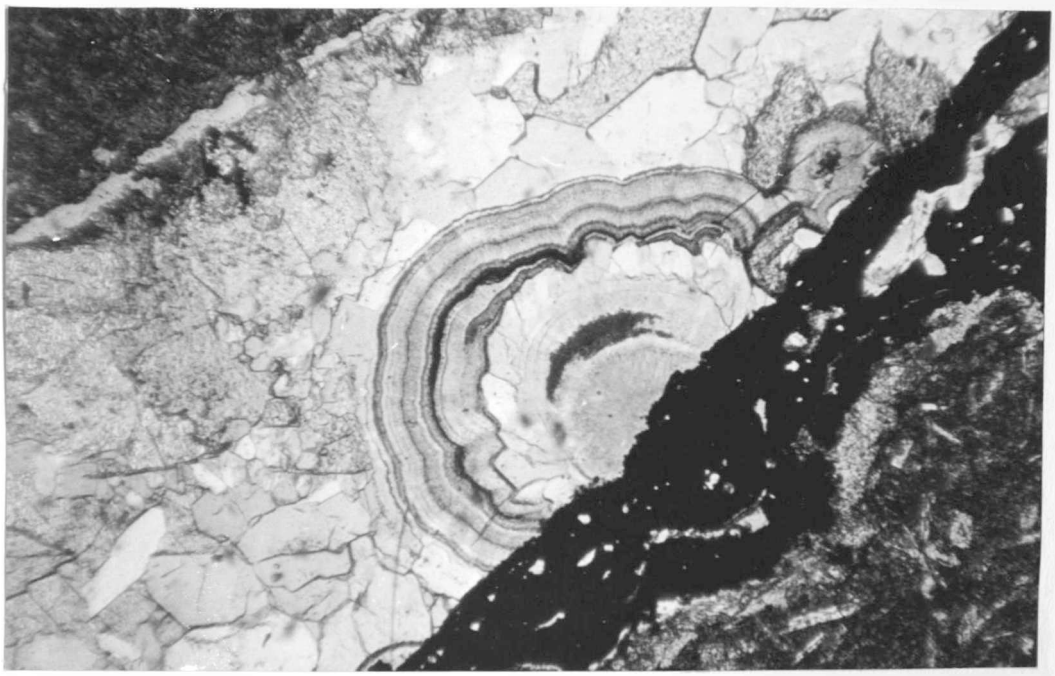

Fig. 48. Photomicrograph of a hydrothermal vein in the contact rock of a thin sill in Coalseam Cliffs. The specimen is an intimate mixture of dolerite and sediment veined by quartz and calcite with a colloform texture in parts (Z.501.5, ordinary light, x 65).

1963; Compston and others, 1968), though age determinations on dolerites from the Horn Bluff area (169-191 m.yr.; Picciotto and Coppez, 1962) and the Pensacola Mountains (215-225 m. yr.; Ford, 1971) suggest the range may be somewhat greater. The layered series of the Dufek Massif and the Forrestal Range is of similar age (168 ± 5 m. yr.; Ford, 1971), as are the Kirkpatrick basalts of the Beardmore Glacier area (163-179 m. yr.; Elliot, 1971a). Early manifestations of the vulcanicity which preceded extrusion of the Kirkpatrick basalts are seen in the acid tuffs of the Falla Formation (203 ± 12 m. yr.; Hill, 1970) and dolerite boulders in the Prebble Formation (179 m. yr.; Hill, 1970) of the Beacon Supergroup.

Close correlatives in other southern continents include the Jurassic dolerites of Tasmania (160-165 m. yr.; McDougall, 1961) and the Karroo dolerites of South Africa (154-190 m. yr.; McDougall, 1963). Rb-Sr ages of rhyolites, granophyres and granites from Swaziland, Zululand and the Nuanetsi Syncline (177-206 m. yr.; Manton, 1968), which preceded eruption of the Karroo basalts, are similar to those of the Falla Formation.

Closely related, though later in time, are the Serra Geral Formation of South America (101-161 m. yr., with most determinations at 115-135 m. yr. and a slight

precursory peak at 140-150 m. yr.; Creer and others, 1965; Amaral and others, 1966; McDougall and Rüegg, 1966; Vandoros and others, 1966; Melfi, 1967) and the Rajmahal (82-109 m. yr.; McDougall and McElhinny, 1970) and Sylhet traps of India.

The distribution and radiometric ages of these Mesozoic tholeiitic rocks in the Southern Hemisphere are shown on a reconstruction (after Smith and Hallam, 1970) of Gondwanaland (Fig. 11).

CHAPTER VI

GEOCHEMISTRY OF THE JURASSIC DOLERITE INTRUSIONS

A. ANALYTICAL METHODS

Ninety-seven specimens from the Jurassic dolerite intrusions of the Theron Mountains have been analysed for 10 major and 14 trace elements using the Phillips PW 1212 X-ray fluorescence spectrometer of the Geology Department of the University of Birmingham. Clean and fresh specimens were ground to powder in a tungsten-carbide, rotary disc mill (Tema model T100) and a 7 g. sample was mixed with 14-15 drops of Mowiol (Hoechst N50-88) and compressed to a $1\frac{1}{4}$" pellet under a pressure of 15 tons. As a check on sampling errors (Kleeman, 1967) duplicate pellets of one specimen (Z.490.1) and fresh and weathered samples of two specimens (Z.498.5 and 9) were analysed (Table VI). Analysis numbers are those of the Geology Department of the University of Birmingham, with numbers greater than 10,000 being allotted to published analyses from other laboratories. Descriptions of analysed specimens and bibliography of published analyses are given in Appendices I and II.

TABLE VI

DUPLICATE CHEMICAL ANALYSES OF SPECIMENS FROM THE JURASSIC DOLERITE INTRUSIONS OF THE THERON MOUNTAINS, ANTARCTICA

	3694	3748	3725	3726	3729	3730
SiO_2	55.08	55.04	47.57	47.05	48.68	47.89
TiO_2	2.11	2.09	0.89	0.91	0.74	0.70
Al_2O_3	10.83	10.81	12.84	13.28	15.02	15.10
Fe_2O_3*	15.98	16.08	11.98	11.27	9.72	9.70
MnO	0.17	0.17	0.15	0.15	0.12	0.13
MgO	2.16	2.19	10.93	11.08	6.98	10.74
CaO	6.93	6.97	9.17	8.56	11.45	11.23
Na_2O	3.25	3.18	1.55	1.59	1.85	1.35
K_2O	2.03	2.04	0.59	0.69	0.25	0.31
P_2O_5	0.17	0.17	0.06	0.07	0.08	0.08
H_2O+	0.37		2.14	2.95	1.54	2.00
H_2O-	0.04		1.01	1.05	0.60	0.54
CO_2	0.44		1.10	0.92	1.65	1.36
Total	98.21	98.19	99.40	99.54	97.98	100.38
S	442	341	186	219	145	251
Cr	24	24	830	793	535	516
Ni	17	18	25	25	10	9
Zn	111	n.d.	105	123	70	73
Ga	19	n.d.	16	15	16	16
Rb	n.d.	66	32	37	23	9
Sr	n.d.	130	219	240	151	171
Y	n.d.	34	17	18	26	15
Zr	229	229	63	60	159	72
Ba	501	496	213	234	172	185
La	32	27	<3	<3	3	4
Ce	64	69	8	9	7	14
Pb	n.d.	13	17	20	11	6
Th	n.d.	5	3	<3	7	3

* Total iron oxide as Fe_2O_3.

Oxides in per cent, elements in p.p.m.

n.d. = not determined.

3694 Z.490.1 - Chilled porphyritic dolerite from the lower contact of the scarp-capping sill in the escarpment between Goldsmith Glacier and Lenton Bluff.

3748 Z.490.1 - Duplicate pellet from same powder as 3694.

3725 Z.498.5f - Chilled porphyritic dolerite from the contact of a 6 m. dyke above the basal sill of Lenton Bluff. Fresh sample.

3726 Z.498.5a - Weathered sample from same specimen as 3725.

3729 Z.498.9f - Fine-grained dolerite from middle of a minor sill in the sediments between the 200 m. sill and the basal sill of Lenton Bluff. Fresh sample.

3730 Z.498.9a - Weathered sample from same specimen as 3729.

Apart from sample preparation the methods used are essentially similar to those described by Leake and others (1969). These give a standard deviation (σ) for the totals of ten major oxides of 1.64 for repeated analyses of 12 pellets of the ratio standard amphibolite BL3571. Using, therefore, a one σ range, and allowing for deviations in the determinations of FeO, H_2O and CO_2, totals within the range 98.00-102.00 are considered fully acceptable, though totals outside this range are also given in the tables of chemical analyses (Tables VI and IX-XVIII).

FeO was determined by titration with ceric sulphate and Fe_2O_3 by subtraction from total iron oxide; the oxidation effects noted by Fitton and Gill (1970) are not considered significant. H_2O- was determined by drying at 110°C. and total water by the boiling tube method of Penfield (1894). Duplicate analyses for FeO and total water are shown in Tables VII and VIII.

CO_2 was determined by acid-base titration (Grimaldi and others, 1966). Although the method was principally evolved for the analysis of dolomites and limestones, acceptable results comparable to those of Riley's (1958) method have been obtained by other workers on other rocks, such as greenstones and rhyolites (personal communication from G.L. Hendry). In the present study, however,

TABLE VII

DUPLICATE FERROUS IRON ANALYSES OF SPECIMENS FROM THE JURASSIC DOLERITE INTRUSIONS OF THE THERON MOUNTAINS, ANTARCTICA

Specimen number	FeO determinations					
	1	2	3	4	5	Mean
Z.480.1a	14.42	14.56	14.16	14.26	14.69	14.42
Z.480.2	13.27	12.81				13.04
Z.474.1	12.62	13.15	12.99	12.68	12.45	12.78
Z.453.2	8.65	9.23				8.94
Z.453.1	8.24	8.01				8.12
Z.483.4	7.57	6.85				7.21
Z.475.1	6.75	6.72				6.73

Z.480.1a Chilled dolerite, third-phase sill of Marø Cliffs.

Z.480.2 Chilled dolerite, third-phase sill of Marø Cliffs.

Z.474.1 Porphyritic fine-grained dolerite, basal sill of Coalseam Cliffs.

Z.453.2 Chilled dolerite, 15 m. minor sill above the 200 m. sill.

Z.453.1 Medium-grained dolerite, 15 m. minor sill above the 200 m. sill.

Z.483.4 Fine-grained dolerite, minor sill in Marø Cliffs.

Z.475.1 Chilled dolerite, middle sill of Coalseam Cliffs.

TABLE VIII

DUPLICATE TOTAL WATER ANALYSES OF SPECIMENS FROM THE JURASSIC DOLERITE INTRUSIONS OF THE THERON MOUNTAINS, ANTARCTICA

Specimen number	Total water determinations				
	1	2	3	4	Mean
Z.472.3	4.36	4.37			4.37
Z.472.13	4.54	4.02			4.28
Z.498.5a	3.69	4.36	3.91	3.94	3.98
Z.498.5f	2.91	3.38			3.15
Z.497.6	2.92	3.06			2.99
Z.487.2	1.18	1.12			1.15
Z.480.1a	0.58	0.59			0.59

Z.472.3 Hydrothermally altered dolerite, basal sill of Lenton Bluff.

Z.472.13 Hydrothermally altered dolerite, basal sill of Lenton Bluff.

Z.498.5a Weathered sample, chilled dolerite, younger dyke of Lenton Bluff.

Z.498.5f Fresh sample, chilled dolerite, younger dyke of Lenton Bluff.

Z.497.6 Altered medium-grained dolerite, minor sill below 200 m. sill.

Z.487.2 Medium-grained dolerite, 30 m. sill above the 200 m. sill.

Z.480.1a Chilled dolerite, third-phase sill of Marø Cliffs.

the strong correlation with sulphur suggests that both sulphides and carbonates have been dissolved and that CO_2 determinations are, therefore, inaccurate. Although given in Tables VI and IX-XVIII, for all practical purposes CO_2 has been ignored, especially in norm calculation, as allotting CO_2 to calcite produces meaningless results.

Analytical data thus obtained and over 500 published analyses of Jurassic dolerites and basalts from Antarctica, Tasmania and southern Africa have been processed using the University of Birmingham KDF9 computer. Computer programmes used have been written by Dr. J. Tarney, Dr. A.C. Skinner, I.H. Kahn and the author.

B. CHEMISTRY OF INDIVIDUAL INTRUSIONS

Analytical results are discussed first in terms of individual intrusions which have been sampled more extensively than others, and variations between these intrusions. The chemistry of the Jurassic dolerite intrusions is then summarized and compared to other Mesozoic tholeiitic rocks of the Southern Hemisphere. Petrogenetic implications with respect to the timing of the break-up of Gondwanaland are then considered and a model proposed for the evolution of basaltic magmatism in the Southern Hemisphere.

1. Scarp-capping sill

The sill is chemically fairly uniform (Table IX) and chemical variations vertically and laterally are small. It is over-saturated with respect to SiO_2 throughout, even chilled marginal rocks containing 4-14 per cent of normative quartz. It is characterized by high SiO_2, TiO_2, total iron, Rb, Zr, Ba, La and Ce and by relatively low Al_2O_3, MgO, CaO, Cr, Ni and Sr.

K/Rb (217-320), Th/K (3.0-7.1) and Rb/Sr (0.27-0.51) ratios are comparable with normal values in continental crustal rocks and the Cr/Ni ratio is almost constant (1.00-2.06; mean 1.41), excluding analysis 10651 (from Stephenson, 1966; trace elements determined by optical spectrographic methods) which has anomalously high Cr.

2. Different intrusive phases

The different intrusive phases of Marø Cliffs and Lenton Bluff are petrographically and chemically distinct and some chemical correlation of other minor intrusions in this area is possible, particularly on the basis of the Cr/Ni ratio, which is almost constant in each intrusive phase.

a. First-phase sill of Marø Cliffs

Slightly over-saturated with respect to SiO_2, this sill (Table X) is characterized by low TiO_2, total iron, Zn

TABLE IX

CHEMICAL ANALYSES OF SPECIMENS FROM THE SCARP-CAPPING SILL, THERON MOUNTAINS, ANTARCTICA

Analyses

	3710	10651	10652	10653	3654	3670	3686	3705	3682	3700	3713	3695	3678	3714	3715	3716	3694	3688
SiO_2	53.98	53.95	55.82	53.75	54.75	58.90	57.14	55.16	54.66	52.32	54.42	57.15	55.73	54.77	55.14	56.25	55.08	55.57
TiO_2	2.08	1.10	2.01	2.17	2.54	1.82	2.10	1.84	2.46	2.50	1.91	1.87	1.85	2.09	2.07	2.10	2.11	2.08
Al_2O_3	10.98	15.69	12.55	11.55	11.98	12.31	12.08	12.78	11.84	11.44	12.63	12.13	11.48	10.90	10.88	11.37	10.83	10.66
Fe_2O_3	5.77	0.88	4.73	6.63	3.32	2.68	4.12	4.86	3.09	4.79	4.78	4.88	4.73	5.21	5.37	3.32	2.07	2.45
FeO	9.31	7.76	9.60	10.48	11.36	10.31	10.11	9.43	11.46	10.83	9.53	9.05	9.84	9.79	9.60	11.38	12.56	12.25
MnO	0.16	0.17	0.20	0.22	0.16	0.15	0.15	0.16	0.16	0.16	0.15	0.15	0.17	0.16	0.16	0.17	0.17	0.16
MgO	2.34	6.96	2.44	2.64	1.85	1.02	1.29	2.51	1.90	2.77	2.34	0.78	1.77	1.80	1.85	2.05	2.16	2.24
CaO	6.72	8.57	6.96	7.39	7.09	6.04	6.38	7.60	7.19	8.09	7.53	6.77	6.66	6.87	6.80	6.96	6.93	6.81
Na_2O	2.08	2.34	2.59	2.48	2.55	2.80	2.63	2.50	2.41	2.28	2.27	1.06	2.40	2.25	2.20	2.43	3.25	2.35
K_2O	1.52	1.38	1.80	1.58	1.76	2.32	2.11	1.60	1.85	1.28	1.75	1.88	1.86	1.53	1.62	1.71	2.03	1.85
P_2O_5	0.22	0.22	0.32	0.22	0.24	0.38	0.30	0.20	0.24	0.21	0.24	0.24	0.24	0.20	0.21	0.18	0.17	0.16
H_2O+	1.69	0.62	0.99	1.02	0.76	0.62	0.74	0.55	0.68	1.08	0.77	0.91	1.12	1.52	1.66	0.48	0.37	0.44
H_2O-	0.55	0.23	0.33	0.43	0.19	0.19	0.24	0.30	0.29	0.34	0.26	0.30	0.35	0.41	0.29	0.08	0.04	0.18
CO_2*	0.62	0.05	0.01	0.02	0.23	0.25	0.21	0.36	0.36	0.39	0.27	0.38	0.35	0.39	0.37	0.38	0.44	1.20
Total	98.01	99.92	100.35	100.58	98.79	99.79	99.61	99.84	98.58	98.47	98.85	97.56	98.55	97.90	98.22	98.85	98.21	98.42

Trace elements (p.p.m.)

S	528	n.d.	n.d.	n.d.	628	809	152	157	809	531	315	654	398	265	424	369	442	380
Cr	23	700	13	5	22	7	12	46	18	28	38	33	24	23	24	26	24	27
Ni	20	45	7	5	16	7	10	27	14	19	24	16	18	17	17	18	17	18
Zn	116	n.d.	n.d.	n.d.	100	110	109	91	98	100	93	104	111	115	115	115	111	106
Ga	19	18	18	25	16	16	17	14	16	19	16	19	15	16	18	17	19	15
Rb	52	-	40	-	49	73	60	46	48	35	47	60	56	58	62	55	66	61
Sr	140	140	80	100	126	142	128	136	122	130	136	144	140	156	141	128	130	134
Y	35	25	20	25	28	42	36	28	29	27	28	34	35	33	35	36	34	35
Zr	216	200	135	220	169	259	211	165	172	138	169	216	215	209	207	213	229	216
Ba	487	270	350	275	503	563	544	439	495	412	442	513	519	499	484	478	501	513
La	28	-	-	-	26	39	31	24	32	21	25	32	33	30	26	29	32	29
Ce	60	n.d.	n.d.	n.d.	51	79	74	43	52	46	52	65	58	67	77	75	64	63
Pb	14	-	-	-	14	20	12	12	15	8	12	13	13	16	20	16	13	11
Th	9	n.d.	n.d.	n.d.	7	9	8	4	6	6	6	8	8	8	8	9	5	6

TABLE IX continued

Analyses recalculated to 100 per cent anhydrous

	3710	10651	10652	10653	3654	3670	3686	3705	3682	3700	3713	3695	3678	3714	3715	3716	3694	3688
SiO_2	56.36	54.46	56.37	54.22	55.96	59.51	57.94	55.72	56.00	53.91	55.64	59.32	57.41	57.07	57.28	57.23	56.32	56.82
TiO_2	2.17	1.11	2.03	2.19	2.60	1.83	2.13	1.86	2.52	2.57	1.95	1.94	1.91	2.18	2.15	2.13	2.16	2.13
Al_2O_3	11.46	15.84	12.67	11.65	12.24	12.44	12.25	12.91	12.13	11.78	12.91	12.59	11.82	11.36	11.30	11.57	11.07	10.90
Fe_2O_3	6.02	0.89	4.78	6.69	3.39	2.71	4.18	4.91	3.17	4.94	4.89	5.07	4.87	5.43	5.58	3.38	2.12	2.51
FeO	9.72	7.83	9.69	10.57	11.61	10.42	10.25	9.53	11.74	11.16	9.74	9.39	10.14	10.20	9.97	11.58	12.84	12.53
MnO	0.17	0.17	0.20	0.22	0.16	0.15	0.16	0.16	0.16	0.17	0.16	0.16	0.17	0.17	0.17	0.17	0.17	0.17
MgO	2.44	7.03	2.46	2.66	1.89	1.03	1.31	2.53	1.95	2.85	2.39	0.81	1.82	1.88	1.92	2.09	2.21	2.29
CaO	7.02	8.65	7.03	7.45	7.25	6.10	6.46	7.68	7.37	8.34	7.70	7.03	6.86	7.16	7.06	7.08	7.08	6.96
Na_2O	2.17	2.36	2.62	2.50	2.61	2.83	2.67	2.52	2.47	2.34	2.32	1.10	2.48	2.35	2.28	2.47	3.32	2.41
K_2O	1.58	1.39	1.82	1.59	1.80	2.35	2.14	1.62	1.90	1.32	1.78	1.95	1.91	1.60	1.69	1.74	2.08	1.89
P_2O_5	0.23	0.22	0.32	0.22	0.25	0.38	0.31	0.20	0.25	0.21	0.24	0.25	0.25	0.21	0.21	0.18	0.17	0.17
CO_2	0.65	0.05	0.01	0.02	0.24	0.25	0.21	0.36	0.37	0.40	0.28	0.39	0.36	0.41	0.38	0.39	0.45	1.23

C.I.P.W. norms

Q	18.92	4.35	14.74	13.67	13.56	17.03	17.00	14.22	13.57	12.87	14.70	27.44	17.34	18.82	19.36	15.53	8.02	14.15
Or	9.43	8.23	10.74	9.42	10.67	13.90	12.69	9.59	11.24	7.85	10.57	11.57	11.34	9.48	10.00	10.34	12.33	11.33
Ab	18.52	19.98	22.12	21.16	22.11	24.02	22.63	21.40	20.96	19.91	19.67	9.36	21.02	19.92	19.38	21.01	28.21	20.62
An	16.94	28.49	17.47	15.85	16.41	14.33	15.13	19.20	16.48	17.79	19.61	23.72	15.55	15.80	15.68	15.36	9.23	13.52
Wo_{Di}	6.93	5.28	6.35	8.16	7.51	5.64	6.26	7.40	7.76	9.33	7.14	4.01	7.08	7.71	7.55	7.81	10.41	8.49
En_{Di}	2.72	2.99	2.34	3.17	1.94	0.94	1.41	2.80	1.99	3.45	2.58	0.72	2.06	2.40	2.45	2.09	2.52	2.18
Fs_{Di}	4.30	2.07	4.14	5.11	5.99	5.18	5.26	4.73	6.20	6.06	4.73	3.61	5.34	5.61	5.36	6.13	8.51	6.78
En_{Hy}	3.40	14.50	3.80	3.46	2.77	1.63	1.86	3.53	2.87	3.68	3.39	1.31	2.49	2.30	2.35	3.13	3.01	3.59
Fs_{Hy}	5.37	10.06	6.73	5.58	8.57	9.00	6.92	5.96	8.94	6.47	6.22	6.57	6.46	5.39	5.14	9.20	10.16	11.16
Mt	8.79	1.29	6.92	9.70	4.93	3.93	6.07	7.14	4.61	7.18	7.10	7.37	7.09	7.90	8.12	4.92	3.08	3.68
Il	4.14	2.11	3.85	4.16	4.95	3.49	4.04	3.55	4.80	4.90	3.72	3.71	3.64	4.16	4.10	4.06	4.12	4.10
Ap	0.54	0.53	0.76	0.53	0.59	0.90	0.73	0.48	0.58	0.50	0.57	0.60	0.59	0.50	0.51	0.42	0.41	0.40

TABLE IX continued

Elements (weight per cent)

	3710	10651	10652	10653	3654	3670	3686	3705	3682	3700	3713	3695	3678	3714	3715	3716	3694	3688
Si^{4+}	26.35	25.46	26.35	25.35	26.16	27.82	27.09	26.05	26.18	25.21	26.01	27.73	26.84	26.68	26.78	26.75	26.33	26.56
Ti^{4+}	1.30	0.67	1.22	1.31	1.56	1.10	1.27	1.12	1.51	1.54	1.17	1.17	1.14	1.31	1.29	1.28	1.29	1.28
Al^{3+}	6.07	8.38	6.71	6.17	6.48	6.58	6.48	6.83	6.42	6.24	6.83	6.66	6.26	6.01	5.98	6.12	5.86	5.77
Fe^{3+}	4.21	0.62	3.34	4.68	2.37	1.89	2.92	3.43	2.21	3.45	3.42	3.54	3.41	3.80	3.90	2.36	1.48	1.75
Fe^{2+}	7.56	6.09	7.54	8.22	9.03	8.10	7.97	7.40	9.13	8.67	7.57	7.30	7.88	7.93	7.75	9.00	9.98	9.74
Mn^{2+}	0.13	0.13	0.16	0.17	0.13	0.12	0.12	0.12	0.12	0.13	0.12	0.12	0.13	0.13	0.13	0.13	0.13	0.13
Mg^{2+}	1.47	4.24	1.49	1.61	1.14	0.62	0.79	1.53	1.17	1.72	1.44	0.49	1.10	1.13	1.16	1.26	1.33	1.38
Ca^{2+}	5.02	6.18	5.02	5.33	5.18	4.36	4.62	5.49	5.27	5.96	5.50	5.02	4.90	5.12	5.05	5.06	5.06	4.98
Na^{+}	1.61	1.75	1.94	1.86	1.93	2.10	1.98	1.87	1.83	1.74	1.72	0.82	1.84	1.74	1.69	1.83	2.46	1.79
K^{+}	1.32	1.16	1.51	1.32	1.50	1.95	1.78	1.34	1.57	1.10	1.48	1.62	1.59	1.33	1.40	1.45	1.72	1.57
P^{5+}	0.10	0.10	0.14	0.10	0.11	0.17	0.13	0.09	0.11	0.09	0.11	0.11	0.11	0.09	0.09	0.08	0.08	0.07
C^{4+}	0.18	0.01	0.00	0.01	0.06	0.07	0.06	0.10	0.10	0.11	0.08	0.11	0.10	0.11	0.10	0.11	0.12	0.33
O^{2-}	44.69	45.21	44.59	43.89	44.35	45.12	44.79	44.63	44.38	44.04	44.55	45.31	44.71	44.63	44.67	44.57	44.14	44.65

Useful Ratios

Thx10^4 /K	7.1	-	-	-	4.8	4.7	4.6	3.0	3.9	5.7	4.1	5.1	5.2	6.3	6.0	6.3	3.0	3.9
K/Rb	242	-	374	-	299	264	292	289	320	305	308	260	275	220	217	259	255	252
Rb/Sr	0.37	-	0.50	-	0.39	0.51	0.47	0.34	0.39	0.27	0.35	0.42	0.40	0.37	0.44	0.43	0.51	0.46
Cr/Ni	1.15	15.6	1.71	1.00	1.38	1.00	1.20	1.70	1.29	1.48	1.58	2.06	1.33	1.35	1.41	1.36	1.41	1.50

n.d. = not determined.
\- = below sensitivity of optical spectrographic methods (analyses quoted from Stephenson, 1966, table 4).
* = CO_2 of very doubtful accuracy; it is ignored in calculation of norms.

3710	Z.469.3	Altered fine-grained dolerite, just below upper contact.
10651	TAE 351/3	Chilled dolerite, upper contact (Stephenson, 1966, table 4, analysis 8).
10652	TAE 351/3	Fine-grained porphyritic dolerite, about 9 m. below upper contact (Stephenson, 1966, table 4, analysis 9).
10653	TAE 351/6	Granophyric quartz-dolerite, near centre of sill (Stephenson, 1966, table 4, analysis 10).
3654	Z.455.1	Granophyric quartz-dolerite, 40-50 m. below upper contact.
3670	Z.468.1	Granophyric quartz-dolerite, near centre of sill.
3686	Z.484.1	Granophyric quartz-dolerite, upper third of sill.
3705	Z.485.1	Granophyric quartz-dolerite, about 150 m. below upper contact.
3682	Z.486.1	Granophyric quartz-dolerite, about 150 m. below upper contact.
3700	Z.487.1	Granophyric quartz-dolerite, about 150 m. below upper contact.
3713	Z.508.1	Granophyric quartz-dolerite, about 150 m. above lower contact.
3695	Z.478.1	Altered quartz-dolerite, 6-7 m. above lower contact.
3678	Z.483.5	Altered quartz-dolerite, 6-7 m. above lower contact.
3714	Z.498.1	Altered fine-grained dolerite, about 1 m. above lower contact.
3715	Z.497.1	Altered fine-grained dolerite, about a m. above lower contact.
3716	Z.497.2	Chilled dolerite, lower contact.
3694	Z.490.1	Chilled dolerite, lower contact (some trace elements are from pellet No. 3748, see Table VI).
3688	Z.478.2	Chilled dolerite, lower contact.

TABLE X

CHEMICAL ANALYSES OF SPECIMENS FROM THE FIRST PHASE OF INTRUSION IN MARØ CLIFFS AND POSSIBLE RELATED MINOR SILLS

Analyses (weight per cent)

	3697	3667	3737	3673	3738	3702	3741
SiO_2	50.64	51.10	51.35	50.07	50.53	50.78	50.92
TiO_2	0.89	1.02	0.99	0.90	0.91	0.93	1.02
Al_2O_3	15.64	14.81	15.07	12.97	15.62	16.30	14.41
Fe_2O_3	3.21	2.24	2.73	3.05	2.97	2.13	2.94
FeO	6.42	7.50	6.83	6.71	6.57	7.21	6.90
MnO	0.14	0.14	0.13	0.15	0.14	0.14	0.14
MgO	7.49	8.12	7.46	10.41	7.92	7.31	8.73
CaO	10.12	9.87	10.14	8.98	10.36	10.16	9.94
Na_2O	1.99	1.83	1.86	1.65	1.88	2.09	2.16
K_2O	0.77	1.05	1.01	1.14	0.82	0.82	0.84
P_2O_5	0.12	0.18	0.20	0.19	0.15	0.14	0.17
H_2O^+	0.78	0.79	0.89	2.09	0.98	0.72	0.96
H_2O^-	0.32	0.12	0.47	0.41	0.25	0.17	0.31
CO_2	1.25	1.33	1.32	1.11	1.39	1.33	1.53
Total	99.70	100.07	100.45	99.83	100.48	100.22	100.98

Trace Elements (p.p.m.)

S	1179	972	90	426	230	998	916
Cr	641	719	601	682	641	532	762
Ni	31	51	35	32	35	37	59
Zn	85	83	84	86	85	85	88
Ga	16	16	14	16	16	15	15
Rb	31	28	26	27	23	20	24
Sr	189	159	159	174	174	194	164
Y	22	26	28	25	23	24	25
Zr	135	155	160	143	140	137	167
Ba	258	353	381	343	292	280	343
La	12	16	18	12	10	11	15
Ce	27	34	39	26	28	30	38
Pb	5	11	10	15	9	6	14
Th	3	3	3	7	<3	5	8

TABLE X (continued)

Analyses recalculated to 100 per cent anhydrous

	3697	3667	3737	3673	3738	3702	3741
SiO_2	51.32	51.53	51.82	51.44	50.91	51.12	51.07
TiO_2	0.90	1.03	1.00	0.93	0.91	0.94	1.03
Al_2O_3	15.85	14.93	15.21	13.33	15.74	16.41	14.45
Fe_2O_3	3.25	2.26	2.76	3.13	2.99	2.15	2.95
FeO	6.51	7.56	6.89	6.89	6.62	7.26	6.92
MnO	0.14	0.14	0.13	0.15	0.14	0.14	0.14
MgO	7.59	8.18	7.53	10.70	7.98	7.36	8.75
CaO	10.26	9.95	10.23	9.23	10.44	10.23	9.97
Na_2O	2.01	1.84	1.87	1.69	1.89	2.10	2.17
K_2O	0.78	1.05	1.02	1.17	0.83	0.82	0.85
P_2O_5	0.12	0.18	0.21	0.19	0.15	0.14	0.17
CO_2	1.27	1.34	1.33	1.14	1.40	1.34	1.53

C.I.P.W. Norms

Q	3.98	3.05	4.61	2.11	3.16	2.27	1.87
Or	4.69	6.31	6.12	6.99	4.98	4.92	5.08
Ab	17.24	15.80	16.05	14.49	16.23	18.03	18.65
An	32.30	29.76	30.47	25.60	32.45	33.35	27.60
Wo_{Di}	7.70	7.98	8.18	8.11	7.96	7.16	8.96
En_{Di}	5.03	4.94	5.18	5.60	5.20	4.33	5.92
Fs_{Di}	2.14	2.57	2.48	1.85	2.21	2.43	2.40
En_{Hy}	14.11	15.71	13.83	21.34	14.96	14.23	16.21
Fs_{Hy}	6.00	8.16	6.62	7.06	6.34	7.98	6.58
Mt	4.78	3.32	4.05	4.60	4.40	3.15	4.34
Il	1.73	1.98	1.93	1.78	1.76	1.80	1.98
Ap	0.29	0.43	0.49	0.46	0.36	0.34	0.42

TABLE X (continued)

Elements (weight per cent)

	3697	3667	3737	3673	3738	3702	3741
Si^{4+}	23.99	24.09	24.23	24.05	23.80	23.90	23.88
Ti^{4+}	0.54	0.62	0.60	0.56	0.55	0.56	0.62
Al^{3+}	8.39	7.90	8.05	7.05	8.33	8.68	7.65
Fe^{3+}	2.28	1.58	1.93	2.19	2.09	1.50	2.06
Fe^{2+}	5.06	5.88	5.36	5.36	5.15	5.65	5.38
Mn^{2+}	0.11	0.11	0.10	0.12	0.11	0.11	0.11
Mg^{2+}	4.58	4.94	4.54	6.45	4.82	4.44	5.28
Ca^{2+}	7.33	7.11	7.31	6.60	7.46	7.31	7.12
Na^{+}	1.49	1.37	1.39	1.26	1.40	1.56	1.61
K^{+}	0.65	0.87	0.85	0.97	0.69	0.68	0.70
P^{5+}	0.05	0.08	0.09	0.09	0.07	0.06	0.08
C^{4+}	0.35	0.37	0.36	0.31	0.38	0.37	0.42
O^{2-}	45.19	45.09	45.20	45.00	45.17	45.19	45.10

Useful ratios

$Th \times 10^4$ /K	4.7	3.4	3.6	7.4	<4.3	7.4	11.4
K /Rb	207	310	323	350	297	339	292
Rb/Sr	0.16	0.18	0.16	0.16	0.13	0.10	0.15
Cr/Ni	20.7	14.9	17.2	21.3	18.3	14.4	12.9

3697 Z.481.9 Medium-grained dolerite, about 0.5 m. below upper contact.

3667 Z.483.7 Porphyritic chilled dolerite, about 0.8 m. above lower contact.

3737 Z.480.1b Altered coarse-grained dolerite, middle of sill, contact with third-phase sill.

3673 Z.480.3 Altered coarse-grained dolerite, middle of sill, about 5 m. below third-phase sill.

3738 Z.502.1 Medium-grained dolerite, near top of sill.

3702 Z.483.4 Fine-grained dolerite, minor sill in Marø Cliffs.

3741 Z.497.7 Chilled porphyritic dolerite, minor sill on south-west margin of Jeffries Glacier.

and Zr and by relatively high Al_2O_3, MgO, CaO, Cr, Ni and Sr. K/Rb (207-350) and Th/K (3.4-7.4) ratios are similar to those of the scarp-capping sill but Rb/Sr ratios are much lower (0.13-0.18). Cr/Ni ratios range between 14.9 and 21.3.

Minor sills in Marø Cliffs and alongside Jeffries Glacier (3702 and 3741) cannot be related on field or petrographical evidence but they appear to be chemically analogous to the first-phase sill of Marø Cliffs.

b. Third-phase sill of Marø Cliffs

This sill (Table XI) is just saturated with respect to SiO_2 except for the upper contact rock (3736). It is characterized by low SiO_2, MgO, Cr and Sr and by relatively high TiO_2, total iron, Zn, Zr, La and Ce. K/Rb (298-473) and Rb/Sr (0.17-0.23) ratios are relatively high compared to those of the first-phase sill and Th/K ratios (2.7-5.0) are lower. Cr/Ni ratios (2.31-2.93) are very much lower than in the first-phase sill.

Minor sills alongside Jeffries Glacier and in Lenton Bluff (3739, 3740 and 3703) are chemically analogous.

c. Basal sill of Lenton Bluff

Field and petrographical evidence suggests that the second phase of intrusion in Marø Cliffs, which is the apparent branch sill of the scarp-capping sill, continues across Jeffries Glacier as the basal sill of Lenton Bluff.

TABLE XI

CHEMICAL ANALYSES OF SPECIMENS FROM THE THIRD PHASE OF INTRUSION IN MARØ CLIFFS AND POSSIBLE RELATED MINOR SILLS

A Analyses (weight per cent)

	3736	3701	3706	3690	3739	3740	3703
SiO_2	47.96	47.76	47.71	47.72	47.70	45.62	46.13
TiO_2	2.49	2.04	2.01	2.41	2.39	2.33	2.29
Al_2O_3	12.69	13.47	13.62	12.37	12.55	12.46	11.83
Fe_2O_3	1.29	3.16	2.55	2.75	4.18	5.12	4.54
FeO	14.42	11.68	12.10	13.04	11.33	10.88	11.28
MnO	0.19	0.17	0.16	0.19	0.17	0.18	0.18
MgO	4.53	4.92	4.68	4.69	4.46	5.04	5.41
CaO	8.75	8.86	8.77	8.94	8.64	9.02	8.09
Na_2O	2.63	2.26	2.44	2.26	2.12	2.25	1.86
K_2O	1.36	1.20	1.25	1.22	1.25	1.05	1.00
P_2O_5	0.19	0.24	0.24	0.18	0.25	0.22	0.24
H_2O^+	0.45	0.99	0.95	1.00	1.22	2.51	1.95
H_2O-	0.14	0.32	0.24	0.14	0.24	0.48	0.40
CO_2	1.87	1.87	2.04	1.58	1.79	0.86	1.52
Total	98.96	98.92	98.75	98.47	98.29	98.02	96.71

Trace Elements (p.p.m.)

S	999	1607	1373	1106	1521	285	3622
Cr	85	74	73	83	76	87	85
Ni	29	32	30	29	30	31	31
Zn	120	112	115	118	120	137	121
Ga	19	22	19	18	19	19	20
Rb	34	21	30	34	33	29	29
Sr	150	126	178	152	165	184	217
Y	34	23	32	33	35	34	32
Zr	211	190	190	205	217	212	201
Ba	375	317	359	373	393	361	420
La	30	22	25	16	28	20	20
Ce	53	55	49	55	50	49	52
Pb	7	7	7	9	10	11	11
Th	<3	5	3	3	3	4	6

TABLE XI (continued)

Analyses recalculated to 100 per cent anhydrous

	3736	3701	3706	3690	3739	3740	3703
SiO_2	48.75	48.92	48.90	49.02	49.26	48.00	48.88
TiO_2	2.53	2.09	2.06	2.47	2.47	2.46	2.43
Al_2O_3	12.90	13.80	13.96	12.71	12.96	13.11	12.54
Fe_2O_3	1.31	3.24	2.61	2.83	4.32	5.39	4.81
FeO	14.66	11.97	12.40	13.40	11.70	11.45	11.95
MnO	0.19	0.17	0.17	0.19	0.18	0.19	0.19
MgO	4.61	5.04	4.80	4.82	4.61	5.31	5.73
CaO	8.90	9.07	8.99	9.18	8.92	9.49	8.58
Na_2O	2.67	2.32	2.50	2.32	2.19	2.37	1.97
K_2O	1.38	1.23	1.28	1.25	1.29	1.10	1.06
P_2O_5	0.20	0.25	0.24	0.18	0.26	0.23	0.25
CO_2	1.90	1.92	2.09	1.62	1.85	0.90	1.61

C.I.P.W. Norms

Q	0.00	1.43	0.06	1.10	4.47	1.70	4.74
Or	8.34	7.38	7.73	7.53	7.76	6.56	6.36
Ab	23.02	19.99	21.57	19.97	18.89	20.22	16.95
An	19.50	24.09	23.59	20.90	22.12	22.10	22.59
Wo_{Di}	10.10	8.42	8.50	10.11	8.87	9.96	7.93
En_{Di}	3.55	3.67	3.47	4.01	3.95	4.94	3.89
Fs_{Di}	6.81	4.73	5.09	6.20	4.88	4.82	3.90
En_{Hy}	4.89	9.12	8.72	8.18	7.73	8.39	10.62
Fs_{Hy}	9.38	11.75	12.80	12.64	9.55	8.18	10.65
Fo	2.28	0.00	0.00	0.00	0.00	0.00	0.00
Fa	4.83	0.00	0.00	0.00	0.00	0.00	0.00
Mt	1.94	4.78	3.87	4.16	6.38	7.88	7.09
Il	4.89	4.04	4.00	4.77	4.78	4.70	4.68
Ap	0.48	0.59	0.58	0.44	0.63	0.56	0.60

TABLE XI (continued)

Elements (weight per cent)

	3736	3701	3706	3690	3739	3740	3703
Si^{4+}	22.79	22.87	22.86	22.92	23.03	22.44	22.85
Ti^{4+}	1.51	1.25	1.24	1.48	1.48	1.47	1.45
Al^{3+}	6.83	7.30	7.39	6.73	6.86	6.94	6.63
Fe^{3+}	0.92	2.26	1.83	1.98	3.02	3.77	3.36
Fe^{2+}	11.39	9.30	9.64	10.41	9.09	8.90	9.29
Mn^{2+}	0.15	0.13	0.13	0.15	0.14	0.15	0.15
Mg^{2+}	2.78	3.04	2.89	2.91	2.78	3.20	3.46
Ca^{2+}	6.36	6.48	6.43	6.56	6.38	6.78	6.13
Na^{+}	1.98	1.72	1.85	1.72	1.63	1.76	1.46
K^{+}	1.15	1.02	1.06	1.04	1.07	0.91	0.88
P^{5+}	0.09	0.11	0.11	0.08	0.11	0.10	0.11
C^{4+}	0.52	0.52	0.57	0.44	0.50	0.25	0.44
O^{2-}	43.53	43.99	44.01	43.58	43.91	43.33	43.78

Useful ratios

Th x 10^4 /K	<2.7	5.0	2.9	3.0	2.8	4.4	7.2
K /Rb	333	473	346	298	314	299	286
Rb/Sr	0.23	0.17	0.17	0.22	0.20	0.16	0.13
Cr/Ni	2.93	2.31	2.43	2.86	2.53	2.81	2.74

3736	Z.480.1a	Vitrophyric olivine-dolerite, upper contact.
3701	Z.481.11	Coarse-grained olivine-dolerite, middle of sill.
3706	Z.483.6	Coarse-grained olivine-dolerite, middle of sill.
3690	Z.480.2	Vitrophyric olivine-dolerite, lower contact.
3739	Z.497.4	Fine-grained olivine-dolerite, minor sill on south-west margin of Jeffries Glacier.
3740	Z.497.6	Medium-grained dolerite, minor sill on south-west margin of Jeffries Glacier.
3703	Z.498.7	Medium-grained dolerite, minor sill in Lenton Bluff.

This is confirmed by the chemistry (Table XII).

Like the scarp-capping sill, this sill is oversaturated with respect to SiO_2 but there are major differences. SiO_2, K_2O and Rb are slightly lower than in the scarp-capping sill and TiO_2, MgO, P_2O_5, Cr, Ni and Zn are slightly higher; Sr, Y, Zr, Ba, La and Ce are considerably higher in the basal sill of Lenton Bluff. Excluding hydrothermally altered rocks (3720 and 3721), K/Rb ratios (283-455) are relatively high and Th/K (1.8-3.80) and Rb/Sr (0.14-0.20) ratios are lower. Cr/Ni ratios (1.66-1.80) are very constant except for altered rocks.

The hydrothermally altered rocks from near the contacts of sedimentary xenoliths (3720 and 3721) differ from unaltered rocks in containing much less SiO_2, CaO, K_2O, Zn, Rb, Sr and Ba and more TiO_2, Fe_2O_3 and total iron, MgO, H_2O, Cr, Ni and Zr. K/Rb (337) and Rb/Sr (0.03) ratios are lower, Cr/Ni ratios (2.09) slightly higher and Th/K ratios (49.2) very much higher than in unaltered rocks.

d. Younger sills and dykes of Lenton Bluff

The younger transgressive sill of Lenton Bluff, the complex system of dykes and sills at station Z.498 and the dyke below the basal sill at station Z.471 are chemically similar (Table XIII).

They are just saturated with respect to SiO_2 and they may be slightly quartz- or slightly olivine-normative

TABLE XII

CHEMICAL ANALYSES OF SPECIMENS FROM THE APPARENT BRANCH SILL OF THE SCARP-CAPPING SILL AND THE BASAL SILL OF LENTON BLUFF

Analyses

	3680	3681	3672	3675	3669	3663	3722	3723	3720	3721
SiO_2	51.71	51.49	51.09	50.37	52.27	51.09	51.12	50.84	47.35	45.54
TiO_2	2.73	2.79	2.77	3.07	2.96	2.85	2.88	3.13	3.24	3.56
Al_2O_3	12.67	12.27	12.24	11.66	12.93	12.23	11.77	11.61	10.11	11.14
Fe_2O_3	2.94	3.62	4.65	2.95	3.54	3.33	3.52	2.82	5.98	6.85
FeO	10.16	9.80	8.85	10.93	9.80	10.01	9.80	11.28	12.08	9.64
MnO	0.16	0.16	0.16	0.18	0.16	0.16	0.17	0.19	0.15	0.22
MgO	3.04	2.70	2.88	3.57	2.85	2.97	3.08	3.46	4.64	5.30
CaO	7.73	7.62	7.82	8.05	7.78	7.69	7.90	8.37	5.47	4.82
Na_2O	2.81	2.59	2.50	2.46	3.08	2.63	2.37	2.81	2.26	2.40
K_2O	1.91	1.96	1.91	1.57	1.92	2.08	1.79	1.37	0.14	0.18
P_2O_5	0.43	0.47	0.47	0.39	0.41	0.44	0.46	0.32	0.38	0.39
H_2O+	0.88	1.00	1.30	1.41	0.61	0.98	1.27	0.76	4.12	3.80
H_2O-	0.22	0.40	0.28	0.49	0.24	0.22	0.26	0.26	0.24	0.48
CO_2	0.80	0.43	0.81	0.84	0.86	1.08	0.70	0.91	0.48	0.77
Total	98.18	97.29	97.72	97.94	99.40	97.77	97.08	98.12	96.63	95.07

Trace elements (p.p.m.)

S	616	483	1449	373	701	1061	732	623	361	117
Cr	61	53	58	58	58	57	53	63	78	83
Ni	34	31	35	33	33	33	33	35	38	39
Zn	110	113	106	97	116	117	155	125	79	90
Ga	17	20	22	20	18	23	20	21	22	27
Rb	36	37	35	34	35	38	36	40	4	4
Sr	227	230	232	238	218	219	227	201	171	117
Y	47	50	51	50	48	48	51	50	64	48
Zr	313	318	321	316	314	311	343	339	359	399
Ba	664	685	662	604	652	631	743	603	194	216
La	41	44	42	48	40	38	42	37	43	49
Ce	76	92	90	80	76	86	88	80	89	111
Pb	14	13	10	5	15	9	12	5	5	5
Th	6	3	6	4	4	5	4	<3	7	6

Analyses recalculated to 100 per cent anhydrous

SiO_2	53.26	53.69	53.14	52.46	53.04	52.91	53.49	52.36	51.31	50.16
TiO_2	2.81	2.90	2.88	3.20	3.00	2.95	3.02	3.23	3.51	3.92
Al_2O_3	13.05	12.80	12.73	12.14	13.12	12.66	12.31	11.95	10.96	12.26
Fe_2O_3	3.03	3.78	4.84	3.07	3.60	3.45	3.68	2.90	6.48	7.55
FeO	10.47	10.22	9.21	11.38	9.94	10.37	10.26	11.62	13.09	10.62
MnO	0.16	0.17	0.16	0.19	0.17	0.16	0.18	0.19	0.16	0.24
MgO	3.13	2.81	3.00	3.72	2.89	3.07	3.22	3.57	5.03	5.83
CaO	7.96	7.95	8.13	8.38	7.90	7.97	8.27	8.62	5.92	5.31
Na_2O	2.90	2.70	2.60	2.56	3.13	2.72	2.48	2.89	2.45	2.64
K_2O	1.97	2.04	1.98	1.63	1.95	2.15	1.88	1.41	0.15	0.20
P_2O_5	0.45	0.49	0.49	0.40	0.41	0.46	0.48	0.33	0.41	0.43
CO_2	0.82	0.45	0.84	0.87	0.87	1.12	0.73	0.94	0.52	0.85

C.I.P.W. Norms

Q	7.10	9.50	10.48	7.68	6.98	7.71	10.25	6.46	13.30	12.54
Or	11.73	12.12	11.82	9.71	11.61	12.87	11.17	8.39	0.91	1.19
Ab	24.71	22.93	22.15	21.88	26.68	23.28	21.13	24.67	20.81	22.51
An	16.93	16.85	17.37	16.94	16.14	16.15	17.04	15.63	18.55	21.20
Wo_{Di}	8.32	8.16	8.38	9.33	8.62	8.67	8.83	10.57	3.47	1.04
En_{Di}	3.26	3.19	3.89	3.83	3.51	3.48	3.71	4.16	1.66	0.65
Fs_{Di}	5.17	5.08	4.41	5.56	5.19	5.28	5.15	6.54	1.75	0.33
En_{Hy}	4.60	3.85	3.64	5.50	3.75	4.26	4.36	4.80	10.93	13.99
Fs_{Hy}	7.30	6.13	4.12	7.98	5.54	6.46	6.06	7.55	11.51	6.97
Mt	4.43	5.50	7.07	4.49	5.26	5.06	5.38	4.25	9.44	11.03
Il	5.38	5.54	5.52	6.13	5.75	5.67	5.77	6.19	6.70	7.50
Ap	1.06	1.16	1.16	0.96	0.98	1.10	1.14	0.79	0.97	1.03

C.I,P.W. Norms

Q	7.10	9.50	10.48	7.68	6.98	7.71	10.25	6.46	13.30	12.54
Or	11.73	12.12	11.82	9.71	11.61	12.87	11.17	8.39	0.91	1.19
Ab	24.71	22.93	22.15	21.88	26.68	23.28	21.13	24.67	20.81	22.51
An	16.93	16.85	17.37	16.94	16.14	16.15	17.04	15.63	18.55	21.20
Wo_{Di}	8.32	8.16	8.38	9.33	8.62	8.67	8.83	10.57	3.47	1.04
En_{Di}	3.26	3.19	3.89	3.83	3.51	3.48	3.71	4.16	1.66	0.65
Fs_{Di}	5.17	5.08	4.41	5.56	5.19	5.28	5.15	6.54	1.75	0.33
En_{Hy}	4.60	3.85	3.64	5.50	3.75	4.26	4.36	4.80	10.93	13.99
Fs_{Hy}	7.30	6.13	4.12	7.98	5.54	6.46	6.06	7.55	11.51	6.97
Mt	4.43	5.50	7.07	4.49	5.26	5.06	5.38	4.25	9.44	11.03
Il	5.38	5.54	5.52	6.13	5.75	5.67	5.77	6.19	6.70	7.50
Ap	1.06	1.16	1.16	0.96	0.98	1.10	1.14	0.79	0.97	1.03

Elements (weight per cent)

Si^{4+}	24.90	25.10	24.84	24.52	24.80	24.73	25.01	24.48	23.99	23.45
Ti^{4+}	1.68	1.74	1.73	1.92	1.80	1.77	1.81	1.94	2.10	2.35
Al^{3+}	6.91	6.77	6.74	6.42	6.94	6.70	6.52	6.32	5.80	6.49
Fe^{3+}	2.12	2.64	3.38	2.15	2.51	2.41	2.58	2.03	4.53	5.28
Fe^{2+}	8.13	7.94	7.16	8.85	7.73	8.06	7.97	9.03	10.18	8.25
Mn^{2+}	0.12	0.13	0.13	0.14	0.13	0.13	0.14	0.15	0.13	0.18
Mg^{2+}	1.89	1.70	1.81	2.24	1.74	1.85	1.94	2.15	3.03	3.52
Ca^{2+}	5.69	5.68	5.81	5.99	5.64	5.69	5.91	6.16	4.23	3.79
Na^{+}	2.15	2.00	1.93	1.90	2.32	2.02	1.84	2.14	1.82	1.96
K^{+}	1.63	1.69	1.65	1.35	1.62	1.79	1.56	1.17	0.13	0.17
P^{5+}	0.19	0.21	0.21	0.18	0.18	0.20	0.21	0.15	0.18	0.19
C^{4+}	0.22	0.12	0.23	0.24	0.24	0.31	0.20	0.26	0.14	0.23
O^{2-}	44.35	44.26	44.39	44.10	44.35	44.33	44.32	44.03	43.74	44.14

Useful ratios

$Th \times 10^4$ /K	1.8	3.8	3.8	3.0	2.5	2.9	2.7	<2.6	58.3	40.0
K /Rb	441	439	452	382	455	454	414	283	295	378
Rb/Sr	0.16	0.16	0.15	0.14	0.16	0.17	0.16	0.20	0.02	0.03
Cr/Ni	1.71	1.79	1.66	1.76	1.76	1.73	1.67	1.80	2.05	2.13

a. Apparent branch sill of the scarp-capping sill

3680 Z.483.8 medium-grained quartz-dolerite, lower half of sill.

3681 Z.483.9 Medium-grained quartz-dolerite, 1.2 m. below upper contact.

b. Basal sill of Lenton Bluff

3672 Z.471.16 Medium-grained dolerite, upper third of sill, 0.8 m. above contact of younger transgressive sill.

3675 Z.472.9 Vitrophyric dolerite, lower half of sill, xenolithic contact.

3669 Z.472.11 Fine-grained olivine-dolerite, lower half of sill.

3663 Z.472.4 Medium-grained olivine-dolerite, lower third of sill.

3722 Z.471.11 Fine-grained dolerite, <1 m. above lower contact, near rheomorphic vein.

3723 Z.471.10 Vitrophyric dolerite, lower contact.

c. Hydrothermally altered rocks

3720 Z.472.3 Chlorite-tremolite veins, above xenolith contact.

3721 Z.472.13 Andradite-calcite veins, near small xenolith.

TABLE XIII

CHEMICAL ANALYSES OF SPECIMENS FROM THE YOUNGER SILLS AND DYKES OF LENTON BLUFF

Analyses (weight per cent)

	3661	3665	3724	3725	3726	3727	3728	3729	3730	3664	3660	3662
SiO_2	49.07	49.73	49.01	47.57	47.05	48.12	48.07	48.68	47.89	49.34	49.23	49.37
TiO_2	0.72	0.70	0.67	0.89	0.91	0.82	0.66	0.74	0.70	0.69	0.66	0.74
Al_2O_3	15.30	16.09	15.12	12.84	13.28	12.95	14.71	15.02	15.10	14.17	14.48	16.00
Fe_2O_3	3.19	1.91	3.65	4.54	4.55	3.06	1.90	2.66	2.57	2.50	2.27	2.37
FeO	5.79	6.76	5.62	6.85	6.69	7.40	6.84	6.36	6.42	7.45	7.34	7.21
MnO	0.12	0.12	0.13	0.15	0.15	0.17	0.13	0.12	0.13	0.15	0.14	0.14
MgO	10.41	10.17	10.60	10.93	11.08	11.77	12.43	6.98	10.74	10.34	11.41	8.01
CaO	11.53	11.04	10.88	9.17	8.56	10.20	10.74	11.45	11.23	10.99	10.83	11.11
Na_2O	1.64	1.66	1.61	1.55	1.59	1.58	1.39	1.85	1.35	1.76	1.80	1.90
K_2O	0.35	0.52	0.36	0.59	0.69	0.40	0.42	0.25	0.31	0.31	0.41	0.48
P_2O_5	0.08	0.08	0.06	0.06	0.07	0.05	0.07	0.08	0.08	0.07	0.08	0.09
H_2O+	0.91	0.52	1.03	2.14	2.95	0.80	1.48	1.54	2.00	0.86	0.92	0.59
H_2O-	0.71	0.39	0.48	1.01	1.05	0.46	0.36	0.60	0.54	0.42	0.40	0.33
CO_2	1.26	1.35	1.07	1.10	0.02	1.49	1.45	1.65	1.36	1.00	1.22	1.15
Total	101.07	101.05	100.28	99.40	99.54	99.27	100.65	97.98	100.38	100.04	101.18	99.48

Trace elements (p.p.m.)

S	443	1107	149	186	219	254	1021	145	251	588	3368	2340
Cr	586	555	566	830	793	734	540	535	516	869	795	641
Ni	9	8	9	25	25	24	9	10	9	35	33	15
Zn	73	70	71	105	123	71	70	70	73	78	71	74
Ga	14	17	16	16	15	14	16	16	16	15	13	13
Rb	9	17	16	32	37	26	15	23	9	23	23	19
Sr	168	171	210	219	240	189	198	151	171	133	123	130
Y	15	14	15	17	18	17	14	26	15	16	17	18
Zr	73	69	63	63	60	68	68	159	72	68	69	80
Ba	165	172	169	213	234	188	285	172	185	171	150	212
La	4	5	3	<3	<3	<3	<3	3	4	3	6	<3
Ce	10	10	14	8	9	12	3	7	14	9	8	23
Pb	3	6	7	17	20	7	8	11	6	8	8	10
Th	<3	4	<3	3	<3	<3	<3	7	3	<3	3	5

Analyses recalculated to 100 per cent anhydrous

SiO_2	49.34	49.66	49.62	49.42	49.72	49.10	48.65	50.79	48.93	49.95	49.30	50.09
TiO_2	0.72	0.70	0.68	0.93	0.96	0.84	0.67	0.77	0.71	0.69	0.66	0.75
Al_2O_3	15.38	16.07	15.30	13.34	14.03	13.21	14.89	15.67	15.43	14.35	14.49	16.23
Fe_2O_3	3.21	1.91	3.70	4.72	4.81	3.12	1.92	2.78	2.63	2.53	2.27	2.40
FeO	5.82	6.75	5.69	7.12	7.07	7.55	6.92	6.64	6.56	7.54	7.35	7.32
MnO	0.12	0.12	0.13	0.16	0.16	0.17	0.13	0.13	0.13	0.16	0.14	0.14
MgO	10.47	10.15	10.73	11.35	11.71	12.01	12.57	7.28	10.97	10.47	11.43	8.13
CaO	11.59	11.03	11.02	9.53	9.05	10.41	10.87	11.95	11.47	11.12	10.84	11.27
Na_2O	1.64	1.66	1.63	1.61	1.68	1.61	1.41	1.93	1.38	1.78	1.81	1.92
K_2O	0.35	0.52	0.36	0.61	0.73	0.41	0.43	0.26	0.32	0.32	0.41	0.48
P_2O_5	0.08	0.08	0.06	0.07	0.07	0.05	0.07	0.09	0.08	0.07	0.08	0.09
CO_2	1.27	1.35	1.08	1.15	0.02	1.52	1.47	1.72	1.39	1.01	1.22	1.17

C.I.P.W. Norms

Q	0.06	0.00	0.89	1.18	0.42	0.00	0.00	3.86	0.00	0.00	0.00	0.84
Or	2.12	3.12	2.18	3.66	4.29	2.45	2.57	1.56	1.89	1.89	2.43	2.89
Ab	14.09	14.23	13.92	13.77	14.24	13.85	12.07	16.65	11.84	15.21	15.46	16.48
An	33.97	35.33	33.74	27.67	28.59	28.03	33.54	33.89	35.46	30.54	30.62	34.62
Wo_{Di}	9.91	8.17	8.81	8.23	6.61	10.04	8.66	10.78	9.07	10.32	9.71	8.91
En_{Di}	7.10	5.44	6.42	5.86	4.75	6.89	5.99	6.79	6.27	6.76	6.51	5.53
Fs_{Di}	1.93	2.13	1.57	1.65	1.26	2.35	1.96	3.32	2.05	2.83	2.47	2.86
En_{Hy}	19.30	18.01	20.58	22.73	24.41	19.64	16.93	11.66	20.21	18.24	15.13	14.95
Fs_{Hy}	5.24	7.04	5.02	6.38	6.46	6.72	5.54	5.69	6.62	7.63	5.74	7.74
Fo	0.00	1.53	0.00	0.00	0.00	2.68	6.21	0.00	0.85	0.93	5.01	0.00
Fa	0.00	0.66	0.00	0.00	0.00	1.01	2.24	0.00	0.31	0.43	2.10	0.00
Mt	4.71	2.80	5.42	6.92	6.97	4.60	2.83	4.09	3.86	3.71	3.34	3.53
Il	1.39	1.35	1.31	1.78	1.82	1.61	1.29	1.49	1.37	1.33	1.27	1.44
Ap	0.19	0.20	0.15	0.16	0.17	0.13	0.17	0.21	0.20	0.18	0.20	0.21

C.I.P.W. Norms

Q	0.06	0.00	0.89	1.18	0.42	0.00	0.00	3.86	0.00	0.00	0.00	0.84
Or	2.12	3.12	2.18	3.66	4.29	2.45	2.57	1.56	1.89	1.89	2.43	2.89
Ab	14.09	14.23	13.92	13.77	14.24	13.85	12.07	16.65	11.84	15.21	15.46	16.48
An	33.97	35.33	33.74	27.67	28.59	28.03	33.54	33.89	35.46	30.54	30.62	34.62
Wo_{Di}	9.91	8.17	8.81	8.23	6.61	10.04	8.66	10.78	9.07	10.32	9.71	8.91
En_{Di}	7.10	5.44	6.42	5.86	4.75	6.89	5.99	6.79	6.27	6.76	6.51	5.53
Fs_{Di}	1.93	2.13	1.57	1.65	1.26	2.35	1.96	3.32	2.05	2.83	2.47	2.86
En_{Hy}	19.30	18.01	20.58	22.73	24.41	19.64	16.93	11.66	20.21	18.24	15.13	14.95
Fs_{Hy}	5.24	7.04	5.02	6.38	6.46	6.72	5.54	5.69	6.62	7.63	5.74	7.74
Fo	0.00	1.53	0.00	0.00	0.00	2.68	6.21	0.00	0.85	0.93	5.01	0.00
Fa	0.00	0.66	0.00	0.00	0.00	1.01	2.24	0.00	0.31	0.43	2.10	0.00
Mt	4.71	2.80	5.42	6.92	6.97	4.60	2.83	4.09	3.86	3.71	3.34	3.53
Il	1.39	1.35	1.31	1.78	1.82	1.61	1.29	1.49	1.37	1.33	1.27	1.44
Ap	0.19	0.20	0.15	0.16	0.17	0.13	0.17	0.21	0.20	0.18	0.20	0.21

Elements (weight per cent)

Si^{4+}	23.07	23.22	23.20	23.11	23.24	22.95	22.74	23.75	22.88	23.35	23.05	23.42
Ti^{4+}	0.43	0.42	0.41	0.56	0.57	0.50	0.40	0.46	0.43	0.42	0.40	0.45
Al^{3+}	8.14	8.50	8.10	7.06	7.43	6.99	7.88	8.29	8.17	7.59	7.67	8.59
Fe^{3+}	2.24	1.33	2.58	3.30	3.36	2.18	1.34	1.94	1.84	1.77	1.59	1.68
Fe^{2+}	4.53	5.25	4.42	5.53	5.49	5.87	5.38	5.16	5.10	5.86	5.71	5.69
Mn^{2+}	0.09	0.09	0.10	0.12	0.12	0.13	0.10	0.10	0.10	0.12	0.11	0.11
Mg^{2+}	6.31	6.12	6.47	6.85	7.06	7.24	7.58	4.39	6.62	6.32	6.89	4.90
Ca^{2+}	8.29	7.88	7.87	6.81	6.47	7.44	7.77	8.54	8.20	7.95	7.75	8.05
Na^{+}	1.22	1.23	1.21	1.19	1.25	1.20	1.04	1.44	1.02	1.32	1.34	1.43
K^{+}	0.29	0.43	0.30	0.51	0.60	0.34	0.36	0.21	0.26	0.26	0.34	0.40
P^{5+}	0.04	0.04	0.03	0.03	0.03	0.02	0.03	0.04	0.04	0.03	0.04	0.04
C^{4+}	0.35	0.37	0.30	0.31	0.01	0.41	0.40	0.47	0.38	0.28	0.33	0.32
O^{2-}	45.01	45.11	45.01	44.62	44.36	44.71	44.97	45.22	44.98	44.73	44.79	44.92

Useful Ratios

$Th \times 10^4$ /K	<10.3	9.3	<10.0	6.1	<5.3	<9.1	<8.6	33.3	11.5	<11.5	8.8	12.5
K /Rb	325	254	187	153	154	128	234	90	285	113	147	208
Rb/Sr	0.05	0.10	0.08	0.15	0.15	0.14	0.08	0.15	0.05	0.17	0.19	0.15
Cr/Ni	65.1	69.4	62.9	33.2	31.7	30.6	60.0	53.5	57.3	24.4	24.1	42.7

a. Younger transgressive 5 m. thick sill which cuts the basal sill of Lenton Bluff

3661 Z.471.14 Altered chilled olivine-dolerite, just below upper contact.
3665 Z.471.15 Fine-grained altered olivine-dolerite, about 1 m. below upper contact.

b. 1.2 m. wide dyke above basal sill of Lenton Bluff

3724 Z.498.3 Chilled dolerite, middle of dyke

c. 6 m. wide dyke above basal sill of Lenton Bluff

3725 Z.498.5f Porphyritic chilled dolerite, fresh specimen, contact of dyke.
3726 Z.498.5a Porphyritic chilled dolerite, weathered specimen, contact of dyke.
3727 Z.498.6 Chilled dolerite, middle of dyke.

d. 3 m. thick minor sill above basal sill of Lenton Bluff

3728 Z.498.8 Fine-grained dolerite, middle of sill.

e. 3-5 m. thick minor sill above basal sill of Lenton Bluff

3729 Z.498.9f Fine-grained dolerite, fresh specimen, middle of sill.
3730 Z.498.9a Fine-grained dolerite, weathered specimen, middle of sill.

f. 2-3 m. wide dyke below basal sill of Lenton Bluff

3664 Z.471.13a Altered chilled olivine-dolerite, contact of dyke.
3660 Z.471.13b Chilled olivine-dolerite, 0.3 m. from contact of dyke.
3662 Z.471.13c Fine-grained altered olivine-dolerite, middle of dyke.

(4 per cent quartz to 8 per cent olivine). They are characterized by low SiO_2, TiO_2, total iron, MnO, Na_2O, K_2O, P_2O_5, Ni, Zn, Rb, Y, Zr, Ba, La and Ce and relatively high Al_2O_3, MgO, CaO and Cr. K/Rb ratios are very variable (90-325) but generally low, as are Rb/Sr ratios (0.05-0.19). Th/K ratios, however, are higher than normal (5.3-12.5, with one at 33.3) and Cr/Ni ratios are very variable and very high (24.1-69.4).

3. Layered sills

Layering of two types is seen in the cliffs alongside Jeffries Glacier and in Marø Cliffs. Chemical data (Table XIV) do not add very much to the field and petrographical evidence of differentiation mechanisms, which are discussed below.

a. Jeffries Glacier

The normal dolerite (3735) beneath the mafic layer in the middle of the 50 m. sill at station Z.497 is just saturated with respect to SiO_2; it is strongly hypersthene-normative. Material from the mafic layer (3734), however, is very much under-saturated with respect to SiO_2; it is a picro-dolerite with 26.7 per cent normative olivine and 24.6 per cent normative hypersthene. Compared with the normal dolerite it is very much lower in

TABLE XIV

CHEMICAL ANALYSES OF SPECIMENS FROM THE LAYERED SILLS OF JEFFRIES GLACIER AND MARØ CLIFFS

Analyses (weight per cent)

	3734	3735	3731	3732	3733	3668	3674
SiO_2	46.95	50.49	51.63	53.82	51.25	47.83	49.24
TiO_2	0.57	0.83	0.95	1.87	0.93	0.63	0.89
Al_2O_3	12.81	14.15	15.93	12.23	15.28	13.19	12.05
Fe_2O_3	0.51	2.37	1.36	3.05	1.75	0.97	2.75
FeO	9.45	6.65	7.36	9.53	7.71	9.04	8.06
MnO	0.16	0.13	0.14	0.14	0.14	0.16	0.14
MgO	18.24	11.53	10.02	3.27	7.90	16.37	14.39
CaO	6.65	9.72	10.15	7.71	9.93	7.08	8.55
Na_2O	1.34	1.64	1.32	2.05	1.74	1.51	1.46
K_2O	0.49	0.74	0.94	2.17	1.00	0.67	0.95
P_2O_5	0.18	0.18	0.26	0.47	0.21	0.20	0.21
H_2O+	0.93	1.03	0.60	1.13	0.69	0.83	0.84
H_2O-	0.10	0.42	0.27	0.45	0.26	0.34	0.28
CO_2	2.53	1.36	1.17	0.99	1.12	2.76	1.64
Total	100.91	101.23	102.10	98.88	99.90	101.58	101.44

Trace Elements (p.p.m.)

S	1561	1399	630	1555	673	1835	693
Cr	2302	1235	634	42	715	2715	1700
Ni	275	113	41	11	37	293	173
Zn	91	77	85	125	82	92	74
Ga	9	15	15	17	16	12	14
Rb	12	18	9	50	23	15	24
Sr	95	159	181	141	153	103	129
Y	16	21	15	51	25	17	23
Zr	73	116	70	308	143	93	133
Ba	304	286	339	634	349	303	325
La	8	14	14	37	13	9	16
Ce	<3	18	31	84	31	<3	26
Pb	10	12	<3	18	13	7	7
Th	<3	3	<3	8	5	3	5

TABLE XIV (continued)

Analyses recalculated to 100 per cent anhydrous

	3734	3735	3731	3732	3733	3668	3674
SiO_2	47.00	50.60	51.00	55.32	51.80	47.64	49.08
TiO_2	0.57	0.83	0.94	1.92	0.94	0.62	0.89
Al_2O_3	12.83	14.18	15.73	12.57	15.44	13.14	12.01
Fe_2O_3	0.51	2.38	1.34	3.13	1.77	0.97	2.74
FeO	9.46	6.66	7.27	9.80	7.79	9.00	8.03
MnO	0.16	0.13	0.14	0.15	0.14	0.16	0.14
MgO	18.26	11.55	9.90	3.36	7.98	16.31	14.34
CaO	6.66	9.74	10.02	7.93	10.04	7.05	8.52
Na_2O	1.34	1.65	1.31	2.10	1.76	1.50	1.45
K_2O	0.49	0.74	0.93	2.23	1.01	0.67	0.94
P_2O_5	0.18	0.18	0.25	0.48	0.21	0.20	0.21
CO_2	2.53	1.36	1.16	1.02	1.13	2.75	1.63

C.I.P.W. Norms

Q	0.00	0.33	2.34	12.23	3.39	0.00	0.00
Or	2.96	4.45	5.57	13.30	6.01	4.05	5.67
Ab	11.65	14.13	11.18	17.97	15.04	13.08	12.47
An	28.24	29.50	34.71	18.47	31.62	27.89	23.86
Wo_{Di}	1.85	7.65	5.81	7.54	7.25	2.80	7.41
En_{Di}	1.26	5.32	3.75	3.05	4.34	1.89	5.16
Fs_{Di}	0.45	1.69	1.67	4.56	2.52	0.70	1.63
En_{Hy}	18.08	23.83	21.18	5.39	15.76	18.63	21.88
Fs_{Hy}	6.49	7.58	9.42	8.07	9.16	6.88	6.91
Fo	19.13	0.00	0.00	0.00	0.00	14.88	6.49
Fa	7.57	0.00	0.00	0.00	0.00	6.06	2.26
Mt	0.76	3.49	1.97	4.59	2.59	1.44	4.04
Il	1.10	1.59	1.80	3.68	1.80	1.22	1.72
Ap	0.44	0.42	0.61	1.15	0.50	0.48	0.50

TABLE XIV (continued)

Elements (weight per cent)

	3734	3735	3731	3732	3733	3668	3674
Si^{4+}	21.97	23.66	23.84	25.86	24.22	22.27	22.95
Ti^{4+}	0.34	0.50	0.56	1.15	0.56	0.53	0.37
Al^{3+}	6.79	7.50	8.33	6.65	8.17	6.95	6.36
Fe^{3+}	0.36	1.66	0.94	2.19	1.24	0.68	1.92
Fe^{2+}	7.35	5.18	5.65	7.61	6.06	7.00	6.24
Mn^{2+}	0.13	0.10	0.11	0.11	0.11	0.12	0.11
Mg^{2+}	11.01	6.97	5.97	2.02	4.82	9.84	8.65
Ca^{2+}	4.76	6.96	7.16	5.66	7.17	5.04	6.09
Na^{+}	1.00	1.22	0.97	1.56	1.30	1.12	1.08
K^{+}	0.41	0.62	0.77	1.85	0.83	0.55	0.78
P^{5+}	0.08	0.08	0.11	0.21	0.09	0.09	0.09
C^{4+}	0.69	0.37	0.32	0.28	0.31	0.75	0.45
O^{2-}	45.11	45.18	45.26	44.83	45.12	45.23	44.75

Useful ratios

Th x 10^4 /K	<7.3	4.9	<3.8	4.4	6.0	5.4	6.3
K /Rb	338	342	871	360	359	370	328
Rb/Sr	0.13	0.11	0.05	0.36	0.15	0.15	0.19
Cr/Ni	8.4	11.0	15.5	3.82	19.7	9.3	9.8

a. Jeffries Glacier

3734 Z.497.10 Mafic layer in middle of sill.

3735 Z.497.9 Normal dolerite below mafic layer.

b. Marø Cliffs

3731 Z.481.6 Upper contact, near rheomorphic vein.

3732 Z.481.5 Thin finer-grained darker-weathering band in dolerite-pegmatite, 1.8 m. below upper contact.

3733 Z.481.4 Dolerite-pegmatite, 1.8 m. below upper contact.

3668 Z.481.2 Melanocratic layer in lower 8 m.

3674 Z.481.1 Leucocratic layer in lower 8 m.

SiO_2, TiO_2, Fe_2O_3, CaO, Na_2O, Rb, Sr, Y, Zr, La and Ce and higher in FeO and total iron, MnO, MgO, Cr, Ni and Zn. Ratios of K/Rb (340), Rb/Sr (0.12), Th/K (6.1) and Cr/Ni (9.7) are relatively constant between the two specimens.

The mafic layer in this sill is very similar to the olivine-diabase layer of the Palisades sill of New Jersey (Walker, 1940), for which crystal settling has been suggested as a possible origin. Gray and Crain (1969) suggested that, although several major features can be explained, the single model of crystal settling cannot account for the details of olivine distribution in the Palisades sill. Walker (1969) considered the olivine-diabase layer to be due to multiple intrusion of two main magma phases, the degree of differentiation being controlled by the rate of cooling. Bhattacharji (1966, 1967) has shown that flowage differentiation in sills could lead to an accumulation of early-formed crystals approximately in the middle of the sill and his figures show a splitting of these layers very similar to that seen in the mafic layer of station Z.497.

The limited field, petrographical and chemical evidence from the layered sill of Jeffries Glacier suggests that flowage differentiation may be the principal causative agent in the formation of the mafic layer in the middle of the sill.

b. Marø Cliffs

The layered sill of Marø Cliffs shows rhythmic layering in its lower 8 m., dolerite-pegmatite and cross-cutting veins in its upper part and remobilization of roof sediments and rheomorphic injection of the sill by them.

The specimen from a melanocratic layer (3668) is very similar to the mafic layer of the layered sill of Jeffries Glacier except that MgO is slightly lower and SiO_2, Fe_2O_3, K_2O, Cr, Ni and Zr are slightly higher. The specimen from a leucocratic layer (3674) is compositionally about midway between the mafic layer and the normal dolerite of the layered sill of Jeffries Glacier. Both melanocratic and leucocratic layers are strongly under-saturated with respect to SiO_2 (20.9 and 8.8 per cent normative olivine), with the former having high normative hypersthene while the latter has relatively high normative diopside. K/Rb (349), Rb/Sr (0.17), Th/K (5.9) and Cr/Ni (9.6) ratios are remarkably constant between melanocratic and leucocratic layers and very similar to those of the layered sill of Jeffries Glacier.

The dolerite-pegmatite (3733) and upper contact material from the contact of a rheomorphic vein (3731) are alike except that MgO, Na_2O and Sr are slightly lower in the dolerite-pegmatite and Rb, Y and Zr are considerably

higher. Both are just saturated with respect to SiO_2 (2-3 per cent normative quartz) and strongly hypersthene-normative (25-30 per cent). Cr/Ni ratios are much the same but Rb/Sr and Th/K ratios are lower and the K/Rb ratio is very much higher in the contact rock of the rheomorphic vein, possibly as a result of contamination.

The thin band of finer-grained darker-weathering material (3732) is very different from the surrounding dolerite-pegmatite. It is over-saturated with respect to SiO_2 (12.2 per cent normative quartz) and normative diopside is slightly in excess of normative hypersthene. SiO_2, TiO_2, Fe_2O_3, FeO, Na_2O, K_2O, P_2O_5, H_2O, Zn, Y, Zr, Ba, La, Ce, Pb and Th are all higher than in the dolerite-pegmatite and Al_2O_3, MgO, CaO, Cr and Ni are lower. Although K/Rb and Th/K ratios are similar, Rb/Sr and Cr/Ni ratios are very different. This band is similar to the cross-cutting dolerite-pegmatite veins described by Walker (1953) as a later post-injection differentiate of the normal rock than patches and schlieren of dolerite-pegmatite, represented by the host dolerite-pegmatite in this example.

This sill is similar to differentiated intrusions described by many authors except that rhythmic layering is usually confined to thick sills. This sill is only 30 m. thick and rhythmic layering of melanocratic and leucocratic

cumulates is confined to its lower 8 m. Cryptic variation is not very marked.

The causes of the rhythmic variation are difficult to establish but crystal settling and rhythmic nucleation from a supercooled liquid (Wager and Brown, 1968) appear to be the most likely explanation. Crystal settling in thin sills is unusual but it has been noted in thin olivine-basalt flows by Fuller (1939) and in a 5 m. olivine-dolerite sill in Mannefallknausane (Juckes, 1968). Irvine (1970) has suggested that crystal settling acts to shorten the time for an intrusion to solidify and increases contact effects around the upper relative to the lower margins. Heat loss downwards would generally not be rapid enough to supercool the reduced amount of liquid adjoining the floor of the intrusion.

The apparent absence of marked gravity stratification in the layered units of this sill (p. 68) supports the possibility of rhythmic nucleation rather than crystal settling. This would lead, however, to adcumulus or crescumulus growth of crystals, neither of which would show the zoning of plagioclase, pyroxene and, to some extent, olivine which is found in the layered rocks (p. 95).

The increased contact effects around the upper margin of the sill and the rheomorphic injection of the sill

by its roof rocks are in close agreement with Irvine's (1970) theoretical conclusions. This may have been exaggerated by the migration of volatiles into the roof of the intrusion, similar to the liquid fractionation process of Hamilton (1964, 1965).

The even multiple layering and the absence of splitting similar to that of the layered sill of Jeffries Glacier suggests that flowage differentiation is not a causative factor. Multiple intrusion on such a small scale also appears unlikely but this is uncertain.

Shaw (1969) suggested that the flow of basaltic magma tends to increase the average temperature because of viscous heating; the thermal effects in large plutons may influence the distribution of crystalline phases leading to textural banding but it is uncertain to what extent this would operate in a sill only 30 m. thick.

The most likely cause of all the features of the layered sill of Marø Cliffs appears, therefore, to be crystal settling, possibly accentuated by the migration of volatiles into the roof of the intrusion.

4. Middle sill of Coalseam Cliffs

This sill shows the greates petrographical variation of any but the layered sills described above;

the chemical variation, though marked in the granophyric quartz-dolerites of the upper part of the sill, is not as great as would be expected from the petrography (Table XV).

The porphyritic olivine-dolerite and the two-pyroxene quartz-dolerites are very similar despite their different petrography. They are over-saturated with respect to SiO_2 (4-10 per cent normative quartz) and strongly hypersthene-normative (12-23 per cent). They are moderately rich in SiO_2, Al_2O_3, Cr and Ni and relatively poor in TiO_2 and total iron. K/Rb (299-333), Rb/Sr (0.16-0.20) and Th/K (2.7-5.5) ratios are relatively constant but Cr/Ni ratios (7.5-15.2) are more variable.

The fayalitic granophyric dolerite of Parry Point (3698) is strongly iron-enriched. TiO_2, Fe_2O_3, FeO, MnO and Na_2O are higher than in the rest of the sill and Al_2O_3, MgO, Cr, Ni, Sr and Zr are lower. The granophyric dolerite between Coalseam Cliffs and Parry Point (3676) in contrast is strongly silica-enriched. SiO_2, K_2O, P_2O_5, Rb, Y, Zr, Ba, La, Ce, Pb and Th are very much higher than elsewhere in the sill and TiO_2, total iron, Na_2O and Zn are moderately increased; Al_2O_3, MgO, CaO, Cr, Ni and Sr are much lower than in the rest of the sill.

For these two specimens, K/Rb ratios (341, 233) extend the range for the sill, Th/K ratios (5.2, 6.2) are

TABLE XV

CHEMICAL ANALYSES OF SPECIMENS FROM THE MIDDLE SILL OF COALSEAM CLIFFS

Analyses (weight per cent)

	3708	3676	3698	3707	3704	3692
SiO_2	53.94	62.73	53.67	52.83	52.63	52.95
TiO_2	1.14	1.40	2.32	0.96	1.04	1.13
Al_2O_3	15.93	11.72	13.38	16.91	15.68	15.27
Fe_2O_3	3.00	2.80	3.29	2.91	2.52	2.19
FeO	6.06	9.05	11.45	5.64	6.73	7.32
MnO	0.12	0.14	0.17	0.12	0.13	0.13
MgO	5.62	0.66	2.35	6.86	7.62	7.35
CaO	8.56	4.81	8.13	9.05	8.68	8.96
Na_2O	2.19	2.94	2.67	1.94	2.10	2.08
K_2O	1.59	2.72	1.40	1.33	1.32	1.20
P_2O_5	0.19	0.37	0.19	0.16	0.16	0.13
H_2O+	0.70	0.28	0.48	1.08	0.72	0.74
H_2O-	0.27	0.64	0.25	0.26	0.32	0.25
CO_2	0.73	0.36	0.28	0.94	1.00	0.82
Total	100.05	100.70	100.01	100.99	100.65	100.51

Trace elements (p.p.m.)

S	167	635	347	291	490	525
Cr	457	7	31	638	830	620
Ni	30	5	21	61	98	67
Zn	84	115	99	96	95	97
Ga	21	18	18	19	18	17
Rb	41	97	34	37	33	30
Sr	209	142	134	220	197	190
Y	26	52	25	23	24	26
Zr	196	342	137	166	168	172
Ba	434	668	398	356	371	394
La	18	56	22	20	20	18
Ce	38	100	52	38	40	35
Pb	15	26	14	11	10	17
Th	4	14	6	<3	6	4

TABLE XV (continued)

Analyses recalculated to 100 per cent anhydrous

	3708	3676	3698	3707	3704	3692
SiO_2	54.44	62.93	54.06	53.02	52.84	53.21
TiO_2	1.15	1.40	2.33	0.97	1.05	1.13
Al_2O_3	16.08	11.76	13.48	16.97	15.74	15.35
Fe_2O_3	3.03	2.81	3.31	2.92	2.53	2.20
FeO	6.12	9.08	11.53	5.66	6.76	7.36
MnO	0.12	0.14	0.17	0.12	0.13	0.13
MgO	5.67	0.66	2.37	6.88	7.65	7.39
CaO	8.64	4.83	8.18	9.08	8.71	9.00
Na_2O	2.21	2.95	2.69	1.95	2.10	2.09
K_2O	1.60	2.73	1.41	1.34	1.33	1.20
P_2O_5	0.19	0.37	0.19	0.16	0.16	0.13
CO_2	0.74	0.36	0.28	0.94	1.00	0.82

C.I.P.W. Norms

Q	8.52	21.89	9.82	6.61	4.65	5.18
Or	9.55	16.16	8.34	7.97	7.93	7.15
Ab	18.86	25.01	22.80	16.62	17.98	17.85
An	29.42	10.85	20.61	33.95	29.88	29.17
Wo_{Di}	5.23	4.49	7.87	4.38	5.30	6.27
En_{Di}	3.28	0.58	2.33	2.93	3.39	3.82
Fs_{Di}	1.64	4.34	5.88	1.13	1.57	2.09
En_{Hy}	10.95	1.06	3.58	14.37	15.85	14.72
Fs_{Hy}	5.48	7.99	9.05	5.53	7.35	8.05
Mt	4.42	4.09	4.82	4.27	3.70	3.22
Il	2.20	2.68	4.44	1.85	2.00	2.17
Ap	0.45	0.88	0.45	0.37	0.39	0.30

TABLE XV (continued)

Elements (weight per cent)

	3708	3676	3698	3707	3704	3692
Si^{4+}	25.45	29.42	25.27	24.78	24.70	24.87
Ti^{4+}	0.69	0.84	1.40	0.58	0.63	0.68
Al^{3+}	8.51	6.22	7.13	8.98	8.33	8.12
Fe^{3+}	2.12	1.96	2.32	2.04	1.77	1.54
Fe^{2+}	4.75	7.06	8.96	4.40	5.25	5.72
Mn^{2+}	0.10	0.11	0.13	0.09	0.10	0.10
Mg^{2+}	3.42	0.40	1.43	4.15	4.61	4.46
Ca^{2+}	6.18	3.45	5.85	6.49	6.23	6.43
Na^{+}	1.64	2.19	1.99	1.44	1.56	1.55
K^{+}	1.33	2.26	1.17	1.11	1.10	1.00
P^{5+}	0.08	0.16	0.08	0.07	0.07	0.05
C^{4+}	0.20	0.10	0.08	0.26	0.27	0.22
O^{2-}	45.52	45.84	44.19	45.60	45.37	45.25

Useful ratios

Th x 10^4 /K	3.0	6.2	5.2	<2.7	5.5	4.0
K /Rb	322	233	341	299	333	331
Rb/Sr	0.20	0.68	0.25	0.17	0.17	0.16
Cr/Ni	15.2	1.40	1.48	10.5	7.5	9.3

3708 Z.479.2 Two-pyroxene quartz-dolerite, about 3 m. below upper contact.

3676 Z.473.1 Granophyric quartz-dolerite, upper part of sill.

3698 Z.476.1 Fayalitic granophyric quartz-dolerite, upper part of sill.

3707 Z.479.3 Two-pyroxene quartz-dolerite, about 10 m. above lower contact.

3704 Z.475.1 Two-pyroxene quartz-dolerite, about 6 m. above lower contact.

3692 Z.475.2 Porphyritic chilled olivine-dolerite, lower contact.

about the same but Rb/Sr ratios (0.25, 0.68) are markedly different. Cr/Ni ratios (1.48, 1.40) are very much lower than in the rest of the sill and very similar to those of the scarp-capping sill.

The chemical data suggest that the chilled marginal rock is not in equilibrium as the only phenocrysts observed are olivine while the rock is moderately (5 per cent) quartz-normative. Differentiation in the rest of the sill is not very marked except in the granophyric rocks in the upper part of the sill, which are exposed in windows in the ice cliff south-west of Coalseam Cliffs and which show either strong iron- or alkali-silica-enrichment.

5. Basal sill of Coalseam Cliffs

This sill is olivine-bearing throughout and shows little petrographical or chemical variation (Table XVI).

It is just saturated with respect to SiO_2 and it varies from slightly olivine- (2.0 per cent) to slightly quartz-normative (3.5 per cent). It is relatively low in SiO_2, MgO and Cr and high in TiO_2 and total iron. K/Rb (273-339), Rb/Sr (0.19-0.23) and Th/K (2.7-5.6) ratios are relatively constant and of moderate proportions and Cr/Ni ratios (2.48-2.86) are very constant and relatively low.

TABLE XVI

CHEMICAL ANALYSES OF SPECIMENS FROM THE BASAL SILL COALSEAM CLIFFS

Analyses (weight per cent)

	3683	3717	3687	3718	3699	3693	3691
SiO_2	48.10	48.58	46.98	49.14	48.70	48.55	48.29
TiO_2	2.45	2.30	2.07	2.17	2.22	2.45	2.49
Al_2O_3	13.21	14.31	12.68	14.67	13.86	13.58	12.80
Fe_2O_3	2.98	2.30	3.62	2.88	2.55	2.85	3.85
FeO	12.51	12.78	10.94	11.81	11.93	12.77	11.65
MnO	0.18	0.18	0.15	0.18	0.16	0.18	0.18
MgO	4.28	3.84	5.13	3.81	3.87	4.08	4.52
CaO	8.73	8.94	8.41	8.86	8.85	8.75	8.80
Na_2O	2.55	2.74	2.25	2.76	2.56	2.70	2.31
K_2O	1.23	1.34	1.39	1.35	1.28	1.30	1.15
P_2O_5	0.20	0.20	0.25	0.27	0.26	0.21	0.21
H_2O+	0.81	0.57	1.52	0.46	0.95	0.65	1.29
H_2O-	0.13	0.15	0.27	0.22	0.20	0.09	0.24
CO_2	1.42	0.90	1.69	0.90	1.25	1.02	1.45
Total	98.79	99.12	97.35	99.48	98.64	99.17	99.23

Trace elements (p.p.m.)

S	1518	1134	2155	1531	2025	1377	2270
Cr	84	74	92	79	71	83	82
Ni	30	27	34	30	28	29	33
Zn	124	119	83	112	111	119	111
Ga	21	20	20	20	23	20	19
Rb	33	33	41	33	33	35	35
Sr	152	169	178	169	170	156	151
Y	34	33	33	33	34	35	34
Zr	209	197	202	196	201	214	212
Ba	363	369	330	373	368	384	336
La	29	19	28	24	23	21	20
Ce	63	58	53	58	55	48	61
Pb	<3	10	6	9	4	9	11
Th	<3	3	6	4	<3	6	5

TABLE XVI (continued)

Analyses recalculated to 100 per cent anhydrous

	3683	3717	3687	3718	3699	3693	3691
SiO_2	49.16	49.37	49.16	49.73	49.95	49.33	49.43
TiO_2	2.50	2.34	2.17	2.20	2.28	2.49	2.55
Al_2O_3	13.50	14.54	13.27	14.85	14.22	13.79	13.10
Fe_2O_3	3.05	2.34	3.79	2.91	2.62	2.90	3.94
FeO	12.79	12.99	11.45	11.95	12.24	12.97	11.92
MnO	0.19	0.18	0.16	0.18	0.17	0.18	0.19
MgO	4.38	3.90	5.37	3.86	3.97	4.14	4.62
CaO	8.93	9.08	8.80	8.97	9.08	8.89	9.01
Na_2O	2.61	2.78	2.36	2.80	2.62	2.74	2.36
K_2O	1.25	1.36	1.45	1.36	1.31	1.32	1.18
P_2O_5	0.21	0.21	0.26	0.27	0.27	0.21	0.21
CO_2	1.45	0.91	1.77	0.91	1.28	1.04	1.48

C.I.P.W. Norms

Q	0.96	0.00	1.59	0.72	1.77	0.26	3.58
Or	7.52	8.14	8.75	8.12	7.83	7.88	7.07
Ab	22.39	23.76	20.30	23.87	22.48	23.44	20.28
An	21.75	23.38	21.70	24.16	23.45	21.65	22.00
Wo_{Di}	9.10	8.65	8.76	7.91	8.51	8.97	9.17
En_{Di}	3.58	3.06	4.13	2.99	3.20	3.37	4.01
Fs_{Di}	5.64	5.80	4.52	5.05	5.46	5.77	5.15
En_{Hy}	7.48	5.82	9.48	6.71	6.82	7.06	7.68
Fs_{Hy}	11.79	11.02	10.36	11.33	11.62	12.09	9.86
Fo	0.00	0.64	0.00	0.00	0.00	0.00	0.00
Fa	0.00	1.34	0.00	0.00	0.00	0.00	0.00
Mt	4.48	3.42	5.59	4.26	3.84	4.24	5.80
Il	4.82	4.48	4.19	4.22	4.38	4.77	4.91
Ap	0.50	0.50	0.63	0.65	0.65	0.51	0.51

TABLE XVI (continued)

Elements (weight per cent)

	3683	3717	3687	3718	3699	3693	3691
Si^{4+}	22.98	23.08	22.98	23.25	23.35	23.06	23.11
Ti^{4+}	1.50	1.40	1.30	1.32	1.37	1.49	1.53
Al^{3+}	7.15	7.70	7.02	7.86	7.52	7.30	6.93
Fe^{3+}	2.13	1.63	2.65	2.04	1.83	2.03	2.76
Fe^{2+}	9.94	10.09	8.90	9.29	9.51	10.09	9.27
Mn^{2+}	0.14	0.14	0.12	0.14	0.13	0.14	0.15
Mg^{2+}	2.64	2.35	3.24	2.33	2.40	2.50	2.79
Ca^{2+}	6.38	6.49	6.29	6.41	6.49	6.35	6.44
Na^{+}	1.93	2.06	1.75	2.07	1.95	2.03	1.75
K^{+}	1.04	1.13	1.21	1.13	1.09	1.10	0.98
P^{5+}	0.09	0.09	0.11	0.12	0.12	0.09	0.09
C^{4+}	0.40	0.25	0.48	0.25	0.35	0.28	0.41
O^{2-}	43.68	43.58	43.95	43.79	43.90	43.54	43.80

Useful ratios

Th x 10^4 /K	<2.9	2.7	5.2	3.6	<5.6	5.6	5.3
K /Rb	309	338	281	339	321	308	273
Rb/Sr	0.22	0.20	0.23	0.20	0.19	0.22	0.23
Cr/Ni	2.80	2.74	2.71	2.63	2.54	2.86	2.48

3683	Z.478.10	Porphyritic chilled olivine-dolerite, upper contact.
3717	Z.474.1	Glomeroporphyritic chilled olivine-dolerite, about 6 m. below upper contact.
3687	Z.478.11	Ophitic olivine-dolerite, middle of sill.
3718	Z.500.1	Ophitic olivine-dolerite, lower part of sill.
3699	Z.477.4	Ophitic olivine-dolerite, about 6 m. above lower contact.
3693	Z.477.3	Porphyritic chilled olivine-dolerite, lower contact.
3691	Z.478.12	Porphyritic chilled olivine-dolerite, lower contact.

6. Other intrusions

Twenty-eight analyses of specimens from other minor sills and dykes in the Theron Mountains are given in Table XVII.

They are variable in composition and range from slightly under-saturated (8.4 per cent normative olivine) to slightly over-saturated (11.2 per cent normative quartz) rocks. They are generally characterized by low to moderate SiO_2, total iron, K_2O, Rb, Sr, Y, Zr, Ba, La and Ce and moderate to high Al_2O_3, MgO, CaO, Cr and Ni. K/Rb ratios range from 156-447 but they are generally about 300-400. Rb/Sr ratios (0.05-0.18, with two exceptions) are less variable but Th/K ratios range from < 2.1 to about 45.0. Cr/Ni ratios (1.43-60.7) are also variable; some may be used to correlate with the major sills described above but this has not been done because of the geographical distances involved.

There is apparently little significant difference between the chemistry of sills and dykes, though the latter are both rarer and less extensively sampled.

C. SUMMARY OF THE CHEMISTRY OF THE JURASSIC DOLERITE INTRUSIONS OF THE THERON MOUNTAINS

The main features of the chemistry of individual intrusions are summarized in the mean analyses of Table XVIII and the variation diagrams (Figs. 49-60). Published analyses of dolerites and basalts from Heimefrontfjella (Juckes, in press) and Vestfjella (Hjelle and Winsnes, 1971) in western Dronning Maud Land have been included with the Jurassic dolerite intrusions of the Theron Mountains.

Differentiation within individual intrusions is, except for the layered sills of Jeffries Glacier and Marø Cliffs and the middle sill of Coalseam Cliffs, relatively limited. The intrusions as a whole, however, form a differentiated series of which the cumulates of the layered sills and the granophyres of the middle sill of Coalseam Cliffs form end-points. The series is summarized below, arranged in order of increasing fractionation, irrespective of relative age:

TABLE XVIII

MEAN CHEMICAL ANALYSES OF JURASSIC DOLERITE INTRUSIONS FROM THE THERON MOUNTAINS AND WESTERN DRONNING MAUD LAND

Analyses (anhydrous and volatile-free recalculated to 100)

	A	B	C	D	E	F	G	H	J
SiO_2	57.13	52.01	49.67	53.49	50.14	51.18	55.46	50.08	51.09
TiO_2	1.38	0.97	2.40	3.03	0.76	0.97	1.35	2.39	1.35
Al_2O_3	12.25	15.34	13.37	12.70	15.06	13.93	15.00	14.08	14.87
Fe_2O_3	4.13	2.82	3.54	3.57	3.02	1.86	2.82	3.11	5.25
FeO	10.74	7.05	12.72	10.52	6.95	8.43	7.80	12.50	6.45
MnO	0.18	0.14	0.19	0.18	0.14	0.15	0.13	0.18	0.18
MgO	2.34	8.41	5.07	3.20	10.74	11.90	5.14	4.37	6.69
CaO	7.31	10.18	9.18	8.21	10.98	8.71	8.13	9.08	11.00
Na_2O	2.50	1.97	2.38	2.78	1.69	1.61	2.35	2.64	2.42
K_2O	1.82	0.94	1.25	1.89	0.43	1.01	1.61	1.34	0.51
P_2O_5	0.24	0.16	0.23	0.44	0.07	0.24	0.20	0.24	0.19

Trace elements (p.p.m.)

S	379	687	1502	741	839	1192	409	1716	-
Cr	23*	654	80	58	663	1335	430	81	214
Ni	18	40	30	33	18	135	47	30	87
Zn	90	85	120	117	79	89	98	111	69
Ga	17	15	19	20	15	14	18	20	-
Rb	49	26	30	36	21	22	45	35	7
Sr	131	173	167	224	175	137	182	164	234
Y	32	25	32	49	17	24	29	34	21
Zr	199	148	204	322	76	134	197	204	111
Ba	462	321	371	656	193	363	437	360	224
La	24	13	23	42	4	16	26	23	11
Ce	52	32	52	84	11	28	50	57	27
Pb	12	10	9	10	9	10	15	7	7
Th	6	5	4	4	4	4	6	4	4

Useful ratios

$Th \times 10^4$ /K	4.9	6.0	4.0	2.9	11.4	5.4	4.4	4.4	9.5
K /Rb	277	303	336	415	190	424	310	310	600
Rb/Sr	0.41	0.15	0.18	0.16	0.12	0.16	0.27	0.21	0.03
Cr/Ni	1.41*	17.1	2.66	1.74	46.2	11.1	7.6	2.68	2.46

A. Scarp-capping sill, mean of 19 analyses (* excluding anomalously high Cr of analysis 10654)

B. First phase of intrusion in Marø Cliffs, mean of 7 analyses

C. Third phase of intrusion in Marø Cliffs, mean of 7 analyses

D. Basal sill of Lenton Bluff, mean of 8 analyses (excluding hydrothermally altered rocks)

E. Younger sills and dykes of Lenton Bluff, mean of 12 analyses

F. Layered sills of Jeffries Glacier and Marø Cliffs, mean of 7 analyses

G. Middle sill of Coalseam Cliffs, mean of 6 analyses

H. Basal sill of Coalseam Cliffs, mean of 7 analyses

J. Jurassic basalts from Heimefrontfjella, mean of 8 analyses (after Juckes (in press))

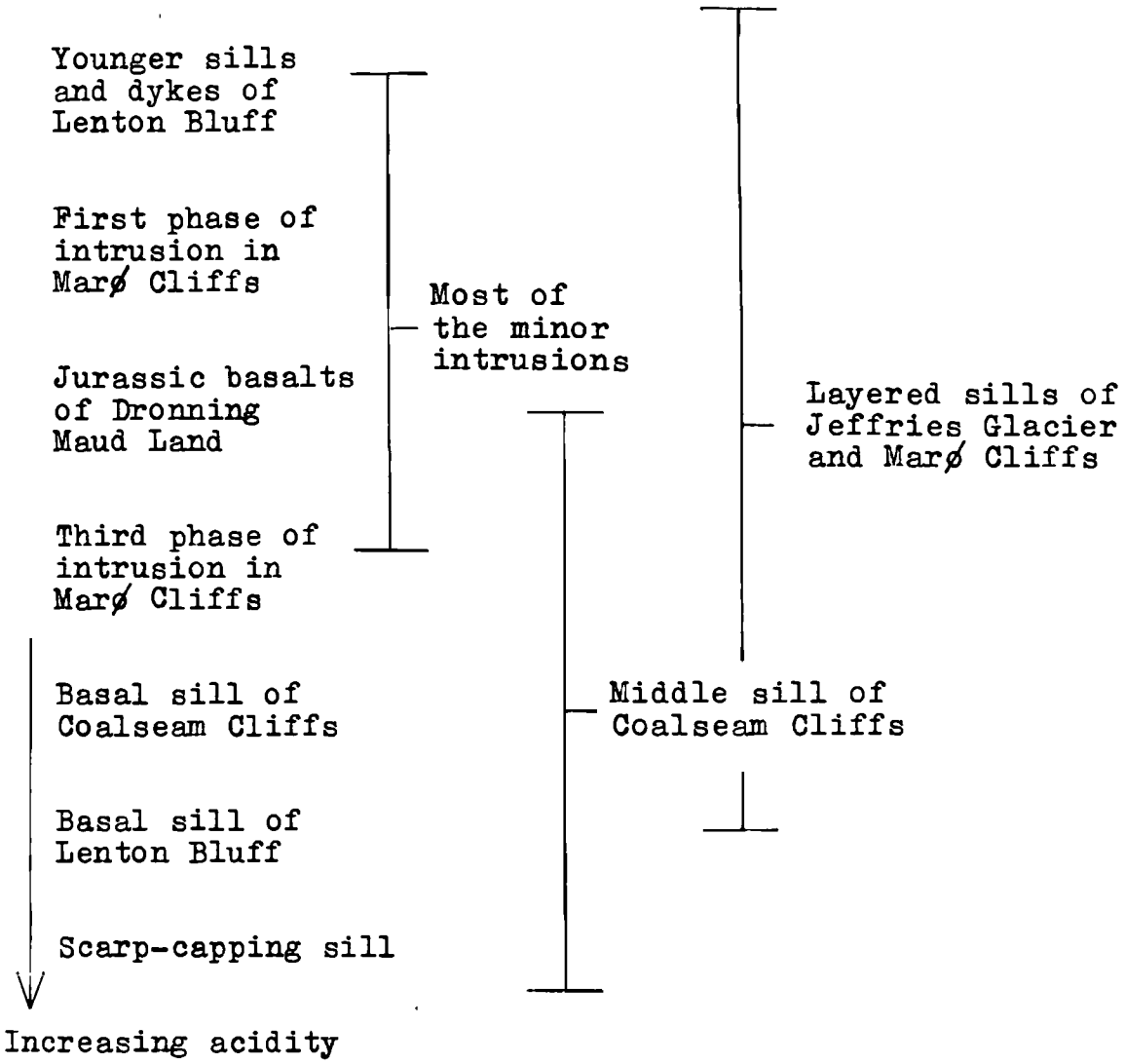
Younger sills and dykes of Lenton Bluff
First phase of intrusion in Marø Cliffs
Jurassic basalts of Dronning Maud Land
Third phase of intrusion in Marø Cliffs
Most of the minor intrusions
Layered sills of Jeffries Glacier and Marø Cliffs
Middle sill of Coalseam Cliffs
Basal sill of Coalseam Cliffs
Basal sill of Lenton Bluff
Scarp-capping sill
Increasing acidity

Computer plots of oxides (weight per cent) and elements (p.p.m.) against various fractionation indices have been examined but for simplicity only those against mafic index (Wager and Deer, 1939) are shown (Figs. 53-60). Computer plots of triangular diagrams of any three of the multi-component system Mg^{2+} — $Fe^{3+} + Fe^{2+}$ — $Na^{+} + K^{+}$ — Ca^{2+} — Al^{3+} — Si^{4+} and of Ca^{2+} — Na^{+} — K^{+} have also been examined. Triangular plots of Mg^{2+} — $Fe^{3+} + Fe^{2+}$ — $Na^{+} + K^{+}$ and Ca^{2+} — Na^{+} — K^{+} are shown in Figs. 49 and 50. Differentiation trends are similar to those of other basaltic provinces except that there is strong iron-enrichment but only a slight tendency towards alkali-enrichment. A plot of mafic index against felsic index (Fig. 51) in the manner described by Simpson (1954) shows that crystallization has been dominated by a steady decrease in MgO relative to total iron and a slight decrease in CaO relative to alkalis.

A plot of $Na_2O + K_2O$ against SiO_2 (Fig. 52) shows two distinct variation trends, both of which show a positive correlation with SiO_2 parallel to the tholeiitic-alkalic boundary (MacDonald and Katsura, 1964; fig. 1). Analyses plotting on the upper trend are those of olivine-bearing intrusions, namely the third phase of intrusion in Marø Cliffs, the basal sills of Coalseam Cliffs and Lenton Bluff

Fig. 49. Triangular plots on the co-ordinates $Mg^{2+} - Fe^{2+} + Fe^{3+} - Na^{+} + K^{+}$ of some Mesozoic tholeiitic rocks from the Southern Hemisphere.

(a) Jurassic dolerites from the Theron Mountains and Dronning Maud Land.

(b) Ferrar dolerites from Antarctica.

(c) Jurassic dolerites from Tasmania.

(d) Karroo dolerites from southern Africa.

(e) Karroo basalts from southern Africa.

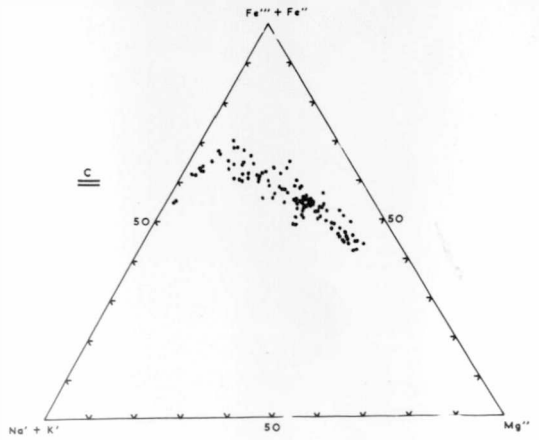
Fe''' + Fe''
c
50
50
Na' + K'
50
Mg''

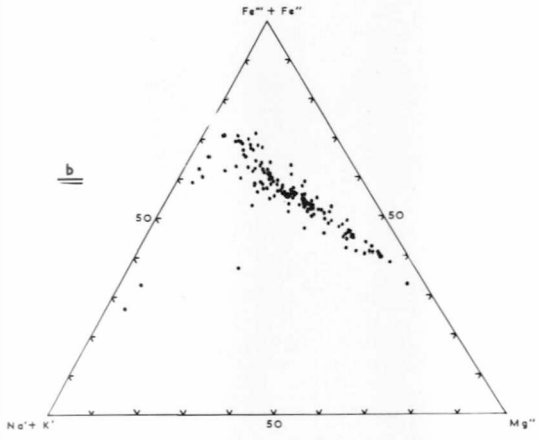
Fe''' + Fe''
b
50
50
Na' + K'
50
Mg''

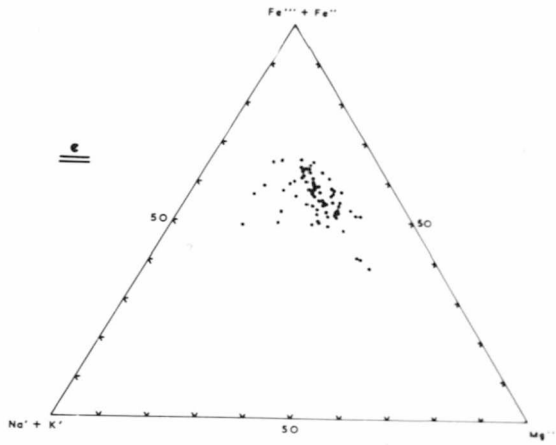
Fe''' + Fe''
e
50
50
Na' + K'
50
Mg''

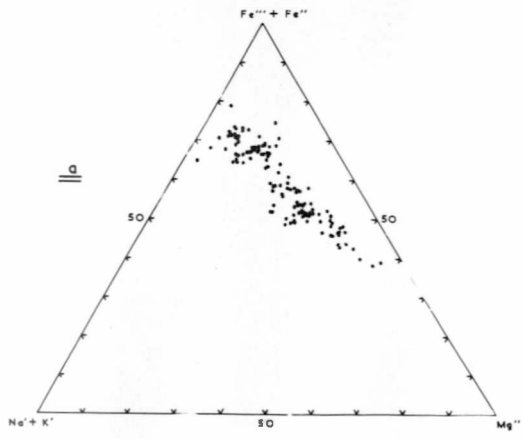
Fe''' + Fe''
a
50
50
Na' + K'
50
Mg''

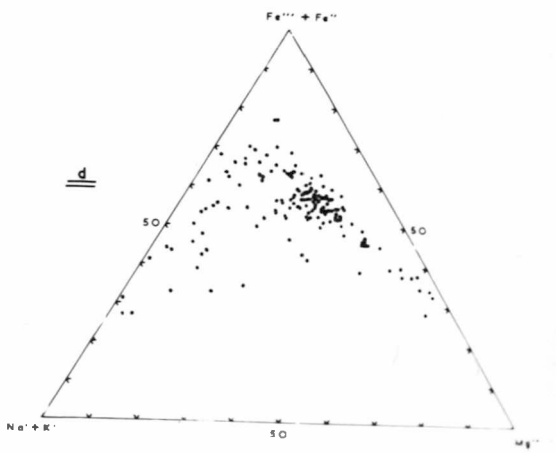
Fe''' + Fe''
d
50
50
Na' + K'
50
Mg''

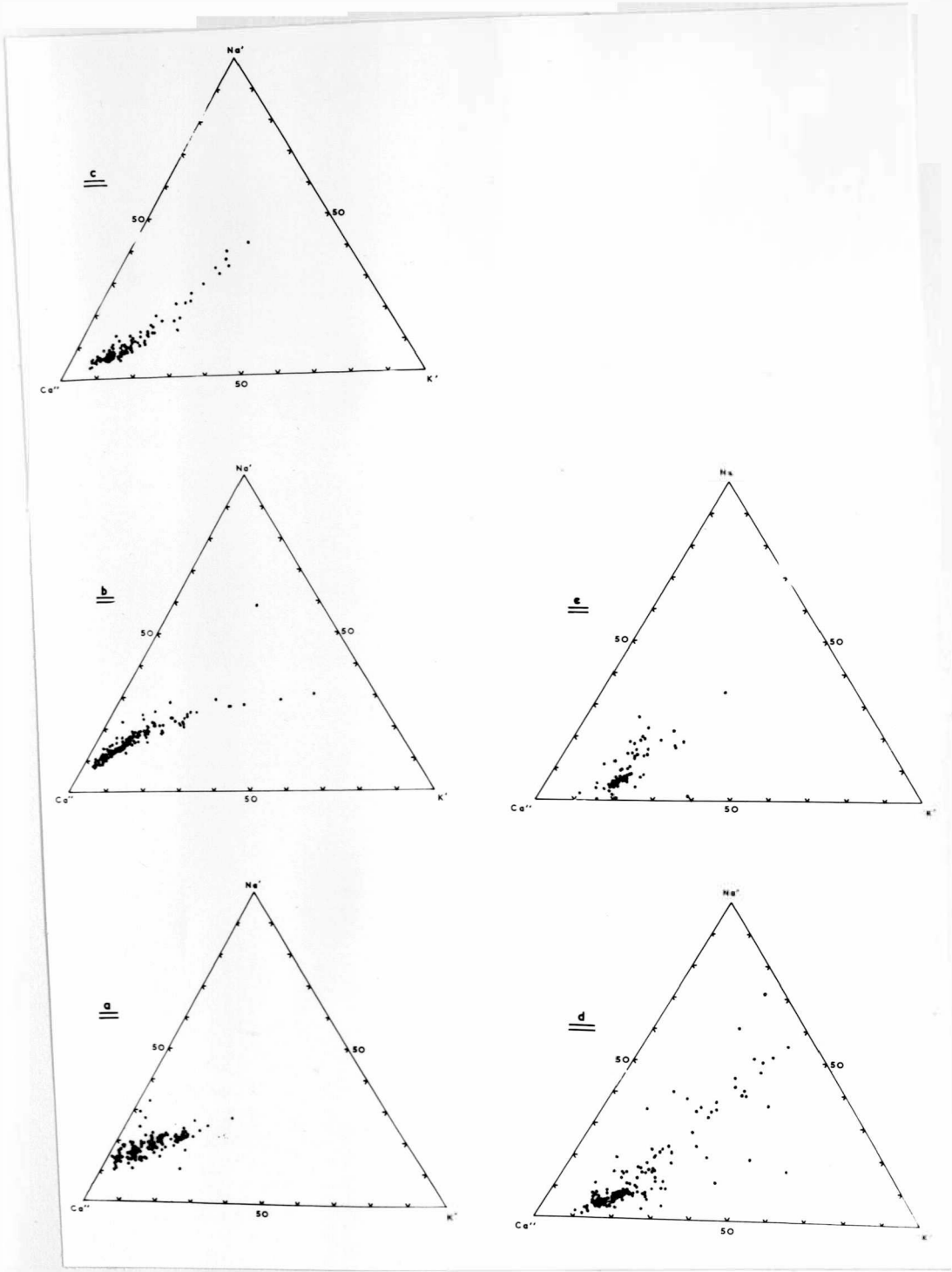

Fig. 50. Triangular plots on the co-ordinates $Ca^{2+} - Na^{+} - K^{+}$ of some Mesozoic tholeiitic rocks from the Southern Hemisphere; lettering as in Fig. 49.

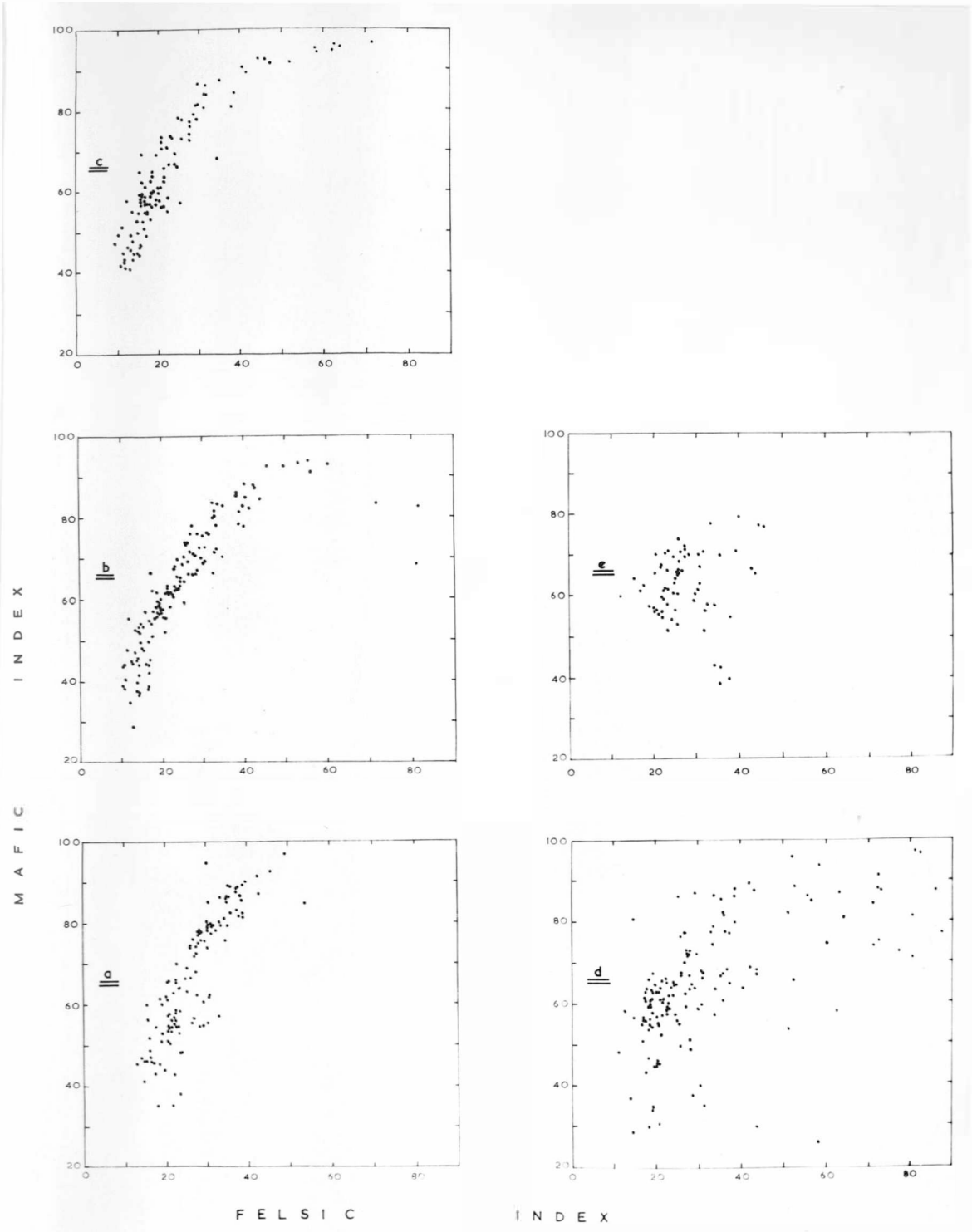

Fig. 51. Plots of mafic index against felsic index for some Mesozoic tholeiitic rocks from the Southern Hemisphere; lettering as in Fig. 49.

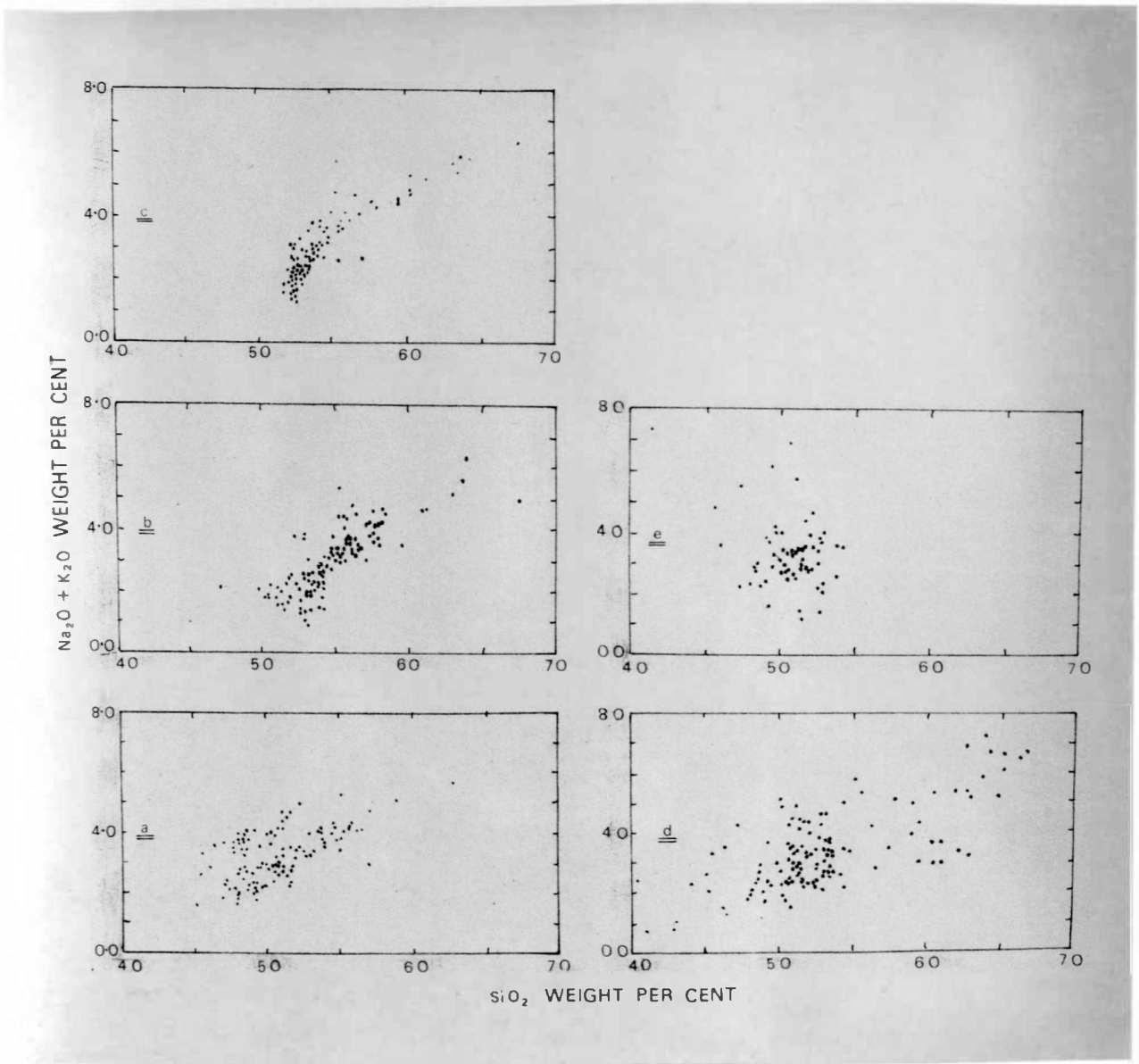

Fig. 52. Plots of $Na_2O + K_2O$ against SiO_2 for some Mesozoic tholeiitic rocks from the Southern Hemisphere; lettering as in Fig. 49.

and one or two minor intrusions from the Theron Mountains and Dronning Maud Land. Analyses plotting on the lower trend range from olivine- to quartz-bearing and they include the layered sills of Jeffries Glacier and Marø Cliffs, the younger sills and dykes of Lenton Bluff, the first phase of intrusion in Marø Cliffs, Jurassic basalts from Dronning Maud Land, the middle sill of Coalseam Cliffs, the scarp-capping sill and most of the minor intrusions of the Theron Mountains. Harker variation diagrams, which are not shown, for all oxides and elements determined rarely produce smooth curves; when they do, there is a distinct tendency towards separation of two trends like those of Fig. 52; this is especially true for Na_2O, K_2O, P_2O_5, Zn, Ga, Rb, Y, Zr, Ba, La and Ce and, to a lesser extent, of TiO_2, MgO and Cr.

Plots of weight per cent of major oxides against mafic index (Figs. 53-57) show relatively smooth curves but with a wide range, which in some cases appears to consist of two separate trends; the two trends differ from those noted on the alkali-silica plot and there is more overlap between them; they are pronounced only in respect of K_2O and P_2O_5. The upper trend consists of the layered sills of Jeffries Glacier and Marø Cliffs, the first phase of intrusion in Marø Cliffs, the middle sill of Coalseam Cliffs, the basal sill of Lenton Bluff and some of the minor

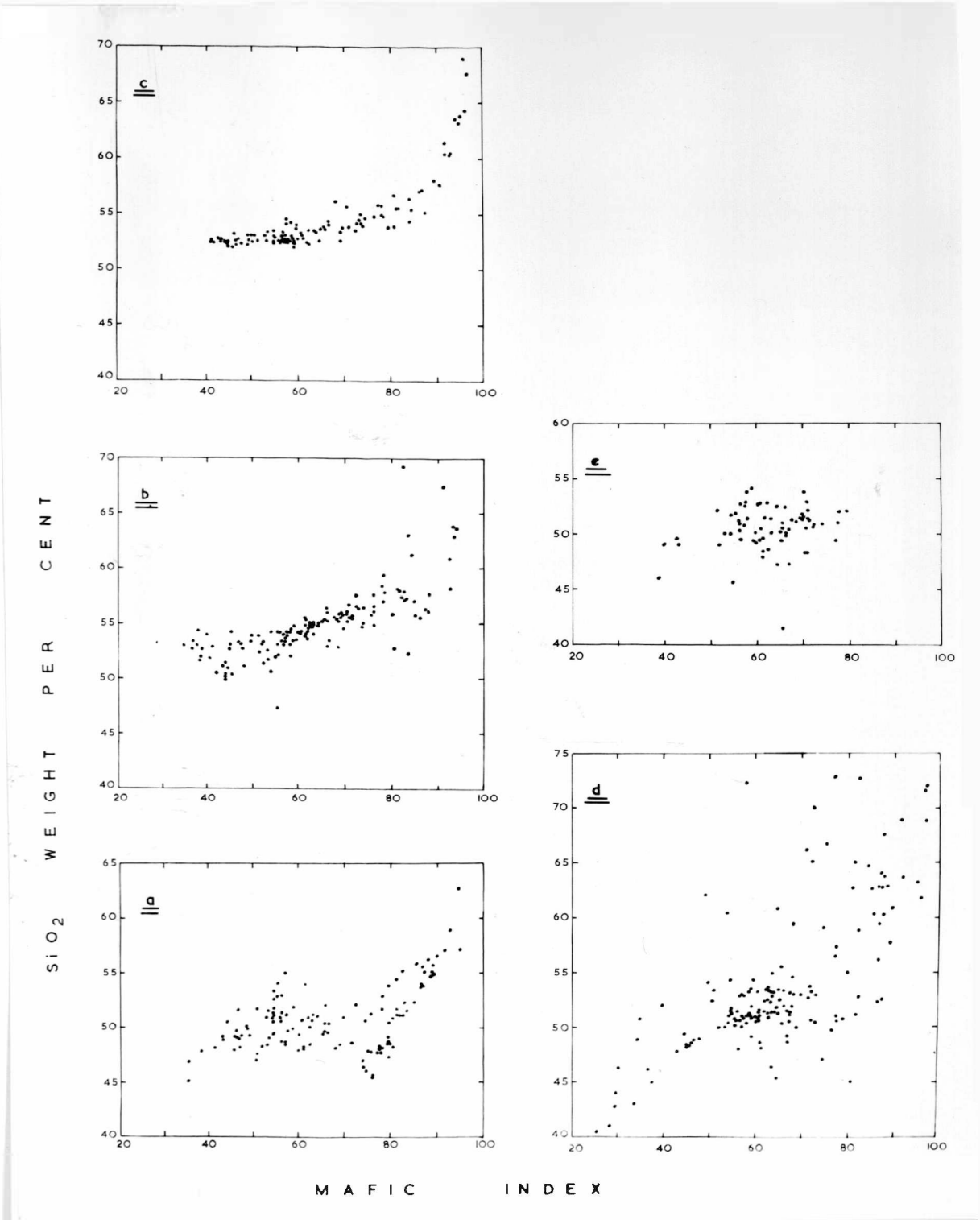

Fig. 53. Plot of SiO_2 against mafic index for some Mesozoic tholeiitic rocks from the Southern Hemisphere; lettering as in Fig. 49.

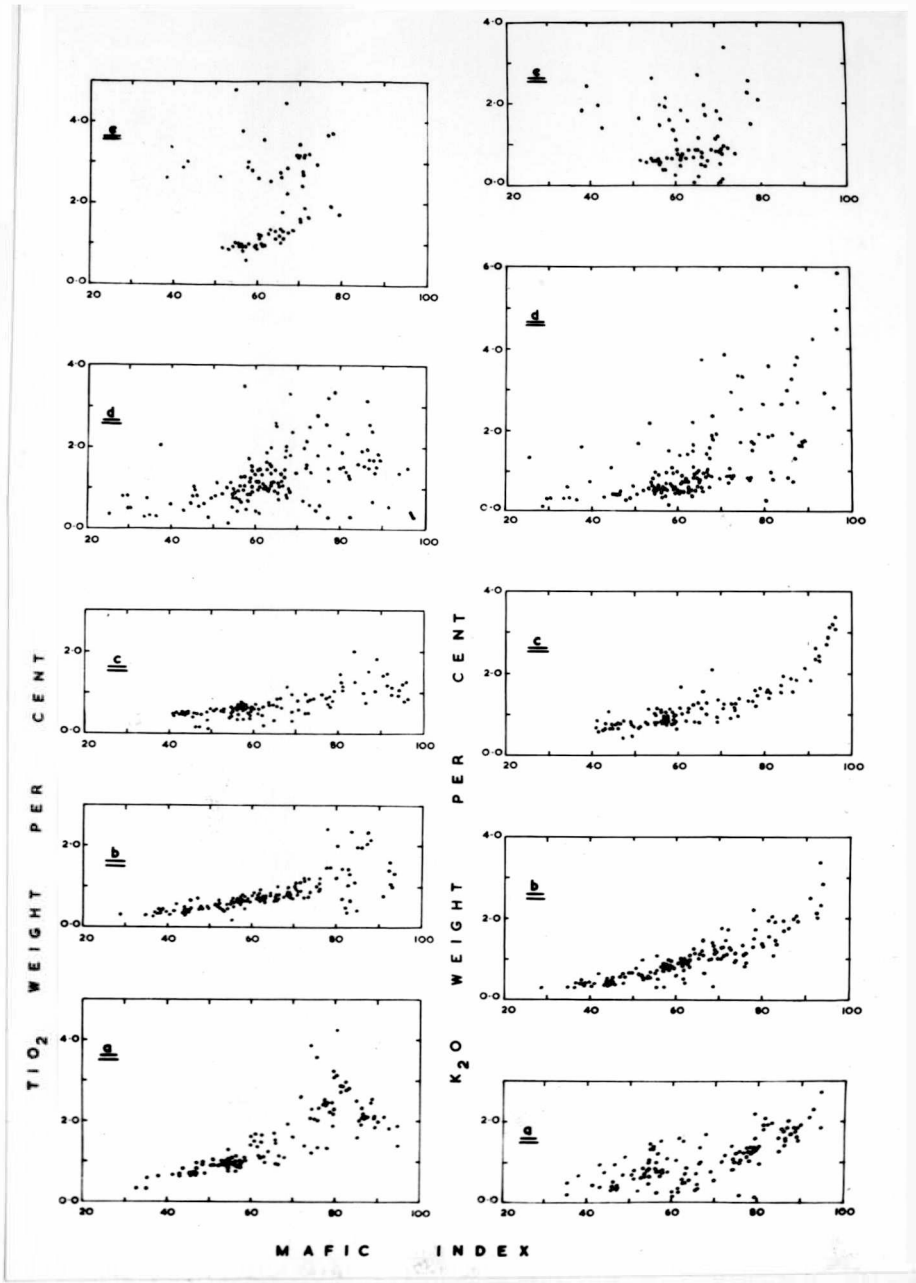

Fig. 54. Plots of TiO_2 and K_2O against mafic index for some Mesozoic tholeiitic rocks from the Southern Hemisphere; lettering as in Fig. 49.

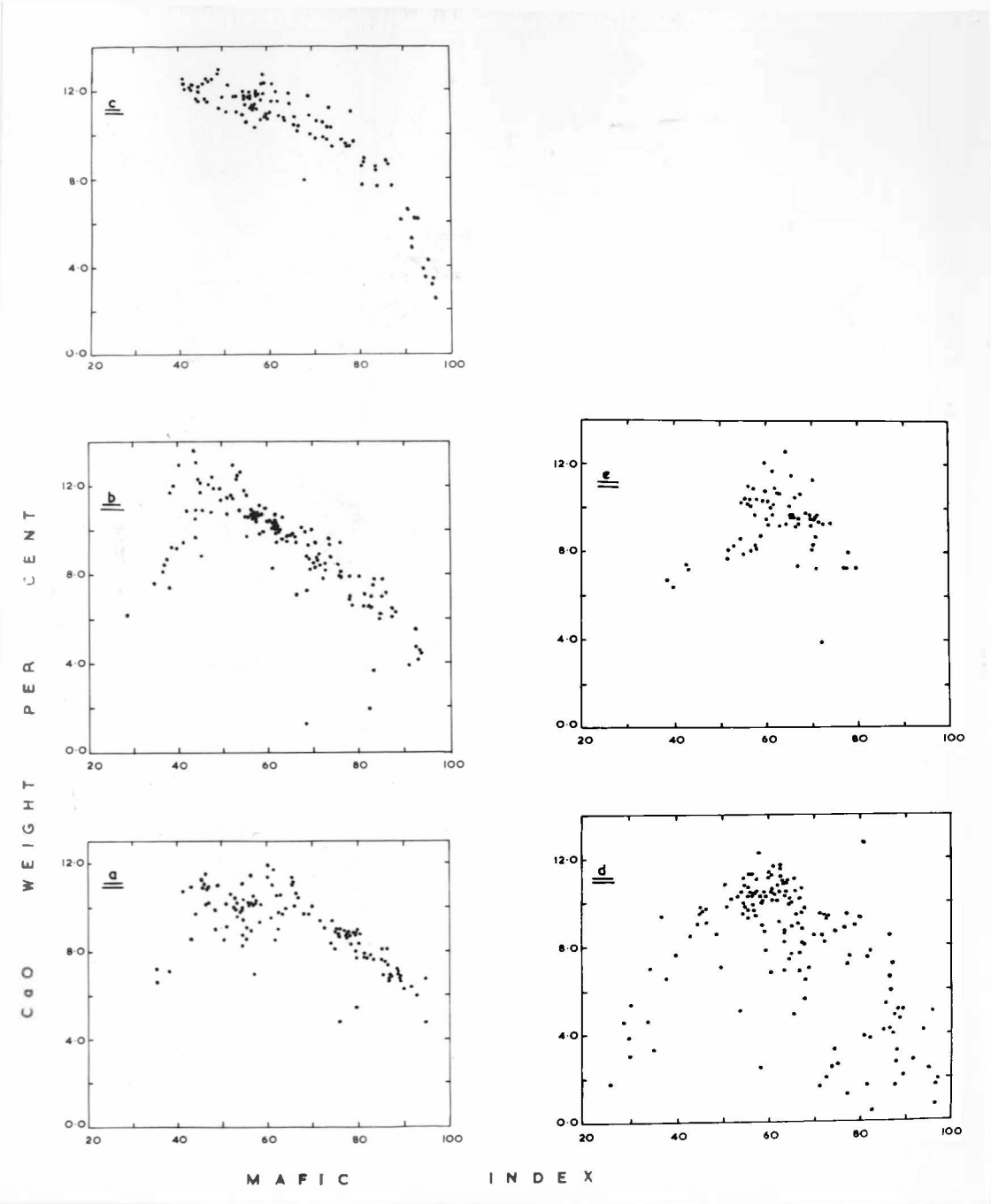

Fig. 55. Plot of CaO against mafic index for some Mesozoic tholeiitic rocks from the Southern Hemisphere; lettering as in Fig. 49.

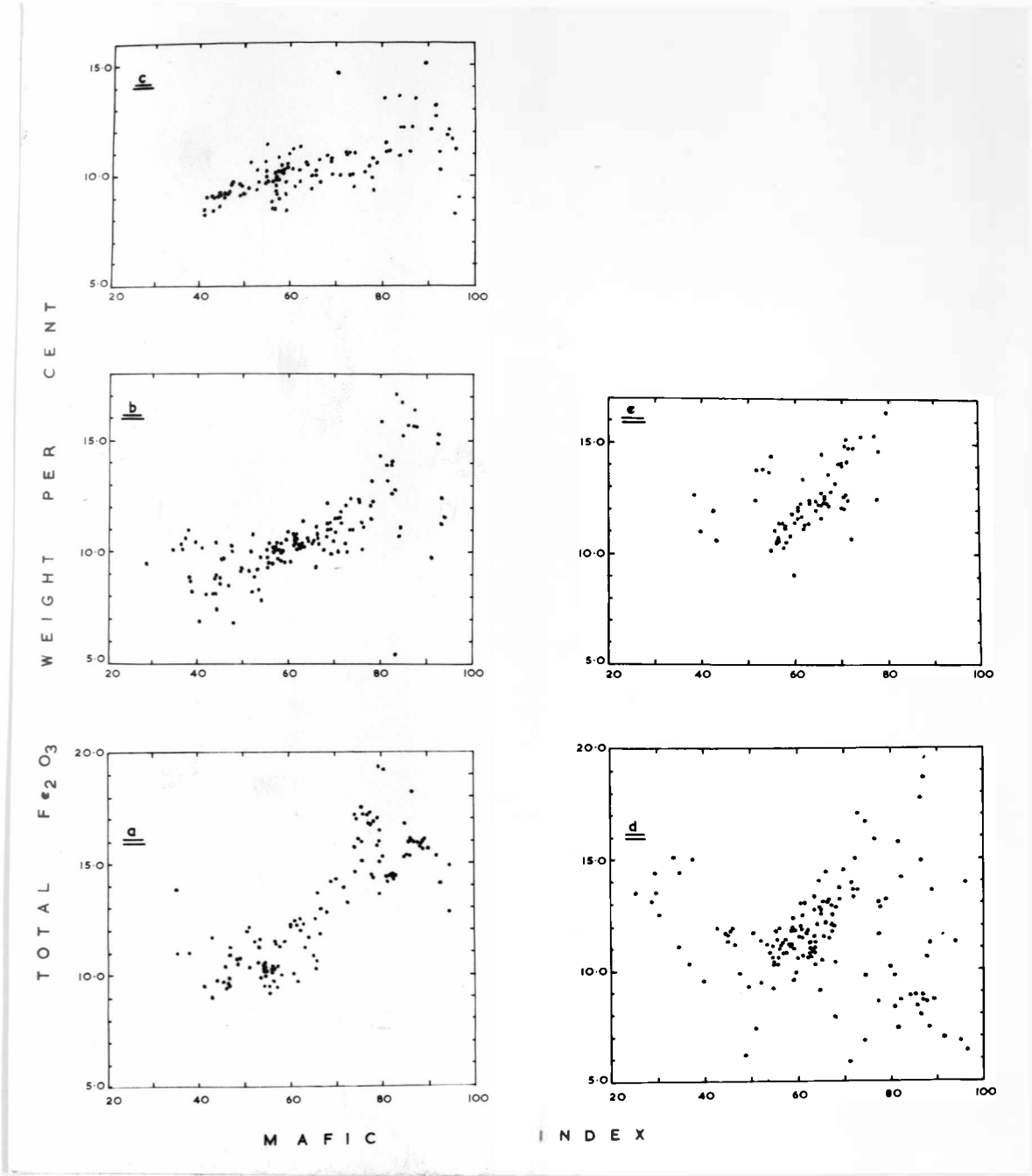

Fig. 56. Plot of total iron (as Fe_2O_3) against mafic index for some Mesozoic tholeiitic rocks from the Southern Hemisphere; lettering as in Fig. 49.

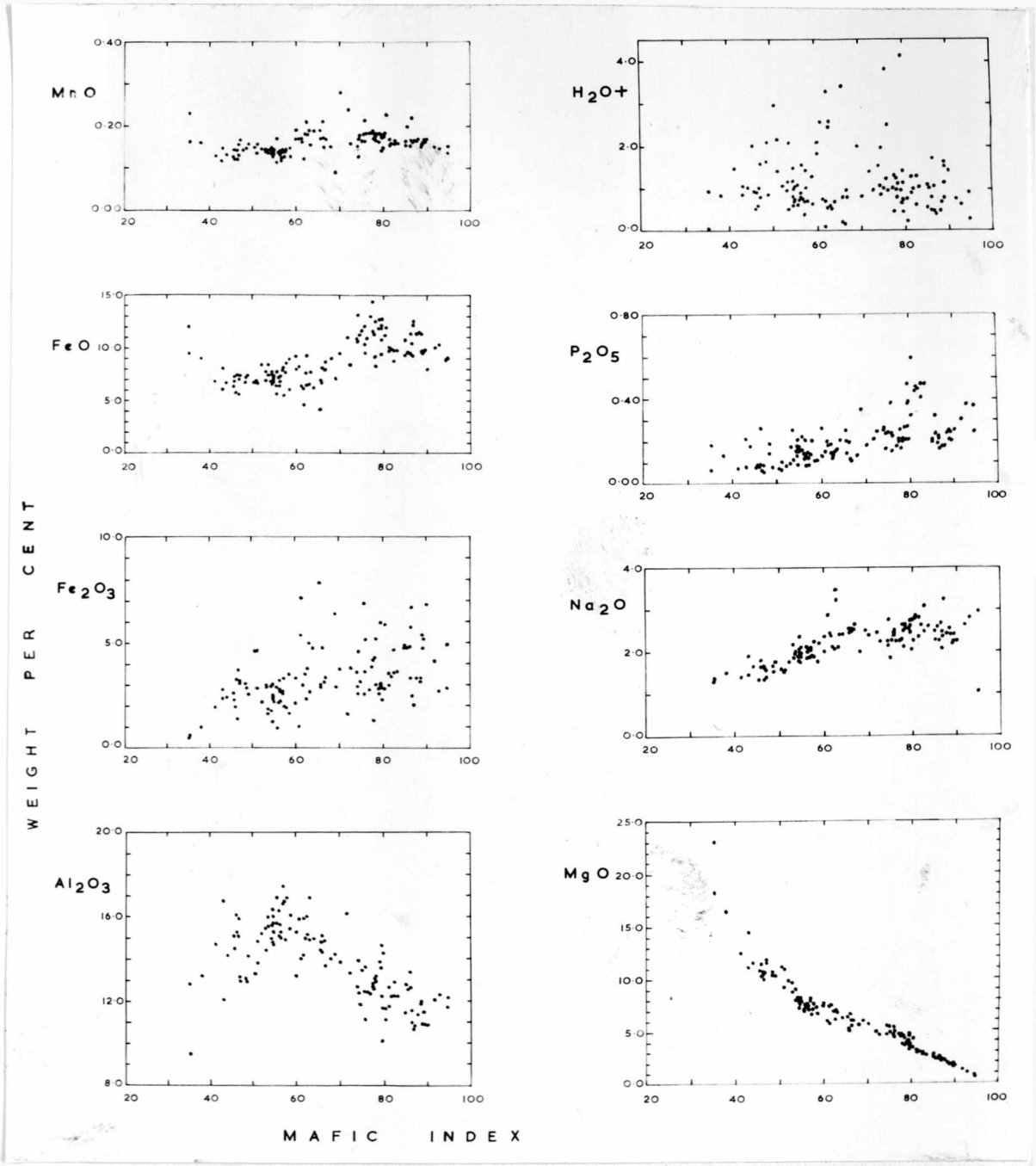

Fig. 57. Plots against mafic index of Al_2O_3, Fe_2O_3, FeO, MnO, MgO, Na_2O, P_2O_5 and H_2O+ for Jurassic dolerites from the Theron Mountains and Dronning Maud Land.

intrusions. The lower trend consists of the younger sills and dykes of Lenton Bluff, Jurassic basalts from Dronning Maud Land, the third phase of intrusion in Marø Cliffs, the basal sill of Coalseam Cliffs, the scarp-capping sill and many of the minor intrusions.

SiO_2, Na_2O, K_2O and P_2O_5 show a steady increase with fractionation while MgO shows a progressive decrease. Al_2O_3 and CaO increase during the first stages of fractionation (up to about mafic index = 60) and then slowly decrease, while TiO_2, total iron and MnO show a steady increase for most of the fractionation (up to about mafic index = 85) and then a sharp decrease.

Plots of trace elements (p.p.m.) against mafic index are shown in Figs. 58-60. These also show a separation into two trends similar to those of the major oxides; there is considerable overlap between the two trends, especially in the early stages of fractionation, and some intrusions are on different trends depending on which element is plotted. This may possibly be interpreted as a separation of the scarp-capping sill from other intrusions in the Theron Mountains, as this is the only intrusion which is constant in its position relative to all the others, irrespective of which element is plotted. The two trends are particularly well seen in plots against mafic index of Rb, Y, Zr, Ba, La and Ce, which

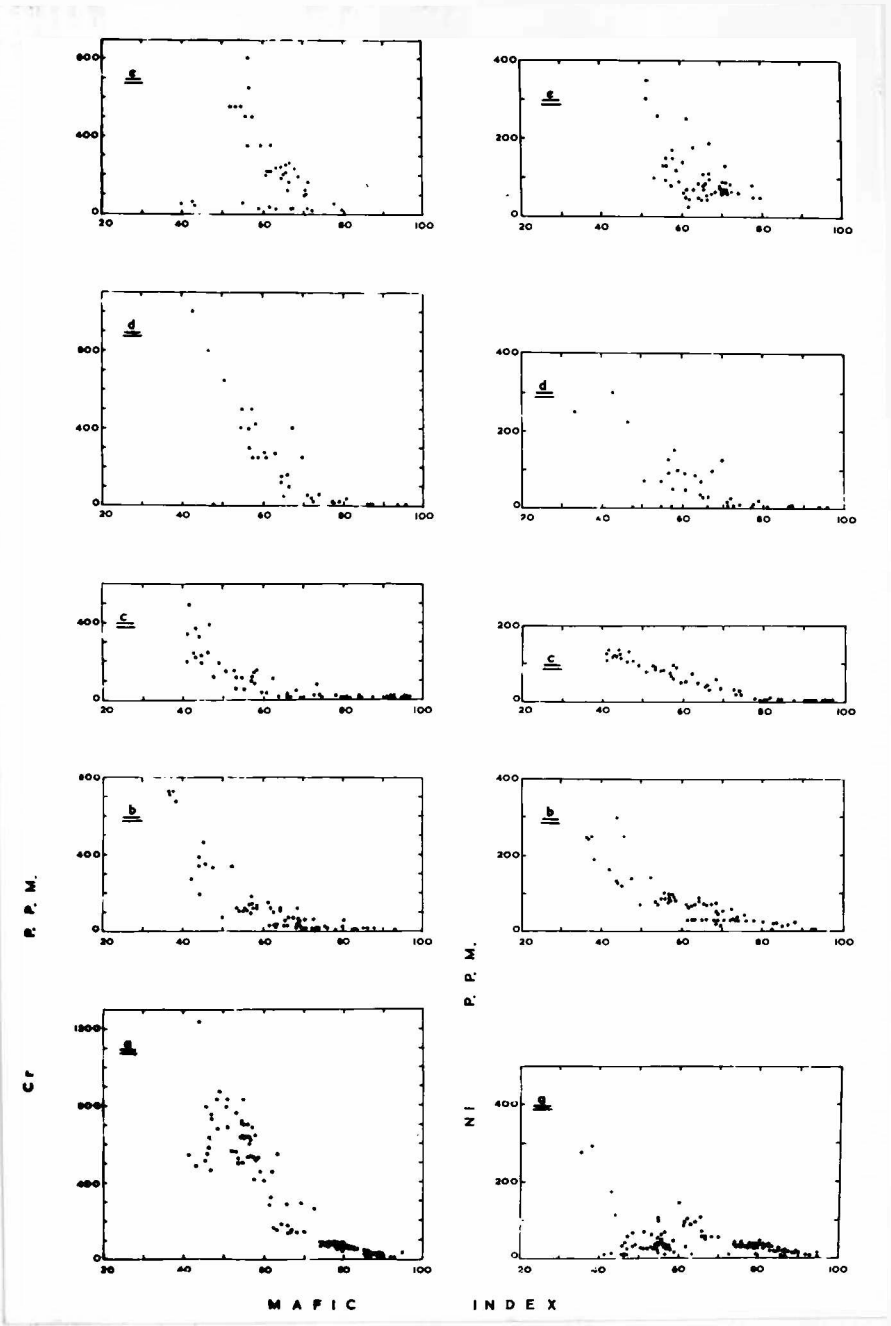

Fig. 58. Plots of Cr and Ni against mafic index for some Mesozoic tholeiitic rocks from the Southern Hemisphere; lettering as in Fig. 49.

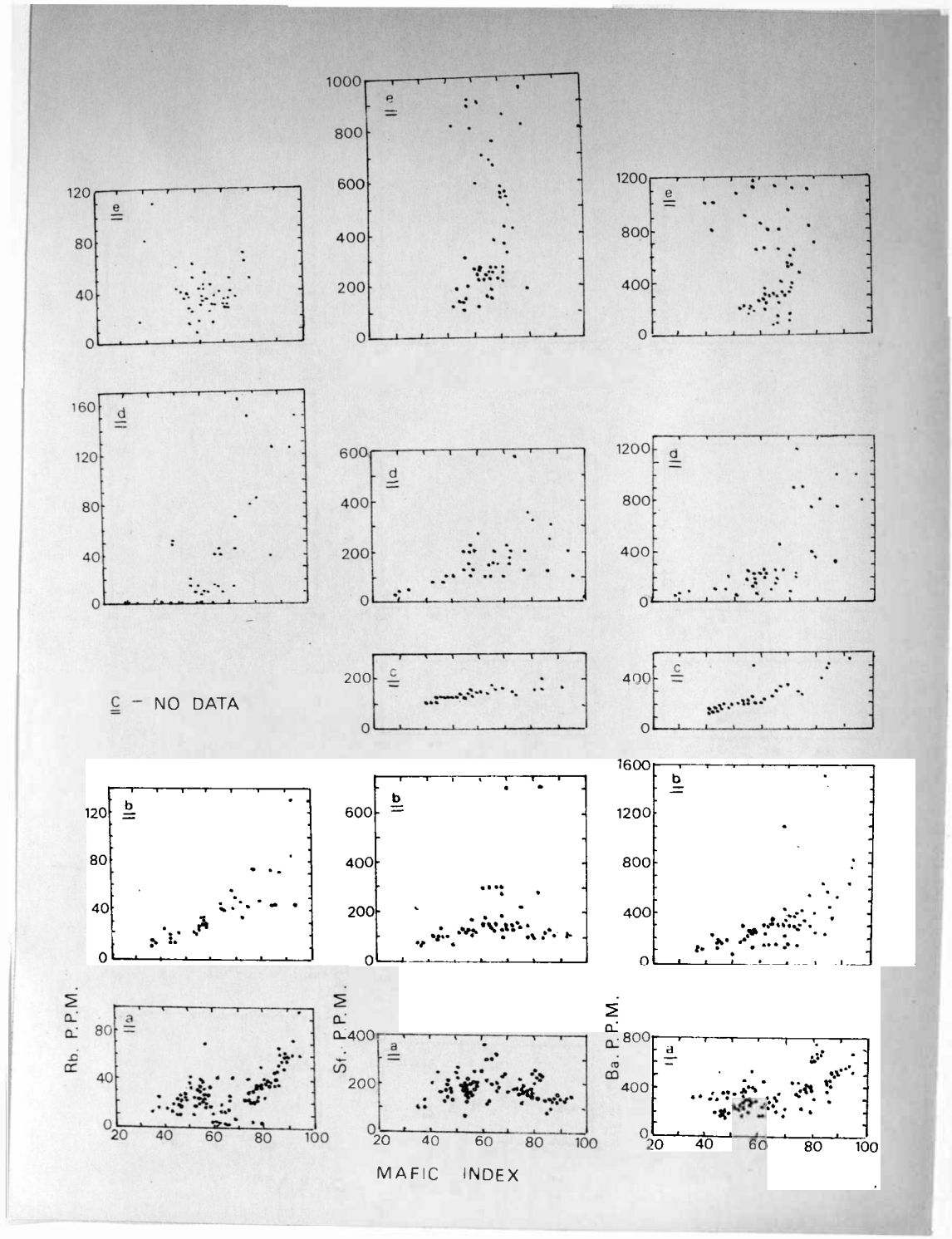

Fig. 59. Plots of Rb, Sr and Ba against mafic index for some Mesozoic tholeiitic rocks of the Southern Hemisphere; lettering as in Fig. 49.

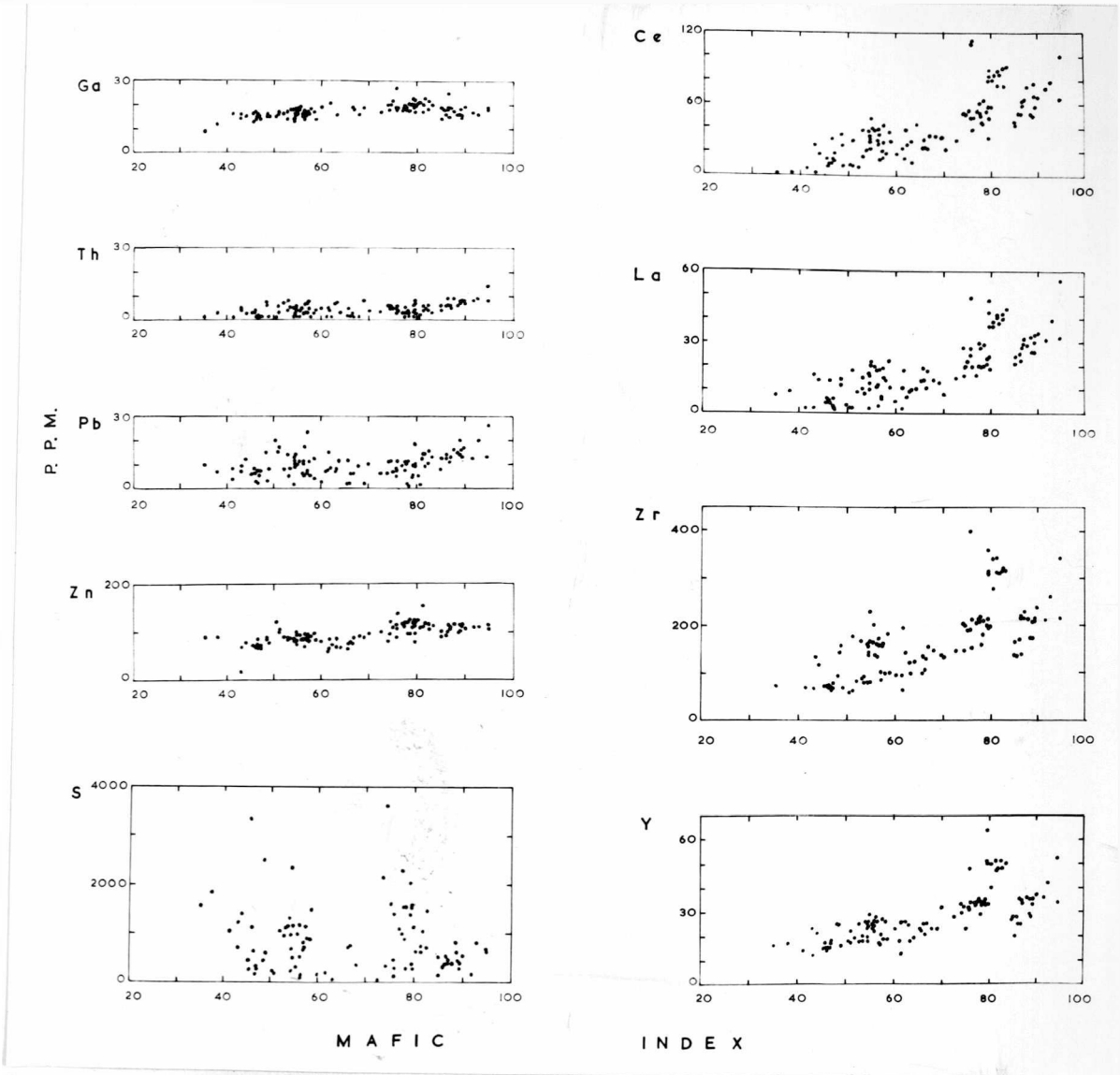

Fig. 60. Plots against mafic index of S, Zn, Pb, Th, Ga, Y, Zr, La and Ce for Jurassic dolerites from the Theron Mountains and Dronning Maud Land.

follow each other very closely; their trends are very similar to those of Na_2O and P_2O_5. Zn, Ga, Rb, Y, Zr, Ba, La, Ce, Pb and Th show progressive increase with fractionation, while Cr shows a sharp decrease. Ni remains relatively constant except for the cumulate rocks of the layered sills of Jeffries Glacier and Marø Cliffs. Sr remains relatively constant but S shows no significant trends.

The main features of the differentiated series of dolerites from the Theron Mountains and Dronning Maud Land are similar, in general, to those of other basaltic provinces. In detail, however, there are differences and these are considered in terms of a regional geochemical correlation of the Mesozoic tholeiitic rocks of the Southern Hemisphere. Of especial significance is the apparent sub-division of the dolerites of the Theron Mountains into two groups on the basis of both major and trace-element geochemistry; the groupings tend to vary depending on which elements are used but there is a consistent separation of the scarp-capping sill from other intrusions in the Theron Mountains.

C. REGIONAL GEOCHEMICAL CORRELATION

The Jurassic dolerites of the Theron Mountains are petrographically and chemically similar to other Mesozoic tholeiitic rocks of the Southern Hemisphere (Table XIX).

They are compared numerically and graphically with published analyses of Jurassic dolerites from western Dronning Maud Land (20 analyses), Ferrar dolerites of eastern Antarctica (148 analyses), Jurassic dolerites of Tasmania (110 analyses), and Karroo dolerites (154 analyses) and basalts (70 analyses) from southern Africa. The sources of these analyses are given in Appendix II.

1. Mean analyses

Mean analyses of Mesozoic tholeiites from the Southern Hemisphere are given in Table XIX. For comparative purposes, the means of quartz- and olivine-tholeiitic basalts and dolerites (after Manson, 1967) are also given.

The Ferrar and Tasmanian dolerites are alike but they are markedly different from the Karroo dolerites and basalts and from the Jurassic dolerites and basalts of the Theron Mountains and Dronning Maud Land. The latter are lower in SiO_2 and Al_2O_3 and higher in TiO_2, total iron, Na_2O and P_2O_5; they are comparable to Manson's (1967) means of

TABLE XIX

MEAN CHEMICAL ANALYSES OF MESOZOIC THOLEIITIC ROCKS FROM THE SOUTHERN HEMISPHERE AND OF QUARTZ- AND OLIVINE-THOLEIITIC BASALTS AND DOLERITES

Analyses (anhydrous and volatile-free, recalculated to 100)

	A	B	C	D	E	F	G	H	I
SiO_2	52.26	55.62	55.10	54.61	51.61	51.95	52.85	48.95	49.99
TiO_2	1.64	0.82	0.73	1.27	2.06	1.57	1.53	1.75	1.34
Al_2O_3	14.15	14.55	15.36	14.39	13.63	16.48	15.43	15.64	15.49
Fe_2O_3	3.38	2.57	1.53	1.77	3.94	3.27	2.41	2.68	1.98
FeO	9.10	7.40	7.99	8.65	7.90	7.49	7.63	8.72	9.74
MnO	0.16	0.19	0.15	0.18	0.16	0.17	0.20	0.17	0.19
MgO	6.48	6.28	5.67	7.07	7.28	5.66	6.26	8.54	7.89
CaO	9.25	9.36	10.36	8.24	9.50	9.86	10.31	10.36	9.98
Na_2O	2.27	1.99	1.76	2.34	2.45	2.56	2.29	2.30	2.29
K_2O	1.09	1.08	1.24	1.31	1.14	0.79	0.90	0.65	0.89
P_2O_5	0.21	0.13	0.12	0.17	0.31	0.21	0.21	0.23	0.21

Th x 10^4 /K	c.4.9	5.6	4.9	2.8
K /Rb	c.312	240	200	407
Rb/Sr	c.0.20	c.0.30	0.25	c.0.13
Initial Sr^{87}/Sr^{86}	0.706	0.712	0.711	0.706

A. Jurassic dolerites from the Theron Mountains and Dronning Maud Land, mean of 123 analyses (Initial Sr^{87}/Sr^{86} ratios from Dronning Maud Land, after Faure and others, 1970)

B. Ferrar dolerites from Antarctica, mean of 138 analyses (minor-element and isotopic ratios after Compston and others, 1968 and Faure and others, 1970)

C. Jurassic dolerites from Tasmania, mean of 110 analyses (minor-element and isotopic ratios after Compston and others, 1968)

D. Karroo dolerites from southern Africa, mean of 147 analyses (minor-element and isotopic ratios after Compston and others, 1968)

E. Karroo basalts from southern Africa, mean of 70 analyses

F. Quartz-basalts, mean of 715 analyses

G. Quartz-dolerites, mean of 283 analyses

(after Manson, 1967)

H. Olivine-tholeiitic basalts, mean of 182 analyses

I. Olivine-tholeiitic dolerites, mean of 48 analyses

tholeiites except that SiO_2 is slightly higher and Al_2O_3 slightly lower. The Ferrar and Tasmanian dolerites are markedly higher in SiO_2 than the mean tholeiites and lower in TiO_2, Na_2O and P_2O_5.

If the Ferrar dolerites are considered in terms of Gunn's (1966) three magma types, then only his olivine-tholeiite is similar in SiO_2 content to the mean tholeiites of Manson (1967); TiO_2, total iron, Na_2O, K_2O and P_2O_5 are, however, very much lower.

If the dolerites of the Theron Mountains are considered in terms of individual intrusions (Table XVIII), then the younger sills and dykes of Lenton Bluff are very similar to Gunn's (1966) olivine-tholeiite. Of the other intrusions, the scarp-capping sill and the middle sill of Coalseam Cliffs are similar in SiO_2 content to the Ferrar and Tasmanian dolerites. The scarp-capping sill has much higher TiO_2, total iron and K_2O than the Ferrar dolerites and much lower Al_2O_3, MgO and CaO; Th/K, K/Rb and Rb/Sr ratios are almost identical with those of Gunn's (1966) pigeonite-tholeiite. The middle sill of Coalseam Cliffs is similarly higher in TiO_2 and K_2O; Th/K and Rb/Sr ratios are about the same as those of the mean Ferrar and Tasmanian dolerites but K/Rb ratios are slightly higher.

In general, both the individual intrusions in the Theron Mountains and the intrusions as a whole are chemically

more like the Karroo dolerites and basalts than either the Ferrar or Tasmanian dolerites.

2. Frequency distribution of oxides

The frequency distributions of some oxide weight percentages of Mesozoic tholeiites of the Southern Hemisphere are shown in Fig. 61. They tend to confirm the differences noted in terms of mean analyses. For comparative purposes, the frequency distributions of Hawaiian tholeiites (see Appendix II) and of quartz- and olivine-tholeiites (Manson, 1967) are also shown.

SiO_2 closely approximates a normal distribution for the Ferrar and Karroo dolerites and basalts, similar to that for quartz- and olivine-tholeiites, but the modal percentages differ; about half the published analyses of Ferrar dolerites lie in the range 53-56 per cent SiO_2, while about half the analyses of Karroo dolerites and basalts lie between 50 and 52 per cent SiO_2. The distribution for the Tasmanian dolerites is strongly positively skewed about a peak of 52-54 per cent SiO_2 and that for the Hawaiin tholeiites is negatively skewed about a peak of 48-51 per cent SiO_2. The distribution for the dolerites and basalts of the Theron Mountains and Dronning Maud Land is positively skewed with a very broad peak area at 48-52 per cent SiO_2

Fig. 61. Frequency distributions of weight percentages of SiO_2, TiO_2, CaO, K_2O and total iron (as Fe_2O_3) for some tholeiitic rocks; the dashed line indicates approximate mean values.

(a) 122 Jurassic dolerites from the Theron Mountains and Dronning Maud Land (see Appendices I and II).

(b) 139 Ferrar dolerites from Antarctica (see Appendix II).

(c) 110 Jurassic dolerites from Tasmania (see Appendix II).

(d) 224 Karroo dolerites and basalts from southern Africa (see Appendix II).

(e) 149 Hawaiian tholeiites (see Appendix II).

(f) 230 olivine-tholeiitic basalts and dolerites (after Manson, 1967).

(g) 998 quartz-basalts and dolerites (after Manson, 1967).

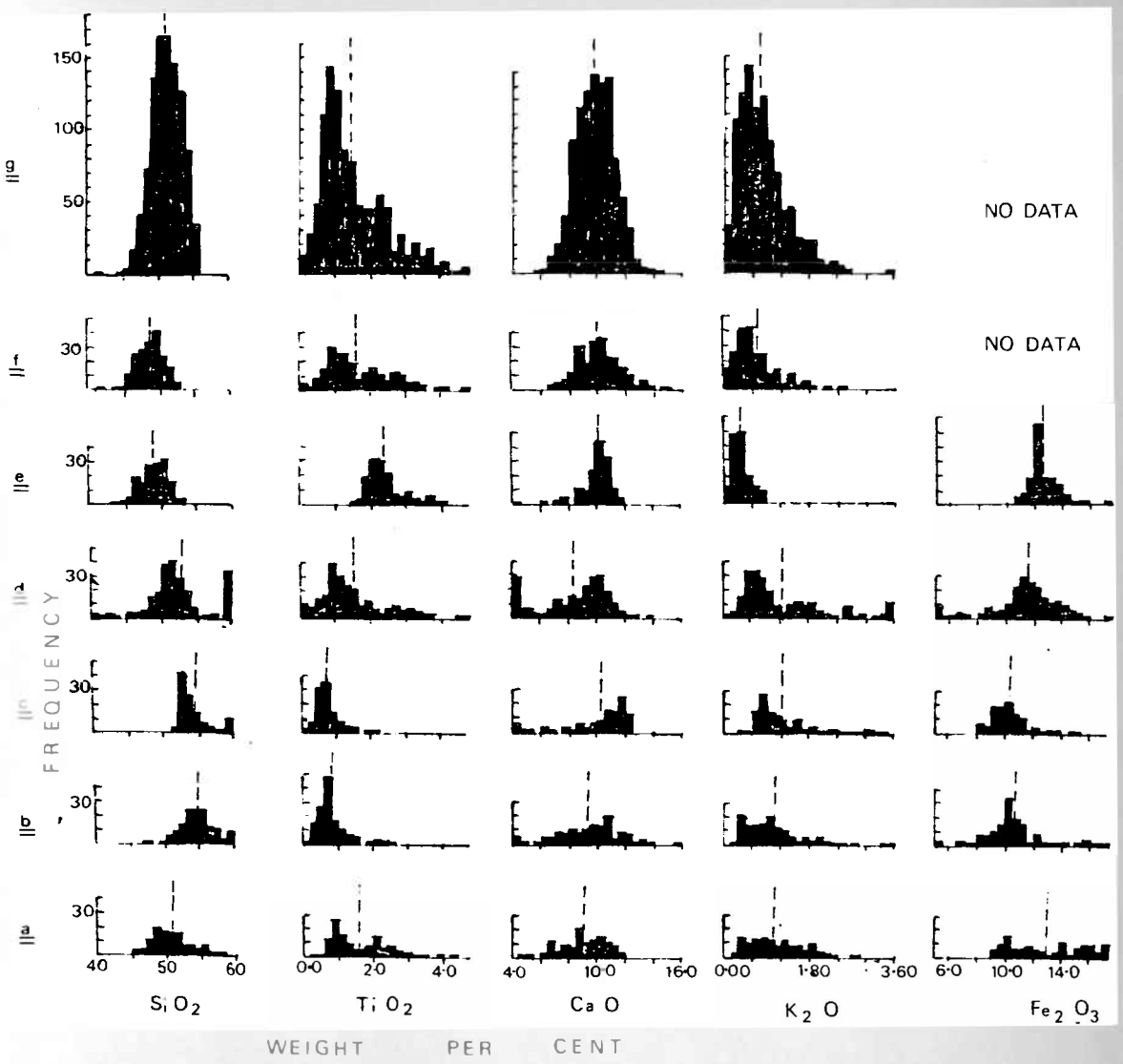
g
f
e
d
c
b
a
150
100
50
30
30
30
30
30
30
40
50
60
0·0
2·0
4·0
4·0
10·0
16·0
0·00
1·80
3·60
6·0
10·0
14·0
NO DATA
NO DATA
FREQUENCY
Si O2
Ti O2
Ca O
K2 O
Fe2 O3
WEIGHT PER CENT

and a slight tendency towards bimodality, with a small subsidiary peak at 55-56 per cent SiO_2. It thus resembles, to some extent a mixture of the Ferrar and Karroo distributions, with the influence of the latter being dominant.

The TiO_2 distribution of the Ferrar and Tasmanian dolerites is markedly different from that of the Karroo dolerites and basalts and those of quartz- and olivine-tholeiites. The Ferrar and Tasmanian dolerites show a strongly unimodal distribution with a peak at 0.6-0.8 per cent TiO_2 and contrast with the Hawaiian tholeiites which are also unimodal but about a peak of 2.0-2.6 per cent TiO_2. Very few analyses of the Ferrar and Tasmanian dolerites exceed 1.6 per cent TiO_2. The Karroo dolerites and basalts show a distinct multimodality, very like that of quartz- and olivine-tholeiites, with a very strong peak at 0.8-1.2 per cent TiO_2 and small subsidiary peaks at 1.8-2.0, 2.4-2.8 and 3.0-3.4 per cent TiO_2. The distribution in the Theron Mountains and Dronning Maud Land is bimodal with the major peak at 0.8-1.0 per cent TiO_2 and another strong peak at 2.0-2.2 per cent TiO_2. It is thus very similar to that of the Karroo dolerites and basalts and significantly different from the distribution in the Ferrar and Tasmanian dolerites.

The distributions of other major oxides show similar strong differences between the Ferrar and Tasmanian

dolerites on the one hand and the Karroo dolerites and basalts and the Jurassic dolerites and basalts of the Theron Mountains and Dronning Maud Land on the other. This is especially so in the case of Al_2O_3 (not shown) and CaO, K_2O and total iron (Fig. 61).

3. Variation diagrams

Variation diagrams for the Ferrar, Tasmanian and Karroo dolerites and Karroo basalts are shown, along with those of Jurassic dolerites and basalts from the Theron Mountains and Dronning Maud Land, in Figs. 49-56 and 58-59. Comparisons are somewhat difficult because of the different analytical methods used by various authors but some general points can be made.

Differentiation trends on all the diagrams are basically similar but the differences between the Ferrar and Tasmanian dolerites and the Karroo and Theron Mountains —Dronning Maud Land dolerites and basalts, which are exhibited by mean analyses and frequency distributions of oxides, are somewhat accentuated.

Both the Ferrar and Tasmanian dolerites show relatively smooth curves with only a slight spread of points on triangular plots of Mg^{2+} — $Fe^{3+} + Fe^{2+}$ — $Na^{+} + K^{+}$ and

Ca^{2+} — Na^{+} — K^{+} (Figs. 49 and 50) and on plots of mafic index against felsic index (Fig. 51). The range is slightly greater and the spread slightly less than those of the Jurassic dolerites and basalts of the Theron Mountains and Dronning Maud Land. The Karroo dolerites show a greater range and spread of points than all these three and the Karroo basalts, though of limited range (in the early - middle stages of fractionation), show as great a spread as the dolerites.

On a plot of $Na_2O + K_2O$ against SiO_2 (Fig. 52), there are significant differences between the two groups. The Ferrar and Tasmanian dolerites show smooth curves with a generally restricted spread of points except at lower SiO_2 values (50-55 per cent SiO_2). The Karroo dolerites, however, show a much greater spread of values (as much as 3-4 per cent $Na_2O + K_2O$ at any SiO_2 value) and a greater range at both high and low SiO_2 values. The Karroo basalts are of restricted range but the spread of $Na_2O + K_2O$ is even greater than in the dolerites. In both the basalts and dolerites of the Karroo, the main concentration of points is in the lower part of the spread of $Na_2O + K_2O$ values. The Jurassic dolerites and basalts of the Theron Mountains and Dronning Maud Land plot as two distinct curves (p.137) whose overall spread is almost as great as that of the

Karroo; the lower curve is almost equivalent to the trends of the Ferrar and Tasmanian dolerites and the main concentration of the Karroo dolerites and basalts.

Plots against mafic index of some major oxides are shown in Figs. 53-56. They similarly show smooth curves with a limited spread of points for the Ferrar and Tasmanian dolerites, especially the latter. The Karroo dolerites have a greater range and spread of points and the Karroo basalts, though limited in range, have a great spread of points. The Jurassic dolerites and basalts of the Theron Mountains and Dronning Maud Land are intermediate between the Ferrar—Tasmanian and the Karroo dolerites and basalts. Some show a tendency towards the separation of two trends, the lower one of which is almost equivalent to the Ferrar and Tasmanian trends and to the main concentrations of the Karroo dolerites and basalts.

Trace-element determinations for Mesozoic tholeiitic rocks of the Southern Hemisphere are relatively few in number. They have been determined by different methods (X-ray fluorescence and optical spectrography) and comparison is difficult, though some general features can be seen on plots against mafic index (Figs. 58 and 59).

The main features are the smooth curves with a limited spread of points for the Ferrar and Tasmanian

dolerites and the greater range and spread for the Karroo dolerites. The Jurassic dolerites and basalts of the Theron Mountains and Dronning Maud Land are intermediate between the two; they often show a tendency towards two separate trends, one of which is equivalent to the Ferrar and Tasmanian trends. The plot of Ni against mafic index (Fig. 58) for the Theron Mountains and Dronning Maud Land is much more restricted than those of other Southern Hemisphere tholeiites; only the cumulates of the layered sills of Jeffries Glacier and Marø Cliffs plot on similar curves in the early stages of fractionation. Otherwise, Ni is generally restricted to < 100 p.p.m. and, if anything, shows a progressive increase in the early stages of fractionation rather than the progressive decrease which would be expected and which is seen in the other Mesozoic tholeiites of the Southern Hemisphere.

4. Isotopic and minor-element ratios

Heier and others (1965) found the Jurassic dolerites of Tasmania to possess unexpectedly high initial $^{87}Sr/^{86}Sr$, Th/K and U/K ratios and low K/Rb ratios as compared with alkali-basalts and oceanic tholeiites; they are similar to those of rocks of crustal derivation.

Because of the general similarities between the Mesozoic tholeiites of South America, South Africa, Antarctica and Tasmania, Compston and others (1968) extended the study to these rocks. They found the Ferrar dolerites of Antarctica were very similar to those of Tasmania in terms of the above parameters but the Karroo and Serra Geral dolerites were significantly different. They suggested a sub-division of the Mesozoic tholeiites of the Southern Hemisphere into a Karroo—Serra Geral suite and a Ferrar—Tasmanian suite.

Mean values of initial $^{87}Sr/^{86}Sr$ ratios for the Karroo and Serra Geral dolerites are the same and slightly higher than those in most alkali-basalts and oceanic tholeiites but much lower than those in the Ferrar and Tasmanian dolerites. K/Rb ratios of Karroo dolerites are intermediate between those of alkali-basalts (and oceanic tholeiites) and those of the Ferrar and Tasmanian dolerites while Th/K and U/K ratios are comparable to those in alkali-basalts, being much lower than in the Ferrar and Tasmanian dolerites. Erlank and Hofmeyr (1968) found K/Rb ratios in the Serra Geral Formation to be similar to those in the Karroo dolerites; the Rajmahal traps of India show a large spread of K/Rb ratios.

Faure and others (1970) found that basaltic rocks of Jurassic age from Vestfjella and Heimefrontfjella in Dronning Maud Land have "normal" initial $^{87}Sr/^{86}Sr$ ratios bimodal about 0.704 and 0.707 while basalts and dolerites from the Ferrar Group average 0.712. The SiO_2 content of Ferrar basalts and dolerites correlates positively with initial $^{87}Sr/^{86}Sr$ ratios and collectively the basaltic rocks of the Ferrar Group and Dronning Maud Land form a co-linear array in a plot of SiO_2 against initial $^{87}Sr/^{86}Sr$ ratios.

Neethling (1971) studied the abundances and ratios of SiO_2, K_2O, Rb, U and Th in Precambrian and Mesozoic tholeiites in western Dronning Maud Land. He concluded that the Mesozoic tholeiites were more similar to those of the Karroo than to the Ferrar dolerites and suggested an extension of the Karroo—Serra Geral suite of Compston and others (1968) into at least the Dronning Maud Land area of Antarctica.

No Sr isotopic work has been done on the dolerites of the Theron Mountains but K/Rb and Th/K ratios are shown in the tables of chemical analyses (Tables IX-XVIII). If the positive correlation suggested by Faure and others (1970) occurs in these rocks, which are geographically between the ones studied by them, then their generally low SiO_2 contents may correlate with "normal" initial $^{87}Sr/^{86}Sr$

ratios. K/Rb and Th/K ratios show a wide spread which extends from the values found in the Karroo—Serra Geral suite to those found in the Ferrar—Tasmanian suite.

5. Summary

Petrographical and chemical data suggest that the Mesozoic tholeiitic rocks of the Southern Hemisphere can be sub-divided into two distinct provinces, a Karroo—Serra Geral and a Ferrar—Tasmanian province.

The Jurassic dolerites of the Theron Mountains are significantly different from the Ferrar dolerites of eastern Antarctica. They may represent an extension of the Karroo—Serra Geral province, as would be expected from their position on a reconstruction of Gondwanaland (Fig. 11). The apparent sub-division of the dolerites may indicate an interdigitation of the two provinces in the area of the Theron Mountains. In this case the most likely representative of the Ferrar—Tasmanian province would be the scarp-capping sill but the majority of intrusions would belong to the Karroo—Serra Geral province.

E. PETROGENESIS OF THE MESOZOIC THOLEIITES OF THE SOUTHERN HEMISPHERE

Because of petrographical and chemical similarities and their close relation in time and space, the petrogenesis of the Jurassic dolerites of the Theron Mountains cannot be divorced from that of other Mesozoic tholeiitic rocks of the Southern Hemisphere. The locations and radiometric ages of these rocks are shown in a reconstruction (after Smith and Hallam, 1970) of Gondwanaland (Fig. 11). Suggested origins for the anomalous Ferrar—Tasmanian magma are discussed below. Possibly the most important consideration with respect to the origin of the magma and its subsequent evolution is the association of basaltic magmatism with the break-up and dispersal of Gondwanaland. The timing of this break-up is discussed and a model, which covers most of the chemical features of the Mesozoic tholeiitic rocks of the Southern Hemisphere, is postulated for their origin. This model is based on a vertical zonation within the upper mantle and the association or otherwise of basaltic magmatism with the dispersal of Gondwanaland. Both geographically and chemically the Jurassic dolerites of the Theron Mountains are in a critical position with respect to this model.

1. Origin of the anomalous Ferrar—Tasmanian magma

Compston and others (1968) suggested a number of possible reasons for the anomalous "crustal" ratios of the Ferrar—Tasmanian province as opposed to the Karroo—Serra Geral province which shows more "normal" ratios. They considered generation of the magma within the crust and within the upper mantle.

Crustal-type isotopic and minor element ratios could not be produced by differentiation of a magma with typical mantle ratios so, if the magma derives from the mantle, either there has been general contamination by crustal material or the mantle beneath Tasmania and Antarctica was of different composition to that elsewhere.

a. Crustal derivation of the magma

The temperature of intrusion of the Tasmanian dolerites was near 1,100°C.(McDougall, 1962) and that of the Ferrar dolerites near 1,000°C. (Hamilton, 1965). Heat flow measurements (Howard and Sass, 1964) give an estimated temperature at the base of a 37 km. thick crust in eastern Australia of 650-780°C. In order to generate the magma within the crust, the temperature gradient during the Jurassic period must have been considerably steeper than at present.

The mere presence of extensive basaltic magmatism, however, indicates a steeper temperature gradient than at

present and this is supported by considerations of plate tectonics. The break-up and dispersal of Antarctica and Australia took place in the Eocene but there may have been some earlier movement along a postulated transcurrent fault zone separating eastern and western Antarctica. It is suggested that magmatism was associated with this fault zone and not with the break-up of the Australia—Antarctica block, possibly due to frictional heating along the fault zone and/or to concentration of any liquid phase in the fault zone, leading to rapid depression of the liquidus. This would lead to a steeper temperature gradient than at present and crustal derivation of the magma cannot, therefore, be discounted on the basis of temperature alone.

A more fundamental problem is the composition of what is regarded as lower crustal material. Spooner and Fairbairn (1970) studied granulite-facies rocks from East Africa, India, Guyana, the Adirondacks and south-eastern Ontario and published work on granulites from India, Scotland and the Ivory Coast. They concluded from geophysical and geochemical evidence that these rocks (pyroxene-granulites and anorthosites) were of igneous origin and developed in the lower crust; although metamorphism has rearranged the assemblages, initial $^{87}Sr/^{86}Sr$ ratios have been unaffected and they are restricted to a narrow range (0.700-0.707).

Studies of K, Rb and Th contents in the Norwegian and Australian Precambrian shields (Heier, 1960; Lambert and Heier, 1968) showed absolute contents of K and Rb to be low but K/Rb ratios to be high.

Available data on apparent lower crustal material would suggest, therefore, that a magma derived from the lower crust would have "normal" mantle-type ratios and not the anomalous ratios found in the Ferrar and Tasmanian dolerites. Upper crustal material would generally produce isotopic and minor element ratios of the right order but major and minor element compositions would differ and it is extremely difficult to envisage the generation of basaltic magma within the upper crust.

b. Derivation of the magma from a homogeneous upper mantle

If the upper mantle is homogeneous, the anomalous chemistry of the Ferrar and Tasmanian dolerites must be due to some form of crustal contamination, for which Compston and others (1968) suggested three possible mechanisms:

i. Bulk assimilation by basaltic magma of granitic material in the crust.

ii. Selective diffusion of certain elements into the magma.

iii. Partial melting of granitic material in the crust and assimilation by basaltic magma of the initial melting fraction.

Erlank and Hofmeyr (1968) considered that K/Rb ratios and the available data for Th and U indicate the possibility of selective crustal contamination in Antarctica (in the Precambrian (Allsopp and Neethling, 1970), not the Jurassic as they thought) while such contamination was absent or present on a smaller scale in the Karroo—Serra Geral province. They were uncertain as to whether the large spread of K/Rb ratios for the Rajmahal traps was due to selective crustal contamination or to secondary alteration.

i. Bulk assimilation

Lower crust granulite-facies rocks are characterized by low initial $^{87}Sr/^{86}Sr$ ratios and high K/Rb ratios typical of mantle-derived igneous rocks (Spooner and Fairbairn, 1970; Heier, 1960; Lambert and Heier, 1968). Assimilation by basaltic magma with mantle-type ratios of these rocks could not, therefore, give rise to the anomalous isotopic and minor element ratios found in the Ferrar and Tasmanian dolerites. If there has been contamination by crustal material then it must have occurred in the upper part of the crust, where acid gneisses predominate. At shallow crustal depths, however, the large temperature contrast usually results in chilling of the magma against its wall rock, resulting in a protective sheath of similar chemistry around the magma. In order to produce isotopic and minor element ratios of the right order the magma would have had

to assimilate a considerable proportion of its own volume. This is difficult to envisage happening at shallow depth with the uniformity found on such a tremendous scale in the Ferrar and Tasmanian dolerites.

ii. Selective diffusion

Heier (1964) postulated the diffusive addition of ^{87}Sr from low-energy sites in Rb-rich phases. This need not entail parallel contamination by other elements but it would require a large amount of time for the accumulation of the large amounts of radiogenic ^{87}Sr required.

Green and Ringwood (1967) suggested that the trace element contents of the Jurassic tholeiites of Antarctica, South Africa and Tasmania have been determined by wall-rock reaction and fractionation processes occurring at low pressures in a crustal environment. Slow ascent of large volumes of basaltic magma through the lower crust led to selective extraction of a low-melting fraction from the wall-rock environment. The elements enriched in the magma would be those least able to substitute in the major phases (i.e. pyroxenes, plagioclase, quartz and possibly hornblende and ilmenite) of the surrounding wall-rock (incompatible elements: K, P, Ba, Cs, Rb, U, Th and the lighter rare earths). The contaminating material would be expected to have high $^{87}Sr/^{86}Sr$ ratios and lead isotopic ratios consistent with geologically old crustal material. They suggest a

lower crust of anhydrous granulitic or anorthositic composition would possibly be suitable wall-rock material for these processes and effects but Spooner and Fairbairn's (1970) isotopic data would tend to mitigate against this conclusion.

Pankhurst (1969) found that the regional gabbro magma of north-east Scotland underwent a progressive increase in its $^{87}Sr/^{86}Sr$ ratio (0.703-0.712) during differentiation. This is similar to the positive correlation with SiO_2 in the Ferrar dolerites (Faure and others, 1970). He considered that there was insufficient time for the diffusive addition of ^{87}Sr (Heier, 1964) to be important and he rejected wall-rock reaction because there was no concomitant increase in other incompatible elements. He suggested instead some form of isotope exchange reaction between Sr in the magma and total Sr in the country rocks. He termed this isotope-equilibration and considered it was probably effected by fluid diffusion. He suggested that the uniformly high initial $^{87}Sr/^{86}Sr$ ratios of the Ferrar and Tasmanian dolerites could be due to isotope-equilibration in a crustal magma chamber prior to intrusion at their present level; trace element concentrations and ratios, however, seem to favour more comprehensive contamination by wall-rock reaction.

The gabbros of north-east Scotland were intruded at the close of orogenic activity and the temperature contrast between the magma and its country rock was only small. Beneath Tasmania and Antarctica, however, the temperature contrast would be greater because this was not an orogenic area subject to regional metamorphism; the effects of isotope-equilibration and wall-rock reaction would not be as pronounced.

Isotope-equilibration and wall-rock reaction would lead to the depletion of the country rock in incompatible elements and this may go some way towards explaining the low initial $^{87}Sr/^{86}Sr$ ratios of granulite-facies rocks when they are associated in time and space with "anomalous" basaltic magma; this does not appear to be the case in Tasmania or Antarctica.

The timing of the break-up and dispersal of Gondwanaland is to some extent consistent with a model which derives the anomalous chemistry of the Ferrar—Tasmanian province by isotope-equilibration and/or wall-rock reaction from a homogeneous mantle. Antarctica—Australia was a solid continental crustal block at the time of intrusion of the dolerites so it is conceivable that the magma was delayed for some considerable time in lower crustal regions before intrusion at its present level. At the same time, the South Africa—Dronning Maud Land area was breaking up

and separating; basaltic magma would not be expected to be delayed as long in such an environment during its ascent to its place of intrusion and would thus have been subject to less contamination by isotope-equilibration and wall-rock reaction. The uniformity of the chemistry of the two provinces of Mesozoic tholeiites in the Southern Hemisphere is, however, still a problem on the necessary scale.

iii. Assimilation of the initial melting fraction

The fraction of granitic material within the crust which would melt first would be that not contained in the major phases of crustal material. This would consist of incompatible elements so this process is essentially similar to that of wall-rock reaction. It is difficult to envisage partial melting of crustal material occurring on a large scale in the upper crust and the composition of the lower crust apparently presents insurmountable problems. If the lower crust is formed of granulite-facies rocks as suggested by Spooner and Fairbairn (1970) then it is difficult to conceive of even the initial melting fraction being sufficiently rich in incompatible elements to produce the anomalies found in the Ferrar and Tasmanian dolerites.

c. Derivation of the magma from an inhomogeneous upper mantle

If the peculiar chemistry of the Ferrar and Tasmanian dolerites is not due to crustal contamination of magma derived from a homogeneous upper mantle, then the upper mantle beneath Tasmania and Antarctica must be of different composition to that elsewhere. There is considerable evidence of both lateral and vertical inhomogeneity of the upper mantle.

Continental and oceanic basalts differ significantly in major and trace element compositions and Gast's (1967) compilation of isotopic data indicates a greater abundance of basalts with high initial $^{87}Sr/^{86}Sr$ ratios (> 0.705) from continental areas rather than oceanic areas. If, therefore, continental and oceanic basalts are abstracted from an initially homogeneous upper mantle, whether this be pyrolite (Green and Ringwood, 1967) or garnet peridotite (Yoder and Tilley, 1962; O'Hara, 1965), the composition of the residual material in the mantle would differ between the two areas. Subsequent magmatism would be expected to lead to even greater differences between oceanic and continental basaltic rocks.

According to the theory of plate tectonics, the upper part of the mantle beneath an oceanic area is constantly

being regenerated; the plate is renewed at the mid-ocean ridge, moves away and is consumed in the subduction zone. Beneath continental areas on the other hand, the upper part of the mantle is not renewed because if a continental plate approaches a subduction zone either movement stops or it reverses and the plate without a continent begins to subduct. Even assuming no major or trace element differences between the two areas, the isotopic geochemistry would be different in the continental mantle which was preserved in perpetuity. Decay of ^{87}Rb with time would, for example, increase the initial $^{87}Sr/^{86}Sr$ ratios of magmas generated within the mantle beneath continental areas. There are, however, also differences in major and trace element geochemistry; Tatsumoto and others (1965) found the contents of K, Th, U and ^{87}Sr to be less in oceanic tholeiites than in other common igneous rocks.

There is some evidence that inhomogeneity of the upper mantle is not restricted to the lateral differences between continental and oceanic areas but there are also differences within oceanic areas which cannot be explained by fractionation processes within the basaltic magmas which derive therefrom.

Hamilton (1965) considered that the variations in the initial $^{87}Sr/^{86}Sr$ ratios of Hawaiian basalts were not

due to natural fractionation in nature. Lessing and Catanzaro (1964) considered that the consistent inverse relation between $^{87}Sr/^{86}Sr$ and K/Rb ratios suggests contamination by assimilation of marine sediments is an influencing factor in Hawaiian petrogenesis. McDougall and Compston (1965) found no change in initial $^{87}Sr/^{86}Sr$ ratio with bulk composition in Reunion and Rodrigues in the Indian Ocean but they demonstrated real local and regional variations which led to the conclusion of inhomogeneity of the Sr isotope composition of the oceanic upper mantle. Le Maitre (1962) noted compositional differences between the alkali-olivine basalt series of Gough and Ascension Islands in the Atlantic Ocean. Gast and others (1964) found these to be accompanied by consistent differences in $^{87}Sr/^{86}Sr$ ratios and they concluded that the isotopic differences reflect differences in the source regions of the upper mantle. Gast's (1967) compilation of isotopic data suggests that regional variations in Rb/Sr ratios in mantle source regions may cause the observed variations of $^{87}Sr/^{86}Sr$ ratios irrespective of rock type. Tatsumoto and others (1965) found the Rb/Sr ratios of high-alumina oceanic tholeiites to be too low to account for the observed $^{87}Sr/^{86}Sr$ ratios; they concluded that either the magmas were not representative of their source in Rb/Sr ratio or the source region had changed its Rb/Sr ratio in the geological past.

There is direct evidence of vertical variations in the composition of the upper mantle in the form of xenoliths preserved within basaltic rocks. Those from Hawaiian alkali-olivine basalts, which are derived from relatively shallow depth, differ from those in kimberlite pipes, which are derived from greater depths. The amount of reliance to be placed on these differences is, however, difficult to estimate because even the peridotites, dunites and eclogites derived from the upper mantle are in part residual.

A vertical zonation in the distribution of incompatible elements is also implied and to a certain extent caused by the wall-rock reaction process of Green and Ringwood (1967). Incompatible elements would be partitioned into any liquid fraction within the mantle and would, therefore, tend to move upwards in a form of de-gassing process. There is evidence that a similar de-gassing process has operated within the continental crust. Lambert and Heier (1968) found that medium to high pressure granulite facies terrains have less acidic major element compositions and show significant depletions of U, Th and Rb compared with typical low pressure granulite and amphibolite facies terrains and the overall surface shield. They suggested that there are strong upward concentrations of Rb, U and Th

in the continental crust and it seems reasonable to assume that the same process operates within the upper mantle (i.e. there is a similar upward concentration of incompatible elements).

2. Break-up and dispersal of Gondwanaland

There is almost overwhelming evidence that the continents of the Southern Hemisphere were once a continuous land mass. Numerous authors have attempted reconstructions of this former super-continent of Gondwanaland based on computer-fits of coastlines at the 500 fathom (914 m.) (e.g. Smith and Hallam, 1970) and 1,000 fathom (1829 m.) isobaths (e.g. Dietz and others, 1971), palaeomagnetic (e.g. Stephenson, 1966), palaeobotanical (e.g. Schopf, 1970) and other geological evidence (e.g. Du Toit, 1937).

For the purposes of the present study, the exact nature of the fit is not necessarily critical and the reconstruction of Smith and Hallam (1970), which closely resembles that of Du Toit (1937), is used arbitrarily in Fig. 11. This reconstruction was based on a computer-fit of continental margins at the 500 fathom (914 m.) isobath, the parts fitted being controlled by a variety of geological features. Elliot (1971b) emphasized the necessity of geological control of drift reconstructions and suggested that

eastern and western Antarctica cannot be regarded as having been in their present relative positions before the break-up of Gondwanaland.

The nature and timing of the break-up and dispersal of Gondwanaland is critical with regard to the petrogenesis of the Mesozoic tholeiitic rocks of the Southern Hemisphere according to the model proposed below (p. 172). Both geological and geophysical criteria have been used to give a rough estimate of the timing of the break-up but their significance is uncertain. The most common criteria used are: initiation of marine transgressions, comparative palaeozoogeography, episodes of basic and/or alkaline igneous activity associated with extensional faulting, palaeomagnetic latitudes and magnetic anomaly patterns in the ocean floors; the timing suggested by these criteria is often contradictory.

Lithostratigraphical comparisons, palaeobotanical and palaeomagnetic evidence indicates that the southern continents were part of a continuous land mass in the Permian but the evidence for the first separation of any parts from this land mass is uncertain. Colbert (1971) considered that recent finds of Triassic tetrapods in Antarctica indicate beyond any reasonable doubt that Antarctica was closely connected to Africa in early Triassic times. An upper limit of about 200 m. yr. is provided for these tetrapod remains by the work of Hill (1970).

Palaeomagnetic evidence has been reviewed by Heirtzler and others (1968), Smith and Hallam (1970) and Creer (1970). It appears to show that Africa, Antarctica, Australia, India and South America were united and close to the south geographic pole in the early Permian. Africa underwent rapid northward movement in the early Mesozoic and Permian but there was little change in palaeomagnetic latitude since the middle Mesozoic. South America similarly underwent a large northward movement in the early Mesozoic and Permian but there was no appreciable change in palaeomagnetic latitude since the Triassic—Jurassic. There is some evidence that there was some movement of Australia relative to the rest of Gondwanaland in late Permian times but this does not appear to be confirmed by other criteria. Investigations on the Triassic—Jurassic lavas that appear in all the Gondwana continents indicate that the break-up of Gondwanaland had already occurred by this time.

Work on marine magnetic anomalies symmetrical about the mid-oceanic ridges in the Pacific (Pitman and others, 1968), South Atlantic (Dickson and others, 1968) and Indian Oceans (Le Pichon and Heirtzler, 1968) was summarized by Heirtzler and others (1968) and by Le Pichon (1968). They derived a history of sea-floor spreading in the Southern Hemisphere along the following lines:

1. Initial northward movement of Africa and South America in the Mesozoic and early Permian due to spreading about the south-west branch of the mid-Indian ridge; this was active during the Lower Mesozoic and the Permian but by the Jurassic spreading had mainly ceased. The split in the South American and African continents may have begun in the Mesozoic almost simultaneous with the break-away of the Africa—South America block.
2. Further separation of South America from Africa and northward movement of India in the Indian Ocean; the direction of spreading in the South Atlantic underwent a major change in the Upper Cretaceous (80 m. yr.) becoming nearly east—west and the separation of India from Antarctica was accomplished by rotation about a pole near 2^{o}N., 26^{o}E. The Upper Cretaceous also saw the separation of the New Zealand block from Antarctica.
3. Change of the pole of rotation in the Indian Ocean to 26^{o}N., 21^{o}E. and start of spreading about the south-east and north-west branches of the mid-Indian ridge at the end of the Eocene (40 m. yr.), caused by the abutting of the Indian sub-continent against the Asian mainland; this led to the rapid separation of Australia from Antarctica.

Dietz and Holden (1970) proposed a very similar time-scheme to this except that the break-up of the

Africa—South America block began sometime in the Jurassic; they explain the overlap of the Antarctic Peninsula onto this block by suggesting it is a Mesozoic accretionary belt. Smith and Hallam (1970) considered that extensional plate margins were established within Gondwanaland during the Jurassic and Cretaceous and that the dispersal of the continental fragments occurred mostly in Upper Cretaceous and Tertiary times; because of the discrepancy between the geometrical and sea-floor spreading poles they suggested the possible existence of an earlier period of spreading between Antarctica and Australia. Schopf (1970) suggested that western Antarctica and the Antarctic Peninsula were not part of the Antarctic crustal unit and that the frontal scarp of the Transantarctic Mountains may represent a "rift" line that was opposed to very different land areas in the Permian. Elliot (1971b) reviewed the geological control of Gondwanaland reconstructions and suggested that the developing mid-oceanic ridge between Africa and Antarctica terminated in a transform fault system which separated eastern and western Antarctica. He considered that this could possibly be related to the Alpine Fault of New Zealand and commented that it was no longer than the fault system along the west coast of North America from the termination of the East Pacific Rise to the Aleutian Trench. Barker

and Griffiths (in press) reviewed geophysical and geological work in the Scotia Sea and the northern part of the Antarctic Peninsula. They suggested that, during the early period of the break-up of Gondwanaland, South America and western Antarctica were fixed relative to each other and that the Weddell Sea was opened by a clockwise rotation of eastern Antarctica; only later did eastern and western Antarctica move as a single unit, distinct from South America, resulting in the present configuration of the Scotia Arc.

A possible history of the dispersal of Gondwanaland, which is related to the model for the evolution of the Mesozoic tholeiitic rocks of the Southern Hemisphere proposed below (p. 172), is outlined below.

During the Permian, the continents of Africa, Antarctica, South America, India and Australia formed a continuous landmass, much along the lines of the reconstruction shown in Fig. 11, except that eastern and western Antarctica were not in their same relative positions. The break-up of this super-continent began in the Upper Triassic (post 200 m. yr.) with the break-away and northward movement of the Africa—South America block from the rest of Gondwanaland; this was accompanied by tholeiitic magmatism in South Africa and Dronning Maud Land as movement continued. In the Upper Jurassic the Africa—South America block had virtually

reached its present latitude but it began splitting with east—west spreading along the mid-Atlantic ridge; this was accompanied by tholeiitic magmatism in South America and alkali-basaltic magmatism (Siedner and Miller, 1968) in South West Africa. The mid-oceanic ridge between Africa and Dronning Maud Land terminated in a transcurrent fault system between eastern and western Antarctica; this was accompanied by tholeiitic magmatism in eastern Antarctica and Tasmania. At the same time there was no movement along the Australian—Antarctic join but there was northward movement of New Zealand due to opening of the Pan-Antarctic rift north of Marie Byrd Land; the plate spreading southwards from this rift was consumed in a subduction zone along the margin of western Antarctica and South America, associated with the orogenic movements in the Andes and the Antarctic Peninsula. In the Eocene, the Antarctica—Australia block split up and Australia drifted rapidly northwards to its present position; this was accompanied by tholeiitic and alkali-basaltic magmatism in eastern and western Australia and in Victoria Land. The northward movement of India took place sometime during the Mesozoic; the exact relationships between this movement and the basaltic magmatism of the Rajmahal, Sylhet and Deccan traps are uncertain.

3. Model for the evolution of the Mesozoic tholeiitic magmas of the Southern Hemisphere

This model, which results largely from discussion with Dr. J. Tarney and K.F. Palmer, is based on a vertical zonation of incompatible elements within the upper mantle and the effects on this of the movements involved in plate tectonics. Although imperfect and highly speculative, it goes a long way towards explaining the anomalous chemistry of the Ferrar—Tasmanian province compared to the more "normal" Karroo—Serra Geral province; it also assists in explaining apparent discrepancies in the variations of major and trace elements in the Jurassic dolerites of the Theron Mountains.

Throughout geological time there has been a continuous de-gassing of the mantle because certain incompatible elements (K, Ti, P, Ba, Rb, Sr, U, Th and the lighter rare earths) are all, because of their ionic radii and valencies, incapable of substitution in the major phases of the upper mantle, be it pyrolite or garnet peridotite. These elements are, therefore, partitioned into any liquid fraction within the upper mantle or in minor phases such as phlogopite and hornblende. This results in a vertical zonation of incompatible elements within the upper mantle with their contents increasing upwards until phlogopite and

hornblende become stable. It is suggested that in the low-velocity zone of the mantle, where there appears to be a certain amount of partial melting, the stability fields of phlogopite and hornblende intersect the geothermal gradients; this leads to a concentration of incompatible elements within the low-velocity zone and consequently within any partial melt derived directly therefrom.

Because this movement of incompatible elements has been going on for a long time and because there is a preferential enrichment of Rb over Sr, Rb/Sr ratios in the low-velocity zone are higher than in the chondritic meteorite Earth model. Decay of ^{87}Rb with time would therefore lead to higher initial $^{87}Sr/^{86}Sr$ ratios in magma derived from the upper mantle than those of chondritic meteorites, as was noted by Gast (1967).

According to the model of plate tectonics, the material above the low-velocity zone in oceanic areas results from the lateral movement away from the mid-oceanic ridges of material derived therefrom by vulcanicity. Some form of convection cell or penetrative convection (Elder, 1970) is necessary to move material away from the mid-oceanic ridges and this would also involve the bringing up of material depleted in incompatible elements into the zone of partial melting. Pitman and others (1968) considered that

the anomalously high heat flow values in the vicinity of mid-oceanic ridges were not explicable by a very simple model of convective flow but that convection of some sort is probably the cause. Oxburgh and Turcotte (1968) considered a simple model of steady cellular convection; their model predicts a reasonable velocity for continental drift and the predicted values for the surface heat flow are in good agreement with observed values. They considered that although many of the arguments for a strong concentration of radioactive elements in the upper part of the mantle are invalid if mantle convection occurs, the currents proposed in their model take so long to complete a cycle that relatively low concentrations of radioactivity could have significant effects; these would include explaining the existence of convection currents with the horizontal dimensions necessary for large continental displacements but at the same time sufficiently shallow to be unaffected by the high viscosities that appear to characterize the deeper parts of the mantle. Mid-ocean ridge volcanism and oceanic plates would be expected, therefore, to be depleted in incompatible elements, and this is the case in oceanic tholeiites.

When a continental plate meets a subduction zone, either movement stops or it is reversed, so the plates

beneath continents are preserved in perpetuity. They are thus more enriched in incompatible elements than oceanic plates because they are not constantly being recirculated by subduction. This means that Rb/Sr ratios beneath continental areas would be higher than those beneath oceanic areas and they have been so for some considerable geological time. Initial $^{87}Sr/^{86}Sr$ ratios of magmas derived therefrom would, therefore, be higher than those in oceanic tholeiites, as is suggested by Gast's (1967) compilation of isotopic data.

If a continental plate began to rift apart, the first material to show itself in volcanism would be that derived from directly beneath the continent but with time more material would be brought up by convection until eventually there existed the true mid-ocean ridge volcanism with oceanic tholeiites being extruded.

If we apply this to the break-up and dispersal of Gondwanaland, then there is a direct connection between the chemistry of basaltic magmatism and its relation in time and space with the rifting apart and dispersal of the southern continents. Rifting apart of Africa and Antarctica began in the Triassic and went on through the Jurassic (at the same time as dolerite intrusion in South Africa and Dronning Maud Land). Rifting apart of Africa and South America began in the latest Jurassic and continued through

the Cretaceous (at the same time as the Serra Geral basalts and dolerites). Rifting apart of Australia and Antarctica, however, did not begin until the Eocene so during the period of intrusion of the Ferrar and Tasmanian dolerites, the Antarctic—Australian area was a solid continental crustal block, though there may have been some transcurrent movement associated with the northward migration of New Zealand and relative movement between eastern and western Antarctica.

With the beginning of the opening of the South Africa—Dronning Maud Land rift, there was first of all partial melting, within the low-velocity zone, of upper mantle material which was enriched in incompatible elements; this partial melting extended because of the local increase in heat flow into the lower part of the continental plate which was also slightly enriched in these elements. The resultant product of magmatism was basalts with anomalous isotopic and minor-element ratios, such as those noted by Manton (1968) in the Karroo basalts of the Lebombo—Nuanetsi region. Gradually, more and more material from the lower part of the upper mantle, depleted in incompatible elements, was brought up by convection into the low-velocity zone. This material suffered partial melting and mixed with the material already in the low-velocity zone, resulting in more "normalized" ratios as in the Karroo dolerites

(Compston and others, 1968); abundances, as opposed to ratios, were, however, more "crustal", as noted by Compston and others (1968) in the Karroo dolerites and by Neethling (1971) in the dolerites and basalts of western Dronning Maud Land. Increasingly more material from the lower part of the upper mantle was brought up with time, the proportion of material derived from the low-velocity zone in the partial melt decreased and ratios and abundances became "normal" like those of the oceanic tholeiites, which are being extruded at present-day mid-oceanic ridges.

A similar situation can be envisaged with the opening of the South America—Africa rift; the alkali-basalts of South West Africa may represent the earlier "enriched" material while more normal mixtures of enriched and depleted material from different depths within the upper mantle are represented by the basalts and dolerites of the Serra Geral Formation.

In contrast to the above, in Antarctica and Tasmania, magmatism occurred before the break-up of the Australia—Antarctica block. The partial melting which caused the magmatism was possibly due to frictional heating along a transcurrent fault zone between eastern and western Antarctica. Alternatively and/or concurrently any liquid phase in the mantle would tend to be concentrated in this

zone of weakness and rapid depression from the anhydrous to a hydrous liquidus would result. This would lead to extensive partial melting and may be a causative factor in the magmatism of the Ferrar and Tasmanian dolerites. The partial melt from which the magma was derived consisted entirely of material from the low-velocity zone and the continental plate above it. This material was enriched in incompatible elements and had anomalous "crustal" isotopic and minor-element ratios. This may also explain the anomalous minor-element ratios of the Precambrian dolerites of Dronning Maud Land (Neethling, 1971), though the tectonic history of this area during the Precambrian is unknown.

With the opening of the Antarctica—Australia rift in the Eocene, however, material from lower down was brought up by convection and began to mix with the material in the low-velocity zone in the new partial melt. This resulted in the more "normalized" isotopic and minor-element ratios of the McMurdo Volcanics of Victoria Land (Faure and others, 1970) and the Tertiary alkali-basalts and tholeiites of Tasmania (Compston and others, 1968).

The wide spread of K/Rb ratios in the Rajmahal traps (Erlank and Hofmeyr, 1968) may be associated with similar variations in the proportions of enriched and depleted material from different depths within the upper mantle in the partial melt.

Many of the chemical features of the Jurassic dolerites of the Theron Mountains suggest that they may represent a mixture of Karroo—Serra Geral and Ferrar—Tasmanian type magmas. This may be due to interdigitation of the two provinces in the area of the Theron Mountains, which to some extent would be expected from their present geographical position and from their position in a reconstruction of Gondwanaland (Fig. 11). There are certain features, however, which mitigate against this conclusion.

SiO_2, TiO_2, total iron, alkalis and associated trace elements and minor-element ratios, in particular, show significant differences from the Ferrar dolerites elsewhere in eastern Antarctica but in many cases they do not vary in concert. Minor-element ratios in the dolerites of the Theron Mountains range from those typical of the Karroo—Serra Geral province to those typical of the Ferrar—Tasmanian province. Th/K ratios are very variable, ranging from 1.8 upwards but they are strongly affected by the amount of secondary alteration. K/Rb ratios range from 90 to 871 but the majority lie between 250-400, which is intermediate between the values for the Ferrar—Tasmanian and Karroo—Serra Geral provinces. Rb/Sr ratios are also variable and they range from 0.02-0.68 but except for the granophyric rocks of the scarp-capping sill, few lie outside the range

0.02-0.25. The earliest differentiates of the dolerites of the Theron Mountains (the younger sills and dykes of Lenton Bluff) are very similar in major and trace element geochemistry to the earliest differentiates of the Ferrar dolerites (olivine-tholeiites; Gunn, 1966). Later differentiates diverge from those of the Ferrar dolerites, however, and though some elements and ratios are similar to those of the Ferrar—Tasmanian province, others are typical of the Karroo—Serra Geral province.

These factors may indicate that, although there has possibly been some mechanical interdigitation of the two provinces in the area of the Theron Mountains, the major features of the chemistry can best be explained by a mixing of the two magmas at depth. One of the major arguments against contamination as the cause of the anomalous chemistry of the Ferrar and Tasmanian dolerites is the uniformity found within these two groups, which would not be expected on such a vast scale with any method of contamination. The same argument can be applied to the present model in that it implies a mixing at depth of enriched and depleted material from different depths within the upper mantle. If, however, the dolerites of the Theron Mountains represent an actual mixture of the two magmatic provinces, then this uniformity of the two provinces of Mesozoic tholeiites of the Southern

Hemisphere is not as great as has been suggested. This is possibly also suggested by the variable isotopic data of Manton (1968) in the Karroo basalts of the Lebombo—Nuanetsi region of South Africa.

The evolution of the Mesozoic tholeiitic magmas of the Southern Hemisphere can thus be summarized according to this model as follows:

i. Latest Triassic

Local increase in heat flow, initiation of convection and extensive tensional basaltic magmatism associated with the doming and uplift of the Africa—Dronning Maud Land rift and transcurrent faulting between eastern and western Antarctica initially without any pulling apart; derivation of magma from the low-velocity zone beneath the continents, which was enriched in incompatible elements.

ii. Jurassic

Pulling apart of the Africa—Dronning Maud Land rift; derivation of the magma from a mixture of enriched and depleted material, typified by the apparent discrepancies in element variations in the dolerites of the Theron Mountains. At the same time there was no movement along the Antarctica—Australia join but basaltic magmatism continued; derivation of magma from the

low-velocity zone.

iii. Latest Jurassic

Beginning of the opening of the Africa—South America rift and initiation of basaltic magmatism; derivation of magma from the low-velocity zone, leading to alkali-basalts in South West Africa.

iv. Cretaceous

Continued opening of the Africa—South America rift and basaltic magmatism of the Serra Geral Formation; derivation of the magma from a mixture of depleted and enriched material from different depths within the upper mantle.

v. Tertiary

Opening of the Antarctica—Australia rift and renewal of basaltic magmatism in the McMurdo Volcanics of Victoria Land and the alkali-basalts and tholeiites of Tasmania; derivation of the magma from a mixture of enriched and depleted material from different depths within the upper mantle.

CHAPTER VII

STRUCTURE AND TECTONICS

The structure of the Theron Mountains is relatively straightforward. There has been some tilting and faulting but it is usually only on a small scale and of very local significance.

The sediments of the Theron Mountains are sub-horizontal in attitude and only rarely can an accurate estimate of their dip be made. The maximum dip observed over any distance is at Coalseam Cliffs (Z.494), where the sediments above the thick wedging sill dip at 5-10^{o} to the south-west. This dip has obviously been imposed by the intrusion of the sill and it is of only local significance. Similar tilting of the sediments directly attributable to dolerite intrusion occurs in many places (e.g. Fig. 31) and locally there are dips of more than 30^{o} over very short distances.

Ford (1971) has described folding about north-east to south-west axes of Devonian to Upper Permian sediments of the Beacon Supergroup in the Pensacola Mountains. The local name Weddell orogeny was given to this event, for which a maximum range of latest Permian to Middle Jurassic is indicated. There is, however, no evidence that the Weddell orogeny had any effect in the Theron Mountains.

On the ridge leading eastwards from point 3300 (Z.453), a small north to south trending reversed fault with a westerly downthrow of about 20 m. offsets the 15 m. thick sill above the scarp-capping sill. A 1-2 m. wide dyke, possibly a feeder to the 6 m. thick sill forming the first shoulder on the ridge leading to point 3300, follows the line of this fault. The dyke is later than the fault but its exact relationships to the two sills are uncertain. The faulting was probably penecontemporaneous with dolerite intrusion. It may have been associated with or possibly caused by intrusion, though the association of compressional features, such as reversed faulting, and tensional features, such as dolerite sills and dykes, is unusual. If the occurrence of sills in a sedimentary sequence is indicative of a state of compression at the time of emplacement (Gretener, 1969), this association would not be unexpected.

Near the south-western end of Marø Cliffs (Z.481), a small reversed fault with a southerly downthrow of not more than 10 m. trends north-east to south-west, parallel to the cliff face. It brings the third-phase sill into contact with the first-phase sill but, as the former varies in horizon by quite large amounts over short distances along the cliffs and in places intrudes the first-phase sill, it is difficult to calculate the downthrow. This fault is not

of great extent and it cannot be traced for more than 50-100 m. along the cliffs. In the two buttresses where is is exposed the actual contacts are covered by a scree-filled gully (Fig. 62). The age of the fault is not known but it is probably not much younger than the sills.

The faults described above are the only ones seen which have significantly displaced the dolerites and sediments but there are examples of very small-scale local faulting penecontemporaneous with sedimentation (p. 27) and of local intrusion-faulting (p. 73).

There is no evidence to suggest any faulting along the tributaries of "Main Glacier" and the scarp-capping sill can be traced at approximately the same altitude across Goldsmith and Jeffries Glaciers and into the thick wedging sill of Coalseam Cliffs across the unnamed southern glacier. Variation in altitude of sills is apparently caused by variation in horizon within the sediments rather than by faulting. The absence of certain sills in some cliff sections at approximately the same horizon is attributed to their being only of local extent and not to their being faulted out.

Stephenson (1966) interpreted the constant trend of the escarpment of the Theron Mountains as a fault scarp with the downthrow to the north-west. The parallel crevassed ice scarp about 50 km. to the north-west supports the

Fig. 62. View from the south-west of a reversed fault cutting dolerite and sediments in Marø Cliffs (Z.481); the downthrow is apparently to the south. The fault plane is not exposed but it follows the scree-filled gully.

suggestion that "Main Glacier" follows the line of a graben. There is, however, no evidence of any major down-faulting to the north-west and little evidence of faulting at all. The evidence for a fault-line origin for the escarpment is thus based largely on inference and the constant trend could be the result of planation by the over-deepened "Main Glacier" in the recent past.

Block-faulting is common in the mountain ranges of the Transantarctic Mountains and of western Dronning Maud Land and, therefore, it is not unlikely that the Theron Mountains are a fault block, separated from its nearest neighbours by faults, or possibly graben, followed by "Main Glacier" and Slessor Glacier. This is based only on inference and there is no direct evidence that the present distribution of rock outcrops and glaciers is a result of block-faulting. If block-faulting has occurred its age is unknown except that it is post-Jurassic. Stephenson (1966) considered that, if the escarpment of the Theron Mountains is due to faulting, the only indication of its age is its sharp profile which infers youth; this could equally well be due to planation by "Main Glacier" and subsequent intensive frost action.

CHAPTER VIII

SUMMARY AND CONCLUSIONS

Pre-Permian events in the Theron Mountains are unknown. Permian and later events are summarized in Table I.

During Permian times a sequence of continental water-lain clastic sediments were deposited. These are wholly of fine grade and consist of fine-grained sandstones, siltstones, mudstones and shales with subordinate carbonaceous beds and coals. They are of variable composition, including arkosic, feldspathic and quartzitic beds and they were probably derived from a metamorphic terrain composed of gneisses and gneissic granites with some slight admixture from an acid volcanic source. Their source area was somewhere to the south-west and the environment of deposition was locally variable. Erosion of the source area was probably fairly rapid with occasional intervals of quiet deposition under fluvial, fluvial-deltaic and lacustrine conditions; glacial and fluvio-glacial deposits and volcaniclastic strata are absent.

Minor breaks in the succession, due to penecontemporaneous erosion, are of very local significance. The sedimentary "break" at Coalseam Cliffs (Stephenson, 1966)

does not indicate a hiatus of any great significance.

The Glossopteris flora within the sediments indicates a Lower Permian age (Plumstead, 1962). This confirms the correlation indicated by lithological and structural comparisons, with the Permian sandstones and coal measures of the Victoria Group of the Beacon Supergroup (Barrett and others, 1971) elsewhere in eastern Antarctica. The Karroo and other Lower Gondwana sediments are homotaxial in other Southern Hemisphere continents.

There is no record of tectonic events between the Permian and Jurassic but the sediments were probably subjected to some diagenetic and metamorphic (lower zeolite facies) changes due to the depth of overburden. These imparted a bituminous rank to the coals. The Lower Permian to Lower Jurassic Weddell orogeny (Ford, 1971), which affected the sediments of the Pensacola Mountains, does not appear to be represented.

During the Jurassic period (154-169 m. yr.; Rex, 1971), the sedimentary sequence was invaded by a great volume of dolerite, correlated with other Mesozoic tholeiitic rocks of the Southern Hemisphere (Fig. 11). Intrusion was largely in the form of sub-horizontal sills, ranging in thickness from <1 m. to over 200 m. and averaging about 30 m., but there are a few impersistent dykes 1-6 m. wide.

Extrusive equivalents of the dolerite intrusions are not present within the mountain range, though they occur in western Dronning Maud Land (Juckes, in press; Hjelle and Winsnes, 1971; Aucamp and others, 1971). At least three phases of intrusion are represented but a top-to-bottom sequence, such as described in the central part of the Karroo Basin (Walker and Poldervaart, 1949), cannot be inferred. Layering of two different types occurs in sills alongside Jeffries Glacier and in Marø Cliffs; the two types are probably due to flowage differentiation and crystal settling, respectively.

Intrusion was accompanied by minor local tilting and faulting, by thermal metamorphism of the intruded sediments and by some hydrothermal mineralization. Obvious metamorphism visible in hand specimen is restricted to contact rocks but there is a general pervasive metamorphism throughout the sedimentary sequence; this is especially noticeable in the coals. Xenoliths are all of local sedimentary origin and they are generally restricted to the basal sill of Lenton Bluff, though they do occur in other intrusions.

The petrography of the dolerite intrusions is variable (Tables III-V); different intrusions are petrographically distinct and there are variations due to

differentiation *in situ*. Many of the intrusions are olivine-bearing throughout and most of them have olivine or altered olivine phenocrysts in chilled marginal rocks. Other intrusions are characterized by a felsic mesostasis and granophyric quartz-dolerites are common. The dolerite intrusions are more similar petrographically to the Karroo dolerites of southern Africa than to either the Ferrar dolerites of Antarctica or the Jurassic dolerites of Tasmania.

The dolerite intrusions vary in chemistry, both individually and due to differentiation *in situ* (Tables IX-XVIII). Some of the minor intrusions can be correlated chemically with major intrusions, the Cr/Ni ratio being of particular value in this respect. Fractionation is largely shown by an increase in total iron relative to magnesia with only a slight increase in alkalis relative to lime. Many of the variation diagrams (Figs. 49-60) show a tendency towards two separate trends, individual intrusions lying on one or the other trend depending on which element is plotted; the scarp-capping sill tends to be consistently separated from other intrusions in the Theron Mountains.

A geochemical comparison with the Mesozoic tholeiitic rocks of the Southern Hemisphere supports the separation of two major basaltic provinces in the Southern

Hemisphere (Compston and others, 1968) but modifies their geographical limits. On the basis of mean analyses, frequency distributions of oxide weight percentages, variation diagrams and isotopic and minor-element ratios, the Jurassic dolerites of the Theron Mountains and Dronning Maud Land differ significantly from the Ferrar dolerites elsewhere in eastern Antarctica and it is suggested that they form an extension of the Karroo—Serra Geral province of Compston and others (1968). This would, to a certain extent, be expected from their geographical position, both at present and in a reconstruction of Gondwanaland (Fig. 11).

The petrogenesis of the Jurassic dolerites of the Theron Mountains is inextricably linked to that of other Mesozoic tholeiitic rocks of the Southern Hemisphere. It seems unlikely, because of compositional difficulties, that the magma could have been derived from crustal material so it must have been derived from the upper mantle. Various contamination mechanisms (bulk assimilation by basaltic magma of granitic material in the crust; selective diffusion of certain elements into the magma; partial melting of granitic material in the crust and assimilation by basaltic magma of the initial melting fraction) may have had some small effect but they are not considered to have caused the anomalous chemistry of the Ferrar and Tasmanian dolerites. This is thought to be due to the mantle beneath Tasmania and

Antarctica differing in composition from that elsewhere due to lateral and vertical inhomogeneities in the distribution of incompatible elements (i.e. those which are incapable of substitution in the major phases of the upper mantle) within the upper mantle.

The relationship of the magmatism of the Karroo—Serra Geral and Ferrar—Tasmanian provinces to the break-up and dispersal of Gondwanaland is considered to be significant. Available evidence suggests a possible chronology of break-up which can be directly linked to the chemistry of the magmatism, according to the model proposed.

The magmatism of the Karroo—Serra Geral province is linked to the break-away of the South America—Africa block from the Dronning Maud Land coast of Antarctica in latest Triassic—Jurassic times and the subsequent break-up and dispersal of this block in Upper Jurassic—Cretaceous times. The presence and chemistry of the magmatism is attributed to the effects of the convection system which caused the break-up on the vertically inhomogeneous upper mantle. The magmatism of the Ferrar—Tasmanian province, on the other hand, does not appear to be linked to dispersive movements within Gondwanaland, though its presence may be linked in some way with possible transcurrent movement between eastern and western Antarctica. The anomalous chemistry of this province is due to a lateral inhomogeneity

of the upper mantle which was caused by the combined effects of vertical inhomogeneity within the upper mantle and the movements involved in plate tectonics. The break-up of the Australia—Antarctica block did not occur till Eocene times and magmatism associated with this break-up (Tertiary tholeiitic and alkali basalts) does not have the anomalous chemistry of the earlier pre-Drift magmatism.

The Theron Mountains were geographically near the boundary of the Karroo—Serra Geral and Ferrar—Tasmanian provinces and, though there may have been some mechanical interdigitation of the two provinces, the chemistry of the Jurassic dolerites is probably attributable to mixing at depth. Apparent discrepancies in the variation patterns of some elements supports this latter possibility.

Little can be inferred of tectonic events since the end of the Jurassic but there may have been some block-fault movement resulting in the preservation of the sediments and dolerites of the Theron Mountains at a lower altitude than in nearby mountain areas, such as the Shackleton Range (Stephenson, 1966) and Heimefrontfjella (Juckes, in press).

Since the last glaciation of Antarctica there has been a period of erosion in which glacial and periglacial processes are dominant. The present-day landforms of the Theron Mountains are ice-sculptured, though they may be

modifications of pre-existing landforms. There is some evidence for retreat of the ice sheet but multiple glaciation (cf. Pewe, 1960; Bull and others, 1962) cannot be inferred.

ACKNOWLEDGEMENTS

I wish to thank Sir Vivian Fuchs, Director of the British Antarctic Survey, for permission to use in this thesis work which is the property of the Survey. Thanks are also due to Professor F.W. Shotton for providing laboratory facilities in the Department of Geology, University of Birmingham, and to Dr. R.J. Adie for his careful supervision during the preparation of this thesis.

The field work was carried out with the assistance of the members of the British Antarctic Survey station at Halley Bay during the years 1966-68, to whom thanks are due. In particular, I am grateful to my field companions, A. Johnston, D.K. McKerrow and C.M. Wornham, who assisted with geomorphological and glaciological observations.

The map on which Figs. 2, 3 and 4 are based was compiled by A. Johnston and the photographs on which Fig. 5 is based were kindly provided by the Directorate of Overseas Surveys.

For assistance with analytical and data-processing techniques, I am grateful to Dr. J. Tarney and Dr. G.L. Hendry. Interpretation of the data has been assisted by much discussion with Dr. J. Tarney, Dr. G.L. Hendry, K.F. Palmer and other colleagues at the University of Birmingham.

REFERENCES

ACKERMANN, P.B. and F. WALKER. 1960. Vitrification of arkose by Karroo dolerite near Heilbron, Orange Free State. Q. Jl geol. Soc. Lond., 116, Pt. 3, 239-54.

ADIE, R.J. 1952. Representatives of the Gondwana System in the Falkland Islands. (In Symposium sur les séries de Gondwana, 19th Int. geol. Congr., Alger, 1952, 385-92.)

ALLEN, A.D. 1962. Geological investigations in southern Victoria Land. Part 7. Formations of the Beacon Group in the Victoria Valley region. N.Z. Jl Geol. Geophys., 5, No. 2, 278-94.

ALLSOPP, H.L. and D.C. NEETHLING. 1970. Rb-Sr isotopic ages of Precambrian intrusives from Queen Maud Land, Antarctica. Earth & Planet. Sci. Letts., 8, No. 1, 66-70.

AMARAL, G., CORDANI, U.G., KAWASHITA, K. and J.H. REYNOLDS. 1966. Potassium-argon dates of basaltic rocks from southern Brazil. Geochim. cosmochim. Acta, 30, No. 2, 159-89.

AMERICAN COMMISSION ON STRATIGRAPHIC NOMENCLATURE. 1961. Code of stratigraphic nomenclature. Bull. Am. Ass. Petrol. Geol., 45, No. 5, 645-65.

ARDUS, D.A. 1964. Some observations at the Tottanfjella, Dronning Maud Land. British Antarctic Survey Bulletin, No. 3, 17-20.

ATHAVALE, R.N., RHADAKRISHNA MURTY, C. and P.W. SAHASRABUDHE. 1962. Palaeomagnetism of some Indian rocks. Geophys. J., 7, 304-13.

AUCAMP, A.P.H., WOLMARANS, L.G. and D.C. NEETHLING. 1971. The discovery of a pre-Beacon sedimentary sequence in the south-western portion of the Kiswan escarpment, western Dronning Maud Land, Antarctica. (In ADIE, R.J. ed. Antarctic geology and geophysics. Oslo, Universitetsforlaget.)

AUGHENBAUGH, N.B. 1961. Preliminary Report on the geology of the Dufek Massif. I.G.Y. Glaciol. Rep., No. 4, 155-93.

AUTENBOER, T. VAN. 1962. Ice mounds and melt phenomena in the Sør-Rondane, Antarctica. J. Glaciol., 4, No. 33, 349-54.

————. 1964. The geomorphology and glacial geology of the Sør-Rondane, Dronning Maud Land, Antarctica. Meded. K. vlaam. Acad., 26, Nr. 8, 7-91.

BARKER, P.F. and D.H. GRIFFITHS. In press. The evolution of the Scotia Ridge and Scotia Sea. Phil. Trans. R. Soc., Ser. A.

BARRETT, P.J. 1969a. Photomicrographs of some sedimentary & volcaniclastic Permian & Triassic Beacon Rocks from the Beardmore Glacier area, Antarctica. Ohio State Univ., Inst. of Polar Studies Rep., No. 31, 30 pp.

BARRETT, P.J. 1969b. Stratigraphy & petrology of the mainly fluviatile Permian & Triassic Beacon rocks, Beardmore Glacier area, Antarctica. Ohio State Univ., Inst. of Polar Studies Rep., No. 34, 132 pp.

————. and D.H. ELLIOT. 1971. The early Mesozoic volcaniclastic Prebble Formation, Beardmore Glacier area, Antarctica. In ADIE, R.J. ed. Antarctic geology and geophysics. Oslo, UniversitetsForlaget.

————., GRINDLEY, G.W. and P.N. WEBB. 1971. The Beacon Supergroup of east Antarctica. In ADIE, R.J. ed. Antarctic geology and geophysics. Oslo, Universitets Forlaget.

BENSON, W.N. 1916. Report on the petrology of the dolerites collected by the British Antarctic Expedition, 1907-09. Brit. Antarct. Exped. 1907-09, Sci. Invs. Repts., Geol., 2, pt. 9, 153-160.

BHATTACHARJI, S. 1966. Experimental scale model studies on flowage differentiation in sills. Spec. Pap. geol. Soc. Am., 87, 11-12.

————. 1967. Scale model experiments on flowage differentiation in sills. In WYLIE, P.J. ed. Ultramafic and related rocks. New York, John Wiley & Sons, Inc., 69-70.

BLUNDELL, D.J. and P.J. STEPHENSON. 1959. Palaeomagnetism of some dolerite intrusions from the Theron Mountains and Whichaway Nunataks, Antarctica. Nature, Lond., 184, No. 4702, 1860.

BROOK, D. and J.R. BECK. In press. Antarctic petrels, snow petrels and south polar skuas breeding in the Theron Mountains. British Antarctic Survey Bulletin.

BROWN, H.R. and G.H. TAYLOR. 1960. Metamorphosed coal from the Theron Mountains. Scient. Rep. transantarct. Exped., No. 12, 11 pp.

BROWN, J.W. 1967. Jurassic dolerites from the Falkland Islands and Dronning Maud Land. British Antarctic Survey Bulletin, No. 13, 89-92.

BROWNE, W.R. 1923. The dolerites of King George Land and Adelie Land. Australasian Antarct. Exped. 1911-14, Sci. Repts., ser. A, 3, pt. 3, 245-58.

BULL, C., McKELVEY, B.C. and P.N. WEBB. 1962. Quaternary glaciations in southern Victoria Land, Antarctica. J. Glaciol., 4, No. 31, 63-78.

CAILLEUX, A. 1962. Ice mounds on frozen lakes in McMurdo Sound, Antarctica. J. Glaciol., 4, No. 31, 131-33.

COLBERT, E.H. 1971. Triassic tetrapods from Antarctica. In ADIE, R.J. ed. Antarctic geology and geophysics. Oslo, UniversitetsForlaget.

COMPSTON, W., McDOUGALL, I. and K.S. HEIER. 1968. Geochemical comparison of the Mesozoic basaltic rocks of Antarctica, South Africa, South America and Tasmania. Geochim. cosmochim. Acta, 32, No. 2, 129-50.

COX, K.G. and G. HORNUNG. 1966. The petrology of the Karroo basalts of Basutoland. Am. Miner., 51, Nos. 9/10, 1414-32.

————., MACDONALD, R. and G. HORNUNG. 1967. Geochemical and petrographic provinces in the Karroo basalts of southern Africa. Am. Miner., 52, Nos. 9/10, 1451-74.

CRARY, A.P. and C.R. WILSON. 1961. Formation of "blue" glacier ice by horizontal compressive forces. J. Glaciol., 3, No. 30, 1045-50.

CREER, K.M. 1962. Palaeomagnetism of the Serra Geral Formation. Geophys. J., 7, 1-22.

————. 1970. A review of palaeomagnetism. Earth Sci. Revs., 6, No. 6, 369-466.

————., MILLER, J.A. and A. GILBERT-SMITH. 1965. Radiometric age of the Serra Geral Formation. Nature, Lond., 207, No. 4994, 282-83.

CROHN, P.W. 1959. A contribution to the geology and glaciology of the western part of Australian Antarctic Territory. A.N.A.R.E. Reps., Ser. A, 3, 103 pp.

DALY, R.A. and T.F.W. BARTH. 1930. Dolerites associated with the Karroo System, South Africa. Geol. Mag., 67, No. 3, 97-110.

DICKSON, G.O., PITMAN, W.C. and J.R. HEIRTZLER. 1968. Magnetic anomalies in the South Atlantic and ocean floor spreading. J. geophys. Res., 73, No. 6, 2087-2100.

DIETZ, R.S. and J.C. HOLDEN. 1970. Reconstruction of Pangaea, its breakup and dispersion of continents - Permian to Present. J. geophys. Res., 75, No. 26, 4939-56.

————., ————. and W.P. SPROLL. 1971. Antarctica and continental drift. In ADIE, R.J. ed. Antarctic geology and geophysics, Oslo, UniversitetsForlaget.

DU TOIT, A.L. 1937. Our wandering continents. Edinburgh and London, Oliver and Boyd, 366 pp.

————. 1954. The geology of South Africa. 3rd ed. Edinburgh and London, Oliver and Boyd, 611 pp.

EALES, H.V. 1959. The Khale Dolerite Sheet. Trans. Proc. geol. Soc. S. Afr., 55, 81-109.

EDWARDS, A.B. 1942. Differentiation of the dolerites of Tasmania. J. Geol., 50, No. 5, 451-80, No. 6, 579-610.

ELDER, J.W. 1970. Quantitative laboratory studies of dynamical models of igneous intrusion. In NEWALL, G. and N. RAST. eds. Mechanism of igneous intrusion. Liverpool geol. Soc., 245-60.

ELLIOT, D.H. 1971a. Major oxide chemistry of the Kirkpatrick Basalt, central Transantarctic Mountains, Antarctica. In ADIE, R.J. ed. Antarctic geology and geophysics. Oslo, UniversitetsForlaget.

ELLIOT, D.H. 1971b. Post-Palaeozoic movements of parts of Gondwanaland with particular reference to Antarctica and its geological record. In ADIE, R.J. ed. Antarctic geology and geophysics. Oslo, UniversitetsForlaget.

ERLANK, A.J. and P.K. HOFMEYER. 1968. K/Rb ratios in Mesozoic tholeiites from Antarctica, Brazil and India. Earth & planet. Sci. Lett., 4, No. , 33-38.

FAURE, G., HILL, R.L., JONES, L.M. and D.H. ELLIOT. 1970. Isotope composition of strontium and silica content of Mesozoic basalt and dolerite from Antarctica. In Studies in the geochronology and geology of the Transantarctic Mountains, Ohio State Univ. Inst. Polar Studies & Dept. of Geol., Laboratory for isotope geology & geochemistry Rep. No. 5, 1-22.

FITTON, J.G. and R.C.O. GILL. 1970. The oxidation of ferrous iron in rocks during mechanical grinding. Geochim. cosmochim. Acta., 34, No. 4, 518-24.

FORD, A.B. 1971. The Weddell Orogeny — Latest Permian to early Mesozoic deformation at the Weddell Sea margin of the Transantarctic Mountains. In ADIE, R.J. ed. Antarctic geology and geophysics. Oslo, Universitets Forlaget.

FRANKEL, J.J. 1938. Studies on Karroo Dolerites - (1) - Note on a Karroo Dolerite Sill at Aliwal North. Trans. geol. Soc. S. Afr., 41, 103-108.

FRANKEL, J.J. 1942. Studies on Karroo Dolerites - (2) - Some younger intrusions of olivine basaltic dolerite. Trans. geol. Soc. S. Afr., 45, 1-26.

————. 1943. Studies on Karroo Dolerites - (3) - A multiple dolerite dyke from Zanddrift Apruit, O.F.S. Trans. geol. Soc. S. Afr., 46, 47-54.

————. 1949. Studies on Karroo Dolerites - (5) - Notes on further occurrences of younger olivine basaltic dolerites. Trans. Proc. geol. Soc. S. Afr., 52, 331-42.

————. 1969. The distribution and origin of the Effingham rock type, a dolerite derivative of intermediate composition, in Natal and Zululand, South Africa. Mem. geol. Soc. Am., No. 115, 149-73.

FULLER, R.E. 1939. Gravitative accumulation of olivine during the advance of basaltic flows. J. Geol., 47, No. 3, 303-13.

GAST, P.W. 1967. Isotope geochemistry of volcanic rocks. In HESS, H.H. and A. POLDERVAART. Eds. Basalts - The Poldervaart treatise on rocks of basaltic composition. New York, Interscience, 325-58.

————., TILTON, G.R. and C.E. HEDGE. 1964. Isotopic composition of lead and strontium from Ascension and Gough Islands. Science, N.Y., 145, No. 3637, 1181-85.

GRAY, N.H. and I.K. CRAIN. 1969. Crystal settling in sills: a model for suspension settling. Canadian J. Earth Sci., 6, No. 5, 1211-16.

GREEN, D.H. and A.E. RINGWOOD. 1967. The genesis of basaltic magmas. Contr. Miner. Petrol. (Beitr. Miner. Petrogr.), 15, 103-190.

GREENLAND, L. and J.F. LOVERING. 1966. Fractionation of fluorine, chlorine and other trace elements during differentiation of a tholeiitic magma. Geochim. cosmochim. Acta, 30, No. 9, 963-82.

GRETENER, P.E. 1969. On the mechanics of the intrusion of sills. Canadian Jl of Earth Sciences, 6, No. 6, 1415-19.

GRIMALDI, F.S., SHAPIRO, L. and M. SCHNEPFE. 1966. Determination of carbon dioxide in limestone and dolomite by acid-base titration. U.S. geol. Surv. Prof. Paper 550-B, 186-88.

GRINDLEY, G.W. 1963. The geology of the Queen Alexandra Range, Beardmore Glacier, Ross Dependency, Antarctica, with notes on the correlation of Gondwana sequences. N.Z. Jl Geol. Geophys., 6, No. 3, 307-47.

————., McGREGOR, V.R. and R.I. WALCOTT. 1964. Outline of the geology of the Nimrod—Beardmore—Axel Heiberg Glaciers region, Ross Dependency. In ADIE, R.J. ed. Antarctic geology, Amsterdam, North-Holland Publishing Co., 206-219.

GRINDLEY, G.W. and G. WARREN. 1964. Stratigraphic nomenclature and correlation in the western Ross Sea region. (In ADIE, R.J. ed. Antarctic geology. Amsterdam, North-Holland Publishing Co., 314-33.)

GROOM, G.E. 1959. Niche glaciers in Bunsow Land, Vest-spitsbergen. J. Glaciol., 3, No. 25, 369-76.

GUNN, B.M. 1962. Differentiation in Ferrar Dolerites, Antarctica. N.Z. Jl Geol. Geophys., 5, No. 5, 820-63.

————. 1963. Layered intrusions in the Ferrar Dolerites, Antarctica. Min. Soc. Am. Spec. Pap. 1, 124-33.

————. 1966. Modal and element variation in some Antarctic dolerites. Geochim. cosmochim. Acta, 30, No. 9, 881-920.

————. and G. WARREN. 1962. Geology. 4. Geology of Victoria Land between the Mawson and Mulock Glaciers, Antarctica. Scient. Rep. transantarct. Exped., No. 11, 157 pp.

HAMILTON, E.I. 1965. Distribution of some trace elements and the isotopic composition of strontium in Hawaiian lavas. Nature, Lond., 206, No. 4981, 251-53.

HAMILTON, W. 1964. Diabase sheets differentiated by liquid fractionation, Taylor Glacier region, south Victoria Land. (In ADIE, R.J. ed. Antarctic geology. Amsterdam, North-Holland Publishing Co., 442-54.)

HAMILTON, W. 1965. Diabase sheets of the Taylor Glacier region, Victoria Land, Antarctica. Prof. Pap. U.S. geol. Surv., No. 456-B, 71 pp.

————. and P.T. HAYES. 1963. Type section of the Beacon Sandstone of Antarctica. Prof. Pap. U.S. geol. Surv., No. 456-A, 18 pp.

HARRINGTON, H.J. 1958. Nomenclature of rock units in the Ross Sea region, Antarctica. Nature, Lond., 182, No. 4631, 190.

HEIER, K.S. 1960. Petrology and geochemistry of high-grade metamorphic and igneous rocks on Langøy, Northern Norway. Norges geol. Undersøk., Nr. 207, 246 pp.

————. 1964. Rubidium/strontium and strontium-87/strontium-86 ratios in deep crustal material. Nature, Lond., 202, No. 4931, 477-78.

————., COMPSTON, W. and I. McDOUGALL. 1965. Th and U concentrations and the isotopic composition of Sr in the differentiated Tasmanian dolerites. Geochim. cosmochim. Acta, 29, No. 6, 643-59.

HEIRTZLER, J.R., DICKSON, G.O., HERRON, E.M., PITMAN, W.C. and X. LE PICHON. 1968. Marine magnetic anomalies, geomagnetic field reversals and motions of the ocean floor and continents. J. geophys. Res., 73, No. 6, 2119-36.

HILL, R.L. 1970. Age of the Falla Formation, Queen Alexandra Range. In Studies in the geochronology and geology of the Transantarctic Mountains, Ohio State Univ., Inst. Polar Studies & Dept. of Geol., Laboratory for isotope geology & geochemistry, Rep. No. 5, 61-66.

HJELLE, A. and T.S. WINSNES. 1971. The sedimentary and volcanic sequence of Vestfjella, Dronning Maud Land. In ADIE, R.J. ed. Antarctic geology and geophysics. Oslo UniversitetsForlaget.

HOWARD, L.E. and J.H. SASS. 1964. Terrestrial heat flow in Australia. J. geophys. Res., 69, No. 8, 1617-26.

IRVINE, T.N. 1970. Heat transfer during solidification of layered intrusions: I. Sheets and sills. Can. Jl of Earth Sci., 7, No. 4, 1031-61.

JACOB, K. 1952. A brief summary of the stratigraphy and palaeontology of the Gondwana System, with notes on the structure of the Gondwana basins and the probable direction of movement of the Late Carboniferous ice sheets. (In Symposium sur les séries de Gondwana, 19th Int. geol. Congr., Alger, 1952, 153-74.)

JAEGER, J.C. 1964. The value of measurements of density in the study of dolerites. J. geol. Soc. Aust., 11, 133-40.

————. and G. JOPLIN. 1954. Rock magnetism and the differentiation of dolerite sill. J. geol. Soc. Aust., 2, 1-19.

JONES, B.F., HAIGH, J. and R. GREEN. 1966. The structure of the Tasmanian dolerite at Great Lake. J. geol. Soc. Aust., 13, pt. 2, 527-42.

JUCKES, L.M. 1968. The geology of Mannefallknausane and part of Vestfjella, Dronning Maud Land. British Antarctic Survey Bulletin, No. 18, 65-78.

————. 1969a. Trace-element values for dolerites from western Dronning Maud Land. British Antarctic Survey Bulletin, No. 22, 95-96.

————. 1969b. Weathering hollows in charnockite at Mannefallknausane, Dronning Maud Land. British Antarctic Survey Bulletin, No. 22, 97-98.

————. In press. The geology of north-east Heimefrontfjella, Dronning Maud Land. British Antarctic Survey Scientific Report.

KENT, L.E. and J.J. FRANKEL. 1948. Studies on Karroo dolerites - (4) - On intrusions of glass in dolerite. Trans. Proc. geol. Soc. S. Afr., 51, 179-93.

KLEEMAN, A.W. 1967. Sampling error in the chemical analysis of rocks. J. geol. Soc. Aust., 14, Pt. 1, 43-48.

KRUMBEIN, W.C. 1941. Measurement and geologic significance of shape and roundness of sedimentary particles. J. sedim. Petrol., 11, 64-72.

LAMBERT, I.B. and K.S. HEIER. 1968. Geochemical investigations of deep-seated rocks in the Australian shield. Lithos., 1, 30-53.

LA PRADE, K.E. 1970. Permian-Triassic Beacon Group of the Shackleton Glacier area, Queen Maud Range, Trans-antarctic Mountains, Antarctica. Geol. Soc. Am. Bull., 81, No. 5, 1403-10.

LEAKE, B.E., HENDRY, G.L., KEMP, A., PLANT, A.G., HARVEY, P.K., WILSON, J.R., COATS, J.S., AUCOTT, J.W., LÜNEL, T. and R.J. HOWARTH. 1969. The chemical analysis of rock powders by automatic X-ray fluorescence. Chem. geol., 5, No. 1, 7-87.

LE MAITRE, R.W. 1962. Petrology of volcanic rocks, Gough Island, South Atlantic. Geol. Soc. Am. Bull., 73, No. 11, 1309-40.

LE PICHON, X. 1968. Sea-floor spreading and continental drift. J. geophys. Res., 73, No. 12, 3661-97.

————. and J.R. HEIRTZLER. 1968. Magnetic anomalies in the Indian Ocean and sea-floor spreading. J. geophys. Res., 73, No. 6, 2101-17.

LESSING, P. and E.J. CATANZARO. 1964. Sr^{87}/Sr^{86} ratios in Hawaiian lavas. J. geophys. Res., 69, No. 8, 1599-1601.

LIGHTFOOT, B. 1938. Notes on the south-eastern part of Southern Rhodesia. Trans. geol. Soc. S. Afr., 41, 193-98.

LINDSAY, D.C. and D. BROOK. 1971. Lichens from the Theron Mountains. British Antarctic Survey Bulletin, No. 25.

LOMBAARD, B.V. 1939. Dykes in the Transvaal. Proc. geol. Soc. S. Afr., 42, xxvii-xlii.

————. 1952. Karroo dolerites and lavas. Trans. Proc. geol. Soc. S. Afr., 55, 175-98.

LONG, W.E. 1964. The stratigraphy of the Horlick Mountains. (In ADIE, R.J. ed. Antarctic geology. Amsterdam, North-Holland Publishing Company, 352-63.)

MACDONALD, G.A. 1949. Hawaiian petrographic province. Bull. geol. Soc. Am., 60, No. 10, 1541-95.

————. and T. KATSURA. 1964. Chemical composition of Hawaiian lavas. J. Petrology, 5, Pt. 1, 82-133.

MANSON, V. 1967. Geochemistry of basaltic rocks: major elements. In HESS, H.H. and A. POLDERVAART. (Eds.) Basalts. The Poldervaart treatise on rocks of basaltic composition. 1, New York, John Wiley & Sons, Inc. 215-70.

MANTON, W.I. 1968. The origin of associated basic and acid rocks in the Lebombo-Nuanetsi igneous province, Southern Africa, as implied by strontium isotopes. J. Petrology, 9, Pt. 1, 23-39.

MATZ, D.B., PINET, P.R. and M.O. HAYES. 1971. Stratigraphy & petrology of the Beacon Group, Southern Victoria Land, Antarctica. In ADIE, R.J. ed. Antarctic geology and geophysics. Oslo UniversitetsForlaget.

McDOUGALL, I. 1961. Determination of the age of a basic igneous intrusion by the potassium-argon method. Nature, Lond., 190, No. 4782, 1184-86.

————. 1962. Differentiation of the Tasmanian dolerites—Red Hill dolerite-granophyre association. Geol. Soc. Am. Bull., 73, No. 3, 279-316.

————. 1963. Potassium-argon age measurements on dolerites from Antarctica and South Africa. J. geophys. Res., 68, No. 5, 1535-45.

————. 1964. Differentiation of the Great Lake dolerite sheet, Tasmania. J. geol. Soc. Aust., 11, 107-32.

————. and W. COMPSTON. 1965. Strontium isotope composition and potassium-rubidium ratios in some rocks from Réunion and Rodriguez, Indian Ocean. Nature, Lond., 207, No. 4994, 252-53.

————. and J.F. LOVERING. 1963. Fractionation of chromium, nickel, cobalt and copper in a differentiated dolerite-granophyre sequence at Red Hill, Tasmania. J. geol. Soc. Aust., 10, 325-38.

————. and M.W. McELHINNY. 1970. The Rajmahal traps of India — K-Ar ages and palaeomagnetism. Earth & planet. Sci. Lett., 9, No. 4, 371-78.

————. and N.R. RÜEGG. 1966. Potassium-argon dates on the Serra Geral Formation of South America. Geochim. cosmochim. Acta, 30, No. 2, 191-95.

McGREGOR, V.R. 1965. Notes on the geology of the area between the heads of the Beardmore and Shackleton Glaciers, Antarctica. N.Z. Jl Geol. Geophys., 8, No. 2, 278-91.

MELFI, A.J. 1967. Potassium-argon ages for core samples of basaltic rocks from Southern Brazil. Geochim. cosmochim. Acta, 31, No. 6, 1079-89.

MOORE, A. 1965. The north Gap Dyke of the Transkei. Trans. Proc. geol. Soc. S. Afr., 68, 89-119.

MOUNTAIN, E.D. 1935. Syntectic phenomena in Karroo dolerite at Coedmore quarries, Durban. Trans. geol. Soc. S. Afr., 38, 93-112.

————. 1943. The dykes of the Transkei Gaps. Trans. geol. Soc. S. Afr., 46, 55-74.

————. 1958. Acidification of dolerite at Coedmore quarries, Durban. Trans. Proc. geol. Soc. S. Afr., 61, 209-220.

————. 1960. Felsic material in Karroo dolerite. Trans. Proc. geol. Soc. S. Afr., 63, 137-52.

MUDGE, M.R. 1968. Depth control of some concordant intrusions. Geol. Soc. Am. Bull., 79, No. 3, 315-32.

MURATA, K.J. and D.H. RICHTER. 1961. Magmatic differentiation in the Uwekahuna laccolith, Kilauea caldera, Hawaii. J. Petrology, 2, Pt. 3, 424-37.

NEETHLING, D.C. 1971. Comparative geochemistry of Proterozoic and Mesozoic tholeiitic intrusives of Western Dronning Maud Land, Antarctica. In ADIE, R.J. ed. Antarctic geology and geophysics, Oslo, UniversitetsForlaget.

NOCKOLDS, S.R. and R.S. ALLEN. 1956. The geochemistry of some igneous rock series, Part III. Geochim. cosmochim. Acta, 9, Nos. 1-2, 34-77.

O'HARA, M.J. 1965. Primary magmas and the origin of basalts. Scot. Jl Geol., 1, Pt. 1, 19-40.

OXBURGH, E.R. and D.L. TURCOTTE. 1968. Mid-ocean ridges and geotherm distribution during mantle convection. J. geophys. Res., 73, No. 8, 2643-61.

PANKHURST, R.J. 1969. Strontium isotope studies related to petrogenesis in the Caledonian basic igneous province of NE Scotland. J. Petrology, 10, Pt. 1, 115-43.

PENFIELD, S.L. 1894. On some methods for the determination of water. Am. J. Sci., 48, No. 283, 30-37.

PEWÉ, T.L. 1960. Multiple glaciation in the McMurdo Sound region, Antarctica. A progress report. J. Geol., 68, No. 5, 498-514.

PICCIOTTO, E. and A. COPPEZ. 1962. Bibliographie des mesures d'ages absolus en Antarctique. Univ. Lib. de Bruxelles, 33 pp.

PITMAN, W.C., HERRON, E.M. and J.R. HEIRTZLER. 1968. Magnetic anomalies in the Pacific and sea floor spreading. J. geophys. Res., 73, No. 6, 2069-85.

PLUMSTEAD, E.P. 1962. Geology. 2. Fossil floras of Antarctica (with an appendix on Antarctic fossil wood, by R. Kräusel). Scient. Rep. transantarct. Exped., No. 9, 154 pp.

————. 1964. Palaeobotany of Antarctica. (In ADIE, R.J. ed. Antarctic geology. Amsterdam, North-Holland Publishing Company, 637-54.)

————. In press. A new assemblage of plant fossils from Milorgfjella, Dronning Maud Land. British Antarctic Survey Bulletin

REX, D.C. 1967. Age of a dolerite from Dronning Maud Land. British Antarctic Survey Bulletin, No. 11, 101.

————. 1971. Potassium-Argon age determinations on volcanic and associated rocks from the Antarctic Peninsula and Dronning Maud Land. In ADIE, R.J. ed. Antarctic geology and geophysics. Oslo, Universitets-Forlaget.

RILEY, J.P. 1958. Simultaneous determination of water and carbon dioxide in rocks and minerals. Anal. chim. Acta, 19, 413-28.

SCHMIDT, D.L., DOVER, J.H., FORD, A.B. and R.D. BROWN. 1964. Geology of the Patuxent Mountains. (In ADIE, R.J. ed. Antarctic geology. Amsterdam, North-Holland Publishing Company, 276-83.)

SCHOLTZ, D.L. 1936. The magmatic nickeliferous ore deposits of East Griqualand and Pondoland. Trans. geol. Soc. S. Afr., 39, 81-210.

SCHOPF, J.M. 1970. Gondwana palaeobotany. Antarct. Jl U.S., 5, No. 3, 62-66.

————. and W.E. LONG. 1960. Antarctic coal geology. (Abstract) Geol. Soc. Am. Bull., 71, No. 12, 1967.

SHAW, H.R. 1969. Rheology of basalt in the melting range. J. Petrology, 10, No. 3, 510-35.

SIEDNER, G. and J. MILLER. 1968. K-Ar determinations on basaltic rocks from South West Africa and their bearing on continental drift. Earth & planet. Sci. Lett., 4, No. , 451-58.

SIMPSON, E.S.W. 1954. On the graphical representation of differentiation trends in igneous rocks. Geol. Mag., 91, No. 3, 238-44.

SKINNER, D.N.B. 1965. Petrographic criteria of the rock units between the Byrd and Starshot Glaciers, southern Victoria Land, Antarctica. N.Z. Jl Geol. Geophys., 8, No. 2, 292-303.

SKINNER, D.N.B. and J. RICKER. 1968. The geology of the region between the Mawson and Priestley Glaciers, north Victoria Land, Antarctica. Part II. Upper Palaeozoic to Quaternary geology. N.Z. Jl Geol. Geophys., 11, No. 4, 1041-75.

SMITH, A.G. and A. HALLAM. 1970. The fit of the southern continents. Nature, Lond., 225, No. 5228, 139-44.

SPOONER, C.M. and H.W. FAIRBAIRN. 1970. Strontium 87/ Strontium 86 initial ratios in pyroxene granulite terranes. J. geophys. Res., 75, No. 32, 6706-13.

STEPHENSON, P.J. 1960. Geology of the Weddell Sea sector, Antarctica. Un. Geod. et Geophys. Int., Monographie, No. 5, 80.

————. 1961. Patterned ground in Antarctica. J. Glaciol., 3, No. 30, 1163-64.

————. 1966. Geology. 1. Theron Mountains, Shackleton Range and Whichaway Nunataks (with a section on the palaeomagnetism of the dolerite intrusions, by D.J. Blundell). Scient. Rep. transantarct. Exped., No. 8, 79 pp.

STEWART, D. 1934. The petrography of some Antarctic rocks. Am. Miner., 19, No. 4, 150-60.

STOCKLEY, G.M. 1940. The geology of Basutoland. Geol. Mag., 77, No. 6, 444-60.

TATSUMOTO, M., HEDGE, C.E. and A.E.J. ENGEL. 1965. Potassium, Rubidium, Strontium, Thorium, Uranium and the ratio of Strontium-87 to Strontium-86 in oceanic tholeiitic basalts. Science, N.Y., 150, No. 3698, 886-88.

TILLEY, C.E. 1960. Differentiation of Hawaiian basalts: some variants in lava suites of dated Kilauean eruptions. J. Petrology, 1, Pt. 1, 47-55.

VANDOROS, P., RÜEGG, N.R. and U. CORDANI. 1966. On Potassium-argon age measurements of basaltic rocks from Southern Brazil. Earth & planet. Sci. Lett., 1, No. , 449-52.

VIALOV, O.S. 1962. Some Problematica of the Beacon Sandstone from Beacon Height West, Antarctica. N.Z. Jl Geol. Geophys., 5, No. 5, 718-32.

WADELL, H. 1932. Volume, shape and roundness of rock particles. J. Geol., 40, No. 5, 443-51.

WAGER, L.R. and G.M. BROWN. 1968. Layered igneous rocks. Edinburgh and London, Oliver & Boyd. 588 pp.

————., ————. and W.J. WADSWORTH. 1960. Types of igneous cumulates. J. Petrology, 1, Pt. 1, 73-85.

————. and W.A. DEER. 1939. Geological investigations in east Greenland. Part III. The petrology of the Skaergaard Intrusion, Kangerdlugssuaq, east Greenland. Medd. om Grøn., 105, No. 4, 1-352.

WALKER, F. 1940. Differentiation of the Palisade diabase, New Jersey. Bull. geol. Soc. Am., 51, No. 7, 1059-1106.

————. 1951. A volcanic vent near Lambert's Bay (Cape Province). Trans. Proc. geol. Soc. S. Afr., 54, 1-7.

————. 1953. The pegmatitic differentiates of basic sheets. Am. J. Sci., 251, No. 1, 41-60.

————. 1956. The dolerites of the Cape Peninsula. Trans. Proc. geol. Soc. S. Afr., 59, 77-92.

————. 1957. Ophitic texture and basaltic crystallisation. J. Geol., 65, No. 1, 1-14.

————. and A. POLDERVAART. 1941. The Hangnest Dolerite Sill, S.A. Geol. Mag., 78, No. 6, 429-50.

————. and ————. 1942. The petrology of the Karroo Dolerites between Sutherland and Middelburg, C.P. Trans. geol. Soc. S. Afr., 45, 55-64.

————. and ————. 1949. Karroo dolerites of the Union of South Africa. Bull. geol. Soc. Am., 60, No. 4, 591-706.

WALKER, K.R. 1969. The Palisades Sill, New Jersey: a reinvestigation. Spec. Pap. geol. Soc. Am., No. 111, 178 pp.

WASHBURN, A.L. 1956. Classification of patterned ground and review of suggested origins. Bull. geol. Soc. Am., 67, No. 7, 823-66.

WEBB, P.N. 1963. Geological investigations in southern Victoria Land, Antarctica. Part 4. Beacon Group of the Wright Valley and Taylor Glacier region. N.Z. Jl Geol. Geophys., 6, No. 3, 362-87.

WENTWORTH, C.K. and H. WINCHELL. 1947. Koolau Basalt Series, Oahu, Hawaii. Bull. geol. Soc. Am., 58, No. 1, 49-78.

WILLIAMS, P.L. 1969. Petrology of upper Precambrian and Palaeozoic sandstones in the Pensacola Mountains, Antarctica. J. sedim. Petrol., 39, 1455-65.

WORNHAM, C.M. 1969. Ice-movement measurements in the Theron Mountains. British Antarctic Survey Bulletin, No. 21, 45-50.

WORSFOLD, R.J. 1967. Physiography and glacial geomorphology of Heimefrontfjella, Dronning Maud Land. British Antarctic Survey Bulletin, No. 11, 49-58.

————. In press. The geology of southern Heimefrontfjella, Dronning Maud Land. British Antarctic Survey Scientific Report.

YODER, H.S. and C.E. TILLEY. 1962. Origin of basalt magmas: an experimental study of natural and synthetic rock systems. J. Petrology, 3, Pt. 3, 342-532.

APPENDIX I

DESCRIPTION OF ANALYSED SPECIMENS FROM JURASSIC DOLERITE INTRUSIONS IN THE THERON MOUNTAINS

Brief descriptions of the rock type and locality of specimens analysed are given with the analyses in Tables IX-XVII. This appendix lists the analyses as they appear in the tables and gives very approximate altitudes, latitudes and longitudes together with a slightly more detailed description of the locality and petrography of specimens.

TABLE IX. Scarp-capping sill

Sill at least 200 m. thick which caps the escarpment for much of its length from Tailend Nunatak in the north-east to the unnamed southern glacier and which appears to cross the latter as the thick wedging sill of Coalseam Cliffs.

3710 Z.469.3 Alt. 740 m., lat. 78°58'S., long. 27°39'W. Near top of sill; rock ridge parallel to and 3 km. south-east of the escarpment just south-west of Goldsmith Glacier.
Highly altered, fine-grained variolitic quartz-dolerite; consists of plagioclase, clinopyroxene, iron ore, micropegmatite, chloritic and biotitic alteration products and some apparently secondary quartz.

10651
10652 see Appendix II.
10653

3654 Z.455.1 Alt. 740 m., lat. 79°09'S., long. 28°26'W. Upper third of sill; cliff outcrop on southern flank of a small tributary of the unnamed southern glacier; bottom of cliffs.
Coarse-grained, ophitic granophyric quartz-dolerite; consists of plagioclase (An_{60}, marginal alkali-feldspar), pigeonite and augite (altered to hornblende and biotite), micropegmatite, iron ore and fayalite (replaced by iddingsite or chlorophaeite) with accessory apatite. Modal analysis Table IV.

3670 Z.468.1 Alt. 640 m., lat. 78°58'S., long. 27°30'W. Near middle of sill; small cliff outcrop on south-western flank of Goldsmith Glacier; bottom of cliffs.
Coarse-grained granophyric quartz-dolerite; consists of plagioclase (An_{60}), clinopyroxene (altered to hornblende, biotite and minute granular fayalite), micropegmatite and iron ore with accessory fayalite, biotite and apatite. Modal analysis Table IV.

3686 Z.484.1 Alt. 840 m., lat. 78°47'S., long. 26°49'W. Upper third of sill; rock ridge at Tailend Nunatak; about two-thirds of the way up the ridge.
Coarse-grained, subophitic granophyric quartz-dolerite; consists of plagioclase (An_{60}), clino-pyroxene, micropegmatite and iron ore with accessory fayalite and apatite and hornblende, biotite and chlorite alteration. Modal analysis Table IV.

3705 Z.485.1 Alt. 620 m., lat. 78°49'S., long. 27°07'W. 100-150 m. below upper contact; large cliff in escarpment between Tailend Nunatak and Goldsmith Glacier; bottom of cliffs.
Coarse-grained granophyric quartz-dolerite; consists of plagioclase (An_{56}), clinopyroxene, micropegmatite

and iron ore with accessory hornblende, biotite, fayalite and apatite. Modal analysis Table IV.

3682 Z.486.1 Alt. 620 m., lat. 78°51'S., long. 27°10'W. 100-150 m. below upper contact; rock window in ice cliffs of escarpment south-west of station Z.485; bottom of cliffs.
Coarse-grained, subophitic granophyric quartz-dolerite; consists of plagioclase (An_{45}, marginal alkali-feldspar), clinopyroxene (altered to hornblende and biotite), micropegmatite and iron ore with accessory hornblende, fayalite (altered to iddingsite), apatite and zircon. Modal analysis Table IV.

3700 Z.487.1 Alt. 570 m., lat. 78°53'S., long. 27°24'W. 100-150 m. below upper contact; long cliff outcrop of escarpment immediately north-east of the mouth of Goldsmith Glacier; bottom of cliffs.
Coarse-grained, ophitic granophyric quartz-dolerite; consists of plagioclase (An_{40-50}, marginal alkali-feldspar), pinkish clinopyroxene (altered to hornblende, biotite and chlorite), micropegmatite, hornblende, iron ore and accessory apatite and zircon. Modal analysis Table IV.

3713 Z.508.1 Alt. 605 m., lat. 78°56'S., long. 27°44'W. About 50 m. above lower contact; rock peak rising from ice cliffs of escarpment just south-west of the mouth of Goldsmith Glacier; top of outcrop.
Coarse-grained granophyric quartz-dolerite; consists of plagioclase (An_{52}), clinopyroxene, micropegmatite and iron ore with accessory hornblende, biotite, fayalite and apatite. Modal analysis Table IV.

3695 Z.478.1 Alt. 485 m., lat. 79°09'S., long. 28°46'W. About 6 m. above lower contact; Coalseam Cliffs below point 2600; thick wedging sill.
Subophitic granophyric quartz-dolerite; consists of plagioclase (An_{55}), clinopyroxene, iron ore, hornblende, biotite, chlorite and micropegmatite. Modal analysis Table IV.

3678 Z.483.5 Alt. 620 m., lat. 79°02'S., long. 28°24'W. About 6 m. above lower contact; north-eastern end of Marø Cliffs.
Medium-grained subophitic altered granophyric quartz-dolerite; consists of plagioclase (An_{45-55}), clinopyroxene, hornblende, iron ore, biotite, chlorite, micropegmatite and apatite. Modal analysis Table IV.

3714 Z.498.1 Alt. 660 m., lat. 78°59'S., long. 28°08'W. About 1 m. above lower contact; higher part of south-western end of Lenton Bluff.
Highly altered fine-grained subvariolitic quartz-dolerite; consists of plagioclase, clinopyroxene, (?) olivine and hornblende—biotite—chlorite alteration products with some secondary quartz and calcite.

3715 Z.497.1 Alt. 601 m., lat. 79°02'S., long. 28°18'W. About 1 m. above lower contact; cliff outcrop on western margin of Jeffries Glacier.
Altered medium-grained quartz-dolerite; consists of plagioclase (An_{60}), clinopyroxene, brown and green alteration products and a fine-grained felsic mesostasis of poorly crystallized feldspar with abundant viridite and iron ore.

3716 Z.497.2 Alt. 600 m., lat. 79°02'S., long. 28°18'W. Lower contact; cliff outcrop on western margin of Jeffries Glacier.
Spherulitic porphyritic dolerite; microphenocrysts of plagioclase (An_{58}) and pigeonite in a glassy groundmass with plagioclase and pyroxene microlites. Modal analysis Table III.

3694 Z.490.1 Alt. 540 m., lat. 78°58'S., long. 27°54'W. Lower contact; largest cliff rising from ice cliff of escarpment between Goldsmith Glacier and Lenton Bluff.
Vitrophyric chilled dolerite; microphenocrysts of plagioclase (An_{55-60}) and pigeonite in a groundmass of devitrified glass with a pseudohexagonal cooling-contraction structure marked by secondary biotite; some secondary quartz. Modal analysis Table III.

3688 Z.478.2 Alt. 480 m., lat. 79°09'S., long. 28°46'W. Lower contact; Coalseam Cliffs below point 2600; thick wedging sill.
Vitrophyric chilled dolerite; microphenocrysts of plagioclase (An_{60-65}) and pigeonite in a hemicrystalline groundmass of partly devitrified glass with plagioclase and pyroxene microlites and minute granular iron ore; some secondary biotite and chlorite. Modal analysis Table III.

TABLE X. First phase of intrusion in Marø Cliffs

Sill 10-30 m. thick which intrudes the sediments beneath the scarp-capping sill and which is intruded by the third-phase sill and seems to be cut by the apparent branch sill (second phase) of the scarp-capping sill.

3697 Z.481.9 Alt. 510 m., lat. 79°04'S., long. 28°32'W. About 0.5 m. below upper contact; south-western end of Marø Cliffs.
Fine- to medium-grained, slightly altered, slightly porphyritic dolerite; (?) phenocrysts of plagioclase (An_{60}) in variolitic groundmass of skeletal plagioclase (An_{55-60}) and augite with intersertal devitrified glass dotted with iron ore; hornblende—biotite—chlorite alteration.

3667 Z.483.7 Alt. 520 m., lat. 79°02'S., long. 28°24'W. About 0.8 m. above lower contact; north-eastern end of Marø Cliffs.
Porphyritic, fine- to medium-grained, variolitic dolerite; pseudomorphs of iron ore, calcite, bowlingite and talc probably after olivine in a variolitic groundmass of plagioclase (An_{62}) and pigeonite with intersertal devitrified glass and iron ore.

3737 Z.480.1b Alt. 350 m., lat. 79°06'S., long. 28°31'W. Upper half of sill; contact with third-phase sill; cliffs beneath point 3300, on eastern flank of unnamed southern glacier.
Altered coarse-grained dolerite; consists dominantly of plagioclase (An_{65}) and pigeonite (biotite—chlorite alteration) and a poorly crystallized felsic mesostasis with some quartz (probably secondary), apatite, iron ore and viridite. Modal analysis Table IV.

3673 Z.480.3 Alt. 335 m., lat. 79°06'S., long. 28°31'W. Lower half of sill; about 5 m. below contact with third-phase sill; cliffs beneath point 3300, on eastern flank of unnamed southern glacier.

Altered coarse-grained dolerite; consists of plagioclase, clinopyroxene and iron ore with a fine-grained felsic mesostasis and chloritic and other alteration.

3738 Z.502.1 Alt. 490 m., lat. 79°02'S., long. 28°26'W. Near top of sill; Marø Cliffs just north-east of the central ice fall.
Slightly altered, medium-grained subvariolitic dolerite; consists dominantly of plagioclase (An_{66}), pigeonite and a poorly crystallized feldspathic mesostasis with apatite needles and rod-like iron ore.

Related minor sills

Minor sills in Marø Cliffs and alongside Jeffries Glacier which petrographically and chemically appear to be related to the first phase of intrusion in Marø Cliffs.

3702 Z.483.4 Alt. 345 m., lat. 79°02'S., long. 28°24'W. Sill of unknown thickness (base not exposed) forming base of cliffs a few metres below the apparent branch sill of the scarp-capping sill; upper contact of sill; north-eastern end of Marø Cliffs.
Fine- to medium-grained subvariolitic dolerite; consists dominantly of plagioclase (An_{60}) and pigeonite with small areas of bowlingite and magnetite possibly after olivine and an intersertal mesostasis of poorly crystallized feldspathic material with rods of iron ore, secondary bowlingite, occasional biotite and some quartz.

3741 Z.497.7 Alt. 520 m., lat. 79°02'S., long. 28°18'W. Thin sill intruding sediments beneath scarp-capping sill; middle of sill; cliff outcrop on western margin of Jeffries Glacier.

Slightly altered, slightly porphyritic, variolitic, hemicrystalline dolerite; phenocrysts are pseudomorphs after (?) olivine or pyroxene in a groundmass of plagioclase, clinopyroxene, iron ore and intersertal glass.

TABLE XI. Third phase of intrusion in Marø Cliffs

Sill 5-15 m. thick which intrudes the first-phase sill and seems to cut through the apparent branch sill (second phase) of the scarp-capping sill.

3736 Z.480.1a Alt. 350 m., lat. 79°06'S., long. 28°31'W. Upper contact, with first-phase sill; cliffs beneath point 3300 on eastern flank of unnamed southern glacier.
Vitrophyric chilled olivine-dolerite; phenocrysts of plagioclase (An_{67}) and olivine in a glassy groundmass grading to minute plagioclase, pyroxene, (?) olivine, iron ore and glass. Modal analysis Table III.

3701 Z.481.11 Alt. 500 m., lat. 79°04'S., long. 28°32'W. Near middle of sill; south-western end of Marø Cliffs. Altered, medium- to coarse-grained, ophitic olivine-dolerite; consists dominantly of plagioclase (An_{70}), augite, olivine (altered to magnetite and talc with some bowlingite) and iron ore with a poorly crystallized, feldspathic, highly altered mesostasis including some quartz (probably secondary). Modal analysis Table IV.

3706 Z.483.6 Alt. 540 m., lat. 79°02'S., long. 28°31'W. Near middle of sill; north-eastern end of Marø Cliffs. Altered, coarse-grained, ophitic olivine-dolerite; consists dominantly of plagioclase (An_{75}), pigeonite

augite, olivine (altered to magnetite, bowlingite and talc) and iron ore; large areas of unidentified green and brown alteration products with some secondary quartz. Modal analysis Table IV.

3690 Z.480.2 Alt. 340 m., lat. 79°06'S., long. 28°31'W. Just above lower contact, with first-phase sill; cliffs beneath point 3300, on eastern flank of unnamed southern glacier.
Vitrophyric chilled olivine-dolerite; phenocrysts of plagioclase (An_{62}), olivine and pigeonite in a cryptocrystalline groundmass of plagioclase, pyroxene and iron ore grading to glass with sporadic plagioclase microlites. Modal analysis Table III.

Related minor sills

Minor sills alongside Jeffries Glacier and in Lenton Bluff which petrographically and chemically appear to be related to the third phase of intrusion in Marø Cliffs.

3739 Z.497.4 Alt. 580 m., lat. 79°02'S., long. 28°18'W. Uppermost thin sill (4 m. thick) intruding the sediments beneath the scarp-capping sill; middle of sill; cliff outcrop on western flank of Jeffries Glacier.
Slightly altered, fine- to medium-grained, ophitic olivine-dolerite; consists dominantly of plagioclase (An_{60}), pink augite, olivine and iron ore with intersertal altered cryptocrystalline mesostasis.

3740 Z.497.6 Alt. 550 m., lat. 79°02'S., long. 28°18'W. Thin sill (<5 m. thick) intruding sediments beneath scarp-capping sill; middle of sill; cliff outcrop on western flank of Jeffries Glacier.
Highly altered, medium- to coarse-grained olivine-dolerite; consists dominantly of plagioclase,

pinkish augite, pseudomorphs of magnetite and viridite (possibly after olivine) and iron ore, with an altered cryptocrystalline mesostasis.

3703 Z.498.7 Alt. 570 m., lat. 78°59'S., long. 28°08'W. Uppermost thin sill (3 m. thick) intruding sediments beneath the scarp-capping sill; middle of sill; higher part of south-western end of Lenton Bluff. Highly altered, medium-grained subophitic dolerite; consists dominantly of plagioclase (An_{55-60}, sericitized), pink augite and pigeonite (altered to biotite) and iron ore with small amounts of interstitial poorly crystallized material.

TABLE XII. Apparent branch sill of the scarp-capping sill

Sill 20-30 m. thick which appears to branch from the scarp-capping sill, to cut through the first-phase sill of Marø Cliffs and to be cut in turn by the third-phase sill; it thus forms the second phase of intrusion in Marø Cliffs.

3681 Z.483.8 Alt. 380 m., lat. 79°02'S., long. 28°24'W. About 1.3 m. below upper contact; north-eastern end of Marø Cliffs.
Altered, medium-grained, subophitic quartz-dolerite; consists of plagioclase (An_{55-60}, sericitized), pink augite (altered to hornblende), iron ore and micropegmatite with accessory apatite, hornblende and biotite and chloritic alteration products.

3680 Z.483.9 Alt. 370 m., lat. 79°02'S., long. 28°24'W. Lower half of sill; north-eastern end of Marø Cliffs. Altered, medium-grained glomeroporphyritic dolerite; glomeroporphs of plagioclase (An_{58}) in groundmass of plagioclase (An_{40-50}), pinkish augite and pigeonite (altered to hornblende), olivine (? fayalitic,

altered to iddingsite), iron ore and micropegmatite with apatite, biotite and viridite. Modal analysis Table IV.

Basal sill of Lenton Bluff

Sill 20-30 m. thick which forms the base of the cliffs of Lenton Bluff for much of their length; it seems to be the continuation across Jeffries Glacier of the apparent branch sill of the scarp-capping sill and is cut by the younger sills and dykes of Lenton Bluff.

3672 Z.471.16 Alt. 416 m., lat. 79°00'S., long. 28°12'W. Upper part of sill; about 0.8 m. above contact of younger transgressive sill; small outcrop at south-western end of Lenton Bluff.
Altered, medium- to coarse-grained granular dolerite; (?) xenocrysts of plagioclase in groundmass of plagioclase, clinopyroxene, micropegmatite, iron ore and chloritic alteration products.

3675 Z.472.9 Alt. 400 m., lat. 78°59'S., long. 28°09'W. Lower half of sill; lower contact of largest xenolith; lower parts of south-western end of Lenton Bluff.
Porphyritic chilled olivine-dolerite; phenocrysts of plagioclase (An_{60-72}), pigeonite and olivine (pseudomorphed by magnetite and serpentine) in fine-grained groundmass of plagioclase, pyroxene, chlorite and iron ore with some secondary biotite. Modal analysis Table III.

3669 Z.472.11 Alt. 395 m., lat. 78°59'S., long. 28°09'W. Lower third of sill; about 5 m. below largest xenolith; lower parts of south-western end of Lenton Bluff.

Slightly altered, fine-grained olivine-dolerite; consists of plagioclase (An_{63}), pinkish augite and pigeonite (altered to hornblende and biotite), and olivine (? fayalitic, altered to iddingsite) in poorly crystallized groundmass of plagioclase, pyroxene, hornblende, biotite and chlorite with interstitial micropegmatite and apatite.

3663 Z.472.4 Alt. 390 m., lat. 78°59'S., long. 28°09'W. Near base of sill; about 10 m. below largest xenolith; lower parts of south-western end of Lenton Bluff.
Altered, medium-grained olivine-dolerite; consists of plagioclase (An_{62}), augite and pigeonite (altered to hornblende and biotite), occasional small olivines (largely pseudomorphed by magnetite and serpentine) and iron ore with interstitial micropegmatite and apatite and some secondary quartz.

3722 Z.471.11 Alt. 391 m., lat. 79°00'S., long. 28°12'W. Lower contact; contact of rheomorphic vein; small outcrop at south-western end of Lenton Bluff.
Altered fine- to medium-grained dolerite; consists of plagioclase (altered), iron ore, chlorite, viridite and minor sphene.

3723 Z.471.10 Alt. 390 m., lat. 79°00'S., long. 28°12'W. Lower contact; small outcrop at south-western end of Lenton Bluff.
Vitrophyric chilled dolerite; phenocrysts of plagioclase (An_{60}), pigeonite and pseudomorphs after olivine in a cryptocrystalline glassy groundmass. Modal analysis Table III.

3720 Z.472.3 Alt. 411 m., lat. 78°59'S., long. 28°09'W. Upper half of sill; just above largest xenolith; near chlorite—tremolite veins; lower parts of south-western end of Lenton Bluff.
Hydrothermally altered porphyritic chilled dolerite; phenocrysts of plagioclase (albitized) in groundmass replaced by chlorite and tremolite with iron ore.

3721 Z.472.13 Alt. 397 m., lat. 78°59'S., long. 28°09'W. Lower half of sill; just above small xenolith; near andradite—calcite veins; lower parts of south-western end of Lenton Bluff.
Hydrothermally altered porphyritic chilled dolerite; epidotized phenocrysts of plagioclase in fine-grained groundmass of plagioclase, iron ore and viridite (? epidote and chlorite).

TABLE XIII. Younger sills and dykes of Lenton Bluff

Sill about 5 m. thick which cuts through the basal sill of Lenton Bluff to intrude the sediments above it.

3661 Z.471.14 Alt. 415 m., lat. 79°00'S., long. 28°12'W. Upper contact; in contact with basal sill; small outcrop at south-western end of Lenton Bluff.
Altered, porphyritic chilled olivine-dolerite; phenocrysts of plagioclase (An_{60}) and pseudomorphs after (?) olivine in groundmass of plagioclase and clinopyroxene with some secondary calcite. Modal analysis Table III.

3665 Z.471.15 Alt. 414 m., lat. 79°00'S., long. 28°12'W. About 1 m. below upper contact; small outcrop at south-western end of Lenton Bluff.
Altered, fine- to medium-grained, intersertal olivine-dolerite; consists of plagioclase, pseudomorphs

after (?) olivine, clinopyroxene (+ pseudomorphs), iron ore and a devitrified glassy mesostasis. Modal analysis Table IV.

Dyke about 1.2 m. wide which intrudes the sediments between the scarp-capping sill and the basal sill of Lenton Bluff.

3724 Z.498.3 Alt. 640 m., lat. 78°59'S., long. 28°08'W. About middle of dyke; higher parts of south-western end of Lenton Bluff.
Fine-grained, intergranular to intersertal dolerite; consists of plagioclase (An_{68-72}), clinopyroxene, pseudomorphs after (?) olivine or pyroxene, intersertal devitrified glass and iron ore with hornblende, biotite and chlorite alteration. Modal analysis Table IV.

Dyke about 6 m. wide which intrudes the sediments between the scarp-capping sill and the basal sill of Lenton Bluff.

3725 Z.498.5f Alt. 600 m., lat. 78°59'S., long. 28°08'W. Contact of dyke; higher parts of south-western end of Lenton Bluff; fresh sample.
Slightly altered, porphyritic intersertal dolerite; pseudomorphs after (?) olivine or pyroxene in groundmass of plagioclase, clinopyroxene and alteration products with some secondary haematite.

3726 Z.498.5a Alt. 600 m., lat. 78°59'S., long. 28°08'W. Same specimen as 3725; weathered and altered sample.
Altered fine-grained subvariolitic dolerite; consists dominantly of plagioclase, alteration products and iron ore with some secondary haematite.

3727 Z.498.6 Alt. 600 m., lat. 78°59'S., long. 28°08'W. Middle of dyke; near zone of calcite mineralization; higher parts of south-western end of Lenton Bluff. Fine-grained variolitic dolerite; consists of plagioclase (An_{60}) laths separated by plagioclase microlites, radiating fibrous clinopyroxene, iron ore, chlorite, tremolite and secondary haematite.

Sill about 3 m. thick which intrudes the sediments between the scarp-capping sill and the basal sill of Lenton Bluff; this is the middle one of three minor sills in this part of the cliffs.

3728 Z.498.8 Alt. 500 m., lat. 78°59'S., long. 28°08'W. Middle of sill; higher parts of south-western end of Lenton Bluff.
Fine-grained variolitic dolerite; consists dominantly of plagioclase (An_{45-70}), clinopyroxene, intersertal glass and unidentified (?) chloritic alteration products liberally dotted with iron ore.

Sill 3-5 m. thick which intrudes the sediments between the scarp-capping sill and the basal sill of Lenton Bluff; this is the lowest of the three sills.

3729 Z.498.9f Alt. 450 m., lat. 78°59'S., long. 28°08'W. Middle of sill; higher parts of south-western end of Lenton Bluff; fresh sample.
Slightly altered, intersertal subophitic dolerite; consists of plagioclase ($?An_{75}$), clinopyroxene and intersertal glass with iron ore and minor alteration products.

3730 Z.498.9a Alt. 450 m., lat. 78°59'S., long. 28°08'W. Same specimen as 3729; weathered and altered sample.
Altered, intersertal subophitic dolerite; similar to

Z.498.9f except that alteration products are more abundant and groundmass possibly includes secondary quartz.

Dyke 2-3 m. wide which intrudes the sediments beneath the basal sill of Lenton Bluff and may intrude the latter.

3664 Z.471.13a Alt. 385 m., lat. 79°00'S., long. 28°12'W. Contact of dyke; small outcrop at south-western end of Lenton Bluff.
Altered, porphyritic chilled olivine-dolerite; chloritic pseudomorphs after (?) olivine in subvariolitic groundmass of plagioclase (An_{55}), clinopyroxene, viridite and iron ore with secondary haematite.

3660 Z.471.13b Alt. 385 m., lat. 79°00'S., long. 28°12'W. About 0.2 m. from contact; small outcrop at south-western end of Lenton Bluff.
Altered, slightly porphyritic, subvariolitic olivine-dolerite; (?) phenocrysts of plagioclase in groundmass of plagioclase, clinopyroxene, pseudomorphs after (?) olivine, iron ore and viridite.

3662 Z.471.13c Alt. 385 m., lat. 79°00'S., long. 28°12'W. About middle of dyke; small outcrop at south-western end of Lenton Bluff.
Medium-grained, subophitic, subvariolitic, altered olivine-dolerite; consists of plagioclase (An_{64}), clinopyroxene, pseudomorphs after (?) olivine, viridite and iron ore. Modal analysis Table IV.

TABLE XIV. Layered sill of Jeffries Glacier

Sill about 50 m. thick which intrudes the sediments beneath the scarp-capping sill; approximately in the middle of the sill is a 1-2 m. thick mafic band which appears to be continuous throughout the sill.

3734 Z.497.10 Alt. 500 m., lat. 79°02'S., long. 28°18'W. About middle of sill; mafic band; cliff outcrop on western margin of Jeffries Glacier.
Very coarse-grained olivine-hypersthene-orthocumulate; cumulus minerals are olivine (altered to talc, bowlingite and magnetite), hypersthene, plagioclase (An_{60}) and clinopyroxene; intercumulus is dominantly plagioclase, clinopyroxene, bowlingite, (?) sericite, apatite, biotite and iron ore. Modal analysis Table IV.

3735 Z.497.9 Alt. 495 m., lat. 79°02'S., long. 28°18'W. Lower half of sill; normal dolerite below mafic band; cliff outcrop on western margin of Jeffries Glacier.
Altered, coarse-grained, ophitic, olivine—two-pyroxene—dolerite; consists dominantly of plagioclase (An_{70}), clinopyroxene, hypersthene (altered to bowlingite), olivine (altered to bowlingite, magnetite and talc) and iron ore with a feldspathic mesostasis including apatite, iron ore, biotite, viridite and some secondary quartz. Modal analysis Table IV.

Layered sill of Marø Cliffs

Sill about 30 m. thick which intrudes the sediments beneath the scarp-capping sill; rhythmic layering is developed in the lower 8 m. of the sill and dolerite-pegmatite in the upper 2-3 m.

3731 Z.481.6 Alt. 360 m., lat. 79°04'S., long. 28°32'W. About 1.2 m. below upper contact; at contact with rheomorphic vein extending downwards from roof of sill; south-western end of Marø Cliffs.
Highly altered, fine- to coarse-grained, variolitic dolerite; consists of plagioclase (An_{70}) and pigeonite in variolitic clusters with interstitial micropegmatite, viridite and rod-like iron ore.

3732 Z.481.5 Alt. 360 m., lat. 79°04'S., long. 28°32'W. About 1.8 m. below upper contact; finer-grained, darker-weathering band in dolerite-pegmatite; south western end of Marø Cliffs.
Altered medium-grained dolerite; consists dominantly of plagioclase (An_{50}), pigeonite, micropegmatite, viridite and iron ore.

3733 Z.481.4 Alt. 360 m., lat. 79°04'S., long. 28°32'W. About 1.8 m. below upper contact; dolerite-pegmatite; south-western end of Marø Cliffs.
Altered, coarse-grained dolerite-pegmatite; consists of plagioclase (An_{64}), pigeonite and iron ore with a poorly crystallized quartzo-feldspathic mesostasis including some micropegmatite and abundant biotite—viridite alteration products.

3668 Z.481.2 Alt. 330 m., lat. 79°04'S., long. 28°32'W. About 2-3 m. above lower contact; melanocratic layer; south-western end of Marø Cliffs.
Coarse-grained, olivine-hypersthene-clinopyroxene-orthocumulate; cumulus minerals are olivine (altered to talc and bowlingite), hypersthene and clinopyroxene; intercumulus is plagioclase (An_{76-50}), clinopyroxene, iron ore and viridite. Modal analysis Table IV.

3674 Z.481.1 Alt. 330 m., lat. 79°04'S., long. 28°32'W. About 2-3 m. above lower contact; leucocratic layer; south-western end of Marø Cliffs.
Coarse-grained clinopyroxene-hypersthene-olivine-plagioclase-orthocumulate; cumulus minerals are clinopyroxene, hypersthene, olivine (often skeletal, altered to talc and serpentine) and plagioclase (An_{70-45}); intercumulus is plagioclase, clinopyroxene, orthopyroxene, olivine, iron ore and viridite. Modal analysis Table IV.

TABLE XV. Middle sill of Coalseam Cliffs

Sill 50-60 m. thick which is the middle of the three major cliff-forming sills in Coalseam Cliffs beneath Stewart Buttress and Mount Faraway and which extends as rock windows in the ice cliffs of the escarpment to Parry Point.

3708 Z.479.2 Alt. 540 m., lat. 79°10'S., long. 28°49'W. About 3 m. below upper contact; Coalseam Cliffs beneath Stewart Buttress.
Coarse-grained, ophitic two-pyroxene quartz-dolerite; consists of plagioclase (An_{76}), hypersthene, pigeonite, augite (altered to hornblende, biotite and chlorite), micropegmatite and iron ore. Modal analysis Table IV.

3676 Z.473.1 Alt. 300 m., lat. 79°20'S., long. 29°32'W. Upper half of sill; rock window in ice cliffs of escarpment about midway between Mount Faraway and Parry Point; base of cliffs.
Medium-grained granophyric quartz-dolerite; consists of plagioclase (An_{47-35}), pigeonite (altered to hornblende and biotite), micropegmatite, hornblende, biotite, fayalite, ilmenite, apatite and some discrete quartz. Modal analysis Table IV.

3698 Z.476.1 Alt. 240 m., lat. 27°30'S., long. 30°21'W. Upper half of sill; rock window in ice cliffs at Parry Point; top of cliffs.
Coarse-grained granophyric quartz-dolerite; consists of plagioclase (An_{40-50}), pigeonite and augite (altered to hornblende and biotite), micropegmatite, iron ore, hornblende, biotite, chlorite, fayalite and apatite. Modal analysis Table IV.

3707 Z.479.3 Alt. 580 m., lat. 79°10'S., long. 28°49'W. About 10 m. above lower contact; Coalseam Cliffs beneath Stewart Buttress.
Coarse-grained, ophitic two-pyroxene quartz-dolerite; consists of plagioclase (An_{66}), hypersthene, pigeonite and augite (altered to hornblende, biotite and chlorite), micropegmatite and iron ore. Modal analysis Table IV.

3704 Z.475.1 Alt. 512 m., lat. 79°11'S., long. 28°52'W. About 2 m. above lower contact; south-western end of Coalseam Cliffs, below Mount Faraway.
Coarse-grained, ophitic two-pyroxene dolerite; consists of plagioclase (An_{64-74}), hypersthene, pigeonite and augite (altered to chlorite), olivine (mainly pseudomorphed by bowlingite and magnetite) and iron ore with intersertal poorly crystallized feldspathic material including (?) micropegmatite, apatite, biotite and chlorite. Modal analysis Table IV.

3692 Z.475.2 Alt. 510 m., lat. 79°11'S., long. 28°52'W. Lower contact; south-western end of Coalseam Cliffs, below Mount Faraway.
Porphyritic chilled olivine-dolerite; phenocrysts of olivine (mainly fresh, some altered to bowlingite

and iddingsite) in subvariolitic groundmass of plagioclase (An_{64}) and pyroxene (altered to hornblende and biotite) with granular iron ore and intersertal devitrified glass; veinlets of quartz, feldspar and iron ore. Modal analysis Table III.

TABLE XVI. Basal sill of Coalseam Cliffs

Sill about 30 m. thick which is the lowest of the three major cliff-forming sills of Coalseam Cliffs and forms the base of the cliffs for much of their length.

3683 Z.478.10 Alt. 260 m., lat. 79°09'S., long. 28°46'W. Upper contact; Coalseam Cliffs below point 2600. Porphyritic chilled olivine-dolerite; phenocrysts of olivine (altered to iddingsite and magnetite or bowlingite), plagioclase (An_{65-70}) with some augite (altered to chlorite) in groundmass grading from glass with plagioclase microlites and iron ore to fine-grained plagioclase (An_{67}), pyroxene, olivine and iron ore with intersertal glass. Modal analysis Table III.

3717 Z.474.1 Alt. 260 m., lat. 79°12'S., long. 28°53'W. About 6 m. below upper contact; just above sedimentary xenolith; small outcrop at south-western end of Coalseam Cliffs.
Glomeroporphyritic fine-grained olivine-dolerite; phenocrysts of olivine (altered to bowlingite and iddingsite) and plagioclase (An_{69}) in fine-grained hemicrystalline groundmass of plagioclase (An_{65}) and olivine in a matrix of devitrified glass with abundant iron ore and probably also olivine, pyroxene and plagioclase. Modal analysis Table IV.

3687 Z.478.11 Alt. 320 m., lat. 79°09'S., long. 28°46'W. About middle of sill; Coalseam Cliffs below point 2600.
Medium-grained ophitic olivine-dolerite; consists of plagioclase (An_{70}), olivine (altered to bowlingite, iddingsite and magnetite), pink augite (altered to chlorite) and iron ore with abundant chloritic alteration products. Modal analysis Table IV.

3718 Z.500.1 Alt. 280 m., lat. 79°09'S., long. 28°47'W. Lower half of sill; Coalseam Cliffs between point 2600 and Stewart Buttress.
Coarse-grained ophitic olivine-dolerite; consists of plagioclase (An_{68}), pink augite (altered to biotite) and olivine (altered to bowlingite and magnetite) with interstitial iron ore and viridite. Modal analysis Table IV.

3699 Z.477.4 Alt. 303 m., lat. 79°08'S., long. 28°44'W. About 3 m. above lower contact; north-eastern end of Coalseam Cliffs.
Medium-grained ophitic olivine-dolerite; consists of plagioclase (An_{64}), pink augite (altered to biotite), olivine (altered to bowlingite and serpentine with some iddingsite and magnetite), iron ore and viridite. Modal analysis Table IV.

3693 Z.477.3 Alt. 300 m., lat. 79°08'S., long. 28°44'W. Lower contact; north-eastern end of Coalseam Cliffs.
Porphyritic chilled olivine-dolerite; phenocrysts of olivine (altered to bowlingite and iddingsite near contact, magnetite elsewhere) and plagioclase (An_{60-74}) with occasional pink augite in groundmass varying from glass to fine-grained hemicrystalline plagioclase, olivine, pyroxene and iron ore; thin deuteric veinlets. Modal analysis Table III.

3691 Z.478.12 Alt. 300 m., lat. 79°09'S., long. 28°46'W. Lower contact; Coalseam Cliffs below point 2600. Porphyritic chilled olivine-dolerite; phenocrysts of olivine (altered to magnetite and bowlingite) and plagioclase (An_{60-72}) in groundmass varying from glass to fine-grained plagioclase, pink augite, olivine, iron ore and chloritic alteration of intersertal glass. Modal analysis Table III.

TABLE XVII. Other intrusions

Sills ranging from <1 m. to about 30 m. in thickness and dykes ranging from <1 m. to about 6 m. in width from various parts of the Theron Mountains; these have been very sporadically collected and they have not been definitely correlated with any of the major intrusions in Tables IX-XVI.

3742 Z.487.3 Alt. 805 m., lat. 78°53'S., long. 27°24'W. Sill about 30 m. thick intruding the sediments above the scarp-capping sill; long cliff of escarpment immediately north-east of the mouth of Goldsmith Glacier; upper contact of sill.
Chilled porphyritic olivine-dolerite; phenocrysts of plagioclase (albitized), olivine and clinopyroxene in a fine-grained hemicrystalline groundmass. Modal analysis Table III.

3743 Z.487.2 Alt. 800 m., lat. 78°53'S., long. 27°24'W. Same sill as analysis 3742; long cliff of escarpment immediately north-east of the mouth of Goldsmith Glacier; upper part of sill.
Altered, coarse-grained ophitic dolerite; consists of plagioclase, clinopyroxene, fayalite, iron ore, alteration products and secondary quartz and calcite.

3659 Z.466.3 Alt. 800 m., lat. 78°54'S., long. 27°23'W. Sill of unknown thickness (top eroded) intruding the sediments above the scarp-capping sill; possibly same sill as analyses 3742 and 3743; truncated spur on north-eastern margin of Goldsmith Glacier; 0.8 m. above lower contact of sill.
Medium-grained, porphyritic, subvariolitic altered dolerite; pseudomorphs after (?) olivine or pyroxene in groundmass of plagioclase, clinopyroxene, alteration products and intersertal mesostasis.

3744 Z.509.1 Alt. 995 m., lat. 78°55'S., long. 27°17'W. Dyke about 6 m. wide intruding the sediments above the scarp-capping sill; appears to merge with a 6 m. thick sill lower down in the outcrop, beneath scree and snow cover; this is at a greater altitude than the sills of analyses 3742, 3743 and 3659 and it is probably not connected with them; boulder-covered ridge on north-eastern margin of Goldsmith Glacier; near centre of dyke.
Fine-grained, granular to subophitic hemicrystalline dolerite; consists of plagioclase, clinopyroxene (?) orthopyroxene, iron ore and intersertal glass with secondary quartz, calcite and biotite. Modal analysis Table IV.

3745 Z.463.2 Alt. 1,080 m., lat. 78°59'S., long. 26°38'W. Sill intruding sediments above the scarp-capping sill; southernmost outcrop on north-eastern margin of Goldsmith Glacier; middle of sill.
Altered, coarse-grained quartz-dolerite; consists of plagioclase, clinopyroxene, micropegmatite, hornblende, biotite, chlorite and iron ore.

3657 Z.463.3 Alt. 1,100 m., lat. 78°59'S., long. 26°38'W. Same sill as analysis 3745; southernmost outcrop on north-eastern margin of Goldsmith Glacier; near top of sill.
Highly altered, fine-grained dolerite; consists of plagioclase, clinopyroxene, viridite and iron ore.

3747 Z.489.1 Alt. 560 m., lat. 78°56'S., long. 27°44'W. Sill about 12 m. thick intruding the sediments immediately below the scarp-capping sill; rock peak rising from ice cliffs of escarpment just south-west of the mouth of Goldsmith Glacier; about 1 m. above lower contact of sill.
Slightly altered, fine-grained granular olivine-dolerite; consists of plagioclase (An_{63}), pigeonite, olivine (altered to magnetite and bowlingite) and iron ore with a poorly crystallized feldspathic mesostasis marked by chloritic alteration.

3679 Z.489.4 Alt. 515 m., lat. 78°56'S., long. 27°44'W. Sill 20-30 m. thick intruding the sediments beneath the scarp-capping sill; this sill forms the base of the outcrop; rock peak rising from ice cliffs of escarpment just south-west of the mouth of Goldsmith Glacier; about 6 m. below upper contact of sill.
Subophitic fine-grained dolerite; consists of plagioclase (An_{55}), pigeonite (zoned to pink augite margins), hornblende and iron ore with a poorly crystallized feldspathic mesostasis with viridite and brownish ferruginous products.

3655 Z.461.1 Alt. 900 m., lat. 79°02'S., long. 28°04'W. Thin sill intruding sediments above the scarp-capping sill; truncated spur about halfway down eastern margin of Jeffries Glacier; lower part of sill.

Altered, coarse-grained subophitic dolerite; consists of plagioclase, clinopyroxene, micropegmatite, iron ore and viridite. Modal analysis Table IV.

3656 Z.461.2 Alt. 910 m., lat. 79°02'S., long. 28°04'W. Same sill as analysis 3655; truncated spur about halfway down eastern margin of Jeffries Glacier; upper part of sill.
Fine-grained granular olivine-dolerite; consists of plagioclase, clinopyroxene, olivine, biotite and iron ore with viridite and (?) micropegmatite. Modal analysis Table IV.

3746 Z.488.1 Alt. 885 m., lat. 78°58'S., long. 27°41'W. Uppermost sill (<5 m. thick), which may be a branch of the sill of analysis 3666, intruding the sediments above the scarp-capping sill; 1.2 m. above lower contact of sill.
Fine-grained, intergranular to subophitic olivine-dolerite; consists of plagioclase (An_{68}), pinkish augite, olivine, iron ore, biotite and rare interstitial micropegmatite with apatite.

3666 Z.469.1 Alt. 860 m., lat. 78°58'S., long. 27°39'W. Uppermost sill (? 15 m. thick) intruding the sediments above the scarp-capping sill; rock ridge parallel to and 3 km. south-east of escarpment, south-west of Goldsmith Glacier; near bottom of sill.
Highly altered, fine- to medium-grained subophitic dolerite; consists of plagioclase, clinopyroxene, (?) orthopyroxene, (?) pseudomorphs after olivine, iron ore, micropegmatite and viridite.

3652 Z.469.2 Alt. 800 m., lat. 78°58'S., long. 27°39'W. Sill about 6 m. thick between the scarp-capping sill and sill of analysis 3666; rock ridge parallel to and 3 km. south-east of the escarpment, south-west of Goldsmith Glacier; middle of sill.
Fine-grained, hemicrystalline, slightly variolitic olivine-dolerite; consists of plagioclase, clinopyroxene, olivine and glass with iron ore.

3711 Z.464.1 Alt. 900 m., lat. 78°59'S., long. 27°18'W. Sill intruding sediments above the scarp-capping sill; may be part of the scarp-capping sill but unlikely as it is petrographically and chemically distinct; southernmost outcrop on south-western margin of Goldsmith Glacier; upper contact of sill.
Glomeroporphyritic chilled olivine-dolerite; phenocrysts of plagioclase (An_{66}) and olivine (altered to bowlingite and magnetite) in devitrified glassy groundmass with minute granular iron ore and patches of secondary biotite; vesicles and veinlets of quartz, feldspar, chlorite and biotite. Modal analysis Table III.

3658 Z.464.2 Alt. 899 m., lat. 78°59'S., long. 27°18'W. Same sill as analysis 3711; southernmost outcrop on south-western margin of Goldsmith Glacier; top of sill.
Fine-grained subophitic olivine-dolerite; consists of plagioclase (An_{70}), clinopyroxene, olivine, orthopyroxene and iron ore with interstitial micropegmatite. Modal analysis Table IV.

3712 Z.464.3 Alt. 890 m., lat. 78°59'S., long. 27°18'W. Same sill as analyses 3711 and 3658; southernmost outcrop on south-western margin of Goldsmith Glacier; middle of sill.
Coarse-grained, ophitic two-pyroxene quartz-dolerite; consists of plagioclase, orthopyroxene, clinopyroxene, intergrowths of ortho- and clinopyroxene, micro-pegmatite, iron ore and viridite. Modal analysis Table IV.

3677 Z.481.10 Alt. 520 m., lat. 79°04'S., long. 28°32'W. Dyke about 1 m. wide intruding sediments beneath the scarp-capping sill and the sill itself; south-western end of Marø Cliffs; middle of dyke.
Fine-grained, altered, slightly porphyritic variolitic dolerite; pseudomorphs of bowlingite and talc after (?) olivine or pyroxene in variolitic groundmass of plagioclase (An_{50}) and clinopyroxene with intersertal glass dotted with iron ore; some secondary haematite and quartz.

3651 Z.453.1 Alt. 860 m., lat. 79°06'S., long. 28°29'W. Sill about 15 m. thick intruding the sediments above the scarp-capping sill; rock ridge leading eastwards from point 3300; near centre of sill.
Coarse-grained ophitic olivine-dolerite; consists of plagioclase (An_{67}), pigeonite (altered to biotite), olivine (altered to bowlingite and magnetite) and iron ore with poorly crystallized feldspathic mesostasis with apatite and some secondary quartz. Modal analysis Table IV.

3671 Z.453.2 Alt. 870 m., lat. 79°06'S., long. 28°29'W. Same sill as analysis 3651; rock ridge leading eastwards from point 3300; top of sill.
Chilled olivine-dolerite; clusters of olivine and (?) orthopyroxene in variolitic groundmass of plagioclase (An_{62}), augite and pigeonite with intersertal glass dotted with iron ore.

3653 Z.453.3 Alt. 880 m., lat. 79°06'S., long. 28°29'W. Dyke about 1 m. wide intruding the sediments above the scarp-capping sill; between the sill of analyses 3651 and 3671 and the thin sill forming the first shoulder on the ridge leading to point 3300; near centre of dyke.
Chilled variolitic dolerite; consists of plagioclase (An_{68}), pigeonite and augite in a glassy groundmass with curved plagioclase crystallites and hollow microlites plus granular iron ore; some secondary calcite and quartz. Modal analysis Table IV.

3684 Z.477.7 Alt. 295 m., lat. 79°08'S., long. 28°44'W. Sill about 2 m. thick intruding the sediments beneath the basal sill of Coalseam Cliffs; north-eastern end of Coalseam Cliffs; middle of sill.
Altered, medium-grained variolitic dolerite; consists of plagioclase, clinopyroxene, pseudomorphs after olivine and iron ore with intersertal glass and secondary quartz and calcite.

10655 TAE350/6 see Appendix II.

3685 Z.477.11 Alt. 290 m., lat. 79°08'S., long. 28°44'W. Sill about 3 m. thick which is the lowest sill intruding the sediments beneath the basal sill of Coalseam Cliffs; north-eastern end of Coalseam Cliffs; middle of sill.

Fine- to medium-grained intersertal dolerite; consists of plagioclase, clinopyroxene, iron ore, biotite—chlorite alteration and intersertal mesostasis. Modal analysis Table IV.

10654 TAE351/7 see Appendix II.

3696 Z.478.3 Alt. 480 m., lat. 79°09'S., long. 28°46'W. Thin wedge of dolerite (<1 m. thick) which is intruded by the thick wedging sill of Coalseam Cliffs (scarp-capping sill); Coalseam Cliffs below point 2600; middle of wedge.
Altered, porphyritic variolitic dolerite; pseudomorphs of talc, serpentine and magnetite probably after olivine in variolitic groundmass of plagioclase (An_{76}) and pigeonite with interstitial glass and iron ore; much chloritic alteration and some chloritic veinlets.

3689 Z.478.7 Alt. 400 m., lat. 79°09'S., long. 28°46'W. Sill about 1.2 m. thick intruding the sediments between the thick wedging sill (scarp-capping sill) and the basal sill of Coalseam Cliffs; Coalseam Cliffs below point 2600; upper contact of sill.
Altered chilled dolerite grading into little altered, fine-grained, hemicrystalline subvariolitic dolerite; consists of plagioclase, pyroxene, iron ore and devitrified glass.

3709 Z.479.1 Alt. 580 m., lat. 79°10'S., long. 28°49'W. Sill about 3 m. thick intruding the sediments between the middle and upper sills of Coalseam Cliffs; Coalseam Cliffs beneath Stewart Buttress; middle of sill.

Fine-grained, intensely variolitic dolerite; consists of plagioclase and pigeonite (biotite—chlorite alteration) with (?) olivine and pseudomorphs after (?) olivine, iron ore and intersertal mesostasis.

3719 Z.495.1 Alt. 1,030 m., lat. 79°10'S., long. 28°46'W. Sill which caps Stewart Buttress; top of Coalseam Cliffs at Stewart Buttress; near base of sill. Highly altered subophitic dolerite; consists of plagioclase (? An_{55}, altered), pinkish clinopyroxene (altered to hornblende, biotite and chlorite), iron ore and micropegmatitic mesostasis with abundant chloritic alteration products.

APPENDIX II

BIBLIOGRAPHY OF PUBLISHED ANALYSES OF MESOZOIC THOLEIITIC ROCKS FROM THE SOUTHERN HEMISPHERE USED IN REGIONAL GEOCHEMICAL CORRELATION AND OF HAWAIIAN THOLEIITIC ROCKS USED FOR THE FREQUENCY DISTRIBUTION HISTOGRAMS OF FIG. 61

! Analysis for major and trace elements
' Analysis for major elements only
. Analysis for trace elements only
* Of unknown age but possibly Jurassic

Where two references are given, the first is the reference to major element analysis and the second to trace element analysis.

a. Jurassic dolerites from the Theron Mountains and Dronning Maud Land

Analysis number	Rock number	Description and locality	Reference
10651! 10652! 10653!	TAE351/3 TAE351/4 TAE351/6	Scarp-capping sill, Coal-seam Cliffs, Theron Mountains	Stephenson, 1966
10654! 10655!	TAE351/7 TAE350/6	Minor sills, Coalseam Cliffs, Theron Mountains	Stephenson, 1966
961! 962! 963! 964! 965! 966! 972! 974!	Z.310.2 Z.349.1 Z.350.1 Z.350.2 Z.370.1 Z.371.7 Z.308.4 Z.372.1	Basalt flows, Heimefrontfjella	Juckes, in press
959!	Z.353.7	Thin sill, Heimefrontfjella	Juckes, in press
*960!	Z.92.1	Thin sill, Heimefrontfjella	Worsfold, in press; Juckes, 1969
*957!	Z.399D.4	Thin sill, Mannefallknausane	Juckes, 1968; 1969

Analysis number	Rock number	Description and locality	Reference
*958!	Z.395.1	Dolerite, Vestfjella	Juckes, 1968; 1969
*10656'	HJW1	Basalt flows, Vestfjella	Hjelle and Winsnes, 1971
*10657'	HJW2		
*10658'	HJW3		
*10659'	HJW4		
*10660'	HJW6	Dolerite sills, Vest-	Hjelle and
*10661'	HJW7	fjella	Winsnes, 1971
*10662'	HJW8		
*10663'	HJW10	Olivine gabbro, Vest- fjella	Hjelle and Winsnes, 1971

b. Ferrar dolerites from Antarctica

10501!	TAE301/1	Dolerite sills, Which-	Stephenson, 1966
10502!	TAE302/5	away Nunataks	
10503!	TAE304/2		
10504!	TAE304/6		
10505!	TAE304/7		
10506!	TAE305/1	Dolerite dyke, Whichaway Nunataks	Stephenson, 1966
10507'	WRB732.A	Quartz dolerite, Horn Bluff	Browne, 1923
10508'	DS10	Diabase, gabbro and	Stewart, 1934
10509'	DS12	melabasalt, Mount	
10510'	DS11	Fridtjof Nansen, Queen Maud Mountains	
10511'	DHE14.1	Dolerite sill, Tillite Glacier, Beardmore Glacier area	Elliot, 1971a
10512'	BMG16790	Mount Harmsworth dyke, Victoria Land	Gunn, 1962
10513!	BMG16792	Mount Harmsworth dyke, Victoria Land. (Granophyre)	Gunn, 1966
10514'	BMG23093	Peneplain sill	Gunn, 1962
10515'	BMG23092	(pigeonite-tholeiite),	
10516'	BMG23091	Solitary Rocks,	
10517'	BMG23094	Victoria Land	
10518'	BMG23090		
10519'	BMG23084		
10520'	BMG23096		

Analysis number	Rock number	Description and locality	Reference
10521'	BMGF2502	Basement sill (hypersthene-tholeiite), Kukri Hills, Victoria Land	Gunn, 1962
10522'	BMG14908		
10523'	BMG14910		
10524'	BMG14913A		
10525'	BMG14914		
10526'	BMG14915		
10527'	BMG16793	Mount Egerton sill, Victoria Land	Gunn, 1962
10528'	BMG16795		
10529'	BMG16797		
10530'	BMG16800		
10531'	BMG21874	Upper Escalade sill, Victoria Land	Gunn, 1962
10532'	BMG21869		
10533'	BMG21870		
10534'	BMG21883		
10535'	BMG21836	Detour Nunatak dyke, Victoria Land	Gunn, 1962
10536'	BMG21837		
10537'	BMG21839		
10538'	BMG21840		
10539'	BMG21842		
10540'	BMG21841		
10541!	BMG4200	Pegmatoid, Terra Cotta Dome (hypersthene-tholeiite), Victoria Land	Gunn, 1966
10542!	BMG4300	Pegmatoid, Emmanuel sheet (hypersthene-tholeiite), Victoria Land	Gunn, 1966
10543!	BMG4031	Lake Vanda sill (hypersthene-tholeiite), Victoria Land	Gunn, 1966
10544!	BMG4030		
10545!	BMG4029		
10546!	BMG4028		
10547!	BMG4027		
10548!	BMG4026		
10549!	BMG4024		
10550!	BMG4021		
10551!	BMG4020		
10552!	BMG4019		
10553!	BMG4018		
10554!	BMG4017		
10555!	BMG4016		
10556!	BMG4013		
10557!	BMG4001		
10558!	BMG4012		

Analysis number	Rock number	Description and locality	Reference
10559!	BMG4174	New Mountain sill (pigeonite-tholeiite), Victoria Land	Gunn, 1966
10560!	BMG4172		
10561!	BMG4170		
10562!	BMG4169		
10563!	BMG4168		
10564!	BMG4165		
10565!	BMG4167		
10566'	BMG4074	North-west Mountain sill, (pigeonite-tholeiite), Victoria Land	Gunn, 1966
10567'	BMG4080	Finger Mountain sill (pigeonite-tholeiite), Victoria Land	Gunn, 1966
10568'	BMG4144	Basement sill (hypersthene-tholeiite), Solitary Rocks, Victoria Land	Gunn, 1966
10569'	BMG4142		
10570'	BMG4137		
10571'	BMG4141		
10572'	BMG4146		
10573'	BMG4147		
10574'	BMG4148		
10575'	BMG4124		
10576'	BMG4112		
10577'	BMG4114		
10578!	BMG4342	Thumb Point sill (olivine-tholeiite), Victoria Land	Gunn, 1966
10579!	BMG28901		
10580!	BMG4345		
10581!	BMG28904		
10582.	BMG28906		
10583!	BMG28908		
10584!	BMG4351		
10585!	BMG28910		
10586!	BMG26903	Painted Cliff sill (olivine-tholeiite), Beardmore Glacier area	Gunn, 1966
10587'	BMG4038	Salina Pond sill (hypersthene-tholeiite), Victoria Land	Gunn, 1966
10588'	BMG4040		
10589'	BMG4044		
10590'	BMG4048		
10591'	BMG4051		
10592!	BMG4285	Emmanuel sill (hypersthene-tholeiite), Victoria Land	Gunn, 1966

Analysis number	Rock number	Description and locality	Reference
10593'	BMG4083	Finger Mountain sheet (hypersthene-tholeiite), Victoria Land	Gunn, 1966
10594'	BMG4229	Basement sill, Kukri Hills, Victoria Land	Gunn, 1966
10595!	BMG4266	Peneplain sill, Victoria Land	Gunn, 1966
10596!	WH1	Basement sill, Kukri Hills, Victoria Land	Hamilton, 1965
10597!	WH2		
10598!	WH3		
10599!	WH4		
10600!	WH5		
10601!	WH6		
10602!	WH7		
10603!	WH8		
10604!	WH9		
10605!	WH10		
10606!	WH11		
10607!	WH12		
10608!	WH13		
10609!	WH14		
10610!	WH15	Peneplain sill, Victoria Land	Hamilton, 1965
10611!	WH16		
10612!	WH17		
10613!	WH18	New Mountain sheet, Victoria Land	Hamilton, 1965
10614!	WH19	Sills of Pyramid Mountain, Victoria Land	Hamilton, 1865
10615!	WH20		
10616!	WH21		
10617!	WH22	Inclined sheet, east end of Pyramid Mountain, Victoria Land	Hamilton, 1965
10618!	WH23		
10619!	WH24		
10620!	WH25		
10621!	WH26	Thin dykes, Beacon Heights, Victoria Land	Hamilton, 1965
10622!	WH27		
10623'	WNB1	Erratics, Cape Royds, Victoria Land	Benson, 1916
10624'	WNB2		
10625'	WNB3	Quartz dolerite, Knob Head Mountain, Victoria Land	Benson, 1916

Analysis number	Rock number	Description and locality	Reference
10626'	BMG21846	Ferrar volcanics, Carapace Nunatak, Victoria Land	Gunn, 1962
10627'	DHE27.45	Kirkpatrick basalts, Beardmore Glacier area	Elliot, 1971a
10628'	DHE27.28		
10629'	DHE33.7		
10630'	DHE27.1		
10631'	DHE27.13		
10632'	DHE27.17		
10633'	DHE27.22		
10634'	DHE27.36		
10635'	DHE27.41		
10636'	DHE55.14		
10637'	DHE55.27		
10638'	DHE55.33		
10639'	DHE55.41		
10640.	BMG4299	Emmanuel sill, Victoria Land	Gunn, 1966
10641.	BMG4296		
10642.	BMG4294		
10643.	BMG4292		
10644.	BMG4290		
10645.	BMG4287		
10646.	BMG4270	Peneplain sill, Victoria Land	Gunn, 1966
10647.	BMG4275		
10648.	BMG4277		

c. Jurassic dolerites from Tasmania

10701'	ABE1	Cataract Gorge	Edwards, 1942
10702'	ABE2	North-west Bay	Edwards, 1942
10703'	ABE3	Mount Nicholas Range	Edwards, 1942
10704'	ABE4	Ben Lomond	Edwards, 1942
10705'	ABE5		
10706'	ABE6		
10707'	ABE7		
10708'	ABE8	Mount Sedgwick	Edwards, 1942
10709'	ABE9		
10710'	ABE10		
10711'	ABE11	Cradle Mountain	Edwards, 1942
10712'	ABE12		

Analysis number	Rock number	Description and locality	Reference
10713'	ABE13	Mount Wellington sill	Edwards, 1942
10714'	ABE14		
10715'	ABE15		
10716'	ABE16		
10717'	ABE17		
10718'	ABE18		
10719'	ABE19		
10720'	ABE20		
10721'	ABE21		
10722'	ABE22		
10723'	ABE23	Gunning's Sugarloaf	Edwards, 1942
10724'	ABE24		
10725'	ABE25		
10726'	ABE26		
10727'	ABE27		
10728'	ABE28		
10729'	ABE29		
10730'	ABE30	Mount Nelson sill	Edwards, 1942
10731'	ABE31		
10732'	ABE32		
10733'	ABE33		
10734'	ABE34		
10735'	ABE35		
10736'	ABE36		
10737'	ABE37		
10738'	ABE38		
10739'	ABE39		
10740'	ABE40	Coarse vein, Mount Sedgwick	Edwards, 1942
10741'	ABE41	Myrtle Gully	Edwards, 1942
10742'	ABE42		
10743'	IM.R76	Chilled dolerites	McDougall, 1962
10744'	IM.PROCRD.		
10745'	IM.8072		
10746'	IM.11(2)	Granophyre	McDougall, 1962
10747!	M200	Chilled dolerite, Red Hill intrusion	McDougall, 1962; McDougall and Lovering, 1963
10748!	M172		

Analysis number	Rock number	Description and locality	Reference
10749!	M212	Quartz-dolerites, Red Hill intrusion	McDougall, 1962; McDougall and Lovering, 1963
10750!	M336N		
10751!	M336P		
10752!	M9		
10753!	M3		
10754!	M209		
10755!	M210		
10756!	M221		
10757!	M222		
10758!	M393		
10759!	M395		
10760!	M223	Fayalite-granophyres, Red Hill intrusion	McDougall, 1962; McDougall and Lovering, 1963
10761!	M384		
10762!	M12		
10763!	M32		
10764!	M206	Granophyres, Red Hill intrusion	McDougall, 1962; McDougall and Lovering, 1963
10765!	M162		
10766!	M8		
10767!	M19		
10768!	M176		
10769'	IM1	Granophyres, Great Lake sheet	McDougall, 1964; Greenland and Lovering, 1966
10770!	IM2		
10771!	IM3	Dolerites of central zone, Great Lake sheet	McDougall, 1964; Greenland and Lovering, 1966
10772!	IM4		
10773!	IM5		
10774!	IM6		
10775!	IM7		
10776!	IM8		
10777!	IM9		
10778!	IM10	Dolerites of lower zone, Great Lake sheet	McDougall, 1964; Greenland and Lovering, 1966
10779!	IM11		
10780!	IM12		
10781!	IM13		
10782!	IM14		
10783!	IM15		
10784!	IM16		
10785!	IM17		
10786!	IM18		
10787!	IM19		
10788!	IM20		

Analysis number	Rock number	Description and locality	Reference
10789'	IM21	Chilled dolerite, Great Lake sheet	McDougall, 1964
10790'	IM22	Dolerites of upper zone, Great Lake sheet	McDougall, 1964
10791'	IM23		
10792'	IM24	Dolerites of central zone, Great Lake sheet	McDougall, 1964
10793'	IM25		
10794'	IM26		
10795'	IM27	Dolerite of lower zone, Great Lake sheet	McDougall, 1964
10796!	IM28	Chilled dolerite, Great Lake sheet	McDougall, 1964; Greenland and Lovering, 1966
10797!	IM29	Dolerites of lower zone, Great Lake sheet	McDougall, 1964; Greenland and Lovering, 1966
10798!	IM30		
10799!	IM31		
10800!	IM32		
10801!	IM33		
10802!	IM34		
10803!	IM35		
10804!	IM36		
10805!	IM37		
10806!	IM38		
10807!	IM39		
10808!	IM40		
10809!	IM41		
10810'	WNB4	Diabase, Launceston	Benson, 1916

d. Karroo dolerites from southern Africa

10901!	WP49.34	Dolerites between Sutherland and Middelburg, Cape Province	Walker and Poldervaart, 1942; Nockolds and Allen, 1956
10902!	WP49.42		
10903'	WP49.81		
10904!	WP49.9		
10905!	WP49.5	500 ft. Bulthouders Bank sill, Alewyn's Gat, Cape Province	Walker and Poldervaart, 1949; Nockolds and Allen, 1956
10906'	WP49.66		
10907'	WP49.11	90 ft. multiple dolerite dyke, Sanddrift Spruit, Orange Free State	Frankel, 1943
10908'	WP49.62		

Analysis number	Rock number	Description and locality	Reference
10909!	WP49.36	Southern gap-dyke, Kentani, Cape Province	Walker and Poldervaart, 1949; Nockolds and Allen, 1956
10910'	WP49.47	Basal zone of 3,000 ft. Insizwa sheet, Sugarbush, Cape Province	Walker and Poldervaart, 1949
10911!	WP49.37	Dykes of the Transkei Gaps, Cape Province	Mountain, 1943; Nockolds and Allen, 1956
10912'	WP49.38		
10913'	WP49.22		
10914!	WP49.85		
10915'	WP49.88		
10916'	WP49.8	Sills and dykes, Paardekop, Transvaal	Walker and Poldervaart, 1949
10917'	WP49.20		
10918'	WP49.23		
10919'	WP49.80	Sill, east of Ermelo, Transvaal	Walker and Poldervaart, 1949
10920'	WP49.78	Dyke, Komatipoort, Transvaal	Lombaard, 1939
10921'	WP49.45	Basal zone of 3,000 ft. Insizwa sheet, Waterfall Gorge, Umzimhlava Poort and Payne's Mining Area, Cape Province	Scholtz, 1936
10922'	WP49.39		
10923'	WP49.44		
10924'	WP49.46		
10925'	WP49.79		
10926'	WP49.84		
10927'	WP49.82		
10928'	WP49.86	Dyke in Insizwa sheet, Payne's Mining Area, Cape Province	Scholtz, 1936
10929'	WP49.89	Sheet in hornfels near floor of Insizwa sheet, Waterfall Gorge, Cape Province	Walker and Poldervaart, 1949
10930'	WP49.35	Basal zone of 3,000 ft. Insizwa sheet, Waterfall Gorge, Cape Province	Walker and Poldervaart, 1949
10931'	WP49.43		

Analysis number	Rock number	Description and locality	Reference
10932!	WP49.15	200 ft. Elephant's Head dyke and 600 ft. New Amalfi sheet, Matatiele, Cape Province	Walker and Poldervaart, 1949; Nockolds and Allen, 1956
10933!	WP49.18		
10934!	WP49.40		
10935!	WP49.41		
10936'	WP49.51		
10937!	WP49.53		
10938!	WP49.54		
10939!	WP49.55		
10940!	WP49.91		
10941!	WP49.92		
10942!	WP49.93		
10943!	WP49.13	Mount Arthur bell-jar intrusion, East Griqualand, Cape Province	Walker and Poldervaart, 1949; Nockolds and Allen, 1956
10944!	WP49.14		
10945'	WP49.52		
10946'	WP49.58		
10947!	WP49.65		
10948!	WP49.71		
10949!	WP49.72		
10950'	WP49.73		
10951!	WP49.74		
10952'	WP49.75		
10953!	WP49.76		
10954!	WP49.77		
10955!	WP49.61	Sills, 100-500 ft., Alewyn's Gat and Rietkop, Cape Province	Walker and Poldervaart, 1949; Nockolds and Allen, 1956
10956'	WP49.69		
10957'	WP49.90		
10958!	WP49.95		
10959!	WP49.96		
10960'	WP49.60	500 ft. sill, Hangnest, Cape Province	Walker and Poldervaart, 1941; Nockolds and Allen, 1956
10961!	WP49.27		
10962!	WP49.70		
10963!	WP49.94		
10964'	WP49.24	Sills from Dover Junction, Orange Free State and Brook's Nek, Insizwa Mountain and De Aar Junction, Cape Province	Daly and Barth, 1930
10965'	WP49.21		
10966'	WP49.10		
10967'	WP49.6		
10968'	WP49.29	Sill, Umhlatuzi Crossing, Natal	Walker and Poldervaart, 1949

Analysis number	Rock number	Description and locality	Reference
10969'	WP49.49	Younger intrusions of olivine-basaltic dolerite, Kranskop, Orange Free State	Frankel, 1942
10970'	WP49.48		
10971'	WP49.50		
10972'	WP49.56		
10973'	WP49.3	20 ft. sill, Aliwal North, Cape Province	Frankel, 1938
10974!	WP49.1	Sills and dykes from Borehole Elandsberg, Natal and Queenstown, Elliot, Perdevlei, Murraysberg, Zwartberg, Execution Rock, Butterworth, Libode, Theekloof, Mount Fletcher, Hangnest, Mount Currie and Calamity Hill, Cape Province	Walker and Poldervaart, 1949; Nockolds and Allen, 1956
10975'	WP49.2		
10976!	WP49.4		
10977'	WP49.7		
10978!	WP49.12		
10979'	WP49.16		
10980!	WP49.17		
10981'	WP49.19		
10982!	WP49.25		
10983!	WP49.26		
10984'	WP49.30		
10985'	WP49.31		
10986'	WP49.32		
10987!	WP49.33		
10988'	WP49.57		
10989'	WP49.59		
10990!	WP49.67		
10991'	WP49.68		
10992'	WP49.83	Bronzite-dolerite from the Falkland Islands	Walker and Poldervaart, 1949
10993'	WP49.87	Vein in dolerite dyke, Poortje, Orange Free State	Walker and Poldervaart, 1949
10994'	WP49.28	200 ft. sill, Downes Mountain, Cape Province	Walker and Poldervaart, 1940
10995'	WP49.63	Intrusions of glass in dolerite, Verulam and Effingham Quarries, Natal	Kent and Frankel, 1948
10996'	WP49.64		
10997'	KF48.3		
10998'	KF48.4		
10999'	KF48.5		
11000'	JJF1	20 ft. sill, Aliwal North, Cape Province	Frankel, 1938
11001'	JJF42.F1	Olivine-dolerite, Filabusi District, Rhodesia	Frankel, 1942

Analysis number	Rock number	Description and locality	Reference
11002'	AW60.1	Sill near Heilbron,	Ackerman and
11003'	AW60.2	Orange Free State	Walker, 1960
11004'	BVL695	Dykes and conical sheets	Lombaard, 1952
11005'	BVL721	around Lady Frere, Indwe	
11006'	BVL734	and Dordrecht, Cape	
11007'	BVL742	Province	
11008'	BVL700		
11009'	BVL728		
11010'	BVL746	Rhyolite, granophyre and	Lombaard, 1952
11011'	BVL758	microgranite from	
11012'	BVL750	northern Lebombo	
11013'	FW51.1	Volcanic vent near	Walker, 1951
11014'	FW51.NB1	Lambert's Bay, Cape Province	
11015'	BL1	Sills and dykes from the	Lightfoot, 1938
11016'	BL2	south-eastern part of	
11017'	BL3	Rhodesia	
11018'	BL4		
11019'	BL5		
11020'	EDM58.12	Acid dolerites, Coedmore	Mountain, 1958
11021'	EDM58.3	Quarries, Durban, Natal	
11022'	EDM58.25		
11023'	EDM58.27		
11024'	EDM58.37		
11025'	FW56.2	Dolerites of the Cape	Walker, 1956
11026'	FW56.3	Peninsula, from Froggy	
11027'	FW56.4	Pond, Logie's Bay,	
11028'	FW56.5	Smitswinkel Bay, Chapman's	
11029'	FW56.6	Peak, Clifton and Llandudno,	
11030'	FW56.7	Cape Province	
11031'	FW56.NB2		
11032'	FW56.NB3		
11033'	FW56.NB4		
11034'	HVE1	Khale dolerite sheet,	Eales, 1959
11035'	HVE2	Bechuanaland	
11036'	HVE3		
11037'	JJF2	Younger olivine-basaltic	Frankel, 1949
11038'	JJF3	dolerite, Trompsburg	
11039'	JJF4	district, Orange Free	
11040'	JJF5	State	

Analysis number	Rock number	Description and locality	Reference
11041'	AM65.2	North gap-dyke of the Transkei, Cape Province	Moore, 1965
11042'	AM65.3		
11043'	AM65.5		
11044'	AM65.6		
11045'	JJF69.1	Effingham rock type in Natal and Zululand	Frankel, 1969
11046'	JJF69.6		
11047'	JJF69.2		
11048'	JJF69.3		
11049'	JJF69.4		
11050'	JJF69.5		
11051'	JJF69.7		
11052'	JJF69.8		
11053'	JJF69.9		
11054'	JJF69.10		

e. Karroo basalts from southern Africa

10831!	CH66B1	Vicinity of Kao mine, northern Basutoland	Cox and Hornung, 1966
10832!	CH66B19		
10833!	CH66B21		
10834!	CH66B31	Between summit of Thaba Bosiu and stream junction 1 mile to west-north-west, northern Basutoland	Cox and Hornung, 1966
10835!	CH66B32		
10836!	CH66B33		
10837!	CH66B36		
10838!	CH66B37		
10839!	CH66B39		
10840!	CH66B42		
10841!	CH66B47		
10842!	CH66B59	On track between Malimabatso River and Kao Mine, northern Basutoland	Cox and Hornung, 1966
10843'	CH66B61		
10844!	CH66B62		
10845!	CH66B63		
10846!	CH66B66	On track from Leribe, between base of basalt succession and Letele Pass, northern Basutoland	Cox and Hornung, 1966
10847!	CH66B67		
10848!	CH66B69		
10849!	CH66B70		
10850!	CH66B71		
10851'	CH66B72		
10852!	CH66B74		
10853!	CH66B76		
10854!	CH66B78		

Analysis number	Rock number	Description and locality	Reference
10855'	BVL714	Lavas from Barkly East	Lombaard, 1952
10856'	BVL715		
10857'	BVL726		
10858'	BVL752	Lavas from northern Lebombo	Lombaard, 1952
10859'	BVL763		
10860'	BVL774		
10861'	BVL775		
10862'	S19400R	Drakensberg lavas, Orange River and Matatiele	Stockley, 1940
10863'	S1940M		
10864'	DB1930.1	Zuurberg lava, De Vlei, Basutoland	Daly and Barth, 1930
10865!	CMHBU1	Nyamandhlovu, Rhodesia	Cox and others, 1967
10866!	CMHBU2		
10867!	CMHBU3		
10868!	CMHBU4		
10869!	CMHBU5		
10870!	CMHBU6		
10871!	CMHBU7		
10872!	CMHBU8		
10873!	CMHF1	Featherstone, Rhodesia	Cox and others, 1967
10874!	CMHF2		
10875!	CMHF3		
10876!	CMHF4		
10877!	CMHF6		
10878!	CMHF8		
10879!	CMHW3	Wankie, Rhodesia	Cox and others, 1967
10880!	CMHW5		
10881!	CMHC922	Nuanetsi, Rhodesia	Cox and others, 1967
10882!	CMHLM341		
10883!	CMHLM126		
10884!	CMHKC58		
10885!	CMHLM619A		
10886!	CMHDW389		
10887!	CMHC868		
10888!	CMHDW21		
10889!	CMHLM434		
10890!	CMHLM436		
10891!	CMHLM428		
10892!	CMHKC37		
10893!	CMHLM432		

Analysis number	Rock number	Description and locality	Reference
10894!	CMHS4	Swaziland	Cox and others, 1967
10895!	CMHS5		
10896!	CMHS9		
10897!	CMHS10		
10898!	CMHS11		
10899!	CMHS13		
10900!	CMHS17		

f. Hawaiian tholeiitic rocks used only in preparation of Fig. 61

Number of analyses	Description and locality	Reference
8	Uwekahuna laccolith, Kilauea Caldera	Murata and Richter, 1961
4	Basalt flows, Kilauea Caldera	Murata and Richter, 1961
6	Basalts of 1921 Kilauea eruption	Tilley, 1960
8	Basalts of 1955 flank eruption of Kilauea in east Puna	Tilley, 1960
11	Koolau Basalt Series, Oahu	Wentworth and Winchell, 1947
2	Lavas from lower and upper vents of 1840 eruption of Kilauea	MacDonald, 1949
2	Earliest and latest lavas from 9,200 ft. vent of 1942 eruption of Mauna Loa	MacDonald, 1949
2	Flank vent and pumice phase of 1926 eruption of Mauna Loa	MacDonald, 1949
39	Lower member of Waianae Volcanic Series, Oahu	MacDonald and Katsura, 1964
5	Middle member of Waianae Volcanic Series, Oahu	MacDonald and Katsura, 1964
14	Pololu Volcanic Series (lower member of Kohala volcano)	MacDonald and Katsura, 1964
2	Upper member of Hamakua Volcanic Series (intermediate member of Mauna Kea volcano)	MacDonald and Katsura, 1964

Number of analyses	Description and locality	Reference
6	Olokele Formation, Waimea Canyon Volcanic Series, Kauai	MacDonald and Katsura, 1964
1	Napali Formation, Waimea Canyon Volcanic Series, Kauai	MacDonald and Katsura, 1964
3	Makaweli Formation, Waimea Canyon Volcanic Series, Kauai	MacDonald and Katsura, 1964
22	Wailuku Volcanic Series, West Maui volcano	MacDonald and Katsura, 1964
6	Historic members of Kau Volcanic Series, Mauna Loa	MacDonald and Katsura, 1964
3	Upper part of Honomanu Volcanic Series, Haleakala (East Maui) volcano	MacDonald and Katsura, 1964
3	Historic members of Puna Volcanic Series, Kilauea	MacDonald and Katsura, 1964

TABLE XVII

CHEMICAL ANALYSES OF SPECIMENS FROM
OTHER INTRUSIONS IN THE THERON MOUNTAINS

Analyses (weight per cent)

	3742	3743	3659	3744	3745	3657	3747	3679	3655	3656	3746	3666	3652	3711	3658	3712	3677	3651	3671	3653	3684	10655	3685	100
SiO_2	50.31	49.52	48.83	51.66	52.93	51.21	48.36	48.13	52.09	48.59	49.03	50.56	48.21	54.96	49.69	51.24	51.67	48.53	49.89	51.82	49.86	51.51	50.85	51.
TiO_2	1.16	0.93	0.68	1.32	1.31	1.35	0.92	1.11	1.39	0.88	0.96	1.22	0.90	0.91	0.99	0.98	1.05	0.88	1.03	1.11	0.97	0.94	1.02	0.
Al_2O_3	13.72	14.84	16.75	13.03	12.92	12.46	15.47	13.98	13.35	16.66	16.00	12.41	15.22	16.73	16.88	16.89	13.79	17.48	16.11	15.45	13.06	15.54	15.00	16
Fe_2O_3	3.31	3.11	2.31	4.25	5.15	3.58	2.94	2.84	3.75	2.63	1.83	2.93	2.17	3.32	1.84	2.64	2.78	2.52	1.60	3.45	2.78	1.58	2.91	1.
FeO	8.71	7.88	6.03	9.22	8.30	10.43	7.78	9.00	8.55	7.91	8.53	10.56	8.42	5.53	8.53	7.74	6.81	8.12	8.94	5.96	7.19	7.51	6.80	7
MnO	0.17	0.15	0.12	0.18	0.17	0.18	0.14	0.15	0.16	0.14	0.14	0.17	0.15	0.13	0.14	0.15	0.13	0.14	0.14	0.13	0.14	0.14	0.14	0
MgO	6.01	5.51	11.09	3.80	3.74	4.46	9.56	5.56	4.68	7.92	8.99	4.69	9.80	6.61	7.57	6.01	9.24	8.04	7.43	6.66	10.56	7.88	8.17	7
CaO	10.43	10.59	10.89	8.91	8.37	8.69	10.45	9.69	9.07	10.51	10.19	9.03	10.61	6.93	10.29	9.70	9.16	10.12	10.15	9.32	9.91	9.58	9.82	9
Na_2O	2.66	2.52	1.89	2.51	2.66	2.50	1.84	1.98	2.26	2.08	1.96	2.13	1.76	1.90	2.26	2.39	1.56	2.08	2.20	1.77	1.52	1.94	1.78	2
K_2O	0.99	0.95	0.39	1.02	1.35	1.00	0.62	1.69	1.18	0.64	0.71	1.07	0.30	1.52	0.73	0.84	0.80	0.77	0.76	1.11	0.72	0.65	0.81	0
P_2O_5	0.11	0.12	0.07	0.17	0.20	0.15	0.10	0.13	0.24	0.12	0.11	0.16	0.08	0.09	0.13	0.16	0.10	0.15	0.11	0.11	0.14	0.25	0.15	0
H_2O+	0.79	0.94	1.04	0.97	1.11	1.23	1.15	1.82	0.96	0.70	0.51	0.86	1.05	1.43	0.70	0.53	1.41	0.38	0.65	1.27	1.62	2.07	1.18	1
H_2O-	0.31	0.21	0.18	0.29	0.31	0.31	0.18	0.35	0.32	0.15	0.22	0.49	0.18	0.22	0.10	0.21	0.36	0.27	0.28	0.41	0.28	0.66	0.20	0
CO_2	1.83	1.73	1.63	1.00	0.85	0.94	1.37	0.76	1.15	1.16	1.75	1.21	1.43	1.76	1.28	0.55	1.57	0.92	1.60	1.14	1.42	0.05	1.39	0
Total	100.50	98.98	101.89	98.32	99.36	98.48	100.87	97.19	99.15	100.09	100.93	97.50	100.28	102.05	101.12	100.04	100.42	100.41	100.89	99.71	100.18	100.30	100.21	100

Trace elements (p.p.m.)

S	739	721	1211	880	267	457	1110	361	56	806	1137	332	1056	698	907	42	130	658	1470	882	2504	n.d.	1294	
Cr	155	144	491	63	53	64	557	143	265	530	526	71	566	413	515	546	688	687	456	524	832	500	635	
Ni	50	55	13	39	37	40	27	54	9	25	24	42	25	24	22	9	68	31	16	45	66	25	35	
Zn	88	76	67	96	96	108	84	90	100	86	87	96	84	94	90	88	99	88	83	96	87	n.d.	87	
Ga	18	19	16	18	18	18	17	16	17	16	18	18	16	17	18	16	17	16	14	17	15	18	14	
Rb	26	22	12	22	25	21	17	41	23	18	16	23	10	69	17	18	41	16	17	33	26	-	30	
Sr	181	202	247	156	155	173	187	224	174	191	194	152	191	250	190	195	264	197	189	202	162	65	178	
Y	25	21	12	29	33	31	18	23	28	17	18	30	19	21	19	18	22	17	19	26	25	20	26	
Zr	154	131	65	159	179	153	89	147	145	84	93	144	82	158	99	100	174	102	101	183	156	80	160	
Ba	269	280	178	386	402	357	239	336	419	235	245	329	198	514	258	296	327	260	268	366	296	140	307	
La	18	11	<3	20	20	28	10	14	15	6	8	16	9	19	14	10	18	7	11	22	14	-	17	
Ce	34	23	<3	45	44	39	16	33	30	15	22	32	7	43	19	12	30	22	29	37	35	n.d.	37	
Pb	6	6	9	<3	11	8	5	9	6	6	8	11	8	23	5	8	15	7	4	12	3	-	<3	
Th	<3	3	4	4	3	5	4	3	3	7	5	5	7	8	<3	7	6	3	4	3	6	n.d.	<3	

Analyses recalculated to 100 per cent anhydrous

SiO_2	50.62	50.61	48.51	53.23	54.04	52.82	48.59	50.65	53.22	48.96	48.94	52.59	48.67	54.74	49.53	51.60	52.38	48.65	49.91	52.86	50.73	52.79	51.45	
TiO_2	1.17	0.95	0.67	1.36	1.34	1.39	0.92	1.16	1.42	0.89	0.96	1.27	0.91	0.91	0.98	0.99	1.06	0.89	1.03	1.13	0.99	0.96	1.03	
Al_2O_3	13.80	15.17	16.64	13.42	13.19	12.85	15.54	14.71	13.64	16.79	15.96	12.91	15.37	16.67	16.83	17.01	13.98	17.52	16.11	15.76	13.29	15.93	15.18	
Fe_2O_3	3.33	3.18	2.29	4.38	5.26	3.69	2.95	2.99	3.83	2.65	1.83	3.05	2.19	3.31	1.83	2.66	2.82	2.53	1.60	3.52	2.83	1.62	2.94	
FeO	8.76	8.05	5.99	9.50	8.47	10.76	7.82	9.47	8.73	7.97	8.51	10.98	8.50	5.51	8.50	7.79	6.90	8.14	8.94	6.08	7.32	7.70	6.88	
MnO	0.17	0.15	0.11	0.18	0.17	0.19	0.14	0.16	0.16	0.14	0.14	0.18	0.15	0.12	0.14	0.16	0.14	0.14	0.14	0.13	0.14	0.14	0.14	
MgO	6.05	5.63	11.01	3.92	3.81	4.60	9.60	5.85	4.78	7.98	8.97	4.88	9.89	6.58	7.54	6.06	9.36	8.06	7.43	6.80	10.75	8.08	8.27	
CaO	10.49	10.82	10.81	9.17	8.55	8.96	10.50	10.20	9.27	10.59	10.17	9.39	10.71	6.91	10.26	9.77	9.28	10.14	10.15	9.50	10.08	9.82	9.93	
Na_2O	2.68	2.58	1.88	2.59	2.72	2.58	1.85	2.09	2.31	2.09	1.96	2.21	1.77	1.90	2.25	2.41	1.58	2.09	2.20	1.80	1.55	1.99	1.80	
K_2O	0.99	0.97	0.39	1.05	1.37	1.03	0.62	1.78	1.21	0.65	0.70	1.11	0.31	1.51	0.73	0.85	0.81	0.77	0.76	1.14	0.73	0.67	0.8	
P_2O_5	0.11	0.12	0.07	0.17	0.21	0.16	0.10	0.14	0.25	0.12	0.11	0.17	0.08	0.09	0.13	0.16	0.10	0.15	0.11	0.11	0.14	0.26	0.1	
CO_2	1.84	1.77	1.62	1.03	0.87	0.97	1.38	0.80	1.17	1.17	1.75	1.26	1.44	1.75	1.28	0.55	1.59	0.92	1.60	1.16	1.44	0.05	1.4	

C.I.P.W. Norms

TABLE XVII

CHEMICAL ANALYSES OF SPECIMENS FROM
OTHER INTRUSIONS IN THE THERON MOUNTAINS

	3745	3657	3747	3679	3655	3656	3746	3666	3652	3711	3658	3712	3677	3651	3671	3653	3684	10655	3685	10654	3696	3689	3709	3719
	52.93	51.21	48.36	48.13	52.09	48.59	49.03	50.56	48.21	54.96	49.69	51.24	51.67	48.53	49.89	51.82	49.86	51.51	50.85	51.67	49.22	51.05	53.28	56.45
	1.31	1.35	0.92	1.11	1.39	0.88	0.96	1.22	0.90	0.91	0.99	0.98	1.05	0.88	1.03	1.11	0.97	0.94	1.02	0.84	0.69	1.00	1.30	1.97
	12.92	12.46	15.47	13.98	13.35	16.66	16.00	12.41	15.22	16.73	16.88	16.89	13.79	17.48	16.11	15.45	13.06	15.54	15.00	16.36	13.15	14.88	14.73	10.87
	5.15	3.58	2.94	2.84	3.75	2.63	1.83	2.93	2.17	3.32	1.84	2.64	2.78	2.52	1.60	3.45	2.78	1.58	2.91	1.18	3.14	1.92	2.17	6.82
	8.30	10.43	7.78	9.00	8.55	7.91	8.53	10.56	8.42	5.53	8.53	7.74	6.81	8.12	8.94	5.96	7.19	7.51	6.80	7.52	7.01	7.64	7.24	8.00
	0.17	0.18	0.14	0.15	0.16	0.14	0.14	0.17	0.15	0.13	0.14	0.15	0.13	0.14	0.14	0.13	0.14	0.14	0.14	0.15	0.15	0.14	0.13	0.17
	3.74	4.46	9.56	5.56	4.68	7.92	8.99	4.69	9.80	6.61	7.57	6.01	9.24	8.04	7.43	6.66	10.56	7.88	8.17	7.24	11.51	7.05	7.77	1.66
	8.37	8.69	10.45	9.69	9.07	10.51	10.19	9.03	10.61	6.93	10.29	9.70	9.16	10.12	10.15	9.32	9.91	9.58	9.82	9.46	10.90	10.21	8.27	6.31
	2.66	2.50	1.84	1.98	2.26	2.08	1.96	2.13	1.76	1.90	2.26	2.39	1.56	2.08	2.20	1.77	1.52	1.94	1.78	2.13	1.37	1.88	1.96	2.24
	1.35	1.00	0.62	1.69	1.18	0.64	0.71	1.07	0.30	1.52	0.73	0.84	0.80	0.77	0.76	1.11	0.72	0.65	0.81	0.65	0.41	0.79	1.46	1.91
	0.20	0.15	0.10	0.13	0.24	0.12	0.11	0.16	0.08	0.09	0.13	0.16	0.10	0.15	0.11	0.11	0.14	0.25	0.15	0.13	0.08	0.14	0.17	0.26
	1.11	1.23	1.15	1.82	0.96	0.70	0.51	0.86	1.05	1.43	0.70	0.53	1.41	0.38	0.65	1.27	1.62	2.07	1.18	1.47	1.57	1.00	1.03	1.41
	0.31	0.31	0.18	0.35	0.32	0.15	0.22	0.49	0.18	0.22	0.10	0.21	0.36	0.27	0.28	0.41	0.28	0.66	0.20	0.48	0.43	0.13	0.23	0.39
	0.85	0.94	1.37	0.76	1.15	1.16	1.75	1.21	1.43	1.76	1.28	0.55	1.57	0.92	1.60	1.14	1.42	0.05	1.39	0.83	1.33	1.55	1.12	0.34
	99.36	98.48	100.87	97.19	99.15	100.09	100.93	97.50	100.28	102.05	101.12	100.04	100.42	100.41	100.89	99.71	100.18	100.30	100.21	100.11	100.98	99.38	100.86	98.80

	267	457	1110	361	56	806	1137	332	1056	698	907	42	130	658	1470	882	2504	n.d.	1294	n.d.	309	1121	1142	1037
	53	64	557	143	265	530	526	71	566	413	515	546	688	687	456	524	832	500	635	500	756	645	702	17
	37	40	27	54	9	25	24	42	25	24	22	9	68	31	16	45	66	25	35	20	56	33	104	15
	96	108	84	90	100	86	87	96	84	94	90	88	99	88	83	96	87	n.d.	87	n.d.	73	83	101	108
	18	18	17	16	17	16	18	18	16	17	18	16	17	16	14	17	15	18	14	18	15	16	17	19
	25	21	17	41	23	18	16	23	10	69	17	18	41	16	17	33	26	-	30	-	22	26	39	59
	155	173	187	224	174	191	194	152	191	250	190	195	264	197	189	202	162	65	178	125	140	173	217	134
	33	31	18	23	28	17	18	30	19	21	19	18	22	17	19	26	25	20	26	20	18	27	29	37
	179	153	89	147	145	84	93	144	82	158	99	100	174	102	101	183	156	80	160	80	78	163	229	238
	402	357	239	336	419	235	245	329	198	514	258	296	327	260	268	366	296	140	307	200	129	391	442	528
	20	28	10	14	15	6	8	16	9	19	14	10	18	7	11	22	14	-	17	-	6	15	22	34
	44	39	16	33	30	15	22	32	7	43	19	12	30	22	29	37	35	n.d.	37	n.d.	19	28	48	66
	11	8	5	9	6	6	8	11	8	23	5	8	15	7	4	12	3	-	<3	-	5	11	14	17
	3	5	4	3	3	7	5	5	7	8	<3	7	6	3	4	3	6	n.d.	<3	n.d.	<3	5	4	7

cent anhydrous

	54.04	52.82	48.59	50.65	53.22	48.96	48.94	52.59	48.67	54.74	49.53	51.60	52.38	48.65	49.91	52.86	50.73	52.79	51.45	52.64	49.73	51.96	53.49	58.20
	1.34	1.39	0.92	1.16	1.42	0.89	0.96	1.27	0.91	0.91	0.98	0.99	1.06	0.89	1.03	1.13	0.99	0.96	1.03	0.86	0.70	1.02	1.31	2.03
	13.19	12.85	15.54	14.71	13.64	16.79	15.96	12.91	15.37	16.67	16.83	17.01	13.98	17.52	16.11	15.76	13.29	15.93	15.18	16.67	13.28	15.14	14.79	11.21
	5.26	3.69	2.95	2.99	3.83	2.65	1.83	3.05	2.19	3.31	1.83	2.66	2.82	2.53	1.60	3.52	2.83	1.62	2.94	1.20	3.17	1.95	2.18	7.03
	8.47	10.76	7.82	9.47	8.73	7.97	8.51	10.98	8.50	5.51	8.50	7.79	6.90	8.14	8.94	6.08	7.32	7.70	6.88	7.66	7.08	7.78	7.27	8.25
	0.17	0.19	0.14	0.16	0.16	0.14	0.14	0.18	0.15	0.12	0.14	0.16	0.14	0.14	0.14	0.13	0.14	0.14	0.14	0.15	0.16	0.14	0.13	0.17
	3.81	4.60	9.60	5.85	4.78	7.98	8.97	4.88	9.89	6.58	7.54	6.06	9.36	8.06	7.43	6.80	10.75	8.08	8.27	7.38	11.63	7.17	7.80	1.71
	8.55	8.96	10.50	10.20	9.27	10.59	10.17	9.39	10.71	6.91	10.26	9.77	9.28	10.14	10.15	9.50	10.08	9.82	9.93	9.64	11.01	10.40	8.30	6.50
	2.72	2.58	1.85	2.09	2.31	2.09	1.96	2.21	1.77	1.90	2.25	2.41	1.58	2.09	2.20	1.80	1.55	1.99	1.80	2.17	1.39	1.91	1.96	2.31
	1.37	1.03	0.62	1.78	1.21	0.65	0.70	1.11	0.31	1.51	0.73	0.85	0.81	0.77	0.76	1.14	0.73	0.67	0.81	0.66	0.42	0.81	1.46	1.97
	0.21	0.16	0.10	0.14	0.25	0.12	0.11	0.17	0.08	0.09	0.13	0.16	0.10	0.15	0.11	0.11	0.14	0.26	0.15	0.13	0.08	0.14	0.17	0.26
	0.87	0.97	1.38	0.80	1.17	1.17	1.75	1.26	1.44	1.75	1.28	0.55	1.59	0.92	1.60	1.16	1.44	0.05	1.41	0.85	1.34	1.58	1.12	0.35

	0.00	0.68	8.59	0.00	0.00	6.48	0.00	11.24	0.00	3.07	6.22	0.00	0.00	8.14	2.04	4.23	4.52	3.65	0.50	4.53	5.98	22.16		
	3.71	10.61	7.22	3.88	4.23	6.65	1.84	9.09	4.35	5.03	4.87	4.62	4.56	6.79	4.40	3.94	4.88	3.95	2.50	4.85	8.75	11.70		
	15.84	17.80	19.77	17.93	16.86	18.95	15.24	16.32	19.30	20.47	13.57	17.82	18.93	15.42	13.29	16.83	15.43	18.51	11.90	16.43	16.81	19.63		

C.I.P.W. Norms

Q.	0.91	1.33	0.00	8.66	10.01	6.59	0.00	0.68	8.59	0.00	0.00	6.48	0.00	11.24	0.00	3.07	6.22	0.00	0.00	8.14	2.04	4.23	4.52	3.65
Or	5.97	5.83	2.33	6.26	8.18	6.14	3.71	10.61	7.22	3.88	4.23	6.65	1.84	9.09	4.35	5.03	4.87	4.62	4.56	6.79	4.40	3.94	4.88	3.95
Ab	23.09	22.22	16.15	22.13	23.18	22.01	15.84	17.80	19.77	17.93	16.86	18.95	15.24	16.32	19.30	20.47	13.57	17.82	18.93	15.42	13.29	16.83	15.43	18.51
An	23.12	27.44	36.41	22.12	19.92	20.65	32.73	25.72	23.56	34.90	33.27	22.29	33.55	33.08	34.09	33.28	29.12	36.48	32.36	31.94	27.53	32.58	31.38	34.07
Wo_{Di}	12.19	11.03	7.36	9.49	8.98	9.68	8.11	10.18	8.90	7.28	7.23	9.92	8.28	0.52	6.92	6.00	7.10	5.57	7.55	6.28	9.30	6.04	7.35	5.54
En_{Di}	6.61	5.99	5.18	4.25	4.44	4.23	5.24	5.19	4.54	4.40	4.35	4.30	5.15	0.35	3.95	3.36	4.76	3.34	4.18	4.18	6.30	3.64	4.80	3.20
Fs_{Di}	5.15	4.66	1.55	5.19	4.36	5.44	2.33	4.74	4.14	2.49	2.49	5.62	2.63	0.13	2.68	2.40	1.81	1.94	3.08	1.64	2.29	2.08	2.04	2.08
En_{Hy}	8.73	8.27	13.67	5.61	5.14	7.35	14.54	9.50	7.50	12.55	13.32	8.01	15.46	16.34	11.80	11.80	18.92	11.67	13.12	12.94	20.86	16.48	16.08	15.32
Fs_{Hy}	6.80	6.42	4.09	6.85	5.04	9.46	6.48	8.66	6.83	7.10	7.63	10.46	7.89	6.09	8.00	8.43	7.19	6.78	9.68	5.07	7.59	9.40	6.84	9.96
Fo	0.00	0.00	6.32	0.00	0.00	0.00	3.13	0.00	0.00	2.21	3.56	0.00	3.07	0.00	2.30	0.00	0.00	3.68	1.06	0.00	0.00	0.00	0.00	0.00
Fa	0.00	0.00	2.08	0.00	0.00	0.00	1.54	0.00	0.00	1.38	2.25	0.00	1.73	0.00	1.72	0.00	0.00	2.36	0.86	0.00	0.00	0.00	0.00	0.00
Mt	4.92	4.69	3.38	6.41	7.69	5.41	4.34	4.37	5.62	3.89	2.70	4.47	3.22	4.88	2.69	3.88	4.15	3.70	2.36	5.16	4.16	2.35	4.33	1.76
Il	2.25	1.83	1.30	2.61	2.57	2.67	1.78	2.23	2.72	1.71	1.85	2.44	1.75	1.76	1.89	1.88	2.04	1.70	1.99	2.17	1.90	1.83	1.99	1.64
Ap	0.25	0.28	0.18	0.41	0.49	0.37	0.23	0.33	0.60	0.29	0.27	0.41	0.20	0.21	0.31	0.39	0.24	0.35	0.26	0.26	0.35	0.61	0.36	0.32

Elements (weight per cent)

Si^{4+}	23.66	23.66	22.68	24.88	25.26	24.69	22.72	23.68	24.88	22.89	22.88	24.59	22.75	25.59	23.15	24.13	24.49	22.74	23.33	24.71	23.72	24.68	24.05	24.61
Ti^{4+}	0.70	0.57	0.40	0.82	0.80	0.83	0.55	0.70	0.85	0.53	0.57	0.76	0.54	0.55	0.59	0.59	0.64	0.53	0.62	0.68	0.59	0.58	0.62	0.51
Al^{3+}	7.30	8.03	8.80	7.10	6.98	6.80	8.22	7.79	7.22	8.89	8.45	6.83	8.13	8.82	8.91	9.00	7.40	9.27	8.53	8.34	7.03	8.43	8.03	8.82
Fe^{3+}	2.33	2.22	1.60	3.06	3.68	2.58	2.07	2.09	2.68	1.85	1.28	2.13	1.53	2.31	1.28	1.86	1.97	1.77	1.12	2.46	1.98	1.13	2.06	0.84
Fe^{2+}	6.81	6.26	4.66	7.38	6.59	8.36	6.08	7.36	6.79	6.20	6.62	8.54	6.61	4.28	6.61	6.06	5.37	6.33	6.95	4.73	5.69	5.98	5.35	5.95
Mn^{2+}	0.13	0.12	0.09	0.14	0.13	0.15	0.11	0.12	0.13	0.11	0.11	0.14	0.11	0.10	0.11	0.12	0.11	0.11	0.11	0.10	0.11	0.11	0.11	0.12
Mg^{2+}	3.65	3.39	6.64	2.36	2.30	2.78	5.79	3.53	2.88	4.81	5.41	2.94	5.97	3.97	4.55	3.65	5.65	4.86	4.48	4.10	6.48	4.87	4.99	4.45
Ca^{2+}	7.50	7.73	7.73	6.56	6.11	6.40	7.50	7.29	6.63	7.57	7.27	6.71	7.66	4.94	7.33	6.98	6.64	7.25	7.25	6.79	7.21	7.02	7.10	6.89
Na^{+}	1.99	1.91	1.39	1.92	2.01	1.91	1.37	1.55	1.71	1.55	1.45	1.64	1.32	1.41	1.67	1.78	1.17	1.55	1.63	1.34	1.15	1.48	1.33	1.61
K^{+}	0.82	0.80	0.32	0.87	1.14	0.85	0.51	1.48	1.00	0.54	0.58	0.92	0.25	1.25	0.60	0.70	0.67	0.64	0.63	0.94	0.61	0.55	0.68	0.55
P^{5+}	0.05	0.05	0.03	0.07	0.09	0.07	0.04	0.06	0.11	0.05	0.05	0.07	0.04	0.04	0.06	0.07	0.04	0.06	0.05	0.05	0.06	0.11	0.07	0.06
C^{4+}	0.50	0.48	0.44	0.28	0.24	0.26	0.38	0.22	0.32	0.32	0.48	0.34	0.39	0.48	0.35	0.15	0.43	0.25	0.44	0.32	0.39	0.01	0.38	0.23
O^{2-}	44.56	44.76	45.21	44.54	44.66	44.30	44.66	44.14	44.80	44.69	44.85	44.38	44.69	46.26	44.79	44.90	45.43	44.63	44.85	45.44	44.98	45.04	45.23	45.36

Useful Ratios

$Th \times 10^4$ /K	<3.7	3.8	12.5	4.7	2.7	6.0	7.9	<2.1	3.1	13.2	8.5	5.6	28.0	6.3	<4.9	10.0	9.0	4.7	6.3	3.3	10.0	-	<45	-
K /Rb	315	358	270	384	447	395	301	343	427	297	366	385	252	183	356	388	162	401	371	280	230	-	223	-
Rb/Sr	0.14	0.11	0.05	0.14	0.16	0.12	0.09	0.18	0.13	0.09	0.08	0.15	0.05	0.28	0.09	0.09	0.16	0.08	0.09	0.16	0.16	-	0.17	-
Cr/Ni	3.10	2.62	37.7	1.62	1.43	1.60	20.6	2.65	29.5	21.2	21.9	1.69	22.6	17.2	23.4	60.7	11.2	22.2	28.5	11.6	12.1	20.0	18.1	25.0

a. Area north-east of Goldsmith Glacier

3742	Z.487.3	Chilled porphyritic olivine-dolerite, upper contact of 30 m. thick sill above scarp-capping sill.
3743	Z.487.2	Coarse-grained olivine-dolerite, upper part of same sill as 3742.
3659	Z.466.3	Chilled dolerite, 0.8 m. above lower contact of minor sill above scarp-capping sill.
3744	Z.509.1	Fine-grained quartz-dolerite, 6 m. wide dyke above scarp-capping sill.
3745	Z.463.2	Altered coarse-grained quartz-dolerite, minor sill above scarp-capping sill, middle of sill.
3657	Z.463.3	Altered chilled dolerite, top of same minor sill as 3745.

b. Area between Goldsmith and Jeffries Glaciers

3747	Z.489.1	Fine-grained olivine-dolerite, 1 m. above lower contact of 20 m. thick sill just below scarp-capping sill.
3679	Z.489.4	Fine-grained dolerite, about 6 m. below upper contact of 20-30 m. thick sill at base of outcrop.
3655	Z.461.1	Altered coarse-grained subophitic dolerite, lower part of minor sill above scarp-capping sill.
3656	Z.461.2	Fine-grained olivine-dolerite, upper part of same sill as 3655.
3746	Z.488.1	Fine-grained olivine-dolerite, 1.2 m. above lower contact of

c. Area between Jeffries Glacier and the unnamed southe

3677	Z.481.10	Altered chilled dolerite, 1 m. wide capping sill.
3651	Z.453.1	Medium-grained ophitic olivine-dole thick sill above scarp-capping sill
3671	Z.453.2	Chilled olivine-dolerite, top of sa
3653	Z.453.3	Chilled dolerite, 1 m. wide dyke be 3671 and thin minor sill above.

d. Area south-west of the unnamed southern glacier

3684	Z.477.7	Medium-grained variolitic dolerite, immediately below basal sill of Coa
10655	TAE350/6	Chilled dolerite. contact of same si Stephenson, 1966).
3685	Z.477.11	Fine-grained dolerite, middle of 3m. lowest below basal sill of Coalseam
10654	TAE351/7	Chilled porphyritic dolerite, top c 3685 (after Stephenson, 1966).
3696	Z.478.3	Altered porphyritic chilled dolerite by thick wedging sill of Coalseam C

8.66	10.01	6.59	0.00	0.68	8.59	0.00	0.00	6.48	0.00	11.24	0.00	3.07	6.22	0.00	0.00	8.14	2.04	4.23	4.52	3.65	0.50	4.53	5.98	22.16
6.26	8.18	6.14	3.71	10.61	7.22	3.88	4.23	6.65	1.84	9.09	4.35	5.03	4.87	4.62	4.56	6.79	4.40	3.94	4.88	3.95	2.50	4.85	8.75	11.70
22.13	23.18	22.01	15.84	17.80	19.77	17.93	16.86	18.95	15.24	16.32	19.30	20.47	13.57	17.82	18.93	15.42	13.29	16.83	15.43	18.51	11.90	16.43	16.81	19.63
22.12	19.92	20.65	32.73	25.72	23.56	34.90	33.27	22.29	33.55	33.08	34.09	33.28	29.12	36.48	32.36	31.94	27.53	32.58	31.38	34.07	29.17	30.83	27.52	14.42
9.49	8.98	9.68	8.11	10.18	8.90	7.28	7.23	9.92	8.28	0.52	6.92	6.00	7.10	5.57	7.55	6.28	9.30	6.04	7.35	5.54	10.71	8.60	5.43	6.77
4.25	4.44	4.23	5.24	5.19	4.54	4.40	4.35	4.30	5.15	0.35	3.95	3.36	4.76	3.34	4.18	4.18	6.30	3.64	4.80	3.20	7.41	5.03	3.41	2.75
5.19	4.36	5.44	2.33	4.74	4.14	2.49	2.49	5.62	2.63	0.13	2.68	2.40	1.81	1.94	3.08	1.64	2.29	2.08	2.04	2.08	2.43	3.16	1.69	4.07
5.61	5.14	7.35	14.54	9.50	7.50	12.55	13.32	8.01	15.46	16.34	11.80	11.80	18.92	11.67	13.12	12.94	20.86	16.48	16.08	15.32	21.94	13.12	16.24	1.52
6.85	5.04	9.46	6.48	8.66	6.83	7.10	7.63	10.46	7.89	6.09	8.00	8.43	7.19	6.78	9.68	5.07	7.59	9.40	6.84	9.96	7.21	8.26	8.06	2.26
0.00	0.00	0.00	3.13	0.00	0.00	2.21	3.56	0.00	3.07	0.00	2.30	0.00	0.00	3.68	1.06	0.00	0.00	0.00	0.00	0.00	0.00	0.00	0.00	0.00
0.00	0.00	0.00	1.54	0.00	0.00	1.38	2.25	0.00	1.73	0.00	1.72	0.00	0.00	2.36	0.86	0.00	0.00	0.00	0.00	0.00	0.00	0.00	0.00	0.00
6.41	7.69	5.41	4.34	4.37	5.62	3.89	2.70	4.47	3.22	4.88	2.69	3.88	4.15	3.70	2.36	5.16	4.16	2.35	4.33	1.76	4.66	2.88	3.19	10.23
2.61	2.57	2.67	1.78	2.23	2.72	1.71	1.85	2.44	1.75	1.76	1.89	1.88	2.04	1.70	1.99	2.17	1.90	1.83	1.99	1.64	1.35	1.97	2.51	3.87
0.41	0.49	0.37	0.23	0.33	0.60	0.29	0.27	0.41	0.20	0.21	0.31	0.39	0.24	0.35	0.26	0.26	0.35	0.61	0.36	0.32	0.20	0.35	0.41	0.62

24.88	25.26	24.69	22.72	23.68	24.88	22.89	22.88	24.59	22.75	25.59	23.15	24.13	24.49	22.74	23.33	24.71	23.72	24.68	24.05	24.61	23.25	24.29	25.01	27.21
0.82	0.80	0.83	0.55	0.70	0.85	0.53	0.57	0.76	0.54	0.55	0.59	0.59	0.64	0.53	0.62	0.68	0.59	0.58	0.62	0.51	0.42	0.61	0.78	1.22
7.10	6.98	6.80	8.22	7.79	7.22	8.89	8.45	6.83	8.13	8.82	8.91	9.00	7.40	9.27	8.53	8.34	7.03	8.43	8.03	8.82	7.03	8.01	7.83	5.93
3.06	3.68	2.58	2.07	2.09	2.68	1.85	1.28	2.13	1.53	2.31	1.28	1.86	1.97	1.77	1.12	2.46	1.98	1.13	2.06	0.84	2.22	1.37	1.52	4.92
7.38	6.59	8.36	6.08	7.36	6.79	6.20	6.62	8.54	6.61	4.28	6.61	6.06	5.37	6.33	6.95	4.73	5.69	5.98	5.35	5.95	5.50	6.04	5.65	6.41
0.14	0.13	0.15	0.11	0.12	0.13	0.11	0.11	0.14	0.11	0.10	0.11	0.12	0.11	0.11	0.11	0.10	0.11	0.11	0.11	0.12	0.12	0.11	0.10	0.13
2.36	2.30	2.78	5.79	3.53	2.88	4.81	5.41	2.94	5.97	3.97	4.55	3.65	5.65	4.86	4.48	4.10	6.48	4.87	4.99	4.45	7.01	4.33	4.71	1.03
6.56	6.11	6.40	7.50	7.29	6.63	7.57	7.27	6.71	7.66	4.94	7.33	6.98	6.64	7.25	7.25	6.79	7.21	7.02	7.10	6.89	7.87	7.43	5.93	4.65
1.92	2.01	1.91	1.37	1.55	1.71	1.55	1.45	1.64	1.32	1.41	1.67	1.78	1.17	1.55	1.63	1.34	1.15	1.48	1.33	1.61	1.03	1.42	1.46	1.72
0.87	1.14	0.85	0.51	1.48	1.00	0.54	0.58	0.92	0.25	1.25	0.60	0.70	0.67	0.64	0.63	0.94	0.61	0.55	0.68	0.55	0.35	0.67	1.22	1.64
0.07	0.09	0.07	0.04	0.06	0.11	0.05	0.05	0.07	0.04	0.04	0.06	0.07	0.04	0.06	0.05	0.05	0.06	0.11	0.07	0.06	0.04	0.06	0.07	0.11
0.28	0.24	0.26	0.38	0.22	0.32	0.32	0.48	0.34	0.39	0.48	0.35	0.15	0.43	0.25	0.44	0.32	0.39	0.01	0.38	0.23	0.37	0.43	0.31	0.10
44.54	44.66	44.30	44.66	44.14	44.80	44.69	44.85	44.38	44.69	46.26	44.79	44.90	45.43	44.63	44.85	45.44	44.98	45.04	45.23	45.36	44.79	45.23	45.41	44.94

4.7	2.7	6.0	7.9	<2.1	3.1	13.2	8.5	5.6	28.0	6.3	<4.9	10.0	9.0	4.7	6.3	3.3	10.0	-	<45	-	<8.8	7.6	3.3	4.4
384	447	395	301	343	427	297	366	385	252	183	356	388	162	401	371	280	230	-	223	-	156	253	310	269
0.14	0.16	0.12	0.09	0.18	0.13	0.09	0.08	0.15	0.05	0.28	0.09	0.09	0.16	0.08	0.09	0.16	0.16	-	0.17	-	0.16	0.15	0.18	0.44
1.62	1.43	1.60	20.6	2.65	29.5	21.2	21.9	1.69	22.6	17.2	23.4	60.7	11.2	22.2	28.5	11.6	12.1	20.0	18.1	25.0	13.4	19.5	6.8	1.13

f Goldsmith Glacier

Chilled porphyritic olivine-dolerite, upper contact of 30 m. thick sill above scarp-capping sill.
Coarse-grained olivine-dolerite, upper part of same sill as 3742.
Chilled dolerite, 0.8 m. above lower contact of minor sill above scarp-capping sill.
Fine-grained quartz-dolerite, 6 m. wide dyke above scarp-capping sill.
Altered coarse-grained quartz-dolerite, minor sill above scarp-capping sill, middle of sill.
Altered chilled dolerite, top of same minor sill as 3745.

lsmith and Jeffries Glaciers

Fine-grained olivine-dolerite, 1 m. above lower contact of 20 m. thick sill just below scarp-capping sill.
Fine-grained dolerite, about 6 m. below upper contact of 20-30 m. thick sill at base of outcrop.
Altered coarse-grained subophitic dolerite, lower part of minor sill above scarp-capping sill.
Fine-grained olivine-dolerite, upper part of same sill as 3655.
Fine-grained olivine-dolerite, 1.2 m. above lower contact of

c. Area between Jeffries Glacier and the unnamed southern glacier

3677	Z.481.10	Altered chilled dolerite, 1 m. wide dyke which cuts scarp-capping sill.
3651	Z.453.1	Medium-grained ophitic olivine-dolerite. Middle part of 15 m. thick sill above scarp-capping sill.
3671	Z.453.2	Chilled olivine-dolerite, top of same sill as 3651.
3653	Z.453.3	Chilled dolerite, 1 m. wide dyke between sill of 3651 and 3671 and thin minor sill above.

d. Area south-west of the unnamed southern glacier

3684	Z.477.7	Medium-grained variolitic dolerite, middle of minor sill immediately below basal sill of Coalseam Cliffs.
10655	TAE350/6	Chilled dolerite, contact of same sill as 3684 (after Stephenson, 1966).
3685	Z.477.11	Fine-grained dolerite, middle of 3m. thick sill which is lowest below basal sill of Coalseam Cliffs.
10654	TAE351/7	Chilled porphyritic dolerite, top contact of same sill as 3685 (after Stephenson, 1966).
3696	Z.478.3	Altered porphyritic chilled dolerite, thin wedge intruded by thick wedging sill of Coalseam Cliffs.
	Z.478.7	Chilled dolerite, upper contact of 1.2 m. thick sill between

Si^{4+}	23.66	23.66	22.68	24.88	25.26	24.69	22.72	23.68	24.88	22.89	22.88	24.59	22.75	25.59	23.15	24.13	24.49	22.74	23.33	24.71	23.72	24.68	24.0
Ti^{4+}	0.70	0.57	0.40	0.82	0.80	0.83	0.55	0.70	0.85	0.53	0.57	0.76	0.54	0.55	0.59	0.59	0.64	0.53	0.62	0.68	0.59	0.58	0.6
Al^{3+}	7.30	8.03	8.80	7.10	6.98	6.80	8.22	7.79	7.22	8.89	8.45	6.83	8.13	8.82	8.91	9.00	7.40	9.27	8.53	8.34	7.03	8.43	8.0
Fe^{3+}	2.33	2.22	1.60	3.06	3.68	2.58	2.07	2.09	2.68	1.85	1.28	2.13	1.53	2.31	1.28	1.86	1.97	1.77	1.12	2.46	1.98	1.13	2.0
Fe^{2+}	6.81	6.26	4.66	7.38	6.59	8.36	6.08	7.36	6.79	6.20	6.62	8.54	6.61	4.28	6.61	6.06	5.37	6.33	6.95	4.73	5.69	5.98	5.3
Mn^{2+}	0.13	0.12	0.09	0.14	0.13	0.15	0.11	0.12	0.13	0.11	0.11	0.14	0.11	0.10	0.11	0.12	0.11	0.11	0.11	0.10	0.11	0.11	0.1
Mg^{2+}	3.65	3.39	6.64	2.36	2.30	2.78	5.79	3.53	2.88	4.81	5.41	2.94	5.97	3.97	4.55	3.65	5.65	4.86	4.48	4.10	6.48	4.87	4.9
Ca^{2+}	7.50	7.73	7.73	6.56	6.11	6.40	7.50	7.29	6.63	7.57	7.27	6.71	7.66	4.94	7.33	6.98	6.64	7.25	7.25	6.79	7.21	7.02	7.1
Na^{+}	1.99	1.91	1.39	1.92	2.01	1.91	1.37	1.55	1.71	1.55	1.45	1.64	1.32	1.41	1.67	1.78	1.17	1.55	1.63	1.34	1.15	1.48	1.3
K^{+}	0.82	0.80	0.32	0.87	1.14	0.85	0.51	1.48	1.00	0.54	0.58	0.92	0.25	1.25	0.60	0.70	0.67	0.64	0.63	0.94	0.61	0.55	0.6
P^{5+}	0.05	0.05	0.03	0.07	0.09	0.07	0.04	0.06	0.11	0.05	0.05	0.07	0.04	0.04	0.06	0.07	0.04	0.06	0.05	0.05	0.06	0.11	0.0
C^{4+}	0.50	0.48	0.44	0.28	0.24	0.26	0.38	0.22	0.32	0.32	0.48	0.34	0.39	0.48	0.35	0.15	0.43	0.25	0.44	0.32	0.39	0.01	0.3
O^{2-}	44.56	44.76	45.21	44.54	44.66	44.30	44.66	44.14	44.80	44.69	44.85	44.38	44.69	46.26	44.79	44.90	45.43	44.63	44.85	45.44	44.98	45.04	45.2

Useful Ratios

Th x 10^4 /K	<3.7	3.8	12.5	4.7	2.7	6.0	7.9	<2.1	3.1	13.2	8.5	5.6	28.0	6.3	<4.9	10.0	9.0	4.7	6.3	3.3	10.0	-	<45
K /Rb	315	358	270	384	447	395	301	343	427	297	366	385	252	183	356	388	162	401	371	280	230	-	223
Rb/Sr	0.14	0.11	0.05	0.14	0.16	0.12	0.09	0.18	0.13	0.09	0.08	0.15	0.05	0.28	0.09	0.09	0.16	0.08	0.09	0.16	0.16	-	0.1
Cr/Ni	3.10	2.62	37.7	1.62	1.43	1.60	20.6	2.65	29.5	21.2	21.9	1.69	22.6	17.2	23.4	60.7	11.2	22.2	28.5	11.6	12.1	20.0	18.1

a. Area north-east of Goldsmith Glacier

3742	Z.487.3	Chilled porphyritic olivine-dolerite, upper contact of 30 m. thick sill above scarp-capping sill.
3743	Z.487.2	Coarse-grained olivine-dolerite, upper part of same sill as 3742.
3659	Z.466.3	Chilled dolerite, 0.8 m. above lower contact of minor sill above scarp-capping sill.
3744	Z.509.1	Fine-grained quartz-dolerite, 6 m. wide dyke above scarp-capping sill.
3745	Z.463.2	Altered coarse-grained quartz-dolerite, minor sill above scarp-capping sill, middle of sill.
3657	Z.463.3	Altered chilled dolerite, top of same minor sill as 3745.

b. Area between Goldsmith and Jeffries Glaciers

3747	Z.489.1	Fine-grained olivine-dolerite, 1 m. above lower contact of 20 m. thick sill just below scarp-capping sill.
3679	Z.489.4	Fine-grained dolerite, about 6 m. below upper contact of 20-30 m. thick sill at base of outcrop.
3655	Z.461.1	Altered coarse-grained subophitic dolerite, lower part of minor sill above scarp-capping sill.
3656	Z.461.2	Fine-grained olivine-dolerite, upper part of same sill as 3655.
3746	Z.488.1	Fine-grained olivine-dolerite, 1.2 m. above lower contact of <5 m. thick minor sill above scarp-capping sill.
3666	Z.469.1	Altered fine- to medium-grained dolerite, <5 m. thick minor sill above scarp-capping sill, possibly same sill as 3746.
3652	Z.469.2	Chilled olivine-dolerite, 6 m. thick sill above scarp-capping sill.
3711	Z.464.1	Porphyritic chilled olivine-dolerite, upper contact of minor sill above scarp-capping sill.
3658	Z.464.2	Fine-grained olivine-dolerite, upper part of same sill as 3711.
3712	Z.464.3	Coarse-grained two-pyroxene, quartz-dolerite, middle of same sill as 3711 and 3658.

c. Area between Jeffries Glacier and the unnam

3677	Z.481.10	Altered chilled dolerite, capping sill.
3651	Z.453.1	Medium-grained ophitic oli thick sill above scarp-cap
3671	Z.453.2	Chilled olivine-dolerite,
3653	Z.453.3	Chilled dolerite, 1 m. wid 3671 and thin minor sill

d. Area south-west of the unnamed southern gla

3684	Z.477.7	Medium-grained variolitic immediately below basal si
10655	TAE350/6	Chilled dolerite, contact Stephenson, 1966).
3685	Z.477.11	Fine-grained dolerite, mid lowest below basal sill of
10654	TAE351/7	Chilled porphyritic doleri 3685 (after Stephenson, 19
3696	Z.478.3	Altered porphyritic chille by thick wedging sill of (
3689	Z.478.7	Chilled dolerite, upper co the basal and thick wedgi
3709	Z.479.1	Chilled olivine-dolerite, middle and upper sills of
3719	Z.495.1	Altered medium-grained do caps Stewart Buttress.

.69	22.72	23.68	24.88	22.89	22.88	24.59	22.75	25.59	23.15	24.13	24.49	22.74	23.33	24.71	23.72	24.68	24.05	24.61	23.25	24.29	25.01	27.21
83	0.55	0.70	0.85	0.53	0.57	0.76	0.54	0.55	0.59	0.59	0.64	0.53	0.62	0.68	0.59	0.58	0.62	0.51	0.42	0.61	0.78	1.22
80	8.22	7.79	7.22	8.89	8.45	6.83	8.13	8.82	8.91	9.00	7.40	9.27	8.53	8.34	7.03	8.43	8.03	8.82	7.03	8.01	7.83	5.93
58	2.07	2.09	2.68	1.85	1.28	2.13	1.53	2.31	1.28	1.86	1.97	1.77	1.12	2.46	1.98	1.13	2.06	0.84	2.22	1.37	1.52	4.92
36	6.08	7.36	6.79	6.20	6.62	8.54	6.61	4.28	6.61	6.06	5.37	6.33	6.95	4.73	5.69	5.98	5.35	5.95	5.50	6.04	5.65	6.41
15	0.11	0.12	0.13	0.11	0.11	0.14	0.11	0.10	0.11	0.12	0.11	0.11	0.11	0.10	0.11	0.11	0.11	0.12	0.12	0.11	0.10	0.13
78	5.79	3.53	2.88	4.81	5.41	2.94	5.97	3.97	4.55	3.65	5.65	4.86	4.48	4.10	6.48	4.87	4.99	4.45	7.01	4.33	4.71	1.03
40	7.50	7.29	6.63	7.57	7.27	6.71	7.66	4.94	7.33	6.98	6.64	7.25	7.25	6.79	7.21	7.02	7.10	6.89	7.87	7.43	5.93	4.65
91	1.37	1.55	1.71	1.55	1.45	1.64	1.32	1.41	1.67	1.78	1.17	1.55	1.63	1.34	1.15	1.48	1.33	1.61	1.03	1.42	1.46	1.72
35	0.51	1.48	1.00	0.54	0.58	0.92	0.25	1.25	0.60	0.70	0.67	0.64	0.63	0.94	0.61	0.55	0.68	0.55	0.35	0.67	1.22	1.64
07	0.04	0.06	0.11	0.05	0.05	0.07	0.04	0.04	0.06	0.07	0.04	0.06	0.05	0.05	0.06	0.11	0.07	0.06	0.04	0.06	0.07	0.11
6	0.38	0.22	0.32	0.32	0.48	0.34	0.39	0.48	0.35	0.15	0.43	0.25	0.44	0.32	0.39	0.01	0.38	0.23	0.37	0.43	0.31	0.10
0	44.66	44.14	44.80	44.69	44.85	44.38	44.69	46.26	44.79	44.90	45.43	44.63	44.85	45.44	44.98	45.04	45.23	45.36	44.79	45.23	45.41	44.94

	7.9	<2.1	3.1	13.2	8.5	5.6	28.0	6.3	<4.9	10.0	9.0	4.7	6.3	3.3	10.0	-	<45	-	<8.8	7.6	3.3	4.4
	301	343	427	297	366	385	252	183	356	388	162	401	371	280	230	-	223	-	156	253	310	269
2	0.09	0.18	0.13	0.09	0.08	0.15	0.05	0.28	0.09	0.09	0.16	0.08	0.09	0.16	0.16	-	0.17	-	0.16	0.15	0.18	0.44
)	20.6	2.65	29.5	21.2	21.9	1.69	22.6	17.2	23.4	60.7	11.2	22.2	28.5	11.6	12.1	20.0	18.1	25.0	13.4	19.5	6.8	1.13

: olivine-dolerite, upper contact of 30 m.
:arp-capping sill.
rine-dolerite, upper part of same sill as 3742.
).8 m. above lower contact of minor sill
; sill.
:-dolerite, 6 m. wide dyke above scarp-capping sill.
ined quartz-dolerite, minor sill above scarp-
le of sill.
lerite, top of same minor sill as 3745.

Glaciers

ne-dolerite, 1 m. above lower contact of 20 m.
low scarp-capping sill.
ite, about 6 m. below upper contact of 20-30 m.
of outcrop.
ined subophitic dolerite, lower part of minor
apping sill.
ne-dolerite, upper part of same sill as 3655.
ne-dolerite, 1.2 m. above lower contact of
sill above scarp-capping sill.
edium-grained dolerite, <5 m. thick minor sill
g sill, possibly same sill as 3746.
lerite, 6 m. thick sill above scarp-capping sill.
d olivine-dolerite, upper contact of minor sill
g sill.
ne-dolerite, upper part of same sill as 3711.
)-pyroxene, quartz-dolerite, middle of same sill

c. Area between Jeffries Glacier and the unnamed southern glacier

3677	Z.481.10	Altered chilled dolerite, 1 m. wide dyke which cuts scarp-capping sill.
3651	Z.453.1	Medium-grained ophitic olivine-dolerite. Middle part of 15 m. thick sill above scarp-capping sill.
3671	Z.453.2	Chilled olivine-dolerite, top of same sill as 3651.
3653	Z.453.3	Chilled dolerite, 1 m. wide dyke between sill of 3651 and 3671 and thin minor sill above.

d. Area south-west of the unnamed southern glacier

3684	Z.477.7	Medium-grained variolitic dolerite, middle of minor sill immediately below basal sill of Coalseam Cliffs.
10655	TAE350/6	Chilled dolerite, contact of same sill as 3684 (after Stephenson, 1966).
3685	Z.477.11	Fine-grained dolerite, middle of 3m. thick sill which is lowest below basal sill of Coalseam Cliffs.
10654	TAE351/7	Chilled porphyritic dolerite, top contact of same sill as 3685 (after Stephenson, 1966).
3696	Z.478.3	Altered porphyritic chilled dolerite, thin wedge intruded by thick wedging sill of Coalseam Cliffs.
3689	Z.478.7	Chilled dolerite, upper contact of 1.2 m. thick sill between the basal and thick wedging sills of Coalseam Cliffs.
3709	Z.479.1	Chilled olivine-dolerite, middle of 4 m. thick sill between middle and upper sills of Coalseam Cliffs.
3719	Z.495.1	Altered medium-grained dolerite, lower part of sill which caps Stewart Buttress.

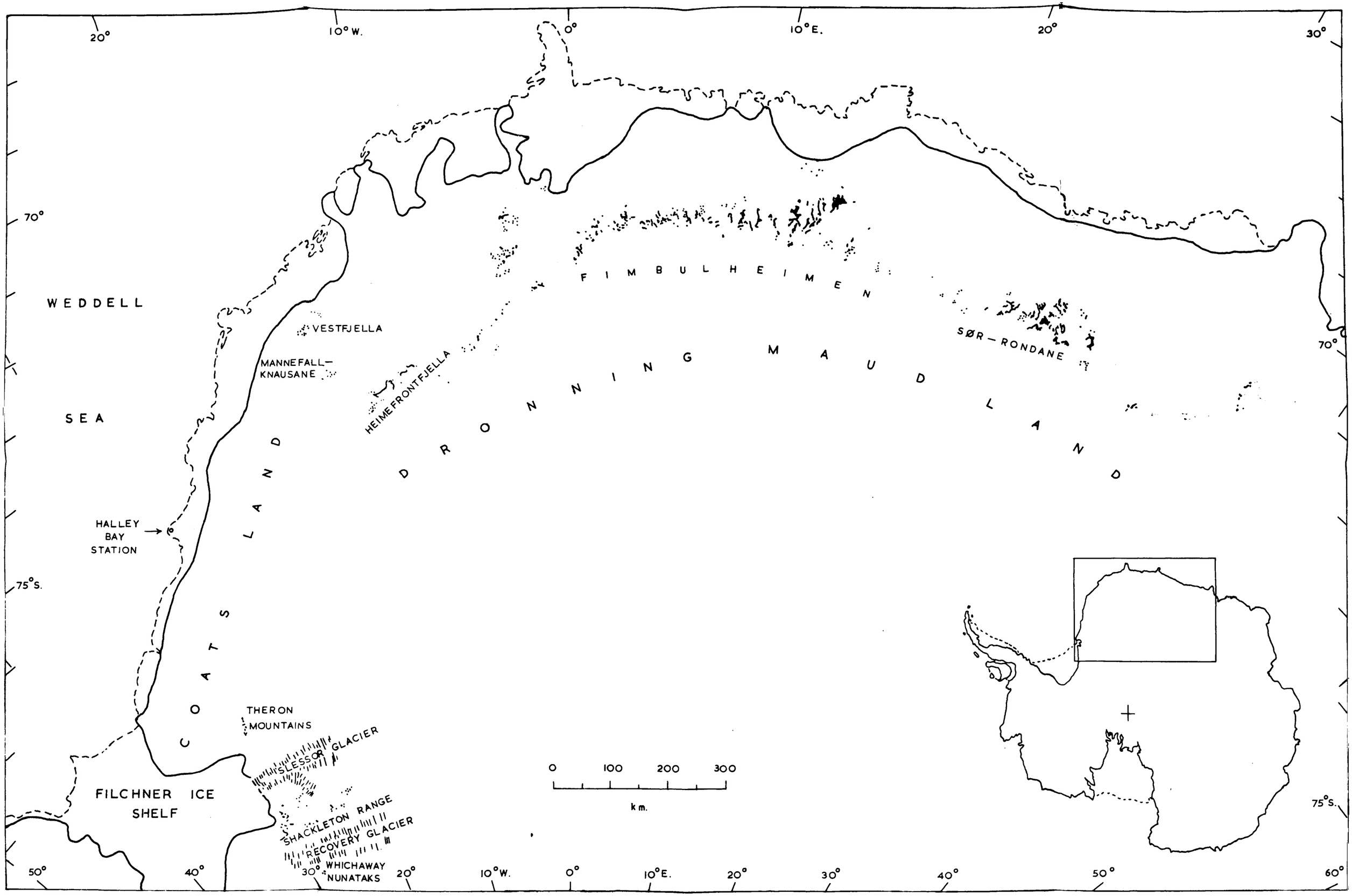

FIG. 1. SKETCH-MAP OF COATS LAND AND DRONNING MAUD LAND SHOWING THE LOCATION OF THE THERON MOUNTAINS AND NEIGHBOURING MOUNTAIN GROUPS. INSET SHOWS THE LOCATION IN ANTARCTICA.

30°

29°

28°W.

27°

2000

TAILEND NUNATAK

3000

1500

"MAIN GLACIER"

GOLDSMITH GLACIER

LENTON BLUFF

1000

3000

79°00'S.

N

POINT 3200

MARØ CLIFFS

POINT 3300

3000

JEFFRIES GLACIER

POINT 2600

COALSEAM CLIFFS

STEWART BUTTRESS

MOUNT FARAWAY

79°00'S.

EXPOSED ROCK WITH NAMED PEAK

ICE FALL

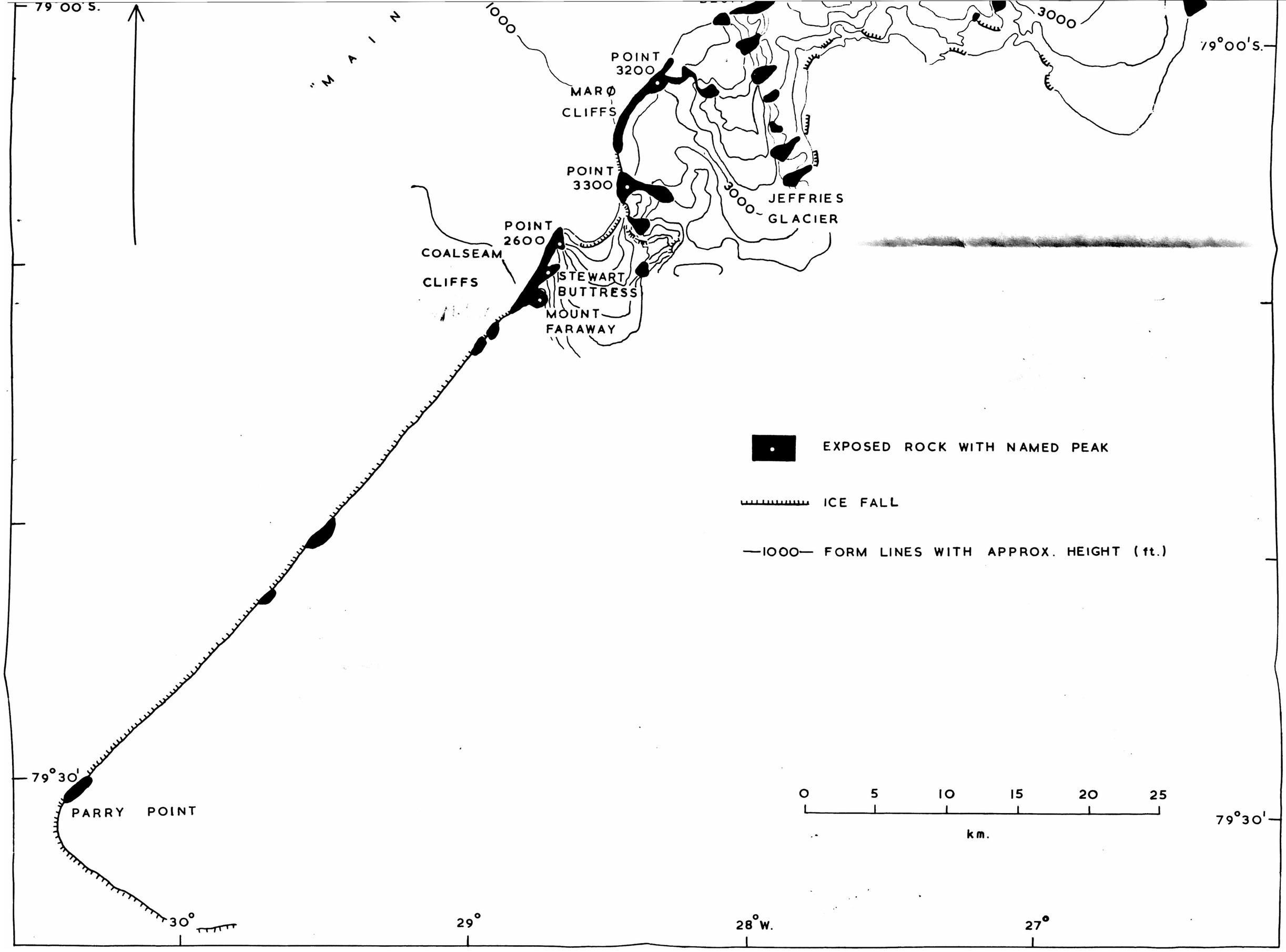

FIG. 2. TOPOGRAPHICAL SKETCH-MAP OF THE THERON MOUNTAINS SHOWING PLACE-NAMES MENTIONED IN THE TEXT. FORM LINES ARE AT 250 ft. (76 m.) INTERVALS.

30°

29°

28° W.

27°

79° 00' S.

N

2000

3000

1500

1000

3000

3000

79° 00' S.

Z·484

Z·485

Z·486

Z·487

Z·467

Z·466

Z·509

Z·465

Z·489

Z·508

Z·470

Z·490

Z·491

Z·506

Z·507

Z·469

Z·468

Z·488

Z·492

Z·505

Z·499

Z·464

Z·463

Z·472

Z·471

Z·498

Z·510

Z·503

Z·483

Z·497

Z·461

Z·502

Z·504

Z·451

Z·482

Z·452

Z·462

Z·481

Z·460

Z·480

Z·453

Z·459

Z·493

Z·477

Z·454

Z·478

Z·494

Z·457

Z·455

Z·500

Z·458

Z·479

Z·495

Z·475

Z·501

Z·496

Z·474

Z·456

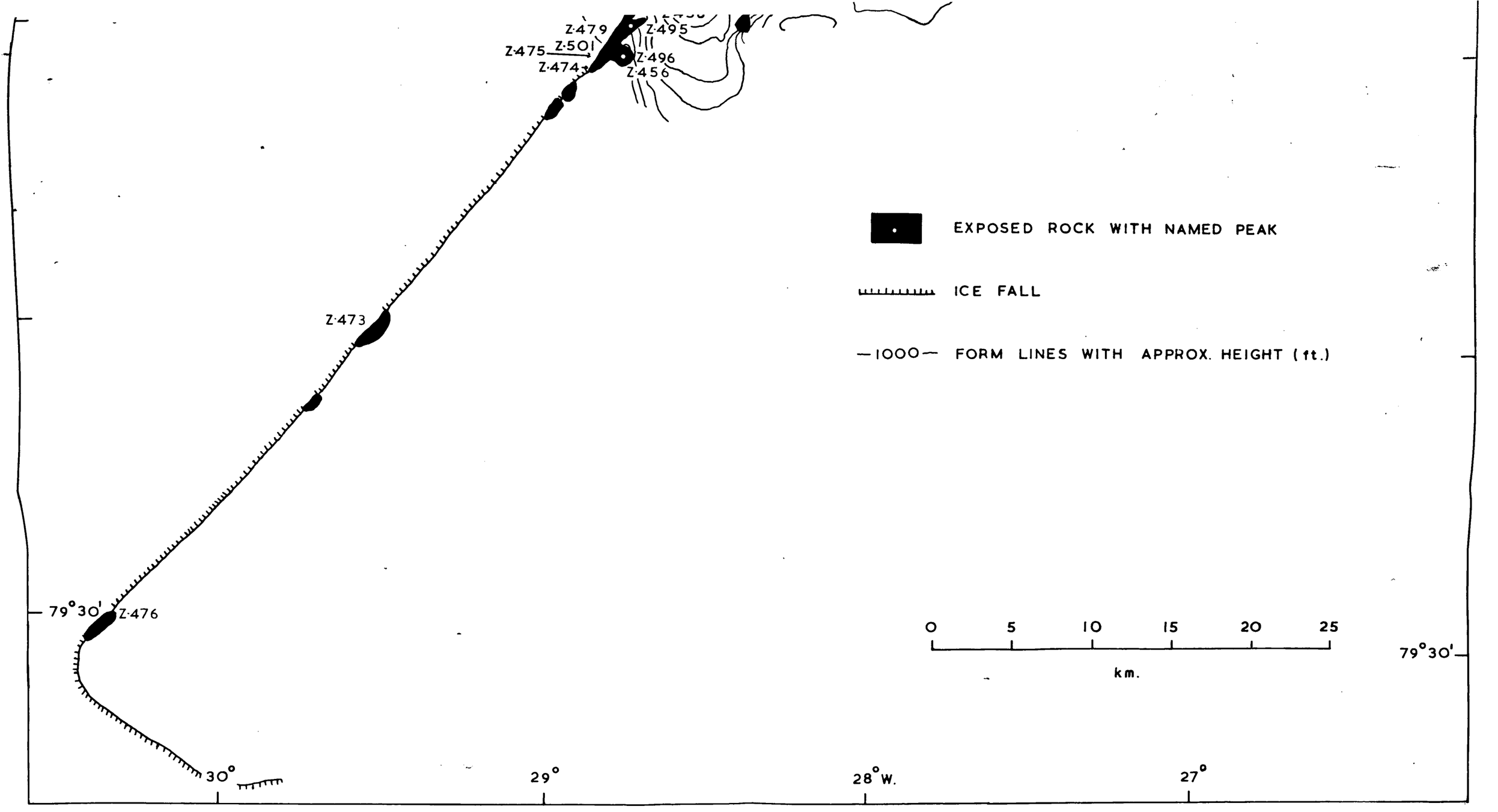

FIG. 3. TOPOGRAPHICAL SKETCH-MAP OF THE THERON MOUNTAINS SHOWING GEOLOGICAL STATIONS VISITED. FORM LINES ARE AT 250 ft. (76 m.) INTERVALS.

30°

28° W.

2000

3000

1500

a.

1000

b.

3000

79°00's.

N

79°00's.

c.

3000

d.

a. SKETCH-SECTIONS OF FIG 5

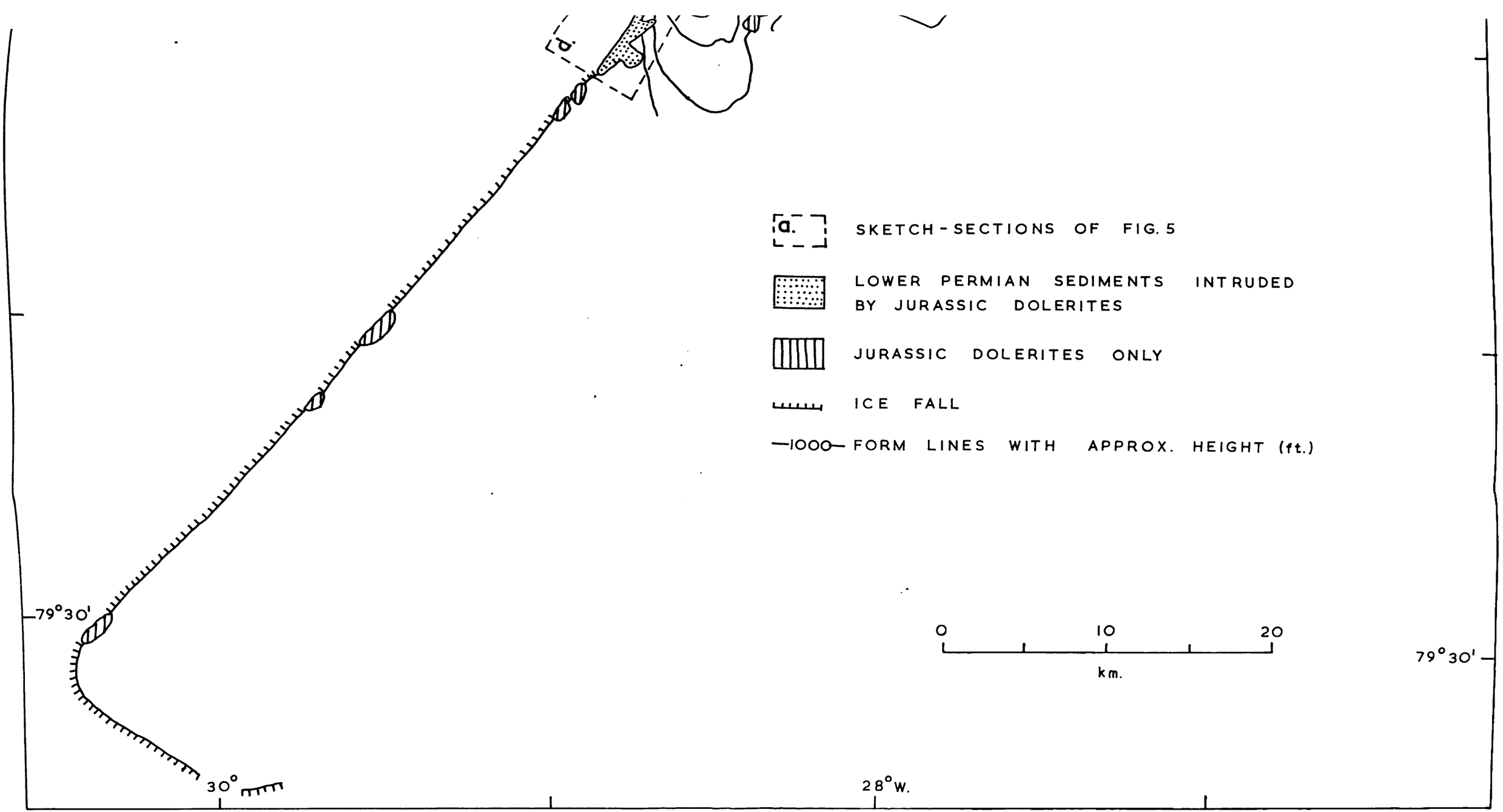

FIG. 4. GEOLOGICAL SKETCH-MAP OF THE THERON MOUNTAINS SHOWING THE DISTRIBUTION OF LOWER PERMIAN SEDIMENTS AND JURASSIC DOLERITES AND THE LOCATION OF THE SKETCH-SECTIONS OF FIG. 5. FORM LINES ARE AT 500 ft. (152 m.) INTERVALS.

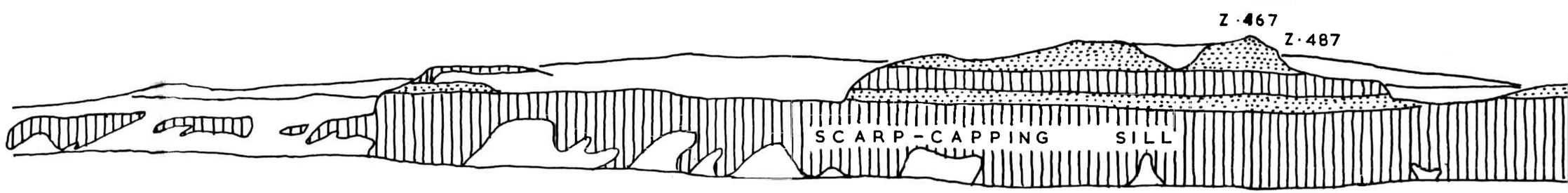

a. CLIFF NORTH-EAST OF GOLDSMITH GLA

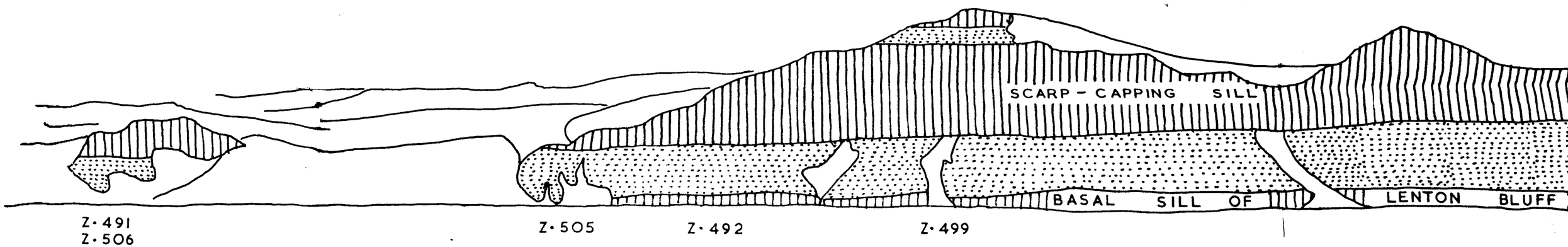

b. LENTON BLUFF

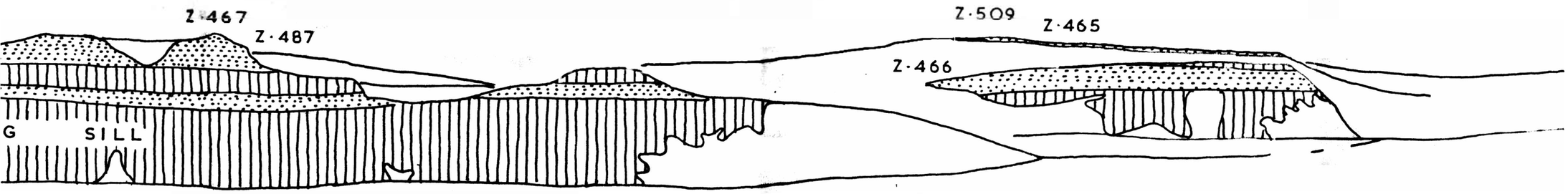

H - EAST OF GOLDSMITH GLACIER

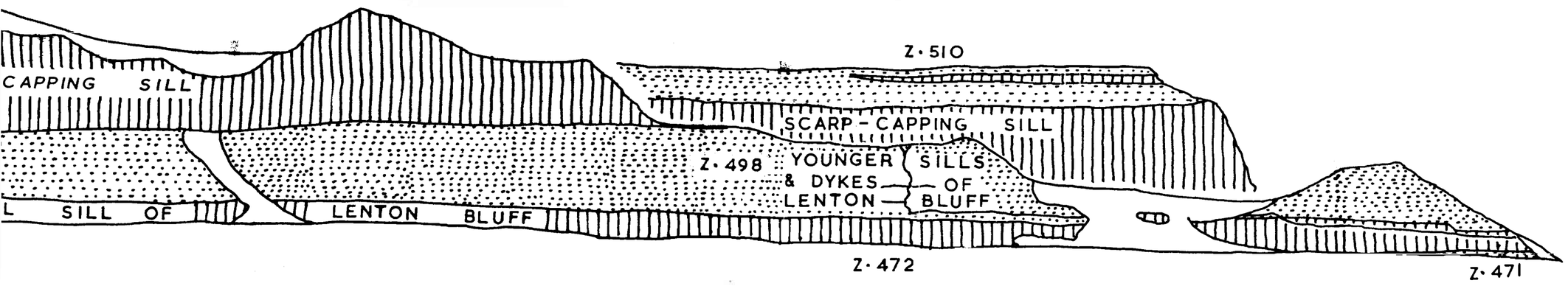

LENTON BLUFF

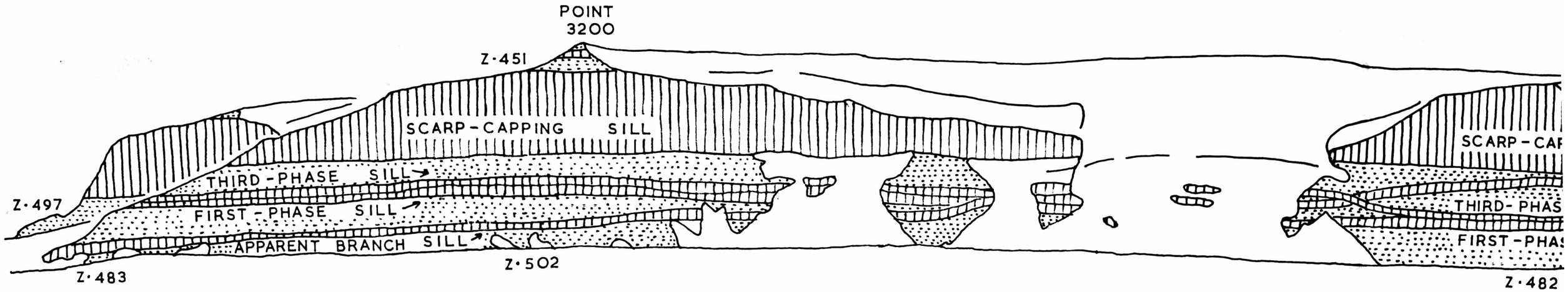

c. MARØ CLIFFS

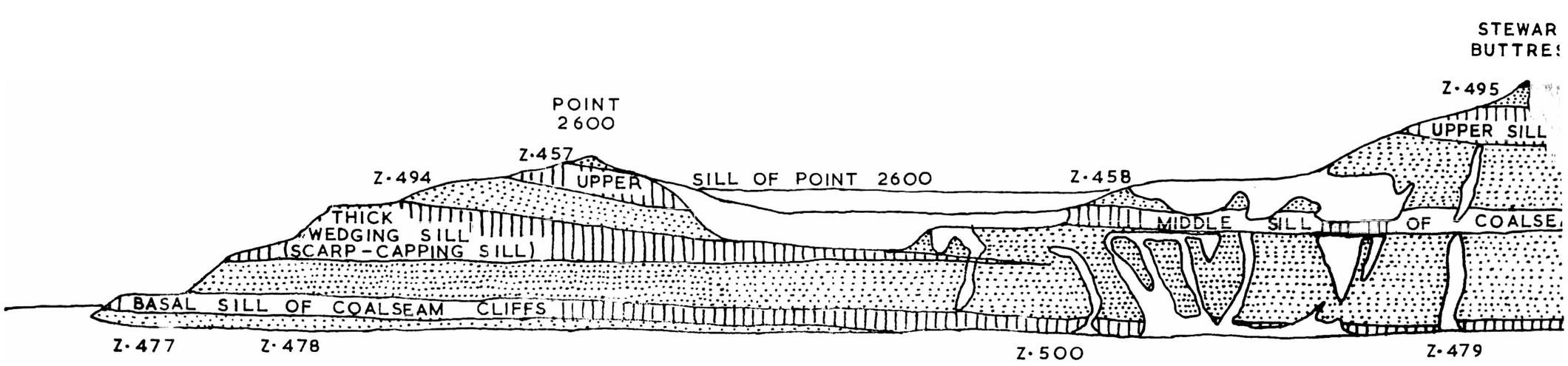

d. COALSEAM CLIFFS

FIG. 5. SKETCH-SECTIONS FROM PHOTOGRAPHS OF THE FOUR MAIN CLIFFS OF THE ESCARPMENT OF THE THERON MOUNTAINS SHOWIN LOWER PERMIAN SEDIMENTS AND THE LOCATION OF GEOLOGICAL STATIONS VISITED. SHADING IS AS IN FIG. 4; UNSHADED AR

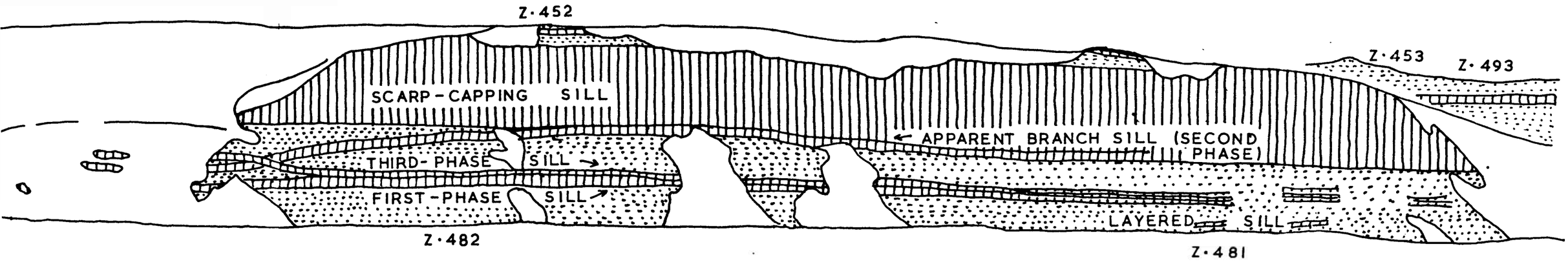

c. MARØ CLIFFS

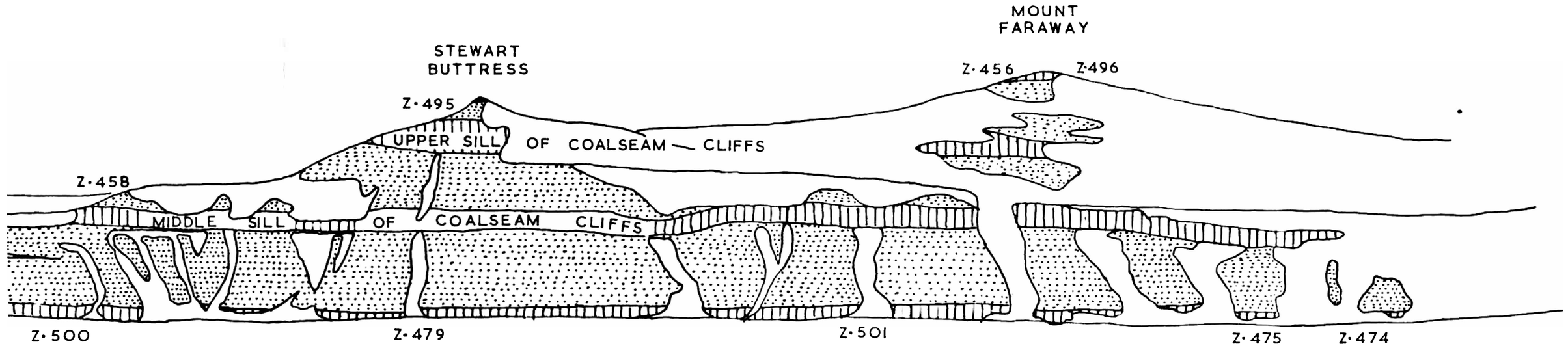

d. COALSEAM CLIFFS

PMENT OF THE THERON MOUNTAINS SHOWING THE DISTRIBUTION AND NOMENCLATURE OF THE MAJOR JURASSIC DOLERITES INTRUDING
SHADING IS AS IN FIG. 4; UNSHADED AREAS ARE SCREE- AND/OR SNOW-COVERED.